Development and application of paleolimnological analyses to disentangle the roles of natural processes and anthropogenic activities on contaminant deposition and hydrological conditions across a northern delta

by

Mitchell Louis Kay

A thesis
presented to the University of Waterloo
in fulfillment of the
thesis requirements for the degree of
Doctor of Philosophy
in
Biology (Water)

Waterloo, Ontario, Canada, 2022

Examining Committee Membership

The following served on the Examining Committee for this thesis. The decision of the Examining Committee is by majority vote.

External Examiner	**Dr. Richard Bindler** Professor Department of Ecology & Environmental Sciences Umeå Universitet, Sweden
Supervisor(s)	**Dr. Roland I. Hall** Professor Department of Biology University of Waterloo **Dr. Brent B. Wolfe** Adjunct Professor Department of Biology Professor, Department of Geography & Environmental Studies, Wilfrid Laurier University
Internal Member(s)	**Dr. Rebecca C. Rooney** Associate Professor Department of Biology University of Waterloo **Dr. Heidi K. Swanson** Associate Professor Department of Biology University of Waterloo
Internal-external Member	**Dr. Mike Stone** Professor Department of Geography and Environmental Management University of Waterloo

Author's Declaration

This thesis consists of material all of which I authored or co-authored: see Statement of Contributions included in the thesis. This is a true copy of the thesis, including any required final revisions, as accepted by my examiners.

I understand that my thesis may be made electronically available to the public.

Statement of Contributions

Mitchell Kay is the sole author for Chapters 1 and 7, which were written under the supervision of Prof. Roland Hall and Prof. Brent Wolfe and were not written for publication.

Prof. Roland Hall and Prof. Brent Wolfe are the primary co-investigators on a collaborative research program that has been supported by multiple grants and contracts. The research presented in this thesis has been supported though federal (NSERC, Global Water Futures, Polar Continental Shelf Program of Natural Resources Canada, Northern Scientific Training Program of Polar Knowledge Canada) and provincial (Alberta Environment and Parks) agencies and industry (Suncor Energy, Canadian Natural Resources Limited, BC Hydro). Logistical support of the fieldwork was provided by Wood Buffalo National Park.

This thesis consists in part of five manuscripts written for publication as peer-reviewed scientific journal papers. Chapters 2, 3, 5 and 6 have already been published as open access peer-reviewed scientific journal papers. Chapter 4 is currently in review. Exceptions to sole authorship of material are as follows:

Research presented in Chapter 2 has been published as: Kay, M.L., Wiklund, J.A., Remmer, C.R., Owca, T.J., Klemt, W.H., Neary, L.K. Brown, K., MacDonald, E., Thomson, K., Vucic, J.M., Wesenberg, K., Hall, R.I., and Wolfe, B.B. 2020. Evaluating temporal patterns of metals concentrations in floodplain lakes of the Athabasca Delta (Canada) relative to pre-industrial baselines. Science of the Total Environment, **20**: 135309. https://doi.org/10.1016/j.scitotenv.2019.135309.

CRediT: Mitchell Kay: Formal analysis, Investigation, Data Curation, Writing – Original Draft, Writing – Review & Editing, Visualization. **Johan Wiklund**: Conceptualization, Methodology, Validation, Writing – Review and Editing. **Casey Remmer**: Investigation, Writing – Review and Editing. **Tanner Owca**: Writing – Review and Editing. **Wynona Klemt**: Validation, Investigation. **Laura Neary**: Investigation, Formal Analysis. **Kathleen Brown**: Investigation, Formal Analysis. **Erin MacDonald**: Investigation, Formal Analysis. **Kate Thomson**: Investigation, Formal Analysis. **Jasmina Vucic**: Investigation, Formal Analysis. **Kristen Wesenberg**: Investigation, Formal Analysis. **Roland Hall**: Conceptualization, Methodology, Writing – Review & Editing, Supervision, Project Administration, Funding Acquisition. **Brent Wolfe**: Conceptualization, Methodology, Writing – Review & Editing, Supervision, Project Administration, Funding Acquisition

Research presented in Chapter 3 has been published as: Kay, M.L., Wiklund, J.A., Sun, X., Savage, C.A.M., Adams, J.K., MacDonald, L.A., Klemt, W.H., Brown, K.C., Hall, R.I., and Wolfe, B.B. Assessment of mercury enrichment in lake sediment records from Alberta Oil Sands development via fluvial and atmospheric pathways. Frontiers in Environmental Science, https://doi.org/10.3389/fenvs.2022.949339.

CRediT: Mitchell Kay: Formal analysis, Investigation, Data Curation, Writing – Original Draft, Writing – Review & Editing, Visualization. **Xiaoyu Sun:** Investigation, Formal Analysis. **Johan Wiklund**: Formal Analysis, Validation, Writing – Review and Editing. **Cory Savage:**

Visualization. **Jennifer Adams:** Investigation, Formal Analysis. **Lauren MacDonald:** Investigation, Formal Analysis, Writing – Review and Editing. **Wynona Klemt:** Investigation, Formal Analysis**. Kathleen Brown**: Investigation, Formal Analysis. **Roland Hall**: Conceptualization, Methodology, Writing – Review & Editing, Supervision, Project Administration, Funding Acquisition. **Brent Wolfe**: Conceptualization, Methodology, Writing – Review & Editing, Supervision, Project Administration, Funding Acquisition

Research Presented in Chapter 4 is in review as: Kay, M.L., Jasiak, I., Klemt, W.H., Wiklund, J.A., Faber, J.A., MacDonald, L.A., Telford, J.V.K., Savage, C.A.M., Cooke, C.A., Wolfe, B.B., and Hall, R.I. Paleolimnological evaluation of metal(loid) enrichment from oil sands and gold mining operations in northwestern Canada.

CRediT: Mitchell Kay: Formal analysis, Investigation, Data Curation, Writing – Original Draft, Writing – Review & Editing, Visualization. **Izabela Jasiak:** Investigation, Formal Analysis. **Wynona Klemt**: Investigation, Formal Analysis. **Johan Wiklund**: Formal Analysis, Validation, Writing – Review and Editing. **Jelle Faber:** Investigation, Formal Analysis. **Lauren MacDonald:** Investigation, Formal Analysis. **James Telford:** Investigation, Formal Analysis, Writing – Review and Editing. **Cory Savage:** Visualization, Formal analysis, Investigation. **Colin Cooke:** Resources, Writing – Review & Editing. **Roland Hall**: Conceptualization, Methodology, Writing – Review & Editing, Supervision, Project Administration, Funding Acquisition. **Brent Wolfe**: Conceptualization, Methodology, Writing – Review & Editing, Supervision, Project Administration, Funding Acquisition

Research presented in Chapter 5 has been published as: Kay, M.L., Wiklund, J.A., Remmer, C.R., Neary, L.K., Brown, K., Ghosh, A., MacDonald. E., Thomson, K., Vucic, J.M., Wesenberg, K., Hall, R.I., and Wolfe, B.B. 2019. Bi-directional hydrological changes in perched basins of the Athabasca Delta (Canada) in recent decades caused by natural processes. Environmental Research Communications **1:** 081001. https://doi.org/10.1088/2515-7620/ab37e7

CRediT: Mitchell Kay: Formal analysis, Investigation, Data Curation, Writing – Original Draft, Writing – Review & Editing, Visualization. **Johan Wiklund**: Conceptualization, Methodology, Validation, Writing – Review and Editing. **Casey Remmer**: Investigation, Writing – Review and Editing. **Laura Neary**: Investigation, Formal Analysis. **Kathleen Brown**: Investigation, Formal Analysis. **Anita Ghosh:** Investigation, Formal Analysis. **Erin MacDonald**: Investigation, Formal Analysis. **Kate Thomson**: Investigation, Formal Analysis. **Jasmina Vucic**: Investigation, Formal Analysis. **Kristen Wesenberg**: Investigation, Formal Analysis. **Roland Hall**: Conceptualization, Methodology, Writing – Review & Editing, Supervision, Project Administration, Funding Acquisition. **Brent Wolfe**: Conceptualization, Methodology, Writing – Review & Editing, Supervision, Project Administration, Funding Acquisition

Research presented in Chapter 6 has been published as: Kay, M.L., H.K. Swanson, J. Burbank, T.J. Owca, C.A.M. Savage, C.R. Remmer, L.K. Neary, J.A. Wiklund, B.B. Wolfe, R.I. Hall. 2021. A Bayesian mixing model framework for quantifying temporal variation in source of sediment to lakes across broad hydrological gradients of floodplains. Limnology and Oceanography Methods **19:** 540-551. https://doi.org/10.1002/lom3.10443

CRediT: Mitchell Kay: Formal analysis, Investigation, Data Curation, Writing – Original Draft, Writing – Review & Editing, Visualization. **Heidi Swanson:** Conceptualization, Methodology, Investigation, Writing – Review & Editing. **Jacob Burbank:** Methodology, Writing – Review & Editing. **Tanner Owca:** Formal Analysis, Writing – Review and Editing. **Lauren MacDonald:** Formal Analysis, Writing – Review and Editing. **Cory Savage:** Formal Analysis, Writing – Review and Editing, Visualization. **Casey Remmer:** Investigation, Writing – Review and Editing. **Laura Neary**: Investigation, Formal Analysis. **Johan Wiklund**: Formal analysis, Writing – Review and Editing. **Roland Hall**: Writing – Review & Editing, Supervision, Project Administration, Funding Acquisition. **Brent Wolfe**: Writing – Review & Editing, Supervision, Project Administration, Funding Acquisition.

Abstract

Freshwater ecosystems across northern Canada provide important habitat for wildlife and have long supported the traditional lifestyles of Indigenous communities. Multiple potential stressors threaten the security of water supply to northern landscapes, which fosters need for information spanning broad spatial and temporal scales to inform adaptive and mitigative strategies. At the Peace-Athabasca Delta (PAD; northern Alberta), the world's largest boreal freshwater delta, existing data records have been too short and too sparse to resolve many concerns over the roles of major energy projects (hydroelectric regulation of river flow, oil sands development) and climate change on decline of flood frequency and magnitude and drawdown of shallow aquatic basins, and on supply of substances of concern. Intensive paleolimnological research during the past two decades at the PAD has evaluated past changes in contaminant deposition and hydroecological conditions to discern effects attributable to oil sands development along the Lower Athabasca River and to regulation of Peace River flow by the W.A.C. Bennett Dam. This thesis builds substantially on these previous studies to address knowledge gaps by applying conventional paleolimnological methods at new locations to improve understanding of temporal changes in contaminant deposition and hydrological change and developing an innovative paleolimnological approach for discerning variation in sediment sources over space and time to lakes within the PAD.

Concerns of pollution in the PAD stem from potential for dispersal of contaminants released by bitumen mining and processing activities within the Alberta Oil Sands Region (AOSR), which straddle the Lower Athabasca River. Unfortunately, systematic monitoring began thirty years after onset of oil sands development and sampling locations have changed over time, which has hampered the ability to accurately track temporal trends or attribute sources of pollution

at the AOSR and downstream locations. Previous paleolimnological studies in the PAD have provided critically missing baseline information by employing lake sediment deposited before oil sands development to evaluate lake or river-bottom sediment deposited after oil sands development for evidence of pollution. Results show no enrichment via fluvial or atmospheric pathways, however, analyses to date were limited to a sediment core from one upland lake and samples of river-bottom sediment collected from a few sites within the Lower Athabasca River and its distributaries within the PAD. In Chapters 2 and 3, contiguous measurements of trace elements (beryllium, chromium, lead, mercury, nickel, vanadium, and zinc) in lake sediment from floodplain and upland lakes were employed to develop knowledge of pre-disturbance concentrations, and to quantify the extent of enrichment in lakes at the PAD since onset of oil sands mining and processing activities via fluvial and atmospheric pathways, respectively. Results demonstrate no enrichment since onset of oil sands development via fluvial pathways. Also, no enrichment via atmospheric pathways was detected for vanadium, nickel and total mercury (THg) at upland lakes coincident with the onset of oil sands activities. Total mercury enrichment was detected at the start of the 20th century in sediment cores from two upland lakes, which is congruent with stratigraphic patterns observed in many other lake sediment records in response to long-range anthropogenic emissions across the northern hemisphere.

Site-specific paleolimnological studies from four regions spanning large-scale bitumen mining on the Lower Athabasca River to gold mining in central Northwest Territories (including AOSR, PAD, Slave River Delta (SRD), Yellowknife region of central NWT) have provided a wealth of information about temporal patterns of deposition of substances of concern. Differences in laboratory methods and data analysis, however, have challenged ability to compare and contrast site-specific studies among regions. Opportunity to coalesce the current state of knowledge was

capitalized on in Chapter 4 via systematic re-analysis of concentrations of key pollution-indicator trace elements in sediment cores from 51 lakes spanning the four key regions. Lake sediment records from lakes within the mining regions (AOSR and central Northwest Territories) illustrate enrichment of pollution-indicators since onset of mining and processing activities via atmospheric pathways, while no enrichment was detected at the PAD or SRD via fluvial pathways since onset of mining activities. The knowledge generated from Chapters 2-4 can be employed by multiple stakeholder groups to assess risks associated with contaminant dispersal across a vast region of northwestern Canada.

Long-term perspectives provided by paleohydrological studies at the PAD have demonstrated that decline of flood frequency and magnitude and lake-level drawdown began decades before onset of Peace River flow regulation by the W.A.C. Bennett Dam. Many of these studies have been concentrated in the northern Peace Delta but concerns also exist about declines in river discharge, flood frequency and lake levels in the southern Athabasca Delta. Chapter 5 tests the hypothesis that the Embarras Breakthrough, a natural geomorphic change in distributary flow of the Athabasca River, is the main driver of recent hydrological change in the Athabasca Delta. Stratigraphic variations in the mineral matter content of sediment cores from nine floodplain lakes, including at sites within the Athabasca River terminus region, demonstrate that flood influence increased after 1982 at lakes along a distributary to the north of the Embarras Breakthrough and declined at lakes east of the Embarras Breakthrough. The timing of this bi-directional change confirms that the Embarras Breakthrough has caused the largest shift in hydrological conditions within the Athabasca Delta during the past ~120 years.

Paleohydrological reconstructions employing conventional analyses have provided valuable insight into the hydrological evolution of the PAD but integration of the results across

sites has remained a challenge due to marked differences in sediment composition across the spectrum of hydrological processes influencing lake water balances. At flood-prone lakes, physical methods (e.g., grain size, magnetic susceptibility) provide high information content, whereas biological or bio-geochemical methods (e.g., diatoms, plant macrofossils, cellulose oxygen isotope composition) provide high information content at perched basins. Elemental concentrations, however, can be determined accurately along the full gradient of mineral-rich to organic-rich sediment of flood-prone and perched basins, respectively, and can be used to delineate the three major sources of sediment supplied to lakes (Athabasca River, Peace River, and local catchment), which is a key advancement over previous paleolimnological studies. In Chapter 6, a mixing model framework was developed and evaluated via application to sediment cores from two adjacent lakes in the Athabasca Delta. Output from the mixing model aligns remarkably well with conventional loss-on-ignition analysis and paleohydrological interpretations from the same two lakes, which further illustrate the profound effect of the 1982 Embarras Breakthrough on hydrological conditions of lakes in Athabasca Delta. Interestingly, model results indicated that ~60% of the sediment originated from the Peace River during the largest ice-jam flood event in the hydrometric record (1974). Due to the success of this model, opportunity exists to apply the model to a network of lakes in the PAD, where elemental concentrations have been analyzed, to reconstruct spatial and temporal variation of pathways of sediment sources and infer changes in hydrological processes. The methods developed and applied in this thesis are anticipated to be broadly applicable to other freshwater landscapes where monitoring records remain too short and too sparse to discern effects of multiple stressors.

Acknowledgements

Hard things are hard, but "appreciation is a wonderful thing.
It makes what is excellent in others belong to us as well." - *Voltaire*

To Dr. Roland Hall and Dr. Brent Wolfe, thank-you for taking a chance on a keen, enthusiastic undergraduate student with absolutely no background in environmental science let alone in paleolimnology. You have enriched my life for the better through the numerous life-changing opportunities you have provided such as going to the North or presenting at international conferences. Your invaluable expertise, guidance and support has made this thesis possible. The whirlwind of the past six years all started by Roland asking if I want to join in this adventure and work together towards completing exciting research. I cannot imagine what my life would look like if I didn't say yes. Little did we know that 'cobbling' together a thesis would turn out the way it did. I will always look back fondly on our Winnipeg Jets versus Toronto Maple Leaf rivalry, which never disappointed and I expect to continue. I am eternally grateful for every moment of the last six years, which was made possible by your untiring support for me.

To Dr. Heidi Swanson and Dr. Rebecca Rooney, thank-you for nurturing my growth as an independent PhD student and researcher. I am forever grateful for the guidance, feedback, and advice you have provided during my PhD. Your stats class, while intimidating in the moment, pushed me to improve my data analysis skills. Your presence on my committee provided valuable perspectives and wisdom that elevated the quality of my thesis and improved my research skillset. Thank-you for listening to my ideas and sharing your own.

To Dr. Mike Stone and Dr. Richard Bindler, thank-you for taking the time out of your busy schedules to serve as examiners for my PhD. Thank-you for the thought-provoking questions, which have provided valuable perspective.

To Dr. Johan Wiklund, your scientific curiosity is unparalleled. I will be forever indebted to you for your guidance and patience throughout this entire process. I am eternally grateful for your ability to develop nuggets of brilliance that have contributed to making my thesis better. You also taught me that a quick 'back of the napkin' calculation can improve a publication. Beyond your scientific contributions, I have learned more about military history and tanks than I ever thought I

would. You are an encyclopedia of knowledge about any topic, which is something I will sorely miss as I depart the research group. Thank-you for every conversation we have had, and I thoroughly enjoyed sharing an office with you. You are the reason I can confidently say I learned something new every day.

To Tanner Owca, together we climbed mountains and fjords across Scandinavia and Scotland, but I would never have been able to finish the journey of my thesis, my tallest mountain, without you. It was a crazy ride with way too many good stories to single specific ones out but, as you said, it was always a party. Thank-you for every single adventure we went on and I look forward to the next adventure. In between all these adventures, we had fantastic conversations about contaminants which provided me with ideas on how to push our data further than either of us could have imagined. I will never forget how to use bear spray because of you. Thank-you for everything.

To James Telford, you were the first person I went to in the lab when I had a problem, and you were always willing to take time out of your day to help me fix the problem. You were incredibly supportive and caring but also challenged me to be a better scientist, and for that I am grateful. I will take the lessons you taught me professionally and personally for the rest of my life. I think anyone who has ever been a member of the Hall/Wolfe Research Group would agree you do things the 'James Way', which often annoyed me in the moment but always knew you would come through. You made even the most mundane tasks enjoyable. I will cherish every memory, especially the days we spent in the field collecting sediment cores with our kayak and tent.

To Wynona Klemt, I have always marveled at your dedication to everything you did while a part of the Hall/Wolfe Research Group. Thank-you for the frequent and long conversations about data analysis and graphical design -- without you I would still wandering mindlessly in random directions. Thank-you for everything, you made the day-to-day more fun than I could have imagined. We made memories in the field and at countless conferences that I will remember for the rest of my life.

To Jelle Faber, you single-handedly have provided me with some of the greatest memories and best laughs during graduate school. No matter the situation you had a smile from ear-to-ear, and

you were always able to make the best out of situations. You stressed me out way more than anyone else in the lab either from wandering off or forgetting your wallet, but we always resolved those challenges and gathered great stories! I could not imagine doing graduate school without you and I would not change any of it for the world.

To Lauren MacDonald, you are a brilliant writer and scientist but the thing I appreciate the most is your blunt honesty. You will tell me exactly what you think about something, which has allowed me to grow as a researcher. The synergy between our skill sets has led to a very productive and efficient working relationship that I only wish started earlier. Thank-you for all the guidance you have provided during my PhD.

To Laura Neary, thank-you for the numerous contributions you have made to my PhD. From collecting samples in the field to endless hours of lab work; without you none of this could have been possible. I admire the competitive spirit you bring to every aspect of your life. Even when you are losing to Johan and I at cards, you never will give up. I will forever cherish the memories gained from the field or simply our morning (and afternoon) coffee breaks.

To Izabela Jasiak, thank-you for being an incredible office mate during the middle part of my PhD. Your tenacity and belief have always inspired me to do the absolute best I can at everything I do. I will always be thankful for the memories and look forward to how our lives will continue to cross in unexpected ways.

To Eva Mehler and Casey Remmer, thank-you for being my first office mates who showed me the ropes of graduate school. You both taught me so much that served as the foundation of my PhD. Eva – I will always strive to be as punctual and devoted as you were to your project. Casey – we have so many incredible memories from fieldwork to conferences that I will cherish for my entire life. One of the hardest learning curves in my PhD was the battle of the thermostat in our office, it could be 30 °C outside but the office still needed to have the heat on because you were cold. Not sure I still fully understand this concept but our discussions around temperature of the office often ended up talking science, which I sorely miss.

To Caleb Girard and Cory Savage, thank-you for all the enjoyable memories in the field and I wish our weekly pickup basketball games didn't end so abruptly. As much as I try to forget all the frustrating battles I have had with R and ArcMap, I knew I could always count on you Cory even if I had already asked multiple times.

To Mia Stratton, it was an absolute pleasure to watch you grow in the lab from a volunteer to co-op student and eventually MSc graduate. Thank-you for all the memories in the lab and field and for never letting my emotions run to low (or high). Thank-you for all the contributions you made to lab work.

To Nelson Zabel, thank-you for being the most organized person I have ever met. Your dedication to the lab manager role and your compassion is a big reason why I survived the early days of graduate school. I am eternally grateful for all of our stats chats, which provided a strong foundation for my PhD.

Thank-you to all the brilliant undergraduate thesis students who put countless hours into lab work and drafting fantastic theses. Your hard work never went unnoticed, and I am truly grateful for the contributions you made to help progress the state of knowledge in our research program. I hope you all enjoyed the experience as much as I did. Additionally, I would like to give a big thank-you to all my lab volunteers, who dedicated many hours to help progress lab work for my PhD. I am indebted to all the research and thesis students and volunteers because, without them, I would probably still be doing lab work.

Thank-you to all the undergraduate research students especially Laura Anderson and Meredith Watson who have worked in the Hall/Wolfe Research Group during my PhD. I am convinced your productivity levels were higher on days when I was not in the lab, but I fully appreciate you all listening (willingly or not) to whatever was on my mind that day from science to sports, and everything in between.

To past and present members of the Wolfe/Hall Research Team, you have made these past six years amazing. Each of you have improved my life in ways you probably don't even realize. I will

cherish every memory I have made here and treasure the opportunity I have had to learn from you all.

To the Graduate House, and especially Manager Cam, thank-you for providing a place where we could discuss science on a Friday afternoon. Some of the best ideas that came into my PhD thesis were generated at the Grad House, and several were sketched out on a napkin. These napkin schematics have formed key chapters in my Thesis that would not have been possible without time spent at Grad House. I will forever cherish every memory at Grad House.

To Dr. Kevin Turner, thank-you for always being an arms length away for the past six years. We did some fantastic science, and I will never forget the memories of meeting for the first time in Fort Chipewyan or my first PALS Conference at Brock University. I will always cherish my first ride in the caboose. I still would like a recount of the votes from the PALS 2019 'Golden Napkin' talks, but I must admit I lost to a worthy competitor.

To Alecia Chevalier, it all started with you being a curious undergraduate student who wanted to gain lab experience. Thank-you for showing up consistently week after week despite all the other pressing deadlines of being a 4th year student. Little did I know the incredible friendship that sprouted from you being a volunteer in the Hall/Wolfe Research Group. I sorely miss our mid-day fieldtrips to Laurier and closing down the GH (more than once). More recently, you have provided me with so much support and laughs. I am eternally grateful for it all and would not have changed any part of the last five years for the world. You remind me continually to do what you love and call it work.

To Ezgi Ulkuseven and Mila Kostic, thank-you for taking an interest in my project and assisting with lab work despite having incredibly difficult course loads. No matter the task, both of you did it with a smile on your face.

To all the friends I made in the Department of Biology during the past six years: Thank-you. You were a welcoming group of students who just wanted to do cool science, and I could not imagine doing my PhD in any other department. I would like to especially thank Justin Knapp, Nikhil

George, Nilanth Yogadasan and Jacob Burbank who have provided endless support and friendships leading to wonderful memories.

To Quinn Abram, you were one of the first people I met in graduate school and our friendship blossomed instantly into something neither of us could imagine. I will cherish our lengthy hallway conversations about the Toronto Maple Leafs and Toronto Blue Jays. One day we will find a way to collaborate on a research project.

To Dan Inglis, Elanna DeMarchi, Phil Guilmette, and Claire Quong, words cannot describe how important the four of you have been during this whole endeavour, but I will try. Thank-you for being an incredible support system and a pillar of stability in my life knowing exactly what I needed. I could not have gotten through this degree without the four of you. Thank-you for believing in me and wanting the best for me in all aspects of my life. You four have made me a better person and it is an absolute honour to call you, my friends. The only constant in life is change, but I hope the four of you never change.

To McKenna Szczepanowski, no matter if it was pouring rain or if there was not a cloud in the sky, you had a smile on your face that could light up the night sky and were ready to listen to my non-sensical rambling. I am grateful for the support during the past couple years and your ability to understand the ups and downs of graduate school was invaluable. Despite all of this, you still don't understand what the word 'paleolimnology' means but that has never stopped you from trying!

To Ryan Cavaliere and Alex Kiciak, we met in first year calculus, which was our first and last 8:30 am class of our undergraduate programs. You both have been with me for every step of the way during the past ten years at UW and I cannot thank you both enough for the words of encouragement and support throughout the entire ride. I would never have finished my undergraduate and PhD without you two.

To Ryan Walker, thank-you for being an incredible friend during the past couple of years. Your enthusiasm and passion are infectious and has been a huge source of positivity in my life. You

knew exactly what to say and I could always count of you for anything. I feel lucky to call you, my friend. I will treasure the memories we have made and look forward to the new adventures.

To Juliana Blossom, thank-you for being the model of consistency during my PhD. You were an amazing support system with a unique way of turning every negative into a positive. You have taught me dedication and dreams are a powerful combination necessary to achieve success. I will always treasure our conversations as they got me through the thick and thin.

To Katie Watson at Molly's Irish Pub, thank-you for always having a spot ready for me no matter the time of day. I am grateful for your enthusiasm and support. Thank-you for providing welcomed distractions in the form of life stories and experiences.

To Waterloo Athletics, it all started with you back in 2012. You provided a home for me during my undergraduate degree and PhD and never in my wildest dreams did I imagine this is how it would play out after accepting my undergraduate offer. Everyone from coaches (notably Tim Pegg, Ben Norris, and Andrew Robb) to administrative staff provided unwavering support of my academic journey from start to finish and I am truly grateful for the opportunities to highlight my PhD research.

To Chris Iltshishin and Kayla Gallagher, despite the crazy day-to-day schedules, we have always found creative ways to make memories that I will remember forever. From day 1, I knew our friendship would be exactly the support I needed during this endeavour. You both provided a calming, rational voice that helped guide me through some of the craziest moments of my PhD.

To Graham Forrester and Robyn Martens, I feel so lucky to have crossed paths with both of you in different aspects of my life. I will treasure every single memory we had from day 1 until the Canadian Prairies called you both back home. You both provided unparalleled encouragement and support in all aspects of my life, and I am incredibly grateful.

To Luke Zettel, Mike Kritz and Stephen Gade, you three are the biggest group of misfits I have ever seen but I would not have changed any of it for the world. Thank-you for the all the late-night

laughs and memories during the past six years. A journey is never too long if you take the heel-toe express and have friends from start to finish.

To Andrew Zettel, I am eternally grateful for the memories and laughs over the last couple of years. Simply put, thank-you for being you. I will always consider you to be the ‘piano man’.

To Liam Kelly, Varun Kuo and Nik Levinski, thank-you for being incredible friends who knew exactly when I needed a break from it all. I will cherish the youthful perspective and energy, which always recharged my energy levels to keep chasing the dream.

To Barbara and Robert Grandjambe, I am eternally grateful for the hospitality and unmatched generosity you both showed during fieldwork. I will forever cherish the moments spent together in Fort Chipewyan or boat rides to the Peace River. You both provided an invaluable perspective of the Peace-Athabasca Delta that I would have not been able to obtain through any other means.

Thank-you to Parks Canada for providing logistical support in the field. I would also like to extend a big thank you to Queenie Gray for her valuable perspectives and thoughts about the Peace-Athabasca Delta.

To Summit Helicopters, thank-you for providing highly skilled pilots (Sean, Mitch, and Rob), who were an absolute pleasure to work with. Holding a helicopter steady while hovering over a lake is not an easy task but the three of them were able to do it without breaking a sweat.

I would like to acknowledge the funding sources for the studies contained within in my thesis. Research support was provided by NSERC Discovery Grant Program, Northern Research Supplement Program, Polar Continental Shelf Program of Natural Resources Canada, Alberta Environment and Parks, Suncor Energy, and Canadian Natural Resources Limited to R.I. Hall and B.B. Wolfe. The W. Garfield Weston Doctoral Award for Northern Research and Ontario Graduate Scholarship and Queen Elizabeth II Graduate Scholarship in Science and Technology supported M.L. Kay. The Northern Scientific Training Program of Polar Knowledge Canada provided funds to allow me to visit the North for numerous multi-week sampling campaigns.

Lastly, to my parents (Michael and Susan), you have encouraged me to chase my dreams since day one of kindergarten and have also been the biggest source of inspiration during this journey. I am deeply grateful for the countless hours of unconditional support and love you have provided. I truly cannot count the ways you have made all my achievements possible, and I would not have made it to this point without you. Thank-you for being my guiding light during this endeavour.

Dedication

This thesis is dedicated to the loving memories of Jacqueline and Todd Jolly, Edwin and Theresa Dietrich and William Kay. Everyday I try to be as knowledgeable, creative, caring and loving as the five of you. I hope my academic journey has made you all proud.

Always on my mind, forever in my heart.

TABLE OF CONTENTS

List of Figures

List of Tables

Chapter 1: General Introduction

Landscapes in northern Canada support an abundance of highly productive shallow lakes, which serve as important habitat for wildlife and have long provided important resources for Indigenous communities to support their traditional lifestyles. Due to their small water volume, shallow lakes are responsive to environmental stressors. During the 20th and 21st centuries, northern latitudes have experienced disproportionate climate warming compared to temperate regions, leading to longer duration of ice-off and alteration of hydrological processes, biogeochemical cycles and limnological conditions (Gleick 2003; Hassan 2005; Prowse et al. 2006; Schindler and Smol 2006; IPCC 2007; Woodward et al. 2010; Vincent et al. 2011; Larsen et al. 2014; Heino et al. 2020). Also, natural resource development has increasingly expanded northwards, encroaching ever closer to remote northern landscapes. Large-scale mining and processing activities have the potential to alter deposition patterns of heavy metals, polycyclic aromatic compounds, and other contaminants of concern (Schindler 2010). Studies attempting to evaluate contaminant deposition in northern Canada have focused mainly on locations proximal to mining sites (Wagemann et al. 1978; Kelly et al. 2009, 2010; Timoney and Lee 2009; Galloway et al. 2012, 2015, 2018; Kirk et al. 2014; Palmer et al. 2015; Donner et al. 2017, 2018), but contaminants may travel farther afield to remote landscapes of high preservation value via atmospheric and fluvial pathways and degrade aquatic ecosystems (McMartin et al. 1999). The pressures of climate change and rapid industrial development have challenged effective stewardship decisions by water resource managers and stimulated concerns about the security of water abundance and water quality in the North. Unfortunately, monitoring programs focusing on water abundance and water quality are almost exclusively developed after industrial development has occurred confounding attempts to disentangle natural processes and anthropogenic activities

(Blais et al. 2015). Thus, there is an urgent need to develop knowledge of past variation in environmental conditions at sufficient spatial and temporal scales to adequately characterize the natural range of variability and the cumulative effects of multiple stressors. Such information will be critical to defining the limits of acceptable change (e.g., Gell 2017) and ensuring informed stewardship of northern freshwater landscapes.

The Peace-Athabasca Delta

Concerns of aquatic ecosystem degradation by multiple stressors have long been a focal point for the Peace-Athabasca Delta (PAD). Located in northern Alberta, the PAD is the world's largest freshwater boreal delta and is comprised of the southern Athabasca Delta (or sector), which is the largest and most active, the northern relic Peace Delta (or sector) and the smaller Birch Delta to the west (Figure 1.1). Similar to other northern freshwater landscapes, the PAD provides extensive wildlife habitat and is of socio-cultural importance for local aboriginal groups, including the Athabasca Chipewyan First Nation (ACFN), Mikisew Cree First Nation (MCFN), and Fort Chipewyan Local 125 of the Métis Nation of Alberta. Most of the PAD lies within Wood Buffalo National Park (WBNP), which is a UNESCO World Heritage Site, and the PAD is recognized as a Ramsar Wetland of International Importance for its ecological, historical, and cultural significance. The delta provides a home to the world's largest herd of free roaming bison and serves as a major resting and nesting ground for birds migrating across North America. The central area of the ~6,000 km^2 delta is characterized by large shallow lakes that are connected to the major rivers by a series of channels (Prowse et al. 2002; Timoney 2002). Hundreds of other smaller shallow lakes, wetlands and grassland comprise the remainder of this productive landscape. Ice-jam flooding on the Peace and Athabasca rivers during the spring freshet is the primary hydrological process that replenishes the shallow perched basins via abandoned channels or

overland flow (Prowse et al. 2002; Timoney 2002; Remmer et al. 2020), although open-water season flooding has been recently identified as an important hydrological process in the Athabasca Delta (Neary et al. 2021). The ecologically important floods, however, also provide a key vector for transport of substances of concern derived from natural geological deposits and potentially anthropogenic activities.

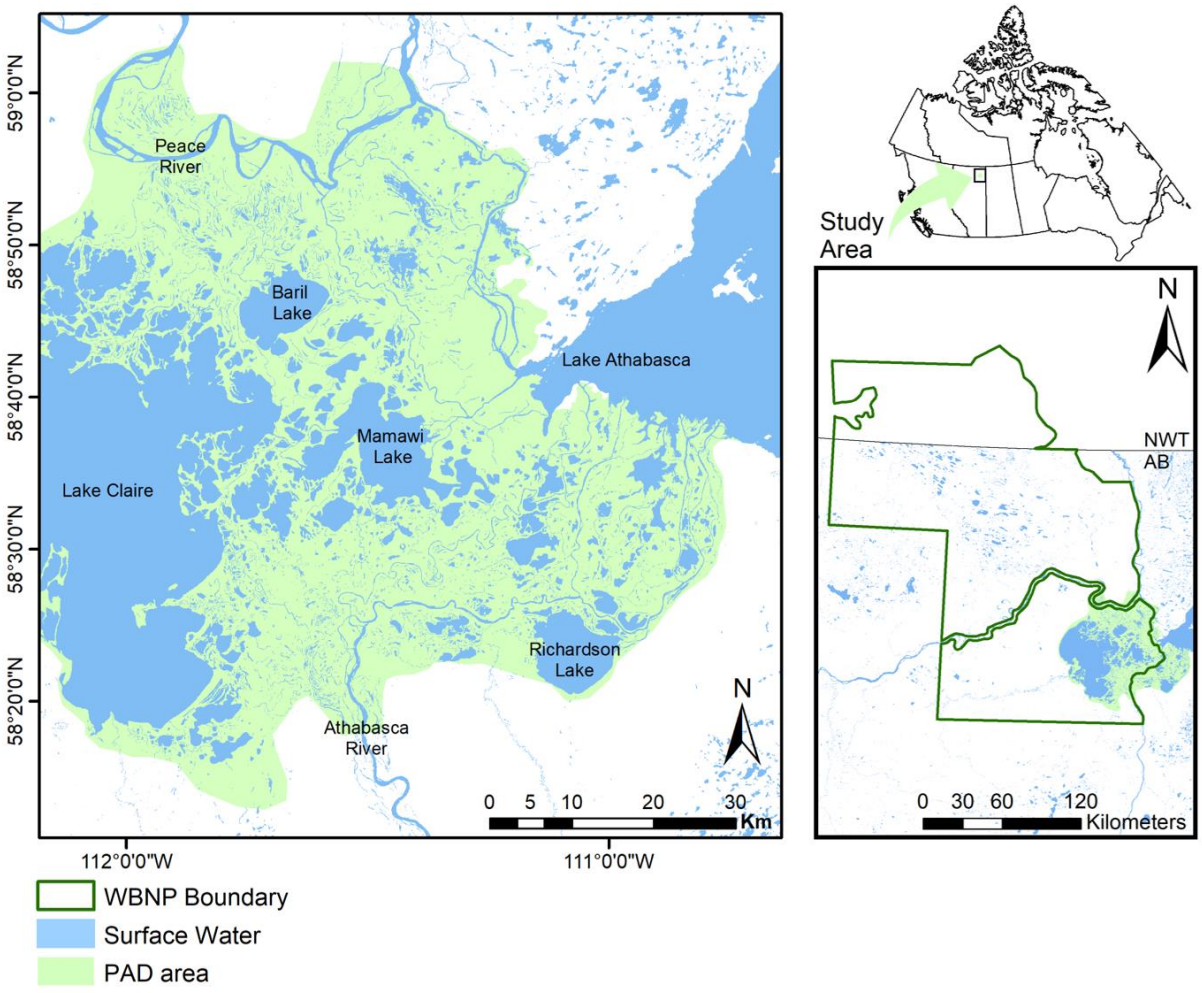

Figure 1.1 Map illustrating the location of the Peace-Athabasca Delta, Alberta, Canada. The area of the Peace-Athabasca Delta is shaded light green, and the boundary of Wood Buffalo National Park is delineated as the dark green outline in the bottom right panel. Source: Government of Canada (national park boundaries: https://open.canada.ca/data/en/dataset/9e1507cd-f25c-4c64-995b-6563bf9d65bd; water bodies: https://open.canada.ca/data/en/dataset/448ec403-6635-456b-8ced-d3ac24143add; PAD area: shapefile generated by Cory Savage.

Despite the efforts of multiple stakeholder groups to protect water quality and quantity of the PAD, concerns have persisted for decades about the potential effects of major energy projects and climate change on the delta's lakes and rivers (PADPG 1973). These concerns have intensified since the 2014 Petition by the Mikisew Cree First Nation to designate WBNP as 'World Heritage in Danger', due in large part to contention that the W.A.C. Bennett Dam, located 1100 km upstream, on the Peace River has reduced flooding and lowered lake levels, and oil sands development along the Lower Athabasca River has increased the supply of contaminants (MCFN 2014). In response to the petition by MCFN, UNESCO initiated a 'monitoring mission' during fall of 2017 and released a subsequent report with 17 recommendations (WHC/IUCN 2017). The World Heritage Committee has tasked the Government of Canada to develop an Action Plan. Among the actions, a key focus is to expand the scope of monitoring in the PAD to understand the effects of major energy projects on aquatic ecosystems (WBNP 2019). The research presented in this PhD thesis was not conducted in response to the UNESCO process but is timely because the collective studies address the effects of these and other stressors using long-term data available in lake sediment cores.

Research Approach

As described above and further identified below for specific research themes, inadequate knowledge of reference conditions commonly hampers the ability to track the drivers of environmental change. In the absence of pre-disturbance monitoring data, paleolimnological studies have long provided continuous sediment records capable of evaluating past changes in hydrological and limnological conditions (Douglas and Smol 1999, 2000; Lotter et al. 1999; Michelutti et al. 2007; Sokal et al. 2008; Brock et al. 2010; Ruhland et al. 2013), and contaminant deposition (Hall et al. 2012; Wiklund et al. 2012, 2014; Kurek et al. 2013; Jautzy et al. 2015;

MacDonald et al. 2016; Thienpont et al. 2016; Cooke et al. 2017; Cheney et al. 2020; Pelletier et al. 2020) in northern freshwater landscapes. Floodplain lakes have been underutilized due to their complex and dynamic sedimentary environment, which may complicate reconstructions of environmental conditions (Rosen 2015). As has been demonstrated repeatedly, paleolimnological research in the PAD during the past 20 years has shown that floodplain lake records provide sensitive and coherent archives of environmental data (reviewed in Wolfe et al. 2012). Studies have focused extensively on addressing questions and concerns about recent lake drying and the role of the W.A.C. Bennett Dam, and more recently to assess for evidence of pollution (e.g., Wolfe et al. 2006, 2008a; Hall et al. 2012; Wiklund et al. 2012, 2014). Indeed, application of both paleohydrological and contaminant approaches are complementary to discern pathways of contaminant deposition (MacDonald et al. 2016; Klemt et al. 2020). Building on these prior studies, the overarching theme of this thesis is to use conventional and novel paleolimnological approaches to reconstruct contaminant deposition and hydrological change from floodplain lakes to improve understanding of the degree to which the lakes in the PAD have been degraded by multiple stressors. The thesis consists of five data chapters, which contribute to two research directions. The first research direction is to assess temporal change in metal(loid) deposition (Chapters 2-4). In the second research direction, I evaluate causes of past hydrological change and develop a novel approach for reconstructing temporal variation in sediment sources at the PAD (Chapters 5, 6). Please note the Chapters are not organized by chronological order of publication, rather they are presented in the sequence of the two research directions to aid in the flow of the Thesis.

Assessment of metal(loid) deposition via fluvial and atmospheric pathways at lakes in the Peace-Athabasca Delta

Industrial development of oil sands deposits in northern Alberta has grown rapidly during the past 60 years, which has stimulated societal concerns about the cumulative downstream environmental effects of mining and processing activities on the Lower Athabasca River watershed (Timoney & Lee 2009; Kelly et al. 2009, 2010; Schindler 2010; Kirk et al. 2014; MCFN 2014; Cooke et al. 2017). Systematic monitoring of the Athabasca River began three decades after onset of oil sands development. In the absence of knowledge of reference conditions (i.e., pre-industrial or pre-disturbance), studies have used upstream versus downstream comparisons (Kelly et al. 2009, 2010; Donner et al. 2017, 2018), contemporary trend analyses (Timoney and Lee 2009) or integration of both (Alexander and Chambers 2017). However, interpretation of results from these approaches is confounded by natural erosion of bitumen deposits along the riverbanks and seasonal variations in river discharge, which may drive changes in contaminant deposition independent of releases from industrial activities (Dowdeswell et al. 2010; Hall et al. 2012; Wiklund et al. 2014). Collectively, this has continued to impede an ability of monitoring programs to accurately detect temporal trends or identify sources of pollution in the Alberta Oil Sands Region (AOSR) and downstream locations including the PAD (Dowdeswell et al. 2010).

The inability to quantify the extent of pollution from mining and processing relative to reference conditions was identified as a critical knowledge gap in a report by the 2010 Oil Sands Advisory Panel to the Minister of the Environment, which stated “it is important to establish as rigorously as possible the background or baseline level of pollution, against which any future trends can be assessed” (Dowdeswell et al. 2010, p. 31). In the PAD, Wiklund et al. (2012, 2014) responded to this recommendation by employing lake sediment deposited before the onset of

industrial development to define baseline concentrations for substances of concern to evaluate if sediment deposition in lakes and rivers post-industrial development exceeded baseline concentrations. Wiklund et al. (2012) focused on evaluating deposition of metal(loids) via atmospheric pathways at one upland lake (i.e., outside the reach of floodwaters) within the PAD. Findings indicated no atmospheric enrichment of metal(loid)s associated with the start of oil sands development despite Kelly et al. (2010) speculating oil sands development has resulted in enhanced long-range (≥ 50 km) deposition of contaminants.

A subsequent study by Wiklund et al. (2014) used lake sediment from two floodplain lakes in the Athabasca Delta to provide baseline concentrations of metal(loid)s conveyed by the Athabasca River, which enabled river-bottom sediment monitoring data to be evaluated against a pre-industrial baseline. Results showed no enrichment of river-bottom sediments due to industrial activities on the Lower Athabasca River. Both studies provided critically missing baseline information to evaluate enrichment of contaminants via fluvial and atmospheric pathways but were limited to one upland lake and surface sediment collection from the Athabasca River and its distributaries within the delta. Due to the dynamic nature of rivers, river-bottom sediment often has an unknown time of deposition whereas lake sediment accretes vertically and is preserved in chronological sequences that can be radiometrically dated. Thus, there remained opportunity to use lake sediment records from multiple lakes within the Athabasca Delta to explore temporal trends of substances of concern to further probe contaminant deposition via the Athabasca River.

Chapter 2 of this thesis, entitled **"Evaluating temporal patterns of metal concentrations in floodplain lakes of the Athabasca Delta (Canada) relative to pre-industrial baselines"**, focused on the use of sediment records from eight lakes that strategically span a 67 river-km transect across the Athabasca Delta. Stratigraphic analyses were used to establish pre-

industrial baseline metal concentrations, assess post-industrial periods for enrichment due to oil sand mining and processing activities via fluvial pathways, and quantify temporal trends. This study focused on oil sands indicator metals (vanadium and nickel) and primary pollutants (beryllium, chromium, lead, and zinc) that Kelly et al. (2010) reported as elevated in snowpack near bitumen mining and in river water downstream. Results reveal no evidence of enrichment of metal concentrations since onset of oil sands mining and processing activities, and identify that natural processes continue to dominate metal deposition at floodplain lakes of the Athabasca Delta.

Chapter 2 has been published as: Kay, M.L., Wiklund, J.A., Remmer, C.R., Owca, T.J., Klemt, W.H., Neary, L.K. Brown, K., MacDonald, E., Thomson, K., Vucic, J.M., Wesenberg, K., Hall, R.I., and Wolfe, B.B. 2020. Evaluating temporal patterns of metals concentrations in floodplain lakes of the Athabasca Delta (Canada) relative to pre-industrial baselines. Science of the Total Environment, **20**: 135309. https://doi.org/10.1016/j.scitotenv.2019.135309

Concerns have continued to center on the extent to which aquatic ecosystems have been polluted by mercury (Hebert et al. 2013, 2019; IEC 2018), because it is a potent neurotoxin with the ability to bioaccumulate and biomagnify through food webs. In **Chapter 3**, entitled "**Assessment of mercury enrichment in lake sediment records from Alberta Oil Sands development via fluvial and atmospheric pathways"**, paleolimnological analysis of total mercury concentration ([THg]) was conducted at nine floodplain lakes within the AOSR and PAD and two upland lakes at the PAD region. Enrichment of [THg] was detected via atmospheric pathways at both upland lakes in the PAD region, but this occurred before onset of oil sands development and aligned with long-range anthropogenic emissions across the northern hemisphere recognized in many other lake sediment records (Drevnick et al. 2016). Similar to the findings of Chapter 2, results show no evidence of [THg] enrichment in floodplain lake sediment via fluvial pathways. Notably, the cumulative inventory of anthropogenic [THg] in the upland lakes is less

than at the Experimental Lakes Area of northwestern Ontario (Canada), widely regarded as a 'pristine' area.

Chapter 3 has been published as: Kay, M.L., Wiklund, J.A., Sun, X., Savage, C.A.M., Adams, J.K., MacDonald, L.A., Klemt, W.H., Brown, K.C., Hall, R.I., and Wolfe, B.B. 2022. Assessment of mercury enrichment in lake sediment records from Alberta Oil Sands development via fluvial and atmospheric pathways. Frontiers in Environmental Science, **10**: 949339 https://doi.org/10.3389/fenvs.2022.949339.

During the past decade, stratigraphic analyses of lake sediment cores have been employed in four key regions of northwestern Canada to determine pre-disturbance metal(loid) concentrations and quantify the degree of enrichment since mining began (AOSR: Cooke et al. 2017; Klemt et al. 2020; PAD: Wiklund et al. 2012; Kay et al. 2020 [*included here as Chapter 2*]; Slave River Delta (SRD): MacDonald et al. 2016; central Northwest Territories: Thienpont et al. 2016; Galloway et al. 2018; Schuh et al. 2018; Van Den Berghe et al. 2018; Cheney et al. 2020; Pelletier et al. 2020; Jasiak et al. 2021). **Chapter 4**, entitled "**Paleolimnological evaluation of metal(loid) enrichment from oil sands and gold mining operations in northwestern Canada",** synthesizes the current state of paleolimnological knowledge via systematic re-analysis of temporal variation in sediment metal(loid) concentrations from 51 lakes across these four key regions spanning 670 km from bitumen mining in the AOSR to gold mining (Giant and Con mines) at Yellowknife in central Northwest Territories. The compilation includes upland and floodplain lakes at varying distances from the mines to evaluate dispersal of pollution-indicator metal(loid)s from bitumen (vanadium and nickel) and gold mining (arsenic and antimony) via atmospheric and fluvial pathways. Results demonstrate 'severe' enrichment of vanadium and nickel at near-field sites within the AOSR and 'severe' (near-field) to 'considerable' (far-field) enrichment of arsenic and antimony due to gold mining at Yellowknife via atmospheric pathways but no evidence of enrichment of these four metal(loid)s via atmospheric or fluvial pathways at the PAD and SRD.

Findings from Chapter 2-4 can be used by decision makers to evaluate risks to ecosystems associated with contaminant dispersal by the large-scale mining activities across a broad region of northwestern Canada.

Chapter 4 is currently in review as: Kay, M.L., Jasiak, I., Klemt, W.H., Wiklund, J.A., Faber, J.A., MacDonald, L.A., Telford, J.V.K., Savage, C.A.M., Cooke, C.A., Wolfe, B.B., and Hall, R.I. Paleolimnological evaluation of metal(loid) enrichment from oil sands and gold mining operations in northwestern Canada.

Hydrological change at the Peace-Athabasca Delta

There has been a substantial amount of research to address hydrological change at the Peace-Athabasca Delta, which has concluded water levels have been declining but the major drivers of hydrological change remain contentious (PADPG 1973; PADTS 1996; Prowse and Conly 2002; Prowse et al. 2006; Wolfe et al. 2005, 2006, 2008a, 2011, 2012, 2020; Beltaos 2014, 2018). Initial concerns over the potential link between river regulation and reduced frequency and influence of flood events on lake water balances at the PAD dates to the period of infilling of the Williston reservoir from 1968-1971 (PADPG 1973). Coincident sharp declines in Peace River flows and water levels on Lake Athabasca stimulated the Canadian, Alberta and Saskatchewan governments to launch the Peace-Athabasca Delta Project Group (PADPG), the first major coordinated set of environmental studies of the PAD, to assess the role of regulation of the Peace River on the PAD. The main conclusion delivered by the PADPG was that the W.A.C. Bennett Dam had caused major, unprecedented changes to the delta (PADPG 1973). The Peace-Athabasca Technical Studies (PADTS) and Northern River Basins Study (NRBS) followed with the goals of understanding the options and strategies for restoring water in the delta, as well as determining the combined effects of multiple developments on the hydrology of the Peace, Athabasca and Slave river basins to ensure long-term protection and management (PADTS 1996; Prowse et al. 2006).

These studies provided understanding of hydrological processes but relied heavily on hydrometric data of limited spatial coverage and temporal extent.

Paleolimnological studies initiated in the early 2000s have provided a long-term perspective of changes in hydrological processes that influence water balance of lakes across the PAD (reviewed in Wolfe et al. 2012). Key findings from a decade of research included that the decline in flood frequency and perched basin drawdown began several decades before hydroelectric regulation of the Peace River, and that climate plays an influential role in hydrological variations within the delta (e.g., Wolfe et al. 2005, 2006, 2008a). The northern Peace Delta has been the focal point of paleolimnological studies, but concerns about declines in lake water-level and reduced river discharge have also occurred in the southern Athabasca Delta (Schindler and Donahue 2006; MCFN 2014; Sauchyn et al. 2015). Paleolimnological investigation of three perched basins across the Athabasca Delta revealed changes in the flow path of the Athabasca River and its distributaries are the primary cause of recent hydroecological changes (Wolfe et al. 2008b). The changes include an engineered straightening of the Athabasca River in 1972 (Athabasca River Cutoff) and a natural avulsion in 1982 know as the Embarras Breakthrough (Timoney 2013; Wolfe et al. 2008b). The Embarras Breakthrough redirected river flow from the Athabasca and Embarras rivers northward to the Mamawi and Cree creeks corridor and away from regions east and northeast of the Embarras Breakthrough including the Athabasca River terminus region. One of the lakes from the paleolimnological investigation along the Mamawi and Cree creek corridor received more frequent flooding while flooding declined at one lake east of the Embarras Breakthrough, which aligned well with distribution of floodwaters in spring of 2003. Thus, it was speculated by Wolfe et al. (2008b) that the Embarras Breakthrough was a major driver of hydrological change across the Athabasca Delta.

In **Chapter 5**, entitled **"Bi-directional hydrological changes in perched basins of the Athabasca Delta (Canada) in recent decades caused by natural processes"**, a hypothesis was tested that the Embarras Breakthrough is the cause of drying of perched basins at the terminus of the Athabasca River. This portion of the Athabasca Delta was not included in the Wolfe et al. (2008b) study but is a key area of concern because of its importance to the ACFN. Loss-on-ignition analysis was performed on sediment cores from nine lakes to reconstruct past changes in flood influence. Results show bi-directional hydrological change since the early 1980s, characterized by reduced flooding east of the Embarras Breakthrough and increased flooding northward along the Mamawi and Cree creek corridor. Findings substantiate that the most profound hydrological change in the Athabasca Delta during the past ~120 years was due to the Embarras Breakthrough, which underscores the need to factor natural deltaic process into stewardship decisions.

Chapter 5 has been published as: Kay, M.L., Wiklund, J.A., Remmer, C.R., Neary, L.K., Brown, K., Ghosh, A., MacDonald. E., Thomson, K., Vucic, J.M., Wesenberg, K., Hall, R.I., and Wolfe, B.B. 2019. Bi-directional hydrological changes in perched basins of the Athabasca Delta (Canada) in recent decades caused by natural processes. Environmental Research Communications **1:** 081001. https://doi.org/10.1088/2515-7620/ab37e7

As discussed above and demonstrated in Chapter 5, paleolimnological studies using conventional methods have provided valuable temporal perspectives about past hydroecological changes in the PAD. However, integration of paleolimnological records from multiple lakes across the PAD has been underdeveloped because different approaches are applied based on the sediment composition. At flood-prone lakes with mineral-rich sediment, physical methods (e.g., grain size and magnetic susceptibility) are often employed while at upland lakes with organic-rich sediment, biological (e.g., diatoms) and geochemical (e.g., carbon and nitrogen elemental and isotope composition, cellulose oxygen isotope composition) methods are widely used. In **Chapter 6**, entitled **"A Bayesian mixing model framework for quantifying temporal variation in source**

of sediment to lakes across broad hydrological gradients of floodplains", sediment elemental concentrations were used to distinguish the three main allochthonous sources of sediment to lakes at the PAD: Athabasca River, Peace River, and local catchment. The distinct differences permitted development of a mixing model with the capability to discern the relative contributions of sediment from the three sources. The mixing model was developed and tested via application to sediment cores from two adjacent lakes at the Athabasca Delta, which demonstrated its effectiveness to discriminate three previously described hydrological phases during the past 300 years. Notably, model results indicated that ~60% of the sediment originated from the Peace River during the largest ice-jam flood event on record (1974), which was unrecognized by other methods. This new, universal method can be applied to sediment cores obtained from a network of lakes to elucidate spatio-temporal variation in sediment sources across the PAD (i.e., novel 'paleohydroscapes'; as presented in **Chapter 7**).

Chapter 6 has been published as: Kay, M.L., H.K. Swanson, J. Burbank, T.J. Owca, C.A.M. Savage, C.R. Remmer, L.K. Neary, J.A. Wiklund, B.B. Wolfe, R.I. Hall. 2021. A Bayesian mixing model framework for quantifying temporal variation in source of sediment to lakes across broad hydrological gradients of floodplains. Limnology and Oceanography Methods **19:** 540-551. https://doi.org/10.1002/lom3.10443

Chapter 2: Evaluating temporal patterns of metals concentrations in floodplain lakes of the Athabasca Delta (Canada) relative to pre-industrial baselines

Citation: Kay, M.L., Wiklund, J.A., Remmer, C.R., Owca, T.J., Klemt, W.H., Neary, L.K. Brown, K., MacDonald, E., Thomson, K., Vucic, J.M., Wesenberg, K., Hall, R.I., and Wolfe, B.B. 2020. Evaluating temporal patterns of metals concentrations in floodplain lakes of the Athabasca Delta (Canada) relative to pre-industrial baselines. Science of the Total Environment, 20: 135309. https://doi.org/10.1016/j.scitotenv.2019.135309

Introduction

Monitoring of river sediment quality is used widely to assess the extent of contamination from industrial activities and protect downstream ecosystems (Reuther 2009). Knowledge of pre-industrial baseline concentrations is essential to these efforts, but often lacking because monitoring is typically initiated after onset of industrial activity (Lindenmayer et al. 2008; Finlayson et al. 2016). This situation has fostered growing concern about contamination of the Athabasca River and downstream Peace-Athabasca Delta (PAD) by the Alberta oil sands mining and processing activities where river sediment quality monitoring began thirty years after industrial development began (Dowdeswell et al. 2010; Schindler 2010; Dillon et al. 2011; Cronmiller and Noble 2018). In the absence of pre-industrial data, comparison of upstream versus downstream concentrations of substances of concern is often used, but the Athabasca River flows through naturally-occurring bitumen deposits, which hinders effectiveness of such spatial approaches (Conly et al. 2007; Hall et al. 2012; Wiklund et al. 2014). Evaluating Athabasca River sediment quality monitoring data for evidence of industrial contamination is also confounded by coincident decline of river discharge during industrial development (Schindler and Donahue 2006; Sauchyn et al. 2015) and seasonal variations in river discharge and associated mobilization of contaminants (Hall et al. 2012).

Ability to evaluate contaminant deposition has become an urgent issue at the southern portion of the PAD, located at the terminus of the Athabasca River. Eighty percent of the PAD is

protected within Wood Buffalo National Park (WBNP) and the remaining 20% falls mainly within traditional territory of the Athabasca Chipewyan First Nation. WBNP is one of 20 UNESCO World Heritage Sites in Canada, in large part owing to exceptional environmental characteristics and cultural values of the PAD. Here, perceived threat of pollution from rapid growth of the oil sands development along the lower Athabasca River, among other concerns, prompted a petition to add WBNP to the list of 'World Heritage in Danger' (MCFN 2014), which would be the first such designation for Canada. UNESCO is in the process of making a decision on the World Heritage status of WBNP and evaluating Canada's response to UNESCO's recommendations (WHC/IUCN 2017) contained in the Wood Buffalo National Park World Heritage Site Action Plan (WBNP 2019).

As recommended by the Federal Expert Oil Sands Advisory Panel (Dowdeswell et al., 2010), a novel method using pre-industrial (~1700 to 1920) sediment from two floodplain lakes in the Athabasca Delta was developed by Wiklund et al. (2014) to define baseline metals concentrations conveyed by the Athabasca River. This approach characterized natural variation in metals concentrations and was used to evaluate river sediment quality monitoring data obtained by the Regional Aquatics Monitoring Program (RAMP). Results demonstrated no enrichment above pre-industrial levels (Wiklund et al. 2014). However, the RAMP data stemmed from surficial river-bottom sediment samples of unknown time of deposition, which has long hampered time-series assessment of RAMP river sediment quality data (Hall et al. 2012; Wiklund et al. 2014). In contrast, floodplain lakes in the Athabasca Delta provide a natural archive for sediment and metals deposition from the Athabasca River that is preserved in a chronological sequence and can be radiometrically dated.

Here we employ the framework developed by Wiklund et al. (2014), expand the number of lakes from two to eight from across the Athabasca Delta, and undertake contiguous stratigraphic analyses to 1) establish pre-industrial baseline metals concentrations, 2) assess post-industrial intervals for evidence of contamination, and 3) quantify enrichment of metals concentrations and evaluate temporal trends since ~1850.

Methods

We collected sediment cores from eight floodplain lakes that span a 67 river-km transect across the southern portion of the PAD (i.e., Athabasca Delta; Figure 2.1). Their stratigraphic records have been ^{210}Pb-dated and used for paleohydrologic reconstruction (Kay et al. 2019 [*included here as Chapter 5*]). Further details regarding study area, core processing and core dating, including estimates of age uncertainty, are presented in Kay et al. (2019). Continuous 1-cm intervals from each of the eight sediment cores were freeze-dried and analyzed for a suite of metals at ALS Canada (Waterloo) following EPA method: 202.2/6020A (aqua-regia hot block digestion followed by analysis by ICP-MSP). In this study, we focus on vanadium (V) and five primary pollutants (beryllium (Be), chromium (Cr), lead (Pb), nickel (Ni), zinc (Zn)). We assessed these metals because Kelly et al. (2010) reported elevated concentrations in the snowpack near the oil sands development and in river water downstream. Bitumen in the McMurray Formation contains high concentrations of V relative to other geological formations (Gosselin et al. 2010) and can be toxic to living organisms (Jacobs and Filby 1982; Irwin et al. 1997).

Wiklund et al. (2014), and many other sediment-based assessments of metals concentrations, have recognized the need for geochemical normalization to account for influence of variation in grain size, as occurs in environments subject to fluctuations in energy conditions (Forstner and Müller 1981; Loring 1991; Covelli and Fontolan 1997; Kersten and Smedes 2002).

Higher energy conditions are associated with coarser grain size and lower sediment metals concentrations. Previous studies in this region used concentrations of lithium (Li) or aluminum (Al) as a geochemical normalizer (Wiklund et al. 2014; MacDonald et al. 2016; Cooke et al. 2017).

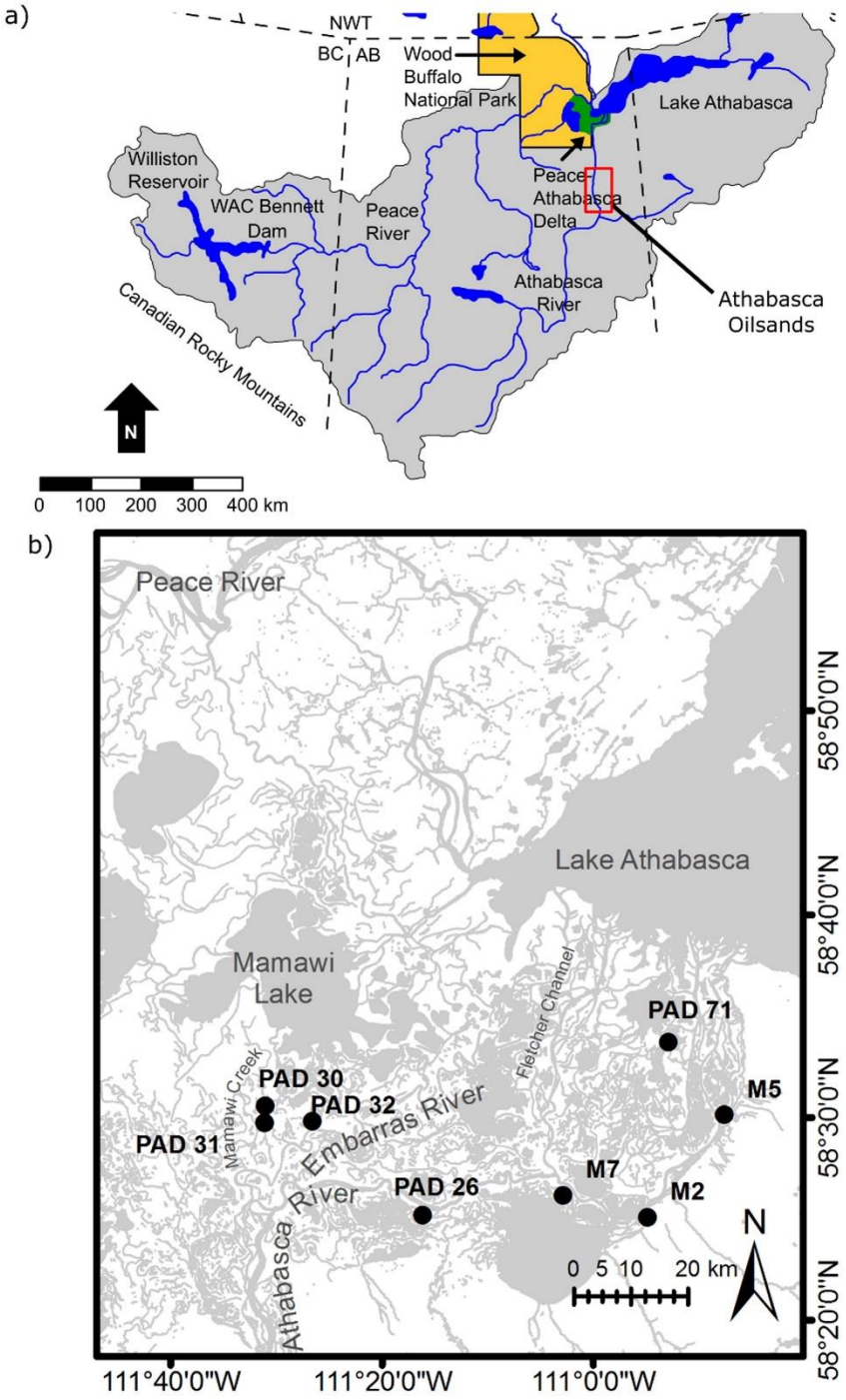

Figure 2.1 a) The Peace-Athabasca Delta, located in northeastern Alberta (Canada), is shown as the central green region at the western end of Lake Athabasca. The red rectangle denotes the approximate area of oil sands operations. b) Sediment core locations are labeled PAD 30, PAD 31, PAD 32, PAD 26, M7, M2, M5 and PAD 71.

Here, we used the small-sample-corrected Akaike's Information Criterion (AICc) (Akaike 1973; Mazerolle 2017) to identify that Al was generally superior to Li (Appendix A Table A1). Furthermore, the six metals presented in this study all have strong positive linear relations with Al and met all requirements for geochemical normalization (Loring 1991).

To generate pre-industrial sediment metals baselines across the 67 river-km transect, we developed linear relations between Al concentrations and each metal of interest using sediment deposited into all the eight lakes before 1920 (n = 128 samples). We established one baseline per metal to encompass the broad range of hydrological conditions that occurred over time and space in the Athabasca Delta. We constructed 95% prediction intervals (PI) about the regression line to characterize the range of natural variability of individual sediment samples. Thus, if >2.5% of post-1920 samples plot above the 95% PI, they were considered enriched due to industrial activities. We assessed each of the eight lake sediment core records for evidence of contamination during two post-industrial time intervals: 1967-present and 1920–1967. The post-1967 interval encompasses the period since onset of oil sands development, whereas the interval 1920–1967 evaluates industrial activities prior to oil sands development.

Time-series of the metals concentrations were expressed as enrichment factors (EF), an effective metric used to quantify the extent of contamination above pre-industrial baselines, and followed the formula used by others in this region (Wiklund et al. 2012; Kurek et al. 2013; Cooke et al. 2017):

$$EF = (X/Al)_i/(X/Al)_{pre\text{-}1920}$$

where X_i and Al_i are the measured concentrations of the metal of interest and Al for a specific sediment interval (i). $X_{pre\text{-}1920}$ and $Al_{pre\text{-}1920}$ are the expected values for the metal of interest and Al in sediments deposited before 1920, derived from the equation of the regression line for the metal-Al relation where $Al_{pre\text{-}1920} = Al_i$. An EF of 1.0 indicates normalized concentrations equivalent to the pre-industrial baseline, whereas an EF of 2.0 indicates a doubling of the metal of interest above baseline. We consider an EF value of <1.5 to represent normal variability of pristine conditions and EFs of 1.5–3.0 to represent minimal modifications, following previous uses (Abrahim and Parker, 2008; Birch, 2017). A generalized additive model (GAM) was used to estimate the temporal trend in EF values synthesized across all eight lakes in the Athabasca Delta for each metal. GAMs are a preferred approach for evaluating paleoenvironmental time-series data (Simpson 2018) and were performed using the mgcv package (version 1.8.28; Wood 2017) in R (version 3.5.2; R Core Team 2019).

Results and Interpretation

Similar to Wiklund et al. (2014), we first focus on V, a metal commonly associated with oil and oil-related pollution (Khalaf et al. 1982; Juichang et al. 1995), including the Alberta oil sands (Baker et al. 2012). Lake sediment from the eight lakes was assessed for evidence of V enrichment in two distinct time periods relative to the pre-1920 baseline (Figure 2.2). The 95% PI for the pre-1920 baseline spans a narrow range, and thus is a sensitive threshold to detect V enrichment due to anthropogenic influences. Collectively, the samples from the eight study lakes span a range of V and Al concentrations that are characteristic of their hydrological setting (Kay et al. 2019). For example, strongly flood-prone PAD 71 has relatively low concentrations of metals consistent with high mineral content and rapid sedimentation rate, and M2 spans a narrow range of V and Al concentrations because the lake has been consistently flood-prone. In contrast, PAD

30 and 31 span the broadest range of metals concentrations because these lakes have experienced prolonged intervals of high and low flood frequency (Kay et al. 2019). Despite the varying paleohydrologic conditions among these lakes, all post-1920 V-Al sediment samples (n = 188) plot below the upper 95% PI and cluster tightly about the regression line. This indicates the source of V has not changed relative to the pre-1920 baseline, including since onset of oil sands development. Similar patterns in Al-normalized metals concentrations occur for the other five primary pollutants (Appendix A Figures A1–A5). An exception is Zn in the core from PAD 30, where 61% of post-1920 samples plot above the upper 95% PI (Figure A5).

Enrichment of V and the five primary pollutants were expressed using EFs and temporal patterns were assessed using GAMs (Figure 2.3). The GAM-estimated trends for all metals (except zinc) remain stable around an EF of 1.0 during the past ~165 years, indicating no enrichment above baseline. The narrow range of the 95% confidence interval of the trend line provides high certainty in this outcome. Beryllium, Cr and V have a very narrow range of EFs (0.78–1.20). The sample with the highest V EF (1.08) was deposited in the early 1960s before oil sands development. The range of EF is greater for Pb, Ni and Zn (0.64–1.71). The highest enrichment factor occurred for Zn (1.71) in a sample deposited ~1977, a peak value following a rising trend that began in the late 1930s in one lake (PAD 30).

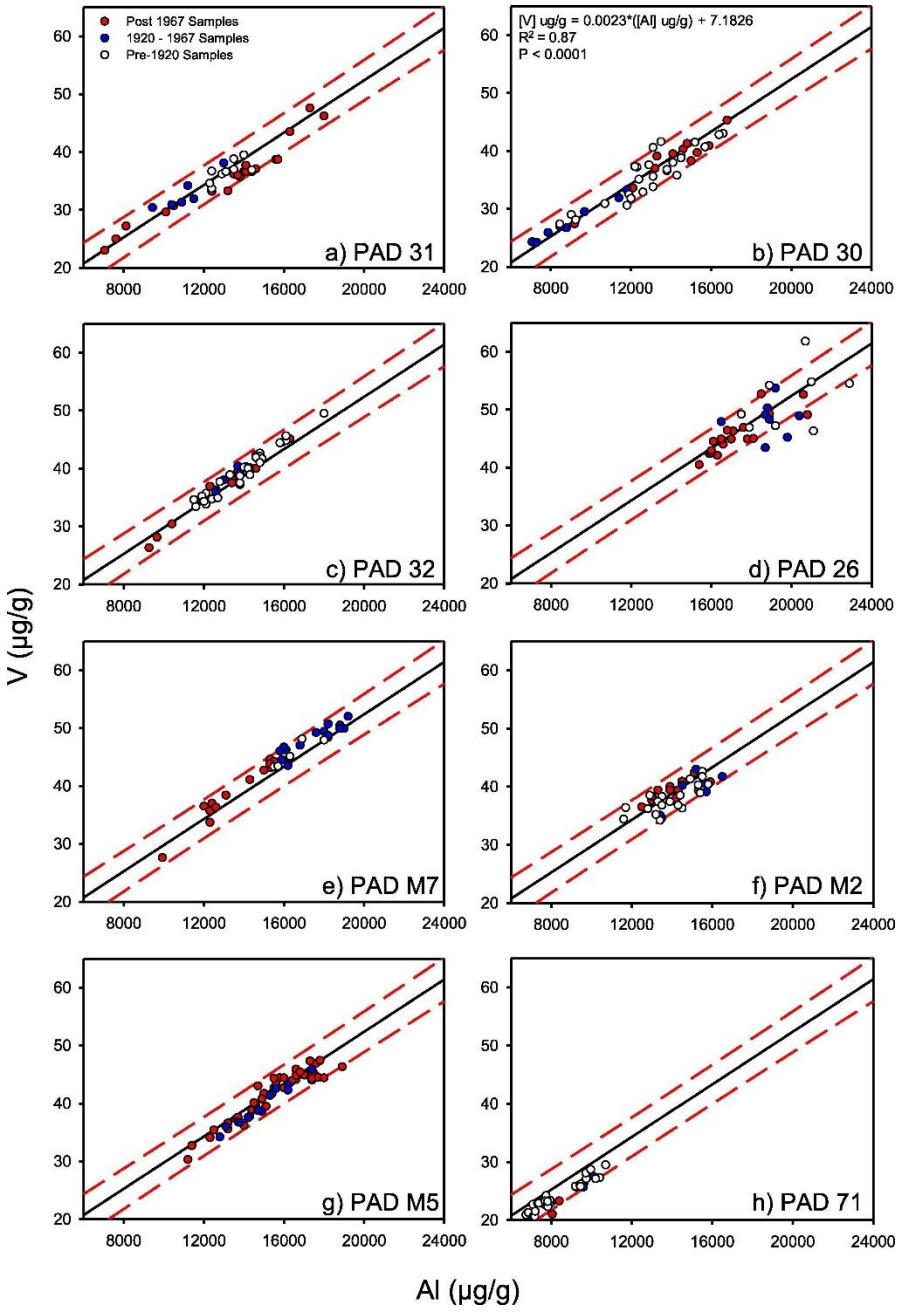

Figure 2.2 The linear relations between sediment concentrations of vanadium and aluminum in pre-1920 floodplain lake sediment (black line) and 95% prediction intervals (red dashed line denoting range of natural variability). Sediment samples are distinguished by time intervals (pre-1920 [open circles; pre-industrial baseline], 1920–1967 [blue circles; pre-oil sands industrial era], and post-1967 [red circles; post-oil sands development era]). Positive collinearity between V and Al is a function of grain size (Loring, 1991; Kersten and Smedes, 2002). Coarse-grained sediment (i.e., sand) deposited during high energy conditions has low extractable metal content, whereas fine-grained sediment (i.e., clay) deposited during low energy conditions has high extractable metal content.

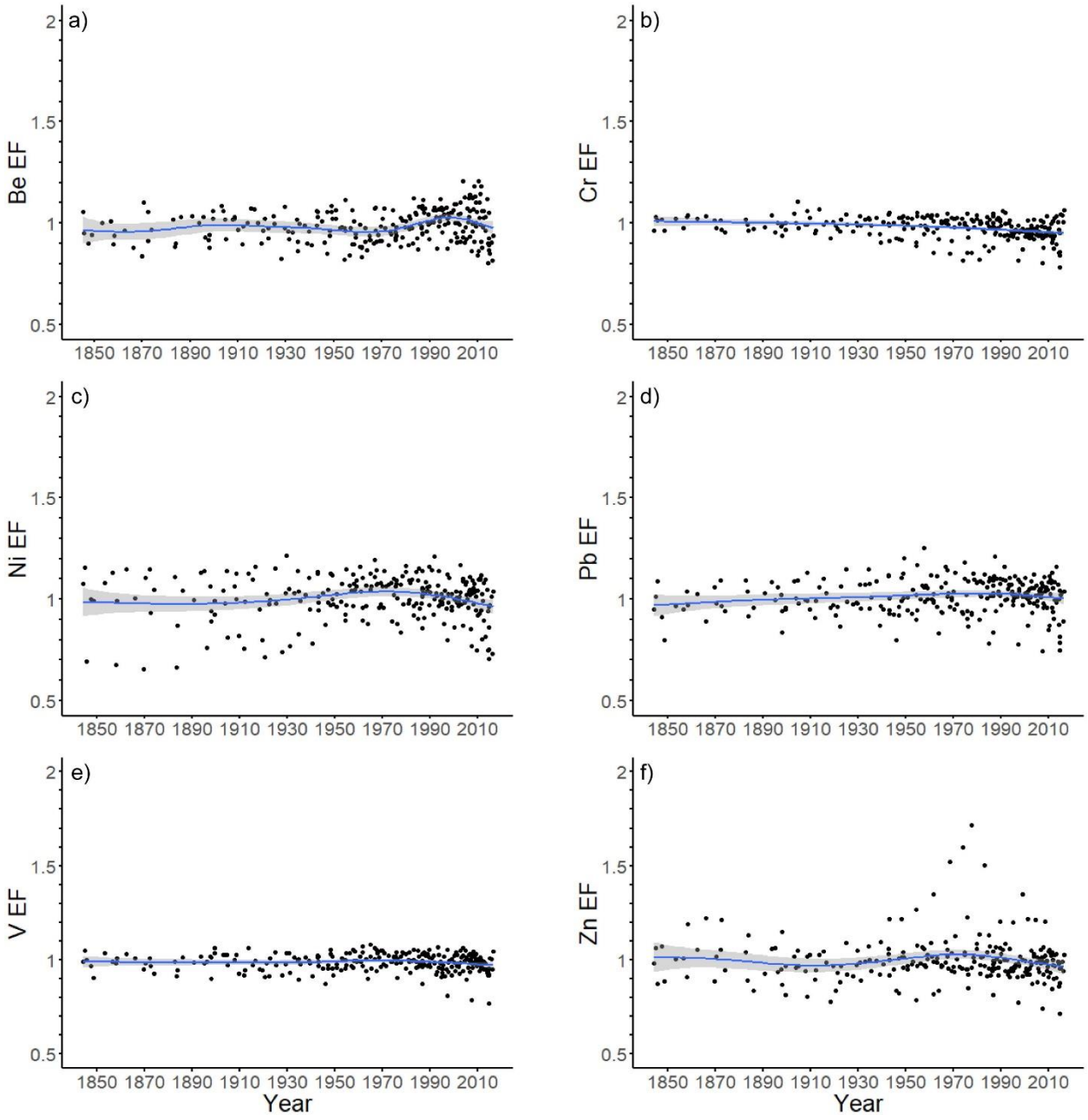

Figure 2.3 GAM-based trends (blue line) fitted to a time series of enrichment factors (EF) relative to the pre-1920 lake sediment baseline for a) Be, b) Cr, c) Ni, d) Pb, e) V and f) Zn for all samples from eight lakes along a 67 river-km transect spanning the Athabasca Delta. The light grey-shaded bands surrounding the GAM-based estimated trends are 95% confidence intervals for the blue trend line.

Discussion and Conclusions

Deciphering the relative roles of natural and anthropogenic influences on Athabasca River sediment quality is crucial for environmental stewardship and requires well-defined pre-industrial baseline conditions – a challenging scientific pursuit given the delay in monitoring activities until decades after initiation of oil sands development (Dowdeswell et al. 2010; Schindler 2010). A perception that oil sands operations are polluting downstream environments stems from studies that, in our opinion, have been challenged to capture sufficient spatial or temporal scales to characterize the natural range of variation of metals concentrations. Here, we used sediment cores as archives of metals concentrations to provide pre-1920 baselines for the Athabasca Delta, which has long been a natural repository for substances of concern carried by sediments in the Athabasca River (Evans et al. 2002; Hall et al. 2012; Wiklund et al. 2014; Evans et al. 2016). For centuries, floodplain lakes at the terminus of the Athabasca River have served as 'passive sampler' monitors of sediment carried by the Athabasca River.

GAM-based trend analysis of sediment cores from eight floodplain lakes spanning a 67 river-km transect across the Athabasca Delta shows no evidence of increasing metals enrichment above pre-1920 baseline concentrations, including since the onset of oil sands development in 1967 (Figure 2.3). Zinc enrichment occurred in one lake (PAD 30) as a discernable rise beginning in the 1930s and decline after ~1977, an interval that is mostly before oil sands development when this lake was less frequently receiving river floodwaters (Kay et al. 2019). A nearby lake (PAD 31) with the same paleohydrologic history does not record Zn enrichment at this time. We suspect that localized, within-lake and direct catchment processes are responsible for this pattern. Our main finding contributes to a growing body of paleolimnological evidence that does not support the perception of oil sands pollution in the PAD via fluvial or atmospheric pathways (Wiklund et

al. 2012; Hall et al. 2012; Wiklund et al. 2014; Owca et al. 2020). Collectively, these studies have extensively probed lake and river sediments in the delta using multiple datasets (including metals and organic compounds) over space and time. We suggest that caution should be exercised in the interpretation of contaminants in biota or other media when no data on reference (i.e., pre-oil sands development) conditions are available.

Federal agencies have been tasked with the challenge to develop long-term monitoring programs in the PAD capable of detecting cumulative effects of multiple stressors, including contaminants from oil sands mining and processing (WBNP 2019). We suggest the pre-1920 sediment metals baselines developed here provide a robust tool to evaluate future surface sediment collection from floodplain lakes in ongoing monitoring efforts, as demonstrated by Owca et al. (2020). Indeed, the records of metal deposition from our eight study lakes, as well as their paleohydrologic reconstructions (Kay et al. 2019), provide a wealth of knowledge spanning several decades to support water quality and quantity monitoring efforts by stakeholder agencies, and should be used to inform decision-making regarding actions to maintain the World Heritage status of WBNP (WBNP 2019).

Chapter 3: Assessment of mercury enrichment in lake sediment records from Alberta Oil Sands Development via fluvial and atmospheric pathways

Citation: Kay, M.L., Wiklund, J.A., Sun, X., Savage, C.A.M., Adams, J.K., MacDonald, L.A., Klemt, W.H., Brown, K.C., Hall, R.I., and Wolfe, B.B. 2022. Assessment of mercury enrichment in lake sediment records from Alberta Oil Sands development via fluvial and atmospheric pathways. Frontiers in Environmental Science, **10**: 949339. https://doi.org/10.3389/fenvs.2022.949339.

Introduction

Oil production from bitumen mining within the Alberta Oil Sands Region (AOSR) has been an important source of economic development and energy security for Canada but it also has garnered societal concern regarding its environmental impacts. These include, but are not limited to, extensive changes to land cover, carbon releases, consumptive water use, and dispersal of contaminants (Gosselin et al. 2010; Rooney et al. 2012; Arcszewski 2021; Roberts et al. 2021). Distress over consequences of contaminant emissions for ecosystems and humans has existed for decades at locations proximal to the industry within the Lower Athabasca River watershed and at the Peace-Athabasca Delta (PAD), a Ramsar Wetland of International Importance located ~200 km downstream within Wood Buffalo National Park, a UNESCO World Heritage Site (Dowdeswell et al. 2010; Gosselin et al. 2010; Schindler 2010; MCFN 2014; WHC/IUCN 2017, 2021; IEC 2018; WBNP 2019). Yet, evaluation of contaminant dispersal requires understanding of natural, pre-disturbance concentrations to decipher the roles of anthropogenic and natural processes.

During the past decade, paleolimnological studies spanning from the AOSR to the PAD have provided critical knowledge of baseline, reference concentrations of contaminants and changes in contaminant deposition in aquatic ecosystems since onset of industrial development (Wiklund et al. 2012; Hall et al. 2012; Kurek et al. 2013; Wiklund et al. 2014; Cooke et al. 2017; Kay et al. 2020 [*included here as Chapter 2*], in review [*included here as Chapter 4*]; Klemt et al.

2020). For example, analyses of sediment cores from lakes within the AOSR have demonstrated 2.5- to 23-fold increases in flux of total PACs (polycyclic aromatic compounds) above pre-industrial levels via atmospheric pathways, with marked increases in C1-C4 alkylated PAHs (polycyclic aromatic hydrocarbons) and dibenzothiophenes which are abundant in the mined bitumen ore (Kurek et al. 2013). At the most enriched site analyzed by Kurek et al. (2013), total PAC concentrations exceeded Canadian interim sediment quality guidelines after the mid-1980s. Concentrations and flux rates of several trace elements (metals, metalloids) have also been shown to increase in lake sediments since onset of oil sands development at near- and mid-field locations within the AOSR via atmospheric pathways (Cooke et al. 2017; Klemt et al. 2020).

To date, paleolimnological studies of trace element deposition within the AOSR have focused primarily on vanadium (V) and nickel (Ni) because they serve as key indicator metals of emissions from oil sands development due to their high concentrations in the McMurray Formation bitumen relative to other geological sources and in wastes released from the mining operations (Gosselin et al. 2010; Shotyk et al. 2021). Paleolimnological analyses at upland lakes and floodplain lakes have demonstrated enrichment of V and Ni within 50 km of oil sands operations via atmospheric pathways but no enrichment of V, Ni or other trace elements (e.g., Be, Cr, Pb, Zn) via fluvial pathways within the AOSR and farther downstream at the PAD (Cooke et al. 2017; Kay et al. 2020; Klemt et al. 2020; Owca et al. 2020; see synthesis by Kay et al. in review). Pre-industrial lake sediments have also been used to evaluate sediment quality monitoring data from the Athabasca River in the AOSR and PAD, which has demonstrated no enrichment of several trace elements due to industrial activities or other causes (Wiklund et al. 2014; Owca et al. 2020; Klemt et al. 2021).

Mercury deposition has been a focus of high concern within and downstream of the AOSR due to emissions from bitumen upgrading facilities, vehicle operations, deforestation, coke piles and dust from open pit mines (Dowdeswell et al. 2010; Kirk et al. 2014). Elevated supply of Hg can pose negative consequences for aquatic and terrestrial ecosystems because Hg can be converted to methylmercury, a toxic organic form that may bioaccumulate and biomagnify through food webs and pose risks to higher trophic levels including human consumers (Gilmour et al. 1992; Ullrich et al. 2001; Driscoll et al. 2013). As reported by Hebert et al. (2013), data from Canada's National Pollutant Release Inventory indicate that total annual Hg emissions from oil sands operations within the AOSR almost tripled between 2000 and 2010. Also, measurements of total Hg concentration ([THg]) in snowpack within the AOSR have demonstrated net loading is highest between the Steepbank and Muskeg rivers, closest to the bitumen upgraders, and declines rapidly in a bullseye pattern with increasing distance from AR6, a central location within the AOSR (Kirk et al. 2014*).* Consistent with these findings, river water [THg] in the AOSR are positively correlated with discharge and have been shown to be higher downstream of mining operations compared to upstream locations (Wasiuta et al. 2019). Such knowledge of the spatial distribution of [THg] has led to fish consumption advisories in the Athabasca River but monitoring of [THg] has not revealed clear temporal trends that would implicate oil sands development as a key source of THg to fish (Evans and Talbot 2012; Kirk et al. 2014). Studies have also identified higher [THg] in aquatic bird eggs at sites downstream of the AOSR located within the PAD and western end of Lake Athabasca than at nearby locations along the Peace River and other locations in western Canada, and that [THg] in eggs at the PAD and Lake Athabasca were higher following years of high discharge of the Athabasca River (Hebert et al. 2013, 2019; Dolgova et al. 2018). These studies identify the Athabasca River is an important vector for Hg transport within the Lower

Athabasca River watershed, which has raised concern for toxicant exposure to wildlife and accumulation in the environment (MCFN 2014; IEC 2018). However, it remains uncertain if releases from oil sands development exert strong control on [THg] in waterbird eggs because measurements were not made until several decades after onset of oil sands development and the paucity of biological monitoring data continues to hamper ability to adequately understand complex interactions among physical and ecological pathways that regulate Hg bioavailability to aquatic biota (Dolgova et al. 2018; Hebert et al. 2019). Importantly, these studies highlight the need for baseline, reference data to accurately discern 1) the roles of natural processes versus industrial activities on THg loading within the AOSR and at the PAD, and 2) loading of anthropogenic THg from localized point sources within the AOSR by oil sands industrial activities versus from diffuse anthropogenic sources outside of the AOSR.

Despite the above concerns and important knowledge gaps about releases of Hg from oil sands development to the Lower Athabasca River watershed, few paleolimnological studies have yet been conducted to establish pre-industrial baselines and assess for temporal patterns of change in Hg deposition via atmospheric and fluvial pathways. To our knowledge, only three studies report temporal analyses of [THg] in lake sediment cores within the Lower Athabasca River watershed (Bourbonniere and Telford 1996; Wiklund et al. 2012; Cooke et al. 2017) and other environmental archives such as peat cores have not been examined for temporal trends in Hg deposition. Bourbonniere and Telford (1996) examined [THg] in a sediment core from the center of Lake Athabasca and demonstrated no enrichment of [THg]. However, this site is distant from the mouth of the Athabasca River and is influenced by numerous input sources beyond the Athabasca River, thus it is unlikely to provide an informative record of temporal variation for [THg] of sediment conveyed by the Athabasca River. Cooke et al. (2017) reports THg deposition

profiles from 20 upland lakes within the AOSR, whereas Wiklund et al. (2012) reports stratigraphic variation in THg deposition from a single upland lake within the PAD. Lakes reported in both these studies receive input of contaminants exclusively via atmospheric pathways (i.e., not via fluvial pathways), yet none of their sediment records have demonstrated evidence of enrichment of [THg] that can be attributed to oil sands development. At the AOSR, the records identify that enrichment of [THg] began in the early to mid-1900s, long before oil sands development, and far-field sites show greater enrichment than one near-field site (Cooke et al. 2017). At the upland lake in the PAD (PAD 18), enrichment of [THg] began before oil sands development (at ~1940) and declined after ~1985 when oil sands production increased rapidly (Wiklund et al. 2012). Both studies concluded that the lake sediment records reflect mid-20th century increases in emissions of Hg from coal combustion and other industrial sources, which is consistent with lake sediment core profiles from other regions at similar and higher latitudes across Canada (Muir et al. 2009), western North America (Drevnick et al. 2016), and elsewhere (Biester et al. 2007; Engstrom et al. 2014). Thus, evidence of [THg] enrichment by oil sands industrial activities via atmospheric pathways has failed to materialize from analyses of upland lake sediment core records in the AOSR and PAD.

Given that the Athabasca River is an important conduit for Hg transport (Hebert et al. 2019), an emerging priority is to determine pre-industrial baseline [THg] for the Lower Athabasca River and apply the baselines to quantify [THg] enrichment in sediment from floodplain lakes where supply will be dominated by fluvial processes. Mercury enrichment at the PAD via fluvial pathways has been identified as a threat by the Mikisew Cree First Nation (MCFN 2014) to the Outstanding Universal Value of the Wood Buffalo National Park World Heritage Site, and a recent Strategic Environmental Assessment concluded "more work needs to be done to determine if these

higher levels are solely a result of greater mercury supply from river-associated sources of THg (e.g., oil sands) or other factors" (IEC 2018, pg. 4-13). Also, knowledge of temporal patterns of THg deposition via atmospheric pathways at the PAD remains based on a single sediment record from upland lake PAD 18. Thus, independent verification is required to confirm temporal patterns of atmospheric Hg deposition at the PAD.

Here, we use measurements of [THg] in sediment cores spanning the past ~220 years at nine floodplain lakes in the AOSR and PAD and two upland lakes in and adjacent to the PAD to evaluate 1) the extent of [THg] enrichment via fluvial pathways at floodplain lakes proximal to the oil sands industry within the AOSR, 2) the extent of [THg] enrichment via fluvial pathways at floodplain lakes distal to the oil sands industry within the PAD, and 3) the extent and origin of [THg] enrichment via atmospheric pathways at upland lakes in the PAD region. Findings provide critical knowledge to inform stewardship of the Lower Athabasca River region, and the baseline reference data serve to identify important locations for ongoing aquatic ecosystem monitoring of [THg] and other contaminants.

Methods

Study lake locations

We took advantage of previously obtained floodplain lake sediment records in the AOSR and floodplain and upland lake sediment records from the PAD region to perform stratigraphic analysis of [THg] (Appendix C Table C1; Figure 3.1). Cores from most of the lakes have been radiometrically dated and measured for concentrations of other trace elements (Wiklund et al. 2012; Kay et al. 2020; Klemt et al. 2020) and are similarly well positioned to evaluate for enrichment of [THg] by oil sands mining and processing activities. Within the AOSR, we analyzed

[THg] in sediment cores from three floodplain lakes located adjacent to the Athabasca River (Down 1, Down 26 and Down 58). These were the best options available based on a prior study by Klemt et al. (2020), which demonstrated that the cores consist predominantly of sediment carried by the Athabasca River. Paleohydrological data at Down 58, the most river-proximal of the three floodplain lakes in the AOSR, indicates strong river influence throughout the entire sediment record. Due to rapid sedimentation at Down 58, the core did not capture sediment deposited before oil sands development, but the lake is located near the downstream perimeter of the AOSR and can serve as an important archive of temporal changes in river sediment [THg]. Down 1 and Down 26 became less river influenced after ~1980 and ~2012, respectively, due to declines in Athabasca River discharge, a feature which enables assessment of THg deposition via atmospheric pathways as river influence waned (Klemt et al. 2020). Of note, the sediment record from Down 26 remained dominated by fluvial processes when Hg emissions from oil sands operations within the AOSR nearly tripled between 2000 and 2010 (Hebert et al. 2013).

Within the PAD, six floodplain lakes (PAD 23, PAD 30, PAD 31, PAD 32, M2 and M5) were selected based on previous studies by Wiklund et al. (2014) and Kay et al. (2019 [*included here as Chapter 5*], 2020), which demonstrated the Athabasca River has been a dominant source of their sediment. In July 1982, a natural geomorphic event known as the Embarras Breakthrough increased frequency and magnitude of river flooding at study lakes PAD 30 and PAD 31 and reduced influence of river flooding at PAD 32 and M5 (Kay et al. 2019). The Embarras Breakthrough provides unique opportunity to identify the role of Athabasca River on THg deposition since these sites have received marked increase (PAD 30, PAD 31) or decrease (PAD 32, M5) in sediment flux via Athabasca River floodwaters since 1982. The Embarras Breakthrough did not discernibly alter the flood regime at PAD 23 and M2 (Kay et al. 2019). Additionally, an

engineered change to the Athabasca River occurred in 1972 (known as the Athabasca River Cutoff), which decreased flood susceptibility at PAD 23 (Wolfe et al. 2008). Upland lakes PAD 18 and AC5 are exclusive archives of atmospheric deposition because PAD 18 is elevated above the reach of ice-jam floods (Yi et al. 2008) and AC5 is located ~10 km outside the delta and beyond the spatial extent of floodwaters. For the above reasons, sediment cores from the study lakes are well situated to develop long-term records of THg deposition for the region via fluvial and atmospheric pathways (See Table C1 for further information about study lakes).

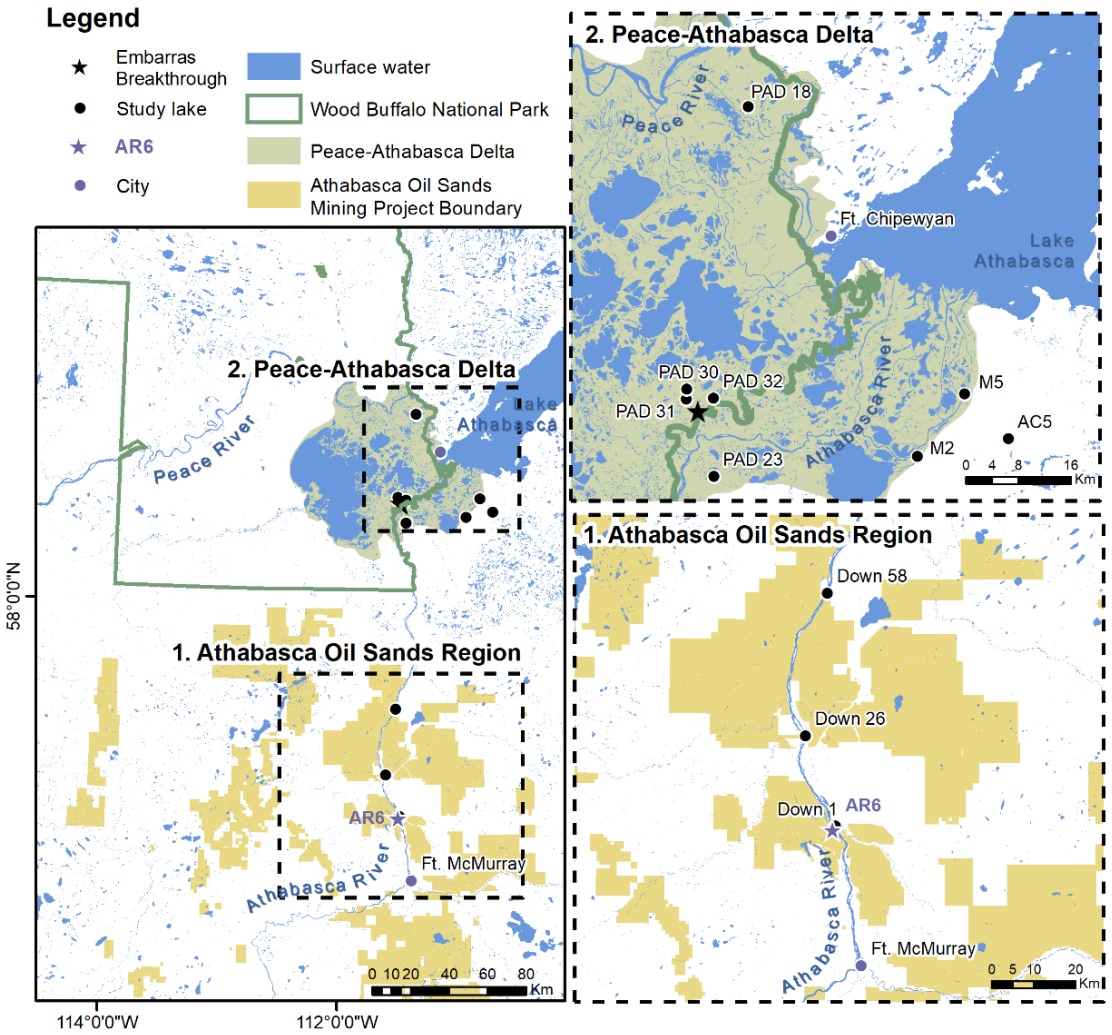

Figure 3.1 Map showing sampling sites for lakes (black circles) in the AOSR and PAD region, located in northeastern Alberta (Canada). The Wood Buffalo National Park boundary is denoted by the dark green line, the PAD is shaded in green and the Athabasca Oil Sands mining footprint including holdings for future developments in 2021 is shaded in brown. Fort McMurray and Fort Chipewyan are denoted by purple circles and AR6, a central location in the AOSR, is a purple star. Source: https://services3.arcgis.com/sLVWntsRoDa37BS8/arcgis/rest/services/OSIP_2015_Project_Boundaries/FeatureServer

Sediment core collection and analyses

Sediment cores were collected from each of the study lakes during 2010 to 2019 using a gravity corer (Glew 1989) or hammer-driven gravity corer (Telford et al. 2021), as described in Wiklund et al. (2012), Kay et al. (2019) and Klemt et al. (2020). Sediment cores were sectioned into 0.5- or 1.0-cm intervals using a vertical extruder (Glew 1988; Telford et al. 2021) within 24 hours of collection at a local field base, and the samples were transported to the University of Waterloo, refrigerated (4 °C) and stored in the dark until further analysis. Because the sediment records had been utilized for other purposes, stratigraphic sampling and analysis was dependent on available material, with the exception of the previously published THg record from PAD 18 (Wiklund et al. 2012). Continuous 1-cm sediment intervals from PAD 23, PAD 31, PAD 32 and M5 were analyzed for [THg]. For cores from PAD 30, M2, Down 1, Down 26 and Down 58, approximately every second 1-cm sediment interval was analyzed for [THg]. At AC5, every second 0.5-cm sediment interval was analyzed for [THg]. Total Hg concentrations were determined on freeze-dried sediment samples from Down 1, Down 26, Down 58, PAD 30, PAD 32, M2, M5, and AC5 at the Biotron Laboratory (Western University, Ontario, Canada) using thermal decomposition and atomic adsorption spectrophotometry and following EPA Method 7473. The analytical uncertainty expressed as a relative percentage difference (RPD) is 3.0% based on sample duplicates. Freeze-dried continuous 1-cm sediment intervals from PAD 23 and PAD 31

were analyzed for [THg] at ALS Canada Ltd. (Edmonton) following EPA Method 200.2/245.7 and the analytical uncertainty is 4.0% based on sample duplicates.

Sediment cores were radiometrically dated using ^{210}Pb and ^{137}Cs methods at the University of Waterloo, and the Constant Rate of Supply (CRS) model was used to calculate ^{210}Pb-based ages and sedimentation rates (Appendix C Figure C1; Appleby 2001; Sanchez-Cabeza and Ruiz-Fernandez 2012). Age-depth relations for all cores used in this study, except Down 58 and AC5, have been previously published (Wiklund et al. 2012; Hall et al. 2012; Kay et al. 2019; Klemt et al. 2020). The complex sedimentary environment of floodplain lakes may challenge sediment core dating by ^{210}Pb and ^{137}Cs. The floodplain lakes in this study span a gradient of flood frequency. Lakes such as PAD 30 and PAD 31 can flood multiple times per year in spring and summer, whereas others flood episodically when ice-jams form on the rivers (e.g., Wiklund et al. 2012; Kay et al. 2019; Remmer et al. 2020). To our knowledge and based on other paleolimnological analyses, the study lakes have retained water throughout the time captured by the sediment cores. Thus, sediment deposition has been continuous, but flood events cause deposition rates to increase markedly due to influx of suspended sediment.

For floodplain lakes in the PAD, sediment core chronologies were based entirely on the ^{210}Pb activity profiles (Kay et al. 2019). Confidence in the chronologies for the floodplain lakes is supported by consistent results obtained on cores collected from PAD 31 in 2001 and 2010 which determined an age of ca. 1982 for a shift from organic-rich to mineral-rich sediment following the Embarras Breakthrough (Wolfe et al. 2008; Kay et al. 2019). At Down 26 and Down 58 in the AOSR, however, ^{210}Pb-based chronologies were not possible due to rapid sedimentation rates that diluted the unsupported ^{210}Pb activity (Klemt et al. 2020; Figure C1). A chronology was developed for the core from Down 26 based on the ^{137}Cs activity profile, and a cumulative dry-mass

sedimentation rate was used to extrapolate the age-depth relation downcore below the 1963 ^{137}Cs activity peak (Klemt et al. 2020). At Down 58, there was no discernible ^{137}Cs activity peak. However, measurable ^{137}Cs activity occurred at the base of the core indicating lowermost sediments are younger than 1963 and that the entire core likely captures a period after onset of oil sands development (Klemt et al. 2020). For upland lakes PAD 18 (Wiklund et al. 2012) and AC5, CRS modelling of ^{210}Pb activity profiles was used to develop age-depth relations and ^{137}Cs and ^{241}Am activity profiles were used for independent assessment at AC5. We provide further supporting details on sediment core dating in Appendix C and report the radiometric dating results for cores from all lakes in Figure C1.

Enrichment factor and anthropogenic flux calculations

Enrichment factors (EFs) are an effective metric for expressing trace element concentrations relative to a pre-industrial reference or baseline, which allows for quantification of temporal patterns of enrichment since onset of industrial activities (Boës et al. 2011). Baseline concentrations were defined as pre-1900 because analyses by Wiklund et al. (2012) demonstrated no evidence of [THg] enrichment until after ~1930, which aligns with data from other lake sediment core studies in western North America (Drevnick et al. 2016). Thus, we define the pre-1900 period as pre-industrial while post-1900 is considered post-industrial even though oil sands development did not begin until 1967. Geochemical and organic matter normalization of [THg] were explored to determine an appropriate agent to account for potential confounding influence of variation in grain size and sediment composition, as was done for assessment of other trace elements in lake sediment cores in the region (Wiklund et al. 2014; Kay et al. 2020, in review; Klemt et al. 2020, 2021; Owca et al. 2020). However, relations between [THg] and lithogenic elements did not meet the requirement for geochemical normalization (Loring et al. 1991) and

organic matter content produced non-significant statistical relations for most lake sediment records. Normalization to organic matter content was used previously at PAD 18 (Wiklund et al. 2012) but was not applied here to remain consistent with data handling and presentation of the other lake sediment records. Thus, EFs were computed without normalization and used [THg] (Tables C2-C12) following Equation 1:

Equation 1: $EF = [THg]_x/[THg]_{pre\text{-}industrial}$

where $[THg]_x$ is the concentration of THg at a specific sediment interval in the core and $[THg]_{pre\text{-}industrial}$ is the pre-1900 average [THg] determined for the core from each individual lake. Two lakes, Down 58 and M5, did not have pre-1900 data for EF computations. At Down 58, an average of pre-1900 [THg] from Down 1 and Down 26 was used to estimate the pre-industrial baseline [THg]. At M5, the closest lake with a similar hydrological setting (M2; Kay et al. 2019; Remmer et al. 2020; Neary et al. 2021) was used to estimate the pre-industrial baseline [THg]. An EF of 1.0 indicates the [THg] in a specific stratigraphic interval is equivalent to the pre-industrial baseline, whereas an EF of 2.0 indicates a doubling above baseline. To quantify the magnitude of enrichment, we incorporated thresholds recommended by Birch (2017), which have been widely applied in this region and elsewhere (Kay et al. 2020, in review; Klemt et al. 2020, 2021; Owca et al. 2020; Jasiak et al. 2021). An EF value of ≤ 1.5 was considered to represent 'pristine conditions' and EFs from 1.5 – 3.0 were considered 'minimal enrichment'.

For the sediment cores obtained from upland lakes PAD 18 and AC5 where [THg] enrichment was identified, anthropogenic THg fluxes were calculated using Equation 2 from Wiklund et al. (2017), which incorporates focus-factor-corrections following recommendations from Muir et al. (2009):

Equation 2: Anthropogenic THg $\text{Flux}_{\text{FF, Excess}_i} = \left(\text{THg}_{\text{conc}_i}\left(\frac{\text{EF}_i\text{-}1}{\text{EF}_i}\right)(r_i)\right)\left(\frac{F^{210}Pb_{\text{u, regional}}}{F^{210}Pb_{\text{u, local}}}\right)$

where $\text{THg}_{\text{conc}i}$ is the total Hg concentration at interval *I*, EF_i is enrichment factor at a given interval *i* calculated from Equation 1, r_i is the sedimentation rate in kg/m^2/year at interval *i*, and $F^{210}Pb_{\text{u,regional}}/F^{210}Pb_{\text{u,local}}$ is the focusing factor.

Anthropogenic inventories of THg were calculated for upland lakes PAD 18 and AC5 as a metric to evaluate the total mass of excess THg deposited per unit area at each lake, and to quantify atmospheric deposition of anthropogenic-sourced Hg. We followed the recommended Equation 5 from Wiklund et al. (2017), where the sum of the excess THg flux was multiplied by the time span of all intervals (Equation 3):

Equation 3: Anthropogenic $I_{\text{FF, Excess}_{\text{THg}}} = \sum_{i=1}^{n} \text{THg}_{\text{conc}_i}\left(\frac{\text{EF}_i\text{-}1}{\text{EF}_i}\right)\left(\frac{\text{mass}_i}{\text{core area}}\right)\left(\frac{F^{210}Pb_{\text{u, regional}}}{F^{210}Pb_{\text{u, local}}}\right)$

where mass_i is the dry mass (kg) of a specific core interval and core area is cross-sectional area of the core tube (m^2).

Results

THg concentrations in sediment cores from the nine floodplain lakes in the AOSR and PAD and two upland lakes in the PAD region span from 0.022 – 0.096 mg/kg (dry wt.), and all values are below the Canadian interim sediment quality guidelines for freshwater (0.17 mg/kg, CCME 1999; Tables C2-C12). Enrichment factors from the floodplain lakes in the AOSR (Down 1, Down 26 and Down 58) remain stable around 1.0 during both the pre-industrial and post-industrial periods and do not exceed the 1.5 threshold for 'minimal enrichment' (Figure 3.2a-c). The only exceptions to this are three samples at the bottom portion of the sediment core from undated Down 58, but growth of oil sands mining and processing activities and associate releases of THg would be expected to result in rising EFs towards the upper strata of the core. Enrichment

factors at Down 1 and Down 26 remain stable around 1.0 during intervals of weaker river influence, which began at ~1985 and ~2012, respectively, when rise of V and Ni enrichment was shown by Klemt et al. (2020). Similarly, floodplain lakes in the PAD (PAD 23, PAD 30, PAD 31, PAD 32, M2, M5) reveal minor variations in THg EFs and values mostly remain stable at ~1.0 (Figure 3.2d-i). Only six sediment samples have THg EFs that exceed the 'minimal enrichment' threshold of 1.5. These include five samples at PAD 30 (~1961, ~1974, ~1983, ~1999, ~2001) and one sample at PAD 31 (~1983; Figure 3.2e-f). Interestingly, EFs in samples deposited at ~1983 at both PAD 30 and PAD 31 identify 'minimal enrichment' in the year following the Embarras Breakthrough. However, the rising trend for THg EFs at PAD 30 started at ~1960 and exceeded the 1.5 'minimal enrichment' threshold before the Embarras Breakthrough, while the increase in THg EFs at PAD 31 occurred after the Embarras Breakthrough. Enrichment factors from floodplain lakes (PAD 32, M2 and M5) downstream of the Embarras Breakthrough do not noticeably change after 1982 and remain below the 'minimal enrichment' threshold throughout their records.

In contrast to the floodplain lakes in both the AOSR and PAD, sediment records at upland lakes PAD 18 and AC5 display systematic rising trends in THg EFs. This trend is more apparent at AC5 than at PAD 18 but the rise began several decades before onset of oil sands development at both lakes (Figure 3.3a,b). At PAD 18, the rising trend began at ~1930 and reached a peak EF value (1.44) in a sample deposited ~1968. At AC5, the rising trend also began at ~1930 and reached a peak of 2.54 in a sample deposited ~1966. A declining trend began shortly after the peak EF values at both lakes with EFs returning to 1.5 (AC5) or lower (PAD 18). Enrichment factors from AC5 exceed the 'minimal enrichment' threshold of 1.5 while EFs from PAD 18 do not. The estimated anthropogenic THg fluxes are similar at both upland lakes, where values ranged 0-1.0

μg THg m^{-2} yr^{-1} before 1900 and rose distinctly after ~1930 (Figure 3.3c,d). Anthropogenic THg fluxes at PAD 18 and AC5 remain relatively stable between ~1960 to ~1990 at ~1.5 μg THg m^{-2} yr^{-1} with some variation about the average value. The peak anthropogenic THg flux for PAD 18 was 2.23 μg THg m^{-2} yr^{-1} in ~1968 while the peak value at AC5 was 1.81 μg THg m^{-2} yr^{-1} in ~2011. In the uppermost strata, both lakes show a general decline in anthropogenic THg flux.

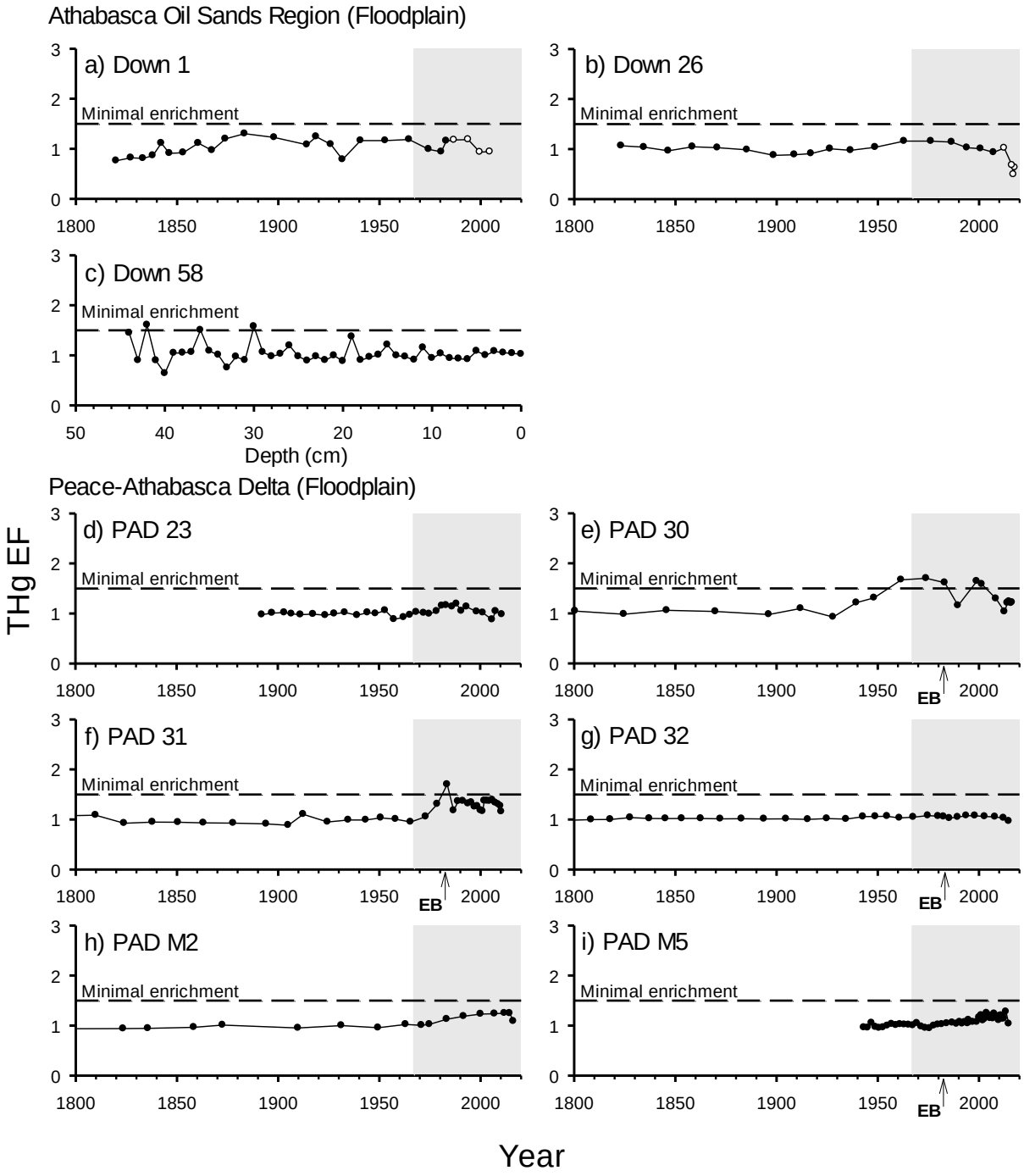

Figure 3.2 Time series of THg enrichment factors (EFs) relative to the average pre-1900 concentration at floodplain lakes in the AOSR (a-c) and PAD (d-i). The horizontal black dashed line at EF of 1.5 marks the 'minimal enrichment' threshold (Birch 2017) and the grey shaded region denotes the interval of oil sands mining and processing activities on the Lower Athabasca River beginning in 1967. The white circles for Down 1 and Down 26 indicate periods of weak river influence identified by Klemt et al. (2020). The EB denotes the 1982 Embarras Breakthrough, which resulted in increased river influence at PAD 30 and PAD 31 and decreased river influence at PAD 32 and PAD M5.

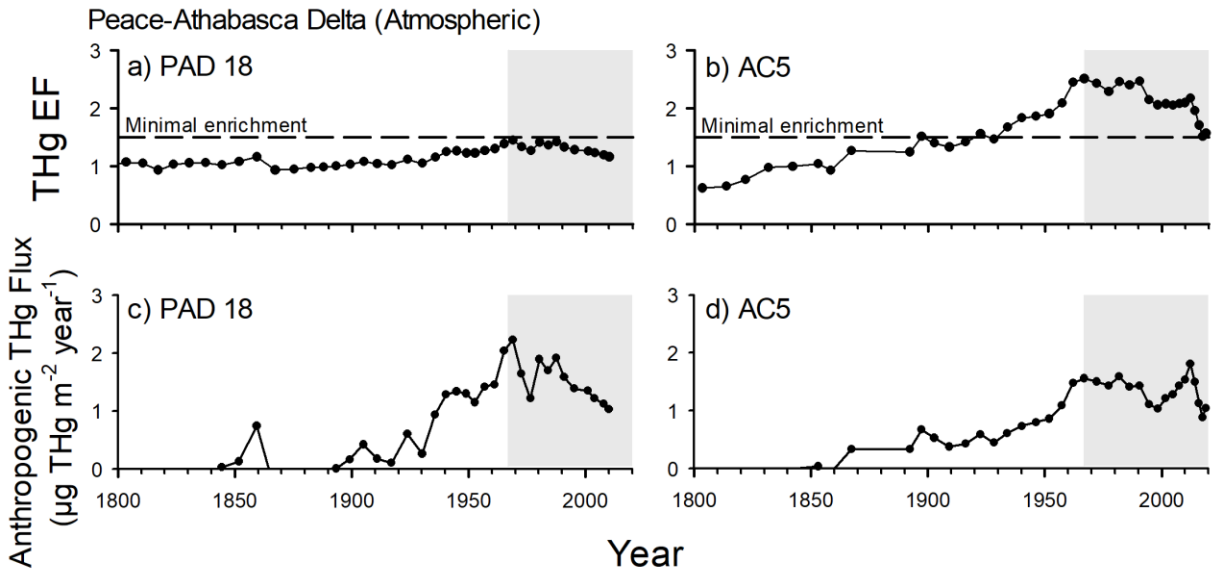

Figure 3.3 Time series of THg enrichment factors (EFs) relative to the average pre-1900 concentration at upland lakes a) PAD 18 and b) AC5. The bottom two graphs are time series of focus factor corrected anthropogenic Hg flux for c) PAD 18 and d) AC5. The grey shaded region denotes the interval of oil sands mining and processing activities on the Lower Athabasca River beginning in 1967.

Discussion

Releases of Hg from oil sands mining and processing have raised questions about the extent of Hg pollution within aquatic ecosystems of the Lower Athabasca River watershed and at the PAD (Kelly et al. 2010; Kirk et al. 2014; Hebert et al. 2019). This is despite evidence that concentrations of Hg are low in geological materials within the AOSR, including oil sands mining source materials, and that spatial distributions of concentrations and stable isotope composition of Hg in a species of epiphytic tree lichen (*Hypogymnia physodes*) have shown no evidence of a significant point source of Hg from oil sands development (Blum et al. 2012). Nonetheless, it has remained difficult to further address these concerns because of insufficient knowledge of pre-industrial, reference [THg]. Our study builds upon similarly designed and executed determination of trace element enrichment in sediment profiles from lakes in the AOSR (Cooke et al. 2017; Klemt et al. 2020), PAD (Kay et al. 2020) and elsewhere (e.g., Slave River Delta: MacDonald et

al. 2016 and Central Northwest Territories: Cheney et al. 2020; Jasiak et al. 2021), which have been crucial for determining pre-industrial baseline concentrations (Kay et al. in review). Here, we capitalized on opportunity to measure [THg] from the same sediment cores used in the trace element studies from the AOSR (Klemt et al. 2020) and PAD (Kay et al. 2020) to determine [THg] before onset of oil sands development, quantify the extent of [THg] enrichment and decipher the roles for emissions from oil sands operations versus other sources and factors operating at local to regional scales. Notably, [THg] measured in the stratigraphic profiles, including both pre- and post-industrial intervals, from floodplain and upland lakes do not exceed the Canadian interim sediment quality guidelines for freshwater (0.17 mg/kg; CCME 1999) and are lower than the mean background [THg] in Canadian lake (0.074 mg/kg) and stream (0.075 mg/kg) sediment (CCME 1999).

Stratigraphic records of THg enrichment factors at the nine floodplain lakes in the AOSR and PAD illustrate that sediments carried by the Lower Athabasca River are not enriched above pre-industrial baselines, including in sediments deposited since the onset of oil sands development. In the PAD, this includes lakes that have received increased river floodwaters and more minerogenic sediment since the 1982 Embarras Breakthrough (PAD 30 and PAD 31) and lakes that have received less river floodwaters and sediment is more organic-rich (PAD 32 and M5). These results identify neither shifting hydrological conditions or sediment composition for lakes examined within this study have measurably influenced [THg]. A minor and single exception is a discernable rise of [THg] enrichment at PAD 30, which began in the late 1930s and peaked in the early 1970s, an interval that mostly precedes oil sands development and corresponds with when the lake received deposition mainly by atmospheric pathways rather than via fluvial pathways (Kay et al. 2019). A similar pattern of Zn enrichment was observed at PAD 30 (Kay et al. 2020)

and we hypothesize that localized catchment or within-lake processes are responsible for this trend (Figure C2). Despite this, PAD 30 remains a strong candidate to track [THg] enrichment via the Athabasca River due to its current, post-Embarras Breakthrough flood-prone status (Kay et al. 2019). Given the absence of evidence for enrichment of [THg] in floodplain lake sediment conveyed by the Lower Athabasca River after 1967, our study suggests oil sands development is not responsible for higher concentrations and altered stable isotope ratios of Hg in aquatic bird eggs at the PAD and Lake Athabasca relative to other locations (Hebert et al. 2013, 2019). As acknowledged by Hebert et al. (2019), periods of elevated flow on the Athabasca River likely increase delivery of THg to the PAD, but our results suggest this occurs via natural processes and at concentrations typical of pre-industrial times.

Delivery of Hg from bitumen mining in the AOSR via atmospheric pathways to aquatic ecosystems at the PAD is another chief concern (Kirk et al. 2014; IEC 2018). Temporal patterns of Hg deposition prior to oil sands development have been assessed from stratigraphic analysis of a sediment core at a single upland lake (PAD 18) within the PAD, and results provided no measurable evidence of far-field [THg] enrichment via atmospheric pathways attributable to oil sands development since 1967 (Wiklund et al. 2012). To further test and verify the findings of that study, [THg] analysis of a sediment core from AC5 was used as an independent replicate of PAD 18. Temporal patterns of variation in [THg] enrichment are similar but differ in magnitude. Since the early 1900s, THg EFs have exceeded the threshold of 'minimal enrichment' at AC5 but not at PAD 18. Anthropogenic flux calculations account for differences in sedimentation rate and focusing factor between the lake sediment records, and their close correspondence provides strong confidence in the reproducibility of the results. Anthropogenic fluxes began to rise several decades before onset of oil sands development at both lakes, then plateaued and declined as oil sands

mining and processing activities increased. This provides compelling evidence that oil sands development has not increased delivery of THg to the PAD via atmospheric pathways. Indeed, the two upland lakes in the PAD region have remarkably similar EF profiles to upland lakes in the AOSR (Cooke et al. 2017), where little to no evidence of increase in enrichment or flux of THg was observed after the onset of oil sands activities. Notably, the temporal patterns of variation in THg EFs and anthropogenic flux are different from those of vanadium, a key oil sands indicator, which increased with onset of oil sands development at the same upland lakes in the AOSR (Cooke et al. 2017). In contrast, stratigraphic patterns of [THg] enrichment from the upland lakes in the AOSR and PAD align with those from other lake sediment records across western North America (Drevnick et al. 2016), attributed to long-range transport of emissions from coal combustion and other anthropogenic sources, and they match closely with industrial development in North America and elsewhere (Callender and van Metre 1997; Couture et al. 2008). Interestingly, a decline in EFs and anthropogenic fluxes is observed at PAD 18 and AC5 since the onset of oil sands development but values have not yet completely returned to baseline. This pattern has been noted as a common feature for sediment deposited in recent decades at remote lakes in northern Canada where contaminants are supplied predominantly via atmospheric pathways (Muir et al. 2009). There, storage and gradual release of anthropogenic THg in catchment soils and biomass (Harris et al. 2007) or maintenance of THg flux from sources in Eurasia have been proposed as mechanisms that account for reduced decline of anthropogenic THg flux in recent decades compared to other trace elements (Muir et al. 2009).

To provide regional context to the anthropogenic THg fluxes and inventories derived from the upland lakes in PAD region, we compared results to other Canadian locations (Figure 3.4). The Experiment Lakes Area (ELA) is a remote region near the Ontario-Manitoba border sufficiently

unaffected by human activities where whole lake experiments are conducted with minimal confounding effects of other anthropogenic influences. In contrast, the Flin Flon smelter was one of the largest point sources of THg in Canada when operational (~1930 – 2010, peak emissions ~1980*;* Pirrone et al. 1998). Data from ELA and Phantom Lake (5 km from a metals smelter near Flin Flon, Manitoba) were obtained from Wiklund et al. (2017), where the same methods were employed to calculate anthropogenic fluxes and inventories. For lakes in the ELA, mean values from 5 lakes (ELA 240, ELA 373, ELA 377, ELA 378 and ELA 442) were computed for THg anthropogenic fluxes and inventories (Wiklund et al. 2017). Distinct differences are noted among the three regions. Anthropogenic THg flux (0 - 2857.59 µg Hg m^{-2} yr^{-1}) and THg inventory (86,857 µg THg m^{-2}) at smelter-proximal Phantom Lake are *~700-fold higher* than corresponding values at ELA (0 – 6.13 µg THg m^{-2} yr^{-1}; 492.82 µg THg m^{-2}), PAD 18 (0 – 2.23 µg THg m^{-2} yr^{-1}; 127.15 µg THg m^{-2}) and AC5 (0 – 1.41 µg THg m^{-2} yr^{-1}; 124.35 µg THg m^{-2}). Since 1930, the cumulative inventory of anthropogenic THg at the two upland lakes in the PAD region parallels the average values for the five lakes in the ELA but the values at the ELA are four-fold higher than at the PAD region (Figure 3.4c). This difference is likely attributed to greater industrial activity in the Great Lakes region. Nonetheless, the ELA is still widely regarded as a 'pristine' environment (Pirrone et al. 1998; Hall et al. 2005; Wiklund et al. 2017) and, thus, it is notable that the upland lakes in the PAD region exhibit lower inventories of anthropogenic THg.

Our study reaffirms that paleolimnological analyses of temporal variation in deposition of substances of concern provide valuable, and often missing, pre-industrial baseline information, which is required to delineate the roles of natural and anthropogenic processes. Temporal patterns of THg EFs align with other paleolimnological studies of metals (Wiklund et al. 2014; Kay et al. 2020; Owca et al. 2020) and polycyclic aromatic compounds (Hall et al. 2012) in floodplain lakes

of the PAD, which also demonstrate oil sands development has not enriched contaminant concentrations at the PAD above pre-industrial baselines via fluvial pathways. Additionally, anthropogenic flux and anthropogenic inventories of THg determined from sediment cores of upland lakes at the PAD region indicate that oil sands development has not increased delivery of THg to the PAD via atmospheric pathways. These findings are important given that the International Committee on Conservation of Nature / World Heritage Committee is currently evaluating Canada's response to their assessment and recommendations regarding the World Heritage status of Wood Buffalo National Park. Degradation of aquatic ecosystems in the PAD by increased delivery of contaminants from oil sands development are prominent among the perceived threats (IUCN/WHC 2021), yet paleolimnological data constrained by knowledge of pre-industrial concentrations of substances of concern do not support such attribution. We suggest lakes presented in this study, equipped with knowledge of pre-industrial baselines, can continue to serve as a useful source of information for evaluating future surficial lake and river-bottom sediment in support of ongoing monitoring of [THg] as well as other trace elements (i.e., V, Ni). The informative nature of this approach has been illustrated previously by Wiklund et al. (2014), Owca et al. (2020) and Klemt et al. (2021) for trace elements but could be expanded readily to be part of an integrated monitoring program, which evaluates [THg] in sediment, air, and biota throughout the Lower Athabasca River watershed. Application of this approach may be especially timely pending discharge of oil sands process waters directly into the Athabasca River (Hicks and Scrimgeour 2019).

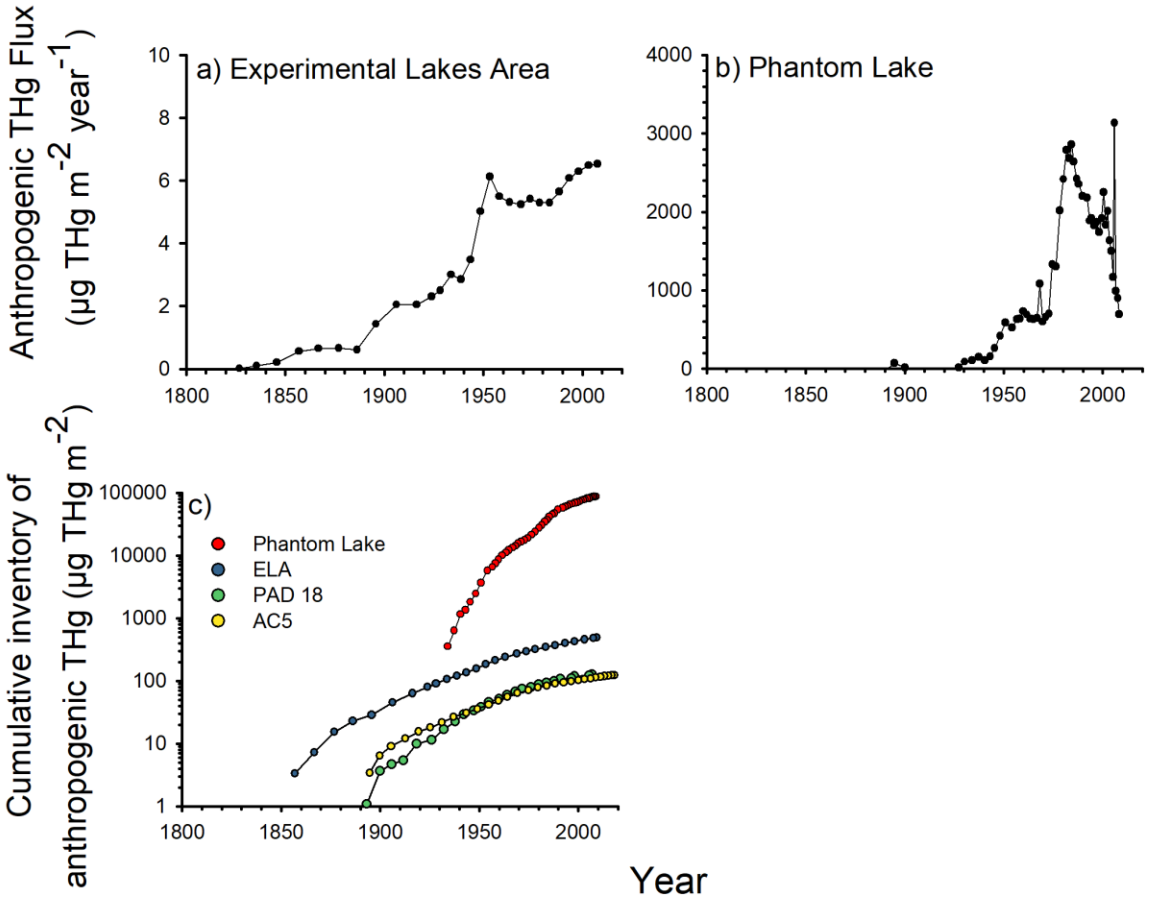

Figure 3.4 Panel a) is the mean anthropogenic Hg flux from 5 lakes (ELA 240, ELA 373, ELA 377, ELA 378, and ELA 442) in the Experimental Lakes Area of Ontario (Wiklund et al. 2017). Panel b) is the anthropogenic Hg flux from Phantom Lake, which is located ~5 km away from a smelter in Flin Flon, Manitoba (Wiklund et al. 2017). Panel c) is the cumulative anthropogenic inventories of Hg for Phantom Lake, ELA, PAD 18 and AC5 plotted on a log-scale. The ELA anthropogenic Hg inventory is a mean value from the same 5 lakes as the anthropogenic flux calculation.

Chapter 4: Paleolimnological evaluation of metal(loid) enrichment from oil sands and gold mining operations in northwestern Canada

Citation: Kay, M.L., Jasiak, I., Klemt, W.H., Wiklund, J.A., Faber, J.A., MacDonald, L.A., Telford, J.V.K., Savage, C.A.M., Cooke, C.A., Wolfe, B.B., and Hall, R.I. In Review. Paleolimnological evaluation of metal(loid) enrichment from oil sands and gold mining operations in northwestern Canada.

Introduction

Discovery of oil and mineral deposits has stimulated rapid growth of large-scale mining and processing activities across northwestern Canada during the past 80 years (Mudroch et al. 1986; Gosselin et al. 2010). Principal among these is exploitation of bitumen-rich deposits in the Alberta Oil Sands Region (AOSR) of northeastern Alberta and gold-bearing sulfide deposits in central Northwest Territories (NWT). Bitumen mining began in the late 1960s, but the high cost of producing commercial-grade oil limited growth initially (Schindler 2010; CAPP 2020). As the price of conventional oil rose, rapid development of the oil sands occurred leading to ~15.3 billion barrels of oil produced since 1967 (CAPP 2020). Most oil production has occurred during the past 25 years, with rates of around 400,000 barrels per day during the 1990s and subsequent increases to ~1.5 million barrels per day by 2010 and ~2.8 million barrels per day by 2020. Among a suite of contaminants, an estimated 164 tonnes of vanadium (V), a metal enriched in McMurray Formation bitumen and waste materials (Gosselin et al. 2010; Shotyk et al. 2021), were released to the atmosphere since 1993 (NPRI 2021).

Pursuit of gold in central NWT during the 20th century resulted in development of two large-scale mines: Consolidated Mining and Smelting Company (Con Mine; opened 1938) and Giant Yellowknife Gold Mines Ltd. (Giant Mine; opened 1948). Giant Mine primarily roasted arsenopyrite at 500°C to generate iron oxides which were subjected to cyanidation (Hocking et al. 1978; Walker et al. 2005, 2015; Fawcett et al. 2015). Arsenic trioxide (As_2O_3) was released from the roaster stack as by-products of the processing and deposited onto the surrounding landscape

(Hutchinson et al. 1982). From 1948 to 1999, >20,000 tonnes of As_2O_3 were emitted by mining operations, with most releases during the early years of operation at Giant Mine (Hocking et al. 1978; Indian and Northern Affairs Canada 2007; Sandlos and Keeling 2012; Jamieson 2014; Galloway et al. 2015). The development of emission controls, including a baghouse dust collector installed in 1958, reduced quantities of pollutants to the atmosphere, however, widespread contamination of the aquatic and terrestrial environment had already occurred due to lack of emission controls prior to 1951 (Wagemann et al. 1978; Hocking et al. 1978; Jamieson et al. 2017; Galloway et al. 2018; Jasiak et al. 2021).

Contaminant releases to the environment from the large-scale mining developments in northeastern Alberta and central NWT have raised concerns about deterioration of ecosystems located downwind and downstream and risks to human health (Hocking et al. 1978; Schindler 2010; Jamieson 2014; Mikisew Cree First Nation 2014; Palmer et al. 2015; WHC/IUCN 2017). However, insufficient knowledge of the spatial extent and temporal persistence of contaminant deposition caused by mining activities has been an impediment to full characterization of the concerns and risks. A key additional challenge has been poor characterization of the natural range of concentrations that existed for substances of concern before onset of the disturbance (Blais et al. 2015). In the absence of pre-disturbance data, studies have used space-for-time substitution designs (Wagemann et al. 1978; Kelly et al. 2010; Palmer et al. 2015, 2021; Donner et al. 2017, 2018; Galloway et al. 2018), temporal-change assessments (Timoney and Lee 2011), or an integration of both approaches (Alexander and Chambers 2017). Such studies have focused mainly on defining the near-field pollution footprint of these industries in the vicinity of Fort McMurray (Alberta) and Yellowknife (NWT) and have contributed to establishing these areas as ‘regions of concern’. However, these approaches can be compromised when natural processes (e.g.,

weathering and erosion) also supply the substances of concern and when confounding factors (e.g., climate change, reduced river discharge) are temporally correlated with the mining development (Bowman and Somers 2005; Wiklund et al. 2014). Such limitations reduce ability to discern the relative roles of natural processes and mining activities, which inhibits development of effective mitigation and remediation policies. These are challenges that have long hampered evaluation of the extent of pollution emanating from the large-scale mining activities in northeastern Alberta and central NWT where there are little to no direct measurements of pre-disturbance concentrations of substances of concern across vast remote regions (Dowdeswell et al. 2010; Palmer et al. 2015).

Expansive remote and protected areas situated between the bitumen mines of the AOSR and gold mines in central NWT support a diversity and abundance of wildlife and the cultural heritage and lifestyles of Indigenous communities. At the Peace-Athabasca Delta (PAD) in northeastern Alberta, located ~200 km north of Fort McMurray, long-standing concerns persist about far-field transport of contaminants from the large-scale open-pit bitumen mines via atmospheric and fluvial pathways (Timoney and Lee 2009; Kelly et al. 2010; Schindler 2010; Mikisew Cree First Nation 2014; WBNP 2019). Concern for pollution of aquatic ecosystems at the PAD by oil sands development threatens a downgrade to Wood Buffalo National Park's (WBNP) UNESCO World Heritage status and is a key consideration of the Federal Action Plan for the park, which encompasses 80% of the PAD (WHC/IUCN 2017, 2021; WBNP 2019). At the Slave River Delta (SRD) in southern NWT, located ~140 km south of Yellowknife and ~650 km north of Fort McMurray, local community concerns also exist about pollution from the bitumen mines in Alberta via fluvial and atmospheric pathways, and uncertainty remains about dispersal of metal(loid)s from the gold mines in central NWT to the SRD (Campbell and Spitzer 2007;

MacDonald et al. 2016). Knowledge of the extent of contaminant dispersal and enrichment is particularly important to Indigenous people who access natural and cultural resources of these remote deltas.

Inadequate knowledge of naturally occurring concentrations of substances of concern before the onset of the mining developments was highlighted by the Federal Oil Sands Advisory Panel more than a decade ago as a critical issue at the AOSR that has impeded ability of monitoring programs to detect temporal trends or identify the source(s) of contamination (Dowdeswell et al. 2010). A key recommendation of the Panel was "to establish as rigorously as possible the background or baseline level of pollution [substances of concern], against which any future trend can be assessed" using information preserved in sediment profiles obtained from lakes and ponds (Dowdeswell et al. 2010, p. 31). At the gold mining region of central NWT, studies based on measurements of recently deposited surficial sediment and water of lakes have delineated a 30-km radius 'zone of immediate influence' or equivalent 'zone of probable influence' from the mines, respectively (Galloway et al. 2012, 2015, 2018; Palmer et al. 2015). These contemporary measurements assess present-day conditions but are unlikely to inform about the spatial extent of contaminant deposition during peak mine emissions in the 1950s, and which may still be present in ecosystems. To address this critical knowledge gap, Palmer et al. (2015; p. 18) recommended "new research in the area should include paleolimnological and paleo-ecotoxicological approaches to better understand long-term trajectories of change in lakes impacted by legacy mining activities."

During the past decade, calls for paleolimnological investigations have spurred several site-specific studies at lakes from the four key regions to establish pre-disturbance concentrations of metal(loid)s of concern, assess their temporal trends and quantify the extent of enrichment since

the mining developments began (AOSR: Cooke et al. 2017; Klemt et al. 2020; Kay et al. 2022 [*included here as Chapter 3*]; PAD: Wiklund et al. 2012; Kay et al. 2020 [*included here as Chapter 2*], 2022; SRD: MacDonald et al. 2016; central NWT: Thienpont et al. 2016; Galloway et al. 2018; Schuh et al. 2018; Van Den Berghe et al. 2018; Cheney et al. 2020; Pelletier et al. 2020; Jasiak et al. 2021). At the AOSR and PAD, paleolimnological analyses have also been employed to evaluate archived data from industry- and government-led aquatic ecosystem monitoring programs for evidence of pollution (Wiklund et al. 2014; Owca et al. 2020; Klemt et al. 2021). Paleolimnological studies of metal(loid)s at the AOSR and PAD have focused mainly on vanadium (V) and nickel (Ni) because they are abundant in carbonaceous sediments and bitumen from the mined McMurray Formation relative to other geological formations, enriched in oil sands waste materials, and toxic to living organisms (Soil Quality Guideline >130 µg/g CCME 1999; Gosselin et al. 2010; Zubot et al. 2012; Nesbitt et al. 2017; Shotyk et al. 2021). Studies in the central NWT and SRD have focused on arsenic (As) and antimony (Sb) due to their elevated concentrations in the mined gold-bearing sulfide deposits and in emissions from Giant and Con mines (Hocking et al. 1978; Wagemann et al. 1978; Hutchinson et al. 1982; Indian and Northern Affairs Canada 2007; Sandlos and Keeling 2012; Jamieson 2014; Galloway et al. 2015). Arsenic remains a metalloid of concern in the region because of links to cancer and respiratory issues in humans (Ng and Gomez-Caminero 2001). Antimony is less mobile in lake sediments than As and, thus, is a useful complementary tracer of emissions from Giant and Con mines (Houben et al. 2016; Schuh et al. 2018; Palmer et al. 2019).

Although the individual paleolimnological studies have provided a wealth of site- and region-specific information, their synthesis would assist decision makers in evaluating risks associated with contaminant dispersal by the large-scale bitumen and gold mining activities across

a broad swath of northwestern Canada. Differences in laboratory methods and data analysis approaches have challenged the ability to compare and contrast the individual studies from different regions. Additionally, shifting hydrological conditions may alter the delivery pathway (atmospheric vs. fluvial) of contaminants within a lake record, further confounding ability to compare results across numerous studies. Here we employ systematic approaches to assemble and re-evaluate metal(loid) concentration data, expressed as enrichment factors relative to pre-disturbance reference concentrations, from sediment cores obtained at 51 lakes within the four key regions, which span 670 km from large-scale bitumen mines in the AOSR to large-scale gold mines in central NWT (Figure 4.1). Our extensive compilation and re-analysis provide an opportunity to coalesce the current state of knowledge regarding spatial and temporal deposition patterns of key pollution indicators from oil sands development (V and Ni) and Giant and Con mines (As and Sb) via atmospheric and fluvial pathways. Although localized pollution by the mines via atmospheric pathways has been documented from analysis of contemporary samples (e.g., Kelly et al. 2010; Kirk et al. 2014; Palmer et al. 2015; Galloway et al. 2018), synthesis at broader spatial and temporal scales across the four regions of interest provides important context to address concerns about enrichment of contaminants via fluvial and atmospheric pathways to remote floodplain landscapes of the PAD and SRD. Furthermore, our synthesis is timely given the recent draft decision by the World Heritage Committee that WBNP "likely meets the criteria for inscription on the List of World Heritage in Danger" in part due to concerns of pollution from upstream oil sands development and inadequate monitoring and assessment (WHC/IUCN 2021, p. 191). We demonstrate that information preserved in lake sediment cores supports quantitative definition of pre-disturbance reference concentrations and the magnitude of enrichment of metal(loid)s of concern at spatial and temporal scales useful to inform decisions by stakeholders. The approaches

applied in this study are also reflected upon to assist others in locations where natural versus industrial sources of metal(loid) deposition remain challenging to differentiate.

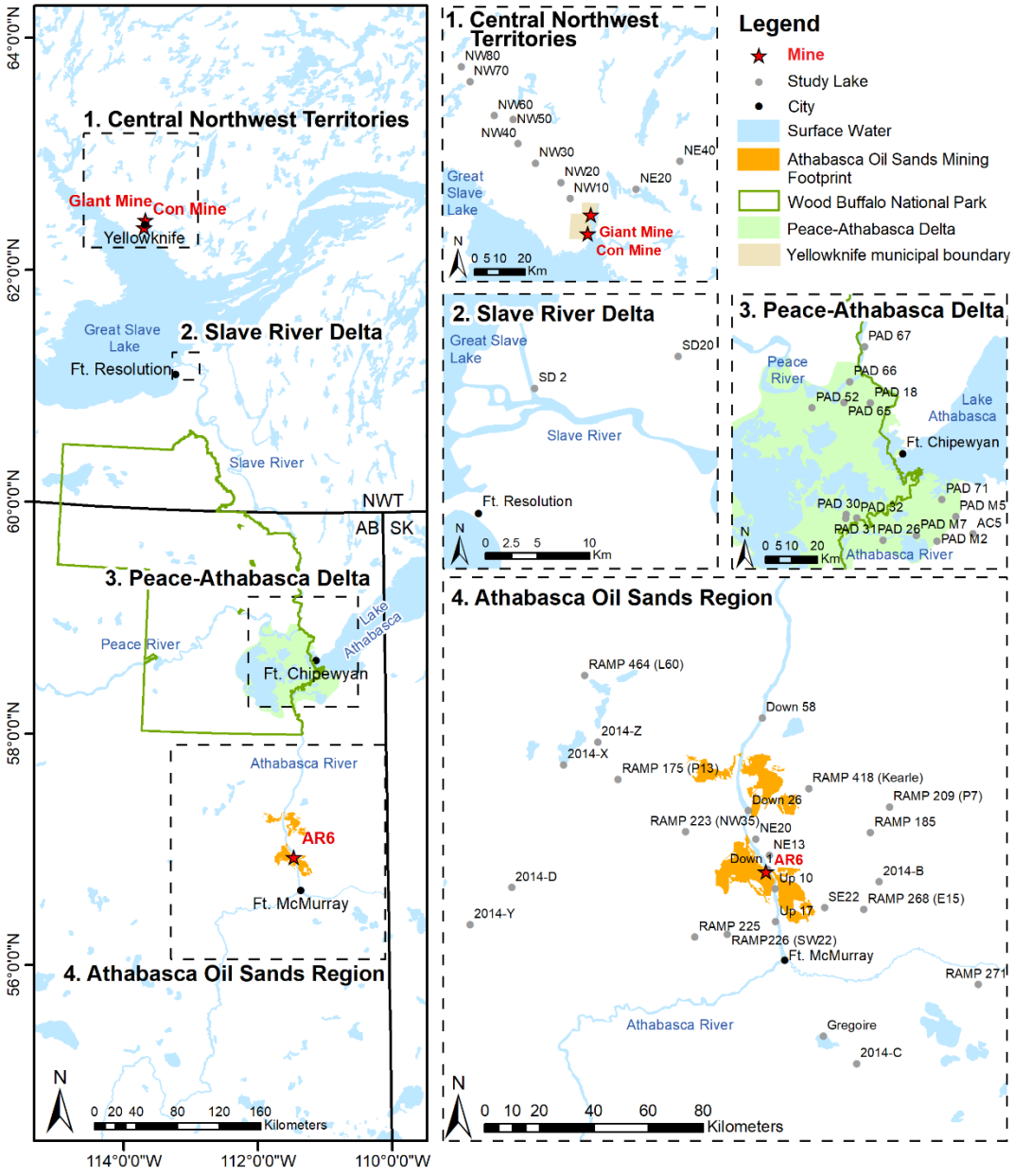

Figure 4.1 Maps showing the four regions of interest with AR6, a central node in the Alberta Oil Sands Region (AOSR), and Giant and Con mines denoted by red stars. The Wood Buffalo National Park boundary is denoted by the green line, the Peace-Athabasca Delta is shaded in green and the Athabasca Oil Sands mining footprint (2010; open source: https://databasin.org/datasets/ca774c8d651a46a1949bdbdb408a2561/) is shaded in orange. The individual study area maps show the locations (grey circles) where lake sediment cores were obtained between 2002 and 2019.

Methodology

Study design

Metal(loid)s released from bitumen mining are potentially dispersed to the study lakes in the AOSR, PAD and SRD via atmospheric and fluvial (Athabasca River, Slave River) pathways, whereas emissions from gold mining in central NWT are potentially dispersed to the study lakes almost exclusively via atmospheric pathways (Figure 4.1). Thus, analysis of sediment cores from small headwater lakes in upland locations of all four regions was used to inform about contaminant supply via atmospheric pathways, whereas analysis of cores from river-proximal floodplain lakes in lowland locations of the AOSR, PAD and SRD was used to inform about contaminant supply via fluvial pathways. Independent paleohydrological reconstructions from the floodplain lakes were key to identify periods of reduced or absent river flooding when contaminant deposition occurred mainly via atmospheric pathways (SRD: MacDonald et al. 2016; AOSR: Klemt et al. 2020). Lake hydrological setting, past and present, thus allowed for the establishment of pathway-appropriate pre-disturbance metal(loid) concentrations (fluvial vs. atmospheric; see below) to evaluate temporal patterns of enrichment after development of the large-scale mining and ore-processing operations.

We recognize the extensive metal(loid)s research using multiple media (e.g., water, snow, soil, vegetation and sediment) in the central NWT and AOSR. Our focus here is to assemble sediment core records from lakes that provide a high resolution (sub-decadal) temporal perspective on the magnitude of As, Sb, V and Ni enrichment relative to pre-disturbance baselines. Important criteria for inclusion of available data in this synthesis include: 1) sediment cores were obtained from central depositional regions of lakes to ensure continuous sediment accumulation, 2) sediment cores were well-dated using standard radiometric methods (^{210}Pb, ^{137}Cs), and 3) pre-

disturbance concentrations of As, Sb, V and Ni were suitably characterized in stratigraphic profiles. The latter criterion is particularly important in the central NWT region because of the possibility of downward mobility of As derived from mine emissions. Thus, multiple measurements spanning decades to centuries prior to mining development are required for rigorous and accurate assessment of lake-specific pre-disturbance baseline concentrations of As and Sb. The criteria described here define the approach that we have taken during the past two decades.

Metal(loid) concentration profiles adhering to the above criteria were assembled from 51 lakes in the AOSR (upland near-field: n = 2; upland mid-field: n = 8; upland far-field: n = 10; floodplain: n = 5), PAD (upland: n = 2; floodplain: n = 12), SRD (upland: n = 1; floodplain: n = 1) and central NWT (upland near-field: n = 4; upland far-field: n = 6; Table 4.1). The spatial distribution of sites is strongly weighted to locations in relatively close vicinity of the mining operations (AOSR: 49% of lake sites; central NWT: 20%), and in the PAD (27%) where there have been persistent and long-held concerns regarding pollution from oil sands operations (Timoney and Lee 2009; Kelly et al. 2010; Schindler 2010; Mikisew Cree First Nation 2014). The SRD (4%) is far less well represented in our compilation. We followed the lake classification scheme used in previous publications and graduate student theses, with some minor modifications. We subdivided lakes into ‘floodplain’ and ‘upland’ based on their hydrological setting to distinguish and assess fluvial and atmospheric pathways of contaminant deposition, respectively. In most cases, entire sediment records were considered to receive contaminants via either fluvial or atmospheric pathways. Exceptions to this include floodplain lakes Down 1 and Up 10 in the AOSR, where the paleohydrological data indicated deposition of contaminants altered from fluvial pathways to predominantly atmospheric pathways after ~1980 (Klemt et al. 2020), and similarly floodplain lake SD2 within the SRD, where flood influence waned during the 1950s (MacDonald

et al. 2016). Within the AOSR, we adopted the lake classification system from Cooke et al. (2017), where upland lakes were categorized by distance from AR6, a central location within the AOSR: near-field as ≤ 20 km, mid-field as > 20-50 km and far-field as > 50 km. In central NWT, upland lakes that exclusively record atmospheric deposition of contaminants were grouped into near-field and far-field based on wind direction and distance from Giant Mine. Lakes located within a 40-km radius in the northwest (downwind) direction were classified as near-field lakes and lakes located outside the 40-km radius in the northwest direction and lakes located in the northeastern direction were classified as far-field lakes. We included northeastern lakes within the far-field category based on their comparable deposition of As and Sb, which is a slight modification from the classification developed by Jasiak et al. (2021).

Table 4.1 Summary of lake names, latitude and longitude, hydrological category (floodplain or upland), and sediment coring year. Source of original lake sediment core data is provided in the footnote.

Region	Lake name	Latitude	Longitude	Category	Sediment coring year
AOSR	Up 17	56.853	-111.433	Floodplain	2016[1]
	Up 10	56.934	-111.455	Floodplain	2016[1]
	Down 1	57.025	-111.485	Floodplain	2016[1]
	Down 26	57.218	-111.604	Floodplain	2018[1]
	Down 58	57.524	-111.523	Floodplain	2016[1]
	NE13	57.071	-111.475	Upland (near-field)	2011[2]
	NE20	57.125	-111.558	Upland (near-field)	2011[2]
	SE22	56.9	-111.140	Upland (mid-field)	2011[2]
	RAMP 226 (SW22)	56.81	-111.723	Upland (mid-field)	2011[2]
	RAMP 223 (NW35)	57.146	-111.983	Upland (mid-field)	2011[2]
	RAMP 268 (E15)	56.894	-110.903	Upland (mid-field)	2012[2]
	RAMP 418 (Kearle)	57.292	-111.238	Upland (mid-field)	2012[2]
	RAMP 225	56.8	-111.918	Upland (mid-field)	2012[2]
	RAMP 185	57.147	-110.863	Upland (mid-field)	2012[2]
	2014-B	56.985	-110.811	Upland (mid-field)	2012[2]
	RAMP 209 (P7)	57.231	-110.746	Upland (far-field)	2014[2]
	Gregoire	56.477	-111.145	Upland (far-field)	2013[2]

	RAMP 175 (P13)	57.315	-112.398	Upland (far-field)	2013[2]
	2014-C	56.386	-110.947	Upland (far-field)	2013[2]
	2014-Z	57.436	-112.527	Upland (far-field)	2014[2]
	2014-X	57.358	-112.731	Upland (far-field)	2014[2]
	RAMP 271	56.645	-110.221	Upland (far-field)	2014[2]
	2014-D	56.95	-113.025	Upland (far-field)	2013[2]
	RAMP 464 (L60)	57.655	-112.617	Upland (far-field)	2014[2]
	2014-Y	56.824	-113.268	Upland (far-field)	2013[2]
Athabasca	PAD 30	58.5090	-111.517	Floodplain	2016[3]
Delta (PAD)	PAD 31	58.4956	-111.518	Floodplain	2010[3]
	PAD 32	58.4968	-111.447	Floodplain	2015[3]
	PAD 26	58.4206	-111.272	Floodplain	2015[3]
	PAD M2	58.4178	-110.914	Floodplain	2016[3]
	PAD M7	58.4376	-111.050	Floodplain	2015[3]
	PAD M5	58.5032	-110.790	Floodplain	2015[3]
	PAD 71	58.5622	-110.881	Floodplain	2017[3]
Peace	PAD 52	58.8771	-111.751	Floodplain	2017[4]
Delta (PAD)	PAD 65	58.8969	-111.536	Floodplain	2016[4]
	PAD 66	58.9686	-111.498	Floodplain	2016[4]
	PAD 67	59.0907	-111.401	Floodplain	2016[4]
Upland (PAD)	PAD 18*	58.8960	-111.360	Upland	2010[5]
	AC5	58.4410	-110.676	Upland	2019[6]
SRD	SD2	61.2822	-113.582	Floodplain	2011[7]
	SD20**	61.3145	-113.326	Upland	2002[8]
central NWT	NW10	62.55289	-114.526	Upland (near-field)	2018[9]
	NW20	62.60833	-114.605	Upland (near-field)	2018[9]
	NW30	62.67228	-114.812	Upland (near-field)	2018[9]
	NW40	62.73889	-114.958	Upland (near-field)	2018[9]
	NW50	62.82556	-115.010	Upland (far-field)	2018[9]
	NW60	62.83469	-115.158	Upland (far-field)	2018[9]
	NW70	62.95111	-115.367	Upland (far-field)	2018[9]
	NW80	63.00206	-115.445	Upland (far-field)	2018[9]
	NE20	62.59838	-114.017	Upland (far-field)	2019[9]
	NE40	62.70584	-113.682	Upland (far-field)	2019[9]

[1]Klemt et al. (2020), [2]Cooke et al. (2017), [3]Kay et al. (2020), [4]Faber (2020), [5]Wiklund et al. (2012), [6]Brown et al. (2022), [7]MacDonald et al. (2016), [8]Mongeon (2008), [9]Jasiak et al. (2021)

* PAD 18 chronology and As and Sb concentrations are reported in Wiklund et al. (2012). Vanadium and Ni data are reported here.

** SD20 chronology and paleohydrology are reported in Mongeon (2008). Metal(loid)s data are reported here.

Sample collection

Sediment cores (one per lake) were collected from a central deep-water location of each study lake in the four regions using Glew (Glew 1989), Uwitec or Uwi-Glew-ee (Telford et al. 2021) gravity corers operated from a small boat or pontoon of a helicopter. Sediment cores were collected between 2002 and 2019, although most were collected during the past decade. Sediment cores were transported to a field base and sectioned within 24 hrs of collection into contiguous 0.5- or 1.0-cm intervals using a vertical extruder (Glew 1988; Telford et al. 2021). Sediment samples were kept refrigerated (4 °C) and in the dark until analysis. To provide consistent evaluation of metal(loid) enrichment across all four regions, we did not group sediment core samples from upland lakes in the AOSR into decadal intervals, as in the original publication by Cooke et al. (2017). Instead, every sediment sample was evaluated individually, as performed on cores from all other lakes. Further details regarding individual study areas, core processing, core dating and paleohydrological reconstructions are available in publications of the individual studies (Wiklund et al. 2012; MacDonald et al. 2016; Cooke et al. 2017; Kay et al. 2019; Klemt et al. 2020; Jasiak et al. 2021) and graduate student theses (SD20 in Mongeon 2008; PAD 52, PAD 65, PAD 66 and PAD 67 in Faber 2020; AC5 in Brown 2022).

Sample analysis

Freeze-dried samples from contiguous intervals of sediment cores from 31 lakes (AOSR floodplain lakes; all lakes in the PAD, SRD and central NWT regions) were analyzed for a suite of metals at ALS Canada (Waterloo or Edmonton) following the EPA method 200.2/6020A (aqua-regia hot block digestion and analysis by CRC-ICP-MS). Sediment samples from selected intervals of the other 20 sediment cores (upland lakes in the AOSR) were freeze-dried and analyzed for a suite of elements by CRC-ICP-MS after aqua-regia digestion (NLET Method 2404; Graney et al.

1995; Gobeil et al. 2013) at the National Laboratory for Environmental Testing (Burlington, Ontario, Canada; Cooke et al. 2017). Concentrations of aluminum (Al), As, Sb, V and Ni are utilized here.

Data analysis

Geochemical normalization

The need for geochemical normalization of metal(loid) concentrations is well recognized for sediment records from floodplain lakes and other aquatic systems where there is a marked range in energy of water flow and natural variability of sediment mineralogy (Foster and Müller 1981; Loring 1991; Covelli and Fontolan 1997; Kersten and Smedes 2002). Relatively high flow energy, for example during input of river flood water, is associated with coarser sediment particle size, which possesses relatively low metal(loid) concentrations due to low surface area to mass ratio of sediment. Conversely, low flow energy is associated with deposition of finer sediment particle size and higher metal(loid) concentrations due to higher surface to mass ratio. Thus, normalization is required to account for shifting metal(loid) concentrations that may be due to changes in flow energy. For this compilation, geochemical normalization was applied to V and Ni for floodplain and upland lakes in the AOSR, PAD, SRD, and central NWT. Although the potential for shifting flow energy is greater at floodplain lakes than at upland lakes, geochemical normalization was exercised at both sets of lakes for consistency. Two early studies by Wiklund et al. (2014) in the PAD and by MacDonald et al. (2016) in the SRD used lithium (Li) as the geochemical normalizer for V and Ni. Since then, studies have used Al, in part to evaluate river sediment monitoring data for evidence of enrichment relative to pre-disturbance metal(loid) concentrations generated from floodplain lake sediment cores because Al concentrations were consistently measured by AOSR-based monitoring programs whereas Li concentrations were not

(Owca et al. 2020; Klemt et al. 2021). Also, use of small-sample-corrected Akaike's Information Criterion (AICc) identified Al is statistically a superior geochemical normalizer compared to Li in the PAD (Kay et al. 2020; Owca et al. 2020). Consequently, we used Al to normalize sediment concentrations of V and Ni. The choice of Al or Li as a geochemical normalizer has little effect, however, since both elements produce comparable results (Kay et al. 2020; Owca et al. 2020).

In contrast to V and Ni, sediment profiles of As and Sb concentration were not normalized to Al because they did not possess positive relations with concentration of Al or other common lithogenic normalizers in the quiescent upland lakes of central NWT (Jasiak et al. 2021), a requirement for geochemical normalization (Loring 1991). In this primary region of investigation of gold mining pollution, relatively unvarying Al concentrations, likely owing to consistent composition and grain size of sediment profiles, contrasts with markedly varying concentrations of As and Sb due to time-varying inputs from the gold mining activities as well as potential redistribution of As and Sb due to diagenetic processes. To evaluate enrichment of As and Sb consistently across all regions, normalization also was not performed at the SRD, PAD, and AOSR.

Development of pre-disturbance baselines

To best achieve comparison of results for V and Ni among regions, where possible, pre-disturbance Al-normalized metal(loid) concentrations (i.e., 'baselines') were derived from pre-1920 sediment (and commonly to ~1700) because 1920 predates all mining activity in the AOSR, as well as enrichment by long-range atmospheric supply of metal(loid)s (Wiklund et al. 2012; Kay et al. 2022). At the AOSR, regional baselines were modified from Klemt et al. (2020) to include only sediment deposited pre-1920 rather than pre-1967. For the PAD, regional (i.e., multi-lake) baselines consisting of sediment deposited before 1920 were applied for lakes within the

Athabasca sector (Kay et al. 2020) and lakes within Peace sector (Table 4.1; Owca et al. 2020). For upland lakes in the PAD region, lake-specific baselines were established for PAD 18 and AC5 using sediment deposited before 1920. At the SRD, a baseline was developed for SD20 (an upland lake) using sediment deposited pre-1920. At SD2 (a floodplain lake), however, the baseline was developed using sediment deposited during the 1920s because no pre-1920 data were available. At central NWT, baselines were developed separately for the subset of near-field lakes and subset of far-field lakes using sediment deposited pre-1920.

In contrast to V and Ni, non-normalized As and Sb baselines were developed for most of the 51 lakes individually (exceptions include Peace Delta and Athabasca Delta floodplain lakes in the PAD and floodplain lakes in the AOSR) using pre-1900 data, where available, given the possibility of downward mobility of these metal(loid)s. Development of lake-specific baselines follows Jasiak et al. (2021) because underlying geology varies among the lakes in central NWT. Mean pre-1900 concentrations were calculated and applied for floodplain lakes in each of the Athabasca Delta, Peace Delta and AOSR, given their similar respective geological settings. For the upland lakes in the PAD region (PAD 18, AC5), lake specific baselines were developed using pre-1900 concentrations. At the SRD, due to a lack of pre-1900 data for SD2, the mean pre-1900 value from SD20 was applied. For upland lakes in the AOSR, pre-1920 concentrations were used due to insufficient pre-1900 data. At central NWT, evidence of downward As mobility in sediment cores from NW10, NW20 and NW40 (Leclerc et al. 2021; Jasiak et al. 2021) prevented use of a static stratigraphic horizon equivalent to 1900 for defining pre-disturbance baseline. Instead, following Jasiak et al. (2021), the mean concentration of As and Sb within a zone of near-constant values in the lower portion of the stratigraphic profile for each lake was considered pre-disturbance to accommodate post-depositional mobility of As.

Enrichment factor calculation

We focus on the use of concentration-based enrichment factors (EF), which are a commonly used metric to quantify and compare the magnitude of enrichment among metal(loid)s and sites relative to a pre-disturbance baseline (Boës et al. 2011; Birch 2017). Concentrations of As, Sb, V and Ni have been published within the individual publications or are publicly available, except for AC5 (see Table 4.1). Enrichment factor profiles are provided for all four metal(loid)s in each of the study regions (AOSR, PAD, SRD, central NWT) even though central NWT is well beyond the expected limit of dispersal of V and Ni from bitumen mining in the AOSR, and the AOSR is well outside the expected limit of dispersal of As and Sb from gold mining in central NWT. Enrichment factors were calculated for Al-normalized concentrations of V and Ni in the AOSR, PAD, SRD and central NWT according to the formula used by previous studies (Wiklund et al. 2014; Cooke et al. 2017; Kay et al. 2020; Klemt et al. 2020; Owca et al. 2020):

Equation (1): $EF = (X/Al)_i/(X/Al)_{pre\text{-}1920}$

where X_i is the measured concentrations of V or Ni, respectively, and Al_i is the measured concentration of Al for a specific sediment interval (i), and $X_{pre\text{-}1920}$ are the expected values for V or Ni in sediment deposited before 1920 as derived from the equation of the regression line for the V-Al or Ni-Al relation when $Al_{pre\text{-}1920} = Al_i$ (Table 4.2).

EF computations used a simplified version of equation (1) for As and Sb because their concentrations were not normalized to Al:

Equation (2): $EF = M_x/(M_{pre\text{-}disturbance})$

where M_x is the concentration of As or Sb at sediment core interval 'x' and $M_{pre\text{-}disturbance}$ is the mean pre-disturbance concentration for As or Sb in the pre-disturbance stratigraphic interval(s) (Table 4.2).

For both variations of the formula (equations 1 and 2), an EF of 1.0 indicates no change in the metal(loid) concentration relative to the pre-disturbance baseline concentration, whereas an EF of 2.0 indicates a doubling of the concentration above the pre-disturbance baseline concentration. Expression of the sediment metal(loid) concentrations as EFs allowed comparable assessments of enrichment across all samples from all four regions (AOSR, PAD, SRD, central NWT) and for all four metal(loid)s analyzed. We used thresholds and terminology presented in the widely cited comprehensive review by Birch (2017) to express the category of enrichment of the metal(loid)s above the pre-disturbance baselines, where EFs ≤ 1.5 represent the range of natural variability or 'pristine conditions', EFs > 1.5-3.0 represent 'minimal enrichment', EFs > 3.0-5.0 represent 'moderate enrichment', EFs > 5.0-10.0 represents 'considerable enrichment' and EFs > 10.0 represent 'severe enrichment'. A generalised additive model (GAM) was used to compute synthetic temporal trends in As, Sb, V and Ni EF values for groups of lakes (AOSR: near-, mid-, far-field upland lakes and floodplain lakes; Athabasca Delta; Peace Delta; Giant Mine near-field; Giant Mine far-field) within each region and for individual lakes (AC5, PAD 18, SD2, SD20) where there was only one in a group. GAMs were computed back to 1850, where possible. GAMs were utilized because they are an unbiased smoother and are recommended for paleolimnological studies where data points are not equally spaced in time (Simpson 2018). GAMs were performed using the *mgcv* (version 1.8.28; Wood 2017) and *Schoenberg* (version 0.0-6; Simpson 2018) packages in R (Version 3.5.2; R Core Team 2020), with a consistent k-value of 10 (number of basis functions used).

Table 4.2 Summary of V and Ni pre-disturbance regression equations, mean pre-disturbance As and Sb (µg/g) concentrations and number of pre-disturbance samples (*n*).

Region or lake	V pre-disturbance equation	Ni pre-disturbance equation	*n*
AOSR	[V] µg/g = 0.0025*([Al] µg/g) + 4.75 Adjusted R^2 = 0.97	[Ni] µg/g = 0.0015*([Al] µg/g) + 13.80 Adjusted R^2 = 0.65	213
Athabasca Delta	[V] µg/g = 0.0023*([Al] µg/g) + 7.18 Adjusted R^2 = 0.87	[Ni] µg/g = 0.0011*([Al] µg/g) + 10.10 Adjusted R^2 = 0.50	123
Peace Delta	[V] µg/g = 0.0031*([Al] µg/g) + 2.84 Adjusted R^2 = 0.96	[Ni] µg/g = 0.0017*([Al] µg/g) + 12.3 Adjusted R^2 = 0.67	80
PAD 18	[V] µg/g = 0.0017*([Al] µg/g) + 5.21 Adjusted R^2 = 0.96	[Ni] µg/g = 0.0009*([Al] µg/g) + 8.18 Adjusted R^2 = 0.83	22
AC5	[V] µg/g = 0.0033*([Al] µg/g) + 2.55 Adjusted R^2 = 0.62	[Ni] µg/g = 0.0007*([Al] µg/g) + 2.32 Adjusted R^2 = 0.65	38
SD2	[V] µg/g = 0.0034*([Al] µg/g) + 0.45 Adjusted R^2 = 0.98	[Ni] µg/g = 0.0017*([Al] µg/g) + 10.87 Adjusted R^2 = 0.97	4
SD20	[V] µg/g = 0.0029*([Al] µg/g) + 3.90 Adjusted R^2 = 0.94	[Ni] µg/g = 0.0013*([Al] µg/g) + 12.30 Adjusted R^2 = 0.78	15
Central NWT Near-Field	[V] µg/g = 0.0021*([Al] µg/g) – 1.32 Adjusted R^2 = 0.94	[Ni] µg/g = 0.0003*([Al] µg/g) + 18.26 Adjusted R^2 = 0.08	44
Central NWT Far-Field	[V] µg/g = 0.0021*([Al] µg/g) + 3.92 Adjusted R^2 = 0.89	[Ni] µg/g = 0.0014*([Al] µg/g) + 14.42 Adjusted R^2 = 0.59	82
	Mean pre-disturbance [As] (µg/g)	Mean pre-disturbance [Sb] (µg/g)	*n*
NW10	16.58	0.39	10
NW20	22.00	0.20	8
NW30	10.56	0.16	11
NW40	9.58	0.22	15
NW50	15.74	0.35	24
NW60	7.41	0.17	10
NW70	15.85	0.37	16
NW80	4.92	0.13	13
NE20 (NWT)	21.44	0.16	16
NE40	2.25	0.10	3
SD2	8.19	0.51	0
SD20	8.19	0.51	15
PAD 18	2.64	0.17	22
AC5	1.35	0.17	38
Peace Delta	12.70	0.73	80
Athabasca Delta	6.68	0.35	123
AOSR Floodplain	9.82	0.54	124
NE20 (AOSR)	0.36	0.04	9
SE22	0.52	0.05	4
RAMP 226	0.71	0.04	3
RAMP 223	0.59	0.04	12
RAMP 268	0.88	0.04	3
RAMP 418	1.27	0.11	9
RAMP 225	0.65	0.68	5
RAMP 185	0.76	0.03	4
2014-B	1.87	0.02	3
RAMP 209	1.24	0.03	3
RAMP 175	1.88	0.08	2
2014-C	2.25	0.12	4
2014-Z	2.93	0.22	4

2014-X	1.91	0.13	5
RAMP 271	3.88	0.06	4
2014-D	1.33	0.08	5
RAMP 464	16.27	0.53	5
2014-Y	2.05	0.06	3
RAMP 282	0.87	0.09	2

Results and Interpretation

Assessment of metal(loid) enrichment from oil sands mining in the AOSR

At lakes within the AOSR, GAM-estimated trends demonstrated marked enrichment of V and Ni via atmospheric pathways (i.e., upland lakes), but not via fluvial pathways (i.e., floodplain lakes; Figure 4.2). Vanadium became enriched above the pre-1920 baseline beginning in the late 1960s at near-field (≤ 20 km) and mid-field (> 20-50 km) upland lakes (Figure 4.2a). GAM-estimated trend lines for V EFs peaked during the 1980s to 1990s at 11.9 ('severe enrichment') for the near-field lakes and 2.4 ('minimal enrichment') for the mid-field lakes, and declined thereafter. Enrichment factors for V (and Ni) during the pre-1920 baseline period exceeded 1.0 for the near- and mid-field lakes, which suggests EFs during the mining period may be overestimated. In contrast, the GAM-estimated pre-disturbance baseline and subsequent mine-era trend line for the far-field lakes (> 50 km) remained stable around 1.0 and did not exceed the 'minimal enrichment' threshold. GAM-estimated trends for Ni EFs did not rise concurrently with V EFs except at the near-field lakes, where the peak value (2.4) suggests 'minimal enrichment' of Ni at the same time as peak 'severe enrichment' occurred for V (~1985) via atmospheric pathways (Figure 4.2b). The GAM-estimated trend lines for Ni EFs identified 'minimal enrichment' of mid-field lakes and 'no enrichment' of far-field lakes. The GAM-estimated trend lines for V and Ni EFs remained stable around 1.0 during the mine era for intervals of strong-flood and weak-flood influence at AOSR floodplain lakes (Figure 4.2c,d). An exception is Down 1, a floodplain lake ~1 km downstream of

AR6, where an interval of weak-flood influence after the 1980s coincided with rising V EFs to a maximum of 1.7, which signifies 'minimal enrichment', when V was supplied by atmospheric pathways (Figure 4.2c; Klemt et al. 2020). During the same interval at Down 1, Ni EFs did not exceed the 'minimal enrichment' threshold (Figure 4.2d). To summarize, results from lakes in the AOSR show mining-era enrichment of V at near-field ('severe') and mid-field ('minimal') upland lakes and during an interval of weak-flood influence at one floodplain lake ('minimal'; Down 1) located within the near-field zone. Also, 'minimal enrichment' of Ni occurred at the near-field upland lakes. Collectively, these findings indicate atmospheric pathways are the primary source of enrichment from oil sands mining in the AOSR. Results provide no evidence of enrichment of V or Ni via fluvial pathways.

In contrast to the AOSR, GAM-estimated V and Ni EF trend lines for lakes in the PAD, SRD and central NWT identified no enrichment since onset of oil sands mining via fluvial or atmospheric pathways based on records from floodplain and upland lakes, respectively (Figure 4.2e-l). Comparable temporal patterns in V and Ni EFs in lakes flooded by the Peace and Athabasca rivers provide compelling evidence that oil sands mining within the AOSR has not increased concentrations of these elements via the Athabasca River to the Athabasca Delta (Figure 4.2e,f). Enrichment factors of V and Ni remained close to 1.0 and did not exceed the 1.5 threshold of 'minimal enrichment' at upland lakes PAD 18 and AC5, identifying that onset and growth of oil sands mining are not associated with V or Ni enrichment of lakes in the PAD via atmospheric pathways (Figure 4.2g,h). Similar results occur at the SRD, where GAM-estimated trend lines for V and Ni EFs remained temporally stable near 1.0 and no individual sediment samples exceeded the 'minimal enrichment' threshold from floodplain lake SD2 and upland lake SD20. At central NWT, GAM-estimated trend lines for V and Ni EFs remain stable around 1.0 (Figure 4.2k,l),

except for one lake (NE40) where Ni EFs are elevated above the ‘minimal enrichment’ threshold during both the pre- and post-mining intervals due to anomalously high concentrations of Ni relative to Al compared to the other lakes.

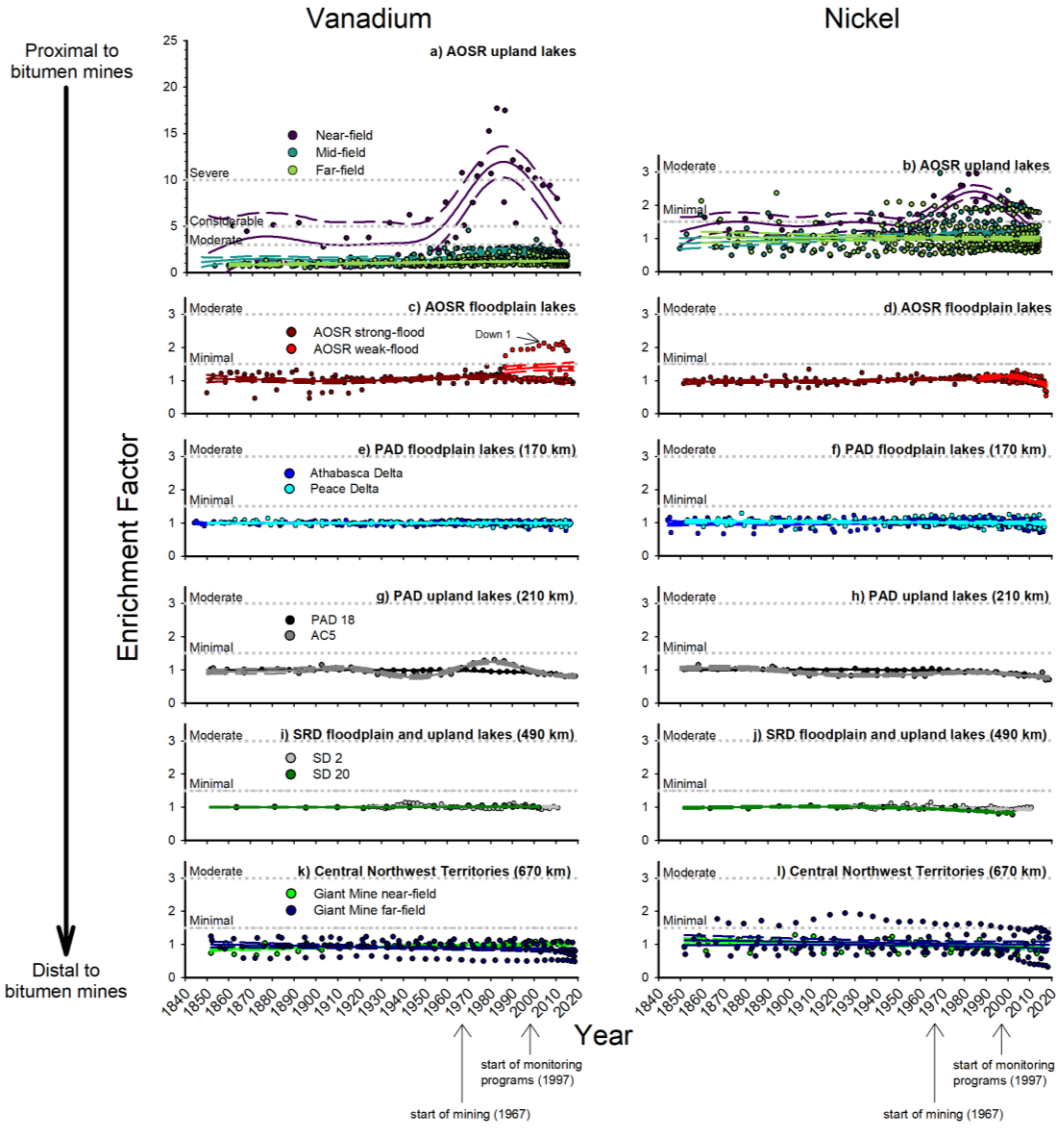

Figure 4.2 GAM-based estimated trends (solid lines) fitted to enrichment factors of vanadium and nickel for a), b) Athabasca Oil Sands Region upland lakes, c), d) Athabasca Oil Sands Region floodplain lakes, e), f) Peace-Athabasca Delta floodplain lakes, g), h) Peace-Athabasca Delta upland lake and i), j) Slave River Delta floodplain and upland lakes with distance from the AOSR in brackets for e) to j). The dashed lines surrounding the solid GAM-based estimated trend lines are the 95% confidence intervals. The horizontal grey dotted lines at EF of 1.5, 3.0, 5.0 and 10.0 mark 'minimal enrichment', 'moderate enrichment', 'considerable enrichment' and 'severe enrichment' thresholds, respectively (following Birch 2017).

Assessment of metal(loid) enrichment from gold mining in central NWT

GAM-estimated trend lines identified enrichment of As and Sb via atmospheric pathways in the central NWT region generally coincident with onset and growth of large-scale gold mining (Figure 4.3a,b). Atmospheric transport and deposition are evident from greater enrichment of As and Sb at near-field versus far-field sites. The latter includes lakes beyond 40 km of Giant Mine in the prevailing wind direction and lakes 20-40 km perpendicular to the prevailing (northeastern) wind direction. At far-field lakes, GAM-estimated trend lines for As and Sb EFs reached 'considerable enrichment' coincident with or shortly after peak emissions in the late 1950s and have since declined to levels indicative of 'moderate enrichment'. At the near-field sites, however, GAM-estimated trend lines for As and Sb EFs have trended upwards since before onset of gold mining, with highest values (As = 62.7, Sb = 44.8) occurring in the uppermost sediment strata indicating 'severe enrichment' relative to pre-disturbance baselines. We note that EFs for As and Sb exceeded 1.0 at near-field lakes prior to start of mining (Figure 4.3a,b), which may be due to uncertainty in characterization of pre-disturbance values and a consequence of interpolation by GAMs given limited downward mobility of arsenic as demonstrated by Leclerc et al. (2021).

At an upland lake in the SRD (SD20), GAM-estimated trend lines for As and Sb EFs were persistently close to 1.0 indicating no evidence of enrichment from gold mining in central NWT via atmospheric pathways (Figure 4.3c,d). Similar patterns were observed at a floodplain lake (SD2) in the SRD for Sb EFs (Figure 4.3d). However, EFs for As at SD2 exceeded the 1.5 threshold for 'minimal enrichment' in three samples from the 1950s during an interval of weak-flood influence and two samples at ~1931 and ~2010 during intervals of strong-flood influence. During the same time periods, there is no corresponding enrichment of Sb at SD2. At an upland lake in the PAD (PAD 18), GAM-estimated trend lines remained within the range of 'no enrichment' for

As and Sb (i.e., EFs did not exceed 1.5), but a slight rising trend was observed during ~1920-1970s, followed by a declining trend to pre-disturbance baselines (Figure 4.3e,f). At AC5, the GAM-estimated trend lines for both As and Sb EFs slightly exceeded the 'minimal enrichment' threshold of 1.5 as part of gradual rising trends from ~1890-1930 and are followed by declines to below baseline post-1940 (Figure 4.3e,f).

GAM-estimated trend lines for As and Sb EFs are temporally consistent around 1.0 for floodplain lakes in the PAD and AOSR (Figure 4.3g-j). Enrichment factors for As exceed the 3.0 threshold for 'moderate enrichment' in samples from one lake (M7) in the Athabasca Delta of the PAD between ~1930 and ~1970. There is no coincidental rise in Sb EFs from the same lake during this time interval. GAM-estimated trend lines for As EFs at near- and far-field upland lakes in the AOSR remain near-constant at 1.0 while there is a slight rising trend beginning ~1930 at the mid-field lakes above the 'minimal enrichment' threshold. Similarly, the GAM-estimated trend lines for Sb EFs at near- and far-field lakes remain constant around 1.0 while the mid-field GAM-estimated trend line exceeds the 'minimal enrichment' threshold during ~1961-~1999 and reached a peak value just below the 'moderate enrichment' threshold.

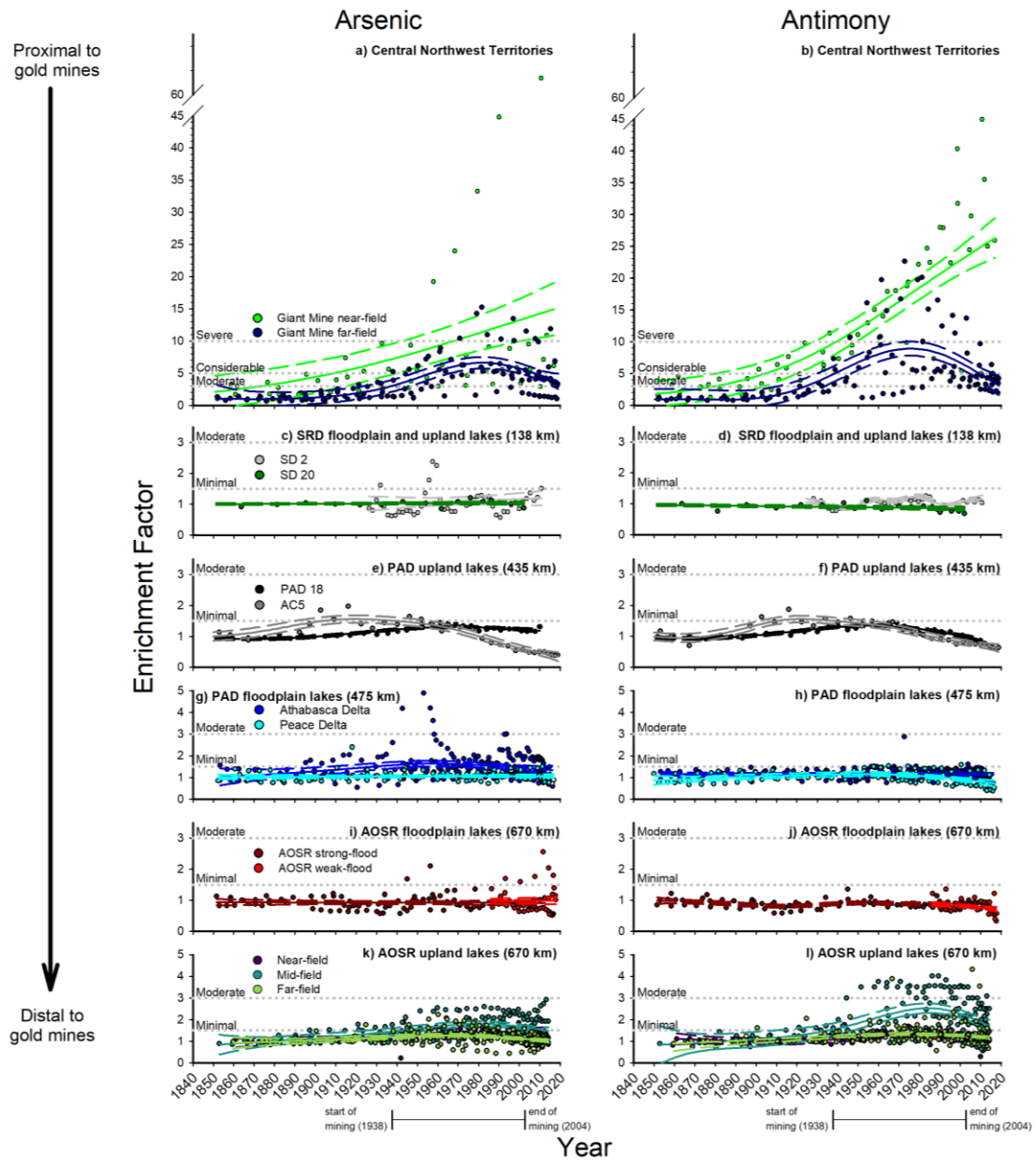

Figure 4.3 GAM-based estimated trends (solid lines) fitted to enrichment factors of arsenic and antimony for a), b) central Northwest Territories, c), d) Slave River Delta floodplain (SD2) and upland (SD20) lakes, e), f) Peace-Athabasca Delta upland lakes, g), h) Peace-Athabasca Delta floodplain lakes, i), j) Alberta Oil Sands Region floodplain lakes and k), l) Alberta Oil Sands Region upland lakes with distance from Yellowknife in brackets for c) to f). The dashed lines surrounding the solid GAM-based estimated trend lines are the 95% confidence intervals. The horizontal grey dotted lines at EF of 1.5, 3.0, 5.0 and 10.0 mark 'minimal enrichment', 'moderate enrichment', 'considerable enrichment' and 'severe enrichment' thresholds, respectively (following Birch 2017).

Discussion and Commentary

Synthesis of findings and their implications

Systematic analysis of metal(loid) concentrations in lake sediment records analyzed from the AOSR to central NWT has permitted characterization of pre-disturbance reference conditions and quantification of enrichment of contaminants of concern from bitumen and gold mining operations via atmospheric and fluvial pathways. Enrichment factors of V and Ni in sediment cores indicate enrichment in the AOSR via atmospheric pathways at near- ('severe') and mid-field ('minimal') upland lakes (i.e., within 50 km of the central AR6 location) but not at greater distances via atmospheric pathways as shown by upland lake sediment records at the PAD region (PAD 18, AC5) and SRD (SD20). Note that use of the term 'severe' follows terminology established by Birch (2017) and is not meant to necessarily imply ecological impairment. Analyses of other environmental archives such as peat cores have also illustrated that atmospheric releases of V and Ni from oil sands mining and processing activities are primarily deposited within a 50-km radius of open pit mines (Shotyk et al. 2021), consistent with snowpack monitoring data (Kirk et al. 2014). Vanadium and Ni are also not enriched at any distance via fluvial pathways to downstream floodplain lakes. As discussed by Klemt et al. (2020), oil sands releases of V to the atmosphere are small relative to the natural base load and immense dilution capacity of the Athabasca River. Thus, there is no evidence of enrichment of these oil sands indicator metal(loid)s at the PAD, at two lakes at the SRD or at lakes in central NWT. Based on the depositional pattern in snow in the AOSR, As has also been associated with oil sands industrial emissions (Kelly et al. 2010). However, As was not enriched at near- or far-field upland lakes in the AOSR. 'Minimal' enrichment was observed at mid-field upland lakes but began in the 1930s before onset of oil sands mining and processing activities.

Consistent, strong evidence among the datasets and metal(loid)s of concern included in our systematic re-analysis identifies that the Peace-Athabasca Delta and Slave River Delta are located well beyond areas of influence from atmospheric emissions from bitumen mines in the AOSR and gold mines in central NWT, and that bitumen mining in the AOSR has not enriched aquatic sediment in the Athabasca River or the downstream deltas. This knowledge is critical to inform impending decisions by the World Heritage Committee and International Union for Conservation of Nature (WHC/IUCN) about the UNESCO World Heritage status of WBNP. Petition for a downgrade in World Heritage status and subsequent documents have identified concerns related to oil sands pollution at the PAD (Mikisew Cree First Nation 2014; WHC/IUCN 2017, 2020; IEC 2018; WBNP 2019). Yet, such evidence has not materialized in the numerous lake sediment cores that have been analysed for metal(loid)s here and in other publications (Wiklund et al. 2012; Kay et al. 2020, 2022). The unique ability to quantify pre-disturbance, reference conditions from lake sediment cores has been instrumental to drawing these conclusions. We recognize that organic contaminants are also of primary concern in the AOSR and PAD, and snowpack and paleolimnological studies (AOSR: Kurek et al. 2013; Chibwe et al. 2021; PAD: Hall et al. 2012; Jautzy et al. 2015; Salat et al. 2021) align well with our conclusions based on the metal(loid)s. The pre-industrial baselines presented in this study can serve as a valuable source of information for evaluating future sediment quality monitoring data (from surficial lake and river-bottom sediments) collected by long-term monitoring programs. This approach may be used to detect enrichment of trace elements following industrial spills (such as occurred in 2013 following failure of a wall of a tailings pond of the Obed Mountain Mine; Cooke et al. 2016) and pending future discharge of treated oil sands process water directly into the Athabasca River (Hicks and Scrimgeour 2019).

In central NWT, lake sediment records of As and Sb EFs identify 'severe' enrichment at near-field distances from the former gold mines (< 40 km), which align with a 'zone of immediate influence' of mine emissions identified by other researchers (Galloway et al. 2012, 2015; Palmer et al. 2015; Cheney et al. 2020), whereas far-field lakes (≥ 40 km to the NW and ≥ 20 km to the NE) provide evidence of considerable enrichment beyond the 'zone of immediate influence'. Except for NW10 and NW20, maximum EFs occurred a few decades ago and are at various stages of returning to pre-disturbance values, indicating risk to ecosystem health is on the decline. In contrast, rising EFs at NW10 and NW20 identify increasing supply from the terrestrial catchment or resupply from within the lakes (Leclerc et al. 2021; Jasiak et al. 2021), reflecting ongoing legacy effects of Giant and Con mine emissions where risks to ecosystem health may need to be investigated further. Similarly, Cheney et al. (2020) illustrated concentrations of As and Sb were highest near Giant Mine and declined with distance. Their lake sediment paleotoxicity results demonstrated lingering aquatic ecosystem effects within this radius two decades after mine closure. We note it is well established that redox-sensitive elements such as As may migrate in the sediment column where there are steep gradients of As concentration in the sediment and porewater (Schuh et al. 2018; Leclerc et al. 2021). Despite little evidence of downward As migration (Leclerc et al. 2021), sufficient downcore measurements in central NWT lakes were performed to ensure pre-1900 stratigraphic intervals of near-constant baseline As concentrations could be identified (see Jasiak et al. 2021). Conversely, upward migration may alter the timing and magnitude of peak EF values. Indeed, upward mobility of As was identified by Leclerc et al. (2021) at NW10, NW20 and NW40 but not at the other NW lakes in central NWT. Thus, upward migration may have led to underestimation of the peak EF values and overestimation of EF values in uppermost sediments for near-field lakes.

In recognition of the potential for post-depositional mobility to alter As concentrations in sediment profiles, we assessed the integrity of the stratigraphic records within the central NWT lakes by comparing the post-mining sediment excess (i.e., anthropogenic) inventories of As and Sb to independent estimates of mining emissions (Bromstad et al. 2017). This comparison identifies striking correspondence between estimates of total landscape anthropogenic deposition for As (9,810 mt) and Sb (240 mt) within a 50-km radius of Giant Mine derived from sediment cores and estimates of lifetime As (9,970 mt) and Sb (200 mt) emissions from Giant and Con mines. The estimates based on sediment cores used wind-weighted calculations of excess inventories following Wiklund et al. (2017; see Appendix D). Close correspondence between releases to air and estimates of atmospheric deposition to the landscape reconstructed from the sediment cores demonstrates the vast majority of mine emissions were deposited within a 50-km radius. This reservoir of legacy deposition has potential to enter lakes via runoff from their terrestrial watersheds and to elevate lake-water concentrations via release from lake sediment.

A semi-empirical predictive model, calibrated using sediment cores from the 10 central NWT lakes, was used to explore the spatial distribution of total atmospheric anthropogenic landscape inventories of As and Sb deposition released during the period of mining operations (1948 – 2004; Figure 4.4; Appendix D). Despite sampling mainly in the prevailing wind direction (NW), we leveraged the sediment core data and wind rose data to predict deposition in all radial directions. The maps display the area with the highest deposition (within ~40 km) is congruent with other assessments of legacy pollution from Giant and Con mines (Galloway et al. 2012, 2015; Palmer et al. 2015; Cheney et al. 2020). These results demonstrate the utility and potential of systematic collection and analyses of lake sediment cores to quantify spatial patterns of anthropogenic metal(loid) deposition in addition to the conventional provision of time-series data.

The predictive landscape model could be further tested by analyzing sediment cores from lakes at varying distances and directions from Giant Mine.

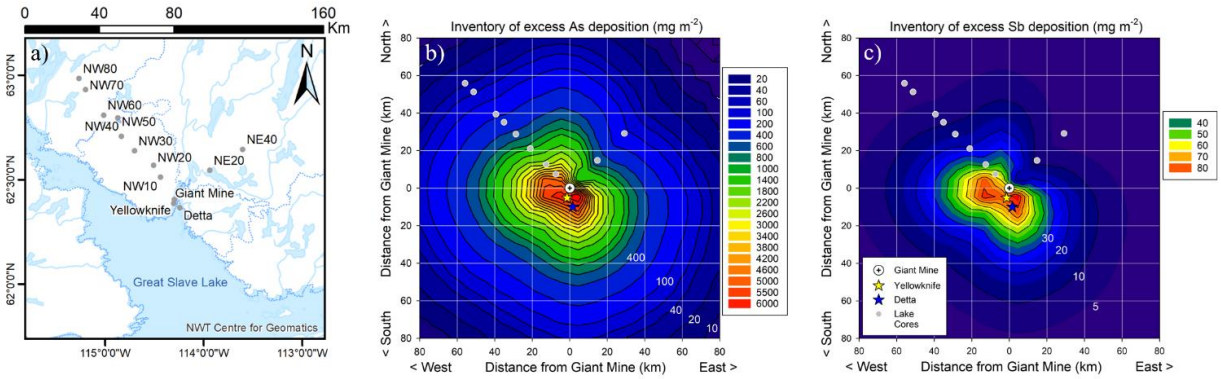

Figure 4.4 a) Map showing locations of the study lakes within central NWT and Giant Mine, Yellowknife and Detta (open source: https://www.geomatics.gov.nt.ca/en/maps-available-base-maps). Panels b) and c) show inferred distributions of locally sourced atmospheric anthropogenic As and Sb inventories (mg m^{-2}), respectively, accumulated on the landscape and centered on Giant Mine. The maps in panels b) and c) are products of a semi-empirical predictive model based on lake sediment core and wind rose data (see Appendix D).

Farther afield, sediment core records from upland lakes in the SRD (SD20) and at the PAD region (PAD 18, AC5) provide no evidence of atmospheric-derived As or Sb enrichment from gold mining activities in central NWT. Minimal enrichment of As, however, was observed at SD2 during the period of peak emissions from Giant Mine and was speculated by MacDonald et al. (2016) as associated with gold mining activities. Interestingly, far-field atmospheric delivery of As has been reported to travel up to 104 km from a smelter in Flin Flon, Manitoba (McMartin et al. 1999). Such knowledge combined with known high emissions at Giant Mine provide reason to suspect that small quantities of As could potentially be transported to the SRD, 138 km to the south of the gold mines. However, a lack of correspondence with SD20, an exclusive recorder of atmospheric pathways, makes this interpretation tenuous especially given the above conclusion that most of the emissions from the gold mines were deposited within a 50-km radius (Figure 4.4).

Alternatively, the peak in As EF at SD2 may have been caused by naturally occurring processes in the lake as the site became less influenced by river floodwaters and more strongly influenced by evaporation (Brock et al. 2010; MacDonald et al. 2016). Thus, the PAD and SRD are the only regions analyzed that present little to no evidence of metal(loid) pollution from either the bitumen mines in the AOSR or the gold mines in central NWT. Although we recognize that this statement includes data from only two lake sediment cores in the SRD, given that V and Ni enrichment from bitumen mines at the AOSR is not identified at the PAD, it seems highly unlikely that V and Ni enrichment has occurred farther away from this source.

Methodological recommendations

During the past decade, we have devoted substantial resources and given considerable thought to developing the methodological aspect of our contaminant studies. Below, we reflect upon some of the key aspects of our methodology including approaches to incorporate paleohydrological knowledge to discriminate atmospheric versus fluvial pathways of contaminant transport to floodplain lakes, apply geochemical normalization, define reference conditions to characterize pre-mining baselines, and employ EFs and recommended thresholds to quantify the degree of contaminant enrichment.

Knowledge of paleohydrological conditions was key for deciphering pathways and sources of contaminant delivery to floodplain lakes. Prior to our studies, paleolimnological analyses of floodplain lake sediment were relatively underutilized as recorders of contaminant deposition because they are situated in hydrologically complex landscapes with multiple potential processes influencing stratigraphic variation in sediment and contaminant deposition. Notable exceptions include a study of floodplain lakes in the Mackenzie River Delta in northwestern Canada by Headley et al. (2002) where spatio-temporal variation in influence of floodwaters was used to

support conclusions of factors influencing composition and concentration of PAH compounds, and a study of billabongs (oxbow lakes) in Australia by Lintern et al. (2016) where flood signal strength was considered in the interpretation of heavy metal concentrations to identify transport pathways for contaminant deposition. We adopted an approach comparable to that used by Lintern et al. (2016) by coupling conventional paleohydrological techniques, including determination of sediment composition and inferred sources via loss-on-ignition analysis and carbon-to-nitrogen ratios, with stratigraphic contaminant profiles to demonstrate floodplain lakes can be sensitive records of both fluvial and atmospheric pathways. For instance, MacDonald et al. (2016) and Klemt et al. (2020) highlighted use of this approach in the SRD and AOSR by delineating intervals of strong- and weak-flood influence to evaluate temporal changes in contaminant deposition via fluvial and atmospheric pathways, respectively. For example, naturally shifting hydrological conditions can mimic the effects of increased anthropogenic supply of contaminants in lake sediment records (Salat et al. 2021).

The numerous studies synthesized here have responded to calls by expert panels and scientists to establish rigorous pre-disturbance baselines for substances of concern as a benchmark to quantify the extent of enrichment caused by mining emissions (e.g., Dowdeswell et al. 2010; Palmer et al. 2015). Paleolimnological approaches allow for robust site- or region-specific determination of reference conditions for metal(loid)s of concern and systematic evaluation of their temporal patterns of enrichment since onset of mining. A critical detail employed by all our studies of V and Ni is the use of geochemical normalization to account for changes in grain size due to shifting flow energy conditions. This is important because grain size influences metal(loid) concentrations, and use of geochemical normalization to account for this phenomenon has long been advocated for by others (e.g., Loring 1991, Kersten and Smedes 2002). As described by

Loring (1991), geochemical normalization has an advantage over granulometric methods (e.g., % fines; Moir et al. 2021) because it accounts for natural mineralogical variability as well as granular variability. Broad distribution of metal concentrations that define pre-disturbance Al-V and Al-Ni relations across numerous hydrologically complex landscapes substantiate the need for geochemical normalization (MacDonald et al. 2016; Kay et al. 2020; Klemt et al. 2020; Owca et al. 2020). Mostly high adjusted R^2 values (Table 2) for the pre-disturbance relations identify strong sensitivity of the approach for tracking enrichment in V and Ni during the post-mining era. Previous studies have demonstrated strong statistical power for detecting enrichment using this approach (Klemt et al. 2020; Owca et al. 2020). Fundamental to achieving these strong relations is extensive measurements of pre-disturbance metal(loid) concentrations in the lake sediment records, where possible, to capture the range of natural variability. While geochemical normalization of trace elements in hydrologically dynamic floodplain lakes is preferable, this is not always possible (e.g., Kay et al. 2022). For upland lakes in central NWT, relations between As and Sb with a geochemical normalizer were explored but were weak and did not meet criteria for geochemical normalization (Loring 1991). However, given that energy of flow did not vary substantially over time at these quiescent upland lakes, inability to normalize did not influence interpretation of the results. We contend that measurement of pre-disturbance metal(loid) concentrations from lake sediment is a robust approach for quantifying pre-disturbance baselines, and we note that central NWT values overlap with geochemical background estimates derived from soils in this region (Palmer et al. 2021).

We recommend caution be exercised when sites span low concentrations of the geochemical normalizer (e.g., < 1000 µg/g of Al) because uncertainty in estimates of Al concentration near the detection limit may cause pre-disturbance EF values to exceed 1.0, as

occurred for V and Ni at the near-field upland lakes in the AOSR (Figure 4.2a,b). Use of samples with such low concentrations anchors the pre-disturbance baselines for application to post-disturbance samples (Klemt et al. 2020, 2021), but may inflate estimates of enrichment factors. Care should also be taken when calculating and interpretating EFs if the pre-disturbance baseline is not adequately defined. Interpretation of EFs at low concentrations of the metal(loid)s of concern can be problematic when a modest rise induces a substantial increase of EF values, because concentrations may remain well below values associated with risk of ecological impairment. We note that maximum As concentrations for the central NWT lakes exceed the CCME Probable Effects Levels (PEL) for protection of aquatic life (Jasiak et al. 2021) whereas V concentrations in lakes of the AOSR (Cooke et al. 2017; Klemt et al. 2020) remained consistently below the Soil Quality Guideline (130 ug/g) despite a 10-fold increase above baseline at near-field upland lakes during the mining era.

Pre-disturbance and enrichment metrics are frequently used by researchers to evaluate the degree of pollution caused by emissions from industrial activities. Examples of the former include common use of global average concentrations (Pekey 2006; Karbassi et al. 2008; Kabir et al. 2011), concentrations measured at pristine areas within the same landscape (Batley and Maher 2001; Simpson et al. 2005) and estimates of source material from local catchment geology (Carral et al. 1995; Salminen and Tarvainen 1997). However, use of these approaches is often compromised because global averages usually cannot accurately represent site-specific pre-disturbance concentrations or inform about the range of natural variation, and contemporary pristine reference conditions are difficult to obtain (Birch 2017). These various methods can then lead to designation of arbitrary enrichment thresholds, which are often tailored to specific study lake(s) (Brady et al. 2015; Birch 2017). To provide a consistent framework for evaluating enrichment, we adopted

thresholds recommended by Birch (2017) because they allow for comparison among multiple landscapes with different background concentrations of metal(loid)s and are suitable to capture a large range of anthropogenic influence. On occasion, we have expressed enrichment as residual concentrations relative to pre-disturbance baseline, which are reported in units of concentration (µg/g of dry sediment; Wiklund et al. 2014; MacDonald et al. 2016). This can complement the use of EFs to inform if the level of enrichment represents a substantial increase in concentration and is advisable to guard against over-interpretation of EFs that may become inflated at low concentrations as discussed above. Using EFs and the Birch (2017) thresholds as a guide, we were able to demonstrate 'severe enrichment' only occurred via atmospheric transport within a 40-km radius of Giant Mine and within a 20-km radius of AR6. Thus, we continue to encourage these thresholds be employed with well-defined baselines by researchers, agencies and stakeholders because of their utility and effectiveness for detecting and communicating the degree to which anthropogenic influences have polluted the landscape.

Future research directions

Our paleolimnological studies have provided a wealth of knowledge about contaminant deposition across a broad swath of northwestern Canada. The focus has been to examine temporal patterns and trends, yet opportunity exists to further develop the spatial dimension as illustrated in Figure 4.4. As another example, we interpolated V EFs and thresholds across upland lakes of the AOSR at three distinct time periods to evaluate the evolution of V enrichment via atmospheric deposition during the past ~100 years in the form of novel 'paleoenrichment-scapes' (Figure 4.5). The time periods selected represent before industrial activities (~1920), during peak fugitive emissions (~1985; Cooke et al. 2017) and a recent interval of more expansive oil sands operations but with advanced emission controls (~2010). Correspondingly, the paleoenrichment-scape for

~1985 shows EFs are highest and greatest within 20 km along the Athabasca River with 'minimal' enrichment occurring outside this corridor. In contrast, the paleoenrichment-scape for ~2010 demonstrates reduced severity of enrichment at near-field locations but spatial expansion of 'moderate' enrichment has occurred due to northward migration of bitumen mining activities. Spatial arrangement and density of study sites could be improved beyond our initial ad-hoc approach by sampling more lakes in a radial orientation around the point source(s). Furthermore, opportunity exists to integrate paleoenrichment-scapes with other approaches such as paleoecotoxicology (Korosi et al. 2017; Cheney et al. 2020) to improve knowledge of the fate and ecological consequences of contaminants in the environment. We advocate that inclusion of paleolimnology in the early design stage of contaminant monitoring programs will contribute to informed policy decisions and effective environmental stewardship for freshwater landscapes.

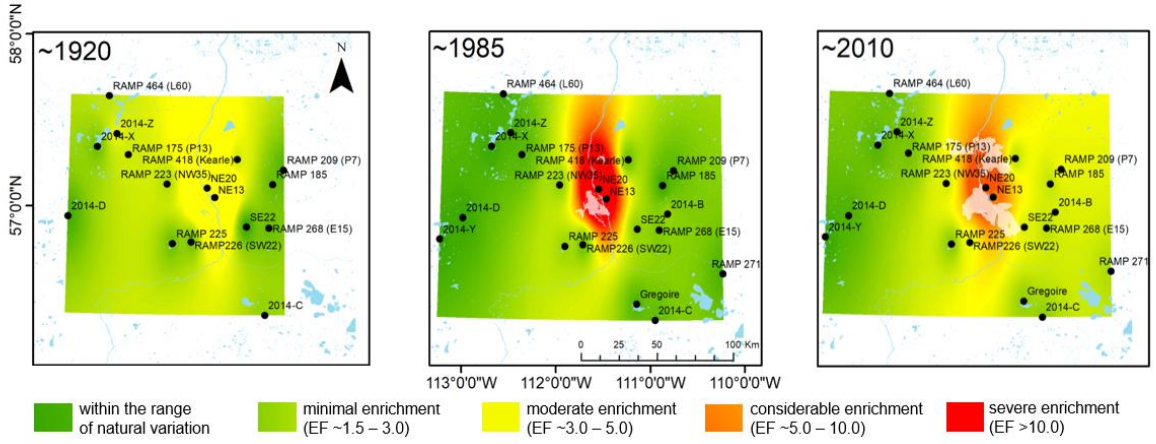

Figure 4.5 'Paleoenrichment-scapes' displaying spatial interpolation of vanadium enrichment factors across the Alberta Oil Sands Region during ~1920, ~1985 and ~2010. Spatial interpolation of the V EFs by ordinary kriging was performed using ArcMap GIS version 10.8.1. The white shaded area represents the Athabasca Oil Sands mining footprint in 1985 and 2010 (note that the 1920s pre-date bitumen mining). Green colours represent 'no to minimal enrichment', yellow represents 'moderate enrichment', orange represents 'considerable enrichment' and red indicates 'severe enrichment'. Sediment core locations are indicated by the black circles. Note that the 'moderate enrichment' in 1920 likely represents overestimation of EFs for this interval due to low

Al concentrations near detection limit (see Discussion and Commentary for details). Consequently, enrichment along the Athabasca River corridor for the ~1985 and ~2010 ‘paleoenrichment-scapes’ may be slightly overestimated.

Chapter 5: Bi-directional hydrological changes in perched basins of the Athabasca Delta (Canada) in recent decades caused by natural processes

Citation: Kay, M.L., Wiklund, J.A., Remmer, C.R., Neary, L.K., Brown, K., Ghosh, A., MacDonald. E., Thomson, K., Vucic, J.M., Wesenberg, K., Hall, R.I., and Wolfe, B.B. 2019. Bi-directional hydrological changes in perched basins of the Athabasca Delta (Canada) in recent decades caused by natural processes. Environmental Research Communications **1:** 081001. https://doi.org/10.1088/2515-7620/ab37e7

Introduction

Many regions of western North America are experiencing decline of water supply and deterioration of ecologically- and culturally-important aquatic habitat, which is challenging the ability of society to respond effectively (Burn et al. 2004, Déry and Wood 2005, Rood et al. 2005, Schindler and Donahue 2006, Barnett et al. 2008, Sauchyn et al. 2015, Scalzitti et al. 2016). This is a focal point for the Peace-Athabasca Delta (PAD), the world's largest freshwater boreal delta. Located at the confluence of the Peace and Athabasca rivers in northern Alberta (Canada; Figure 5.1), this ~6,000km^2 delta provides important habitat for waterfowl, wood bison and other wildlife, and holds traditional importance to the First Nation and Métis communities of the region. Consequently, it is recognized as a Ramsar Wetland of International Importance and contributes significantly to Wood Buffalo National Park's designation as an UNESCO World Heritage Site (Timoney 2013). Despite efforts of federal (Parks Canada, Environment and Climate Change Canada), First Nation (Athabasca Chipewyan and Mikisew Cree) and Métis, provincial (Alberta) and international agencies (UNESCO, Ramsar Convention) to preserve this world-renowned floodplain landscape, concerns have persisted for over 60 years about water-level declines and deterioration of aquatic habitat. Concerns center on the abundant, ecologically important, shallow, perched basins (i.e., restricted- and closed-drainage lakes) within the delta that are prone to drying

and then refill primarily by episodic ice-jam flood events that occur along the Peace and Athabasca rivers (PADPG 1973; Prowse and Conly 1998, Timoney 2013).

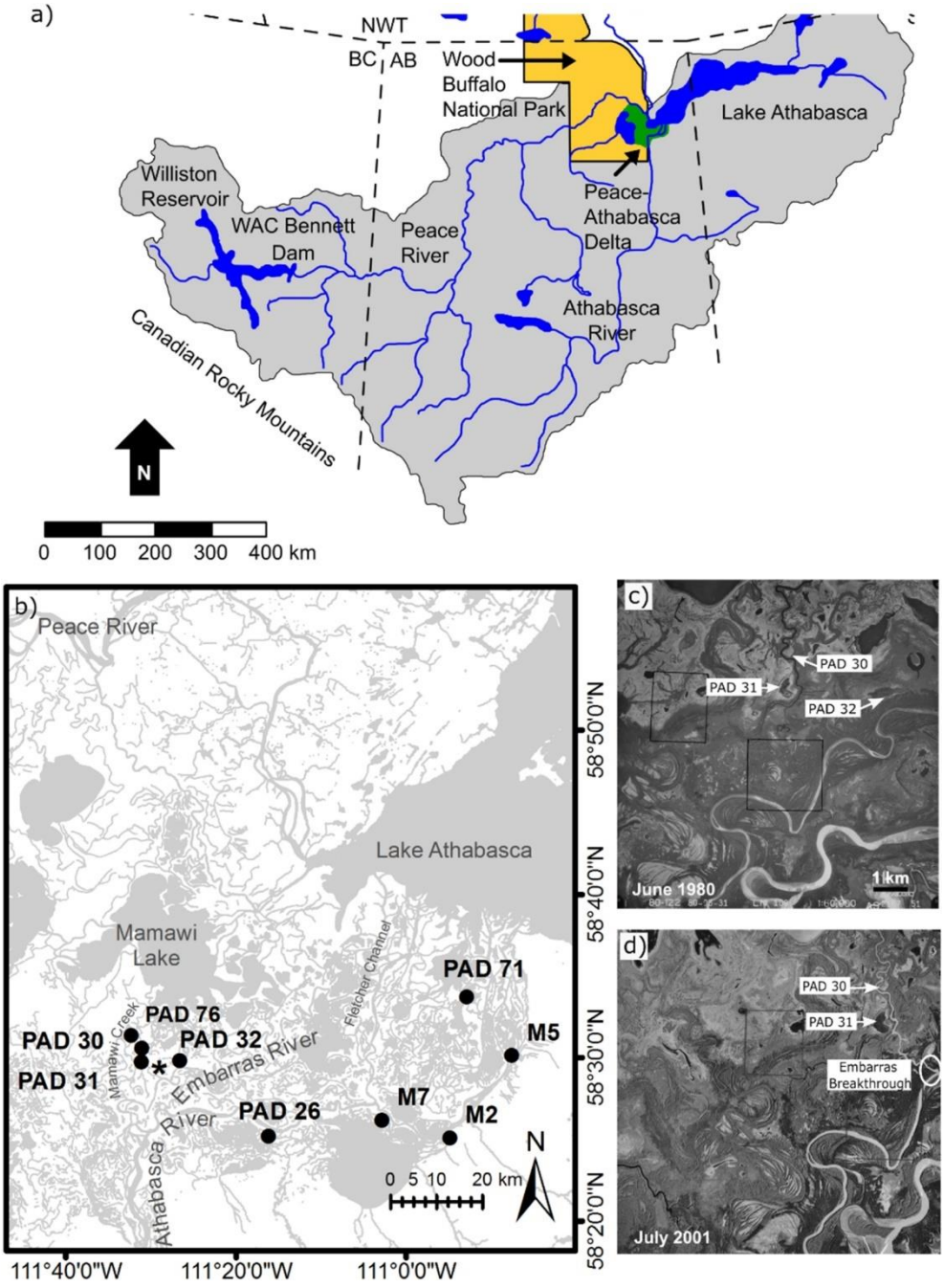

Figure 5.1 The Peace-Athabasca Delta, located in northeastern Alberta (Canada), is shown as the central green region at the western end of Lake Athabasca (Panel a). The locations of lakes where sediment cores were obtained (black circles) and the Embarras Breakthrough (asterisk) are in Panel b. Panels c and d show aerial photos before and after the Embarras Breakthrough, respectively, a natural avulsion that occurred in 1982 and diverts substantial flow northward along Cree and Mamawi creeks to Mamawi Lake.

While there is broad consensus that water levels have been declining in many areas of the PAD during recent decades, the primary cause(s) remain controversial (IEC 2018). On one side, Indigenous knowledge holders and reports by scientists and consultants claim that decline of water levels and ice-jam flood induced recharge of the perched basins throughout the PAD began after 1968, due primarily to hydroelectric regulation at the headwaters of the Peace River (PADPG 1973; Prowse and Conly 1998, 2002, Prowse et al 2006, Dubé and Wilson 2012, Beltaos 2014). The scientific studies are based mainly on analyses of hydrometric records available since the 1950s at a few locations upstream of the PAD in the Peace River. This perspective has gained considerable traction in recent years. In 2014, the Mikisew Cree First Nation (MCFN) petitioned WHC/IUCN to designate Wood Buffalo National Park as 'World Heritage in Danger' based, in large part, on claims that 'dam-induced changes to the Peace River have resulted in a severe deterioration of the PAD's main recharge mechanisms' (MCFN 2014, p 18). This claim was also advanced in the subsequent WHC/IUCN Reactive Monitoring Mission in response to MCFN (2014): 'Regulation of the Peace River … along the upper reaches in British Columbia is widely accepted as a continual and significant threat to the PAD' (WHC/IUCN 2017, p 17) and, based on traditional knowledge, in the ensuing Final Report of the Strategic Environmental Assessment: 'the PAD as a whole is drying, and that this drying has coincided with BC Hydro regulation of the Peace [River]' (IEC 2018, p5–19). These statements imply that Peace River regulation has caused widespread unidirectional change towards less frequent flooding and drying of perched basins across the entire PAD starting after 1968.

On another side, longer temporal data (decades to several centuries) and broader spatial perspectives provided by paleoenvironmental research (e.g., analyses of lake sediment cores and tree-ring records), supported by historic maps and compilations of human observations of ice-jam

flood events, identify that trends of declining river flow, lower delta water levels, reduced flood frequency (Wolfe et al. 2006, 2008a, Sinnatamby et al. 2010, Sauchyn et al. 2015) and directional change to drying of perched basins in the northern Peace sector of the delta (Wolfe et al. 2005, 2008a, Sinnatamby et al. 2010) did not coincide with river regulation. Instead, these records indicate that drying began several decades before hydroelectric regulation and initiation of the Peace River hydrometric records. These findings support conclusions that climatic processes exert overwhelming control on hydrological recharge and water balance of the perched basins, not river regulation (Wolfe et al 2012). In the southern Athabasca sector of the PAD, analyses of sediment records from three perched basins identified two geomorphic events, which modified flow paths of the Athabasca River and its distributaries, as the main causes of hydroecological changes during the past century: one engineered in 1972 (Athabasca River Cutoff) and the other a natural avulsion in 1982 (Embarras Breakthrough; also referred to as Cree Creek Avulsion by Timoney 2013) (Wolfe et al 2008b). One of the lakes situated along Cree/Mamawi creeks became more floodprone after the Embarras Breakthrough event directed increasing flow from the Athabasca/Embarras river network northward toward this lake. It also re-directed river flow away from another lake located east of the Embarras Breakthrough, which subsequently became less flood-prone. A synthesis of the paleoenvironmental studies in the PAD concludes that roles of climate and natural deltaic processes have been underestimated by the other knowledge sources, because these processes operate over broader scales of time and space than captured by available river hydrometric records and observations of land users (Wolfe et al. 2012).

Although speculated upon, the Wolfe et al. (2008b) study does not include sufficient spatial coverage to determine if widespread drying of perched basins across the Athabasca Delta is due to the 1982 Embarras Breakthrough, or, as widely claimed, to initiation of hydroelectric regulation

of the Peace River in 1968. Here, we test these competing hypotheses. Based on prior studies that have identified increases in whole-lake production and sediment organic matter content occur in response to decline of flood frequency (McGowan et al. 2011), we use loss-on-ignition analyses of radiometrically-dated sediment cores from nine flood-susceptible perched basins along an~67-km transect (river distance) across the entire Athabasca Delta to reconstruct hydrological conditions during the past~65–115 years. This includes the terminal region of the Athabasca River that encompasses the Athabasca Chipewyan First Nation traditional territory (Indian Reserve 201) downstream of the Embarras Breakthrough.

Study area

The Athabasca Delta is the largest (~1,970 km^2) and most active of the three deltaic regions that make up the PAD, which also includes the relic Peace Delta to the north (~1,680 km^2) and smaller Birch Delta to the west (~170 km^2; PADPG 1973; Figure 5.1). The Athabasca and Peace deltas have contrasting river hydrology. Under normal flow conditions, tributary channels in the Peace Delta convey water that drains northward out of the PAD towards the adjacent, lower-elevation Peace and Slave rivers. During the spring freshet (late April to early May), episodic ice-jams events develop on the Peace River that persist for a few hours to a week or so in duration and can raise the Peace River sufficiently to cause southward flow reversals and overland flooding in the Peace Delta that can replenish the perched basins.

The Athabasca River flows directly into the Athabasca Delta and divides into a number of smaller distributaries that flow north- and east-ward towards the Athabasca Delta terminus where flow enters Lake Athabasca. Lakes in the Athabasca Delta can receive river floodwater during both spring ice-jam events and the open-water season. During the past 45 years, both engineered and natural changes to river channels have altered the distribution of river flow in the Athabasca

Delta. In 1972, the Athabasca River's impending avulsion into the Embarras River channel (a major distributary of the Athabasca River) was prevented by engineered excavation of a channel across a tight bend in the Athabasca River to maintain the navigable route for river barges and avoid redirection of river flow away from the terminus of the Athabasca River, including Athabasca Chipewyan First Nation traditional lands. Ten years later, in 1982, a natural avulsion of the Embarras River (the 'Embarras Breakthrough'; Figure 5.1) began to divert substantial and increasing flow northward via Cree and Mamawi creeks towards the large, central open-drainage Mamawi Lake and away from the terminus region and Indian Reserve 201 where Athabasca and Embarras river flow enters Lake Athabasca. Estimates from soon after the natural avulsion suggested that the Embarras Breakthrough directs 58% of Embarras River discharge (3%–8% of Athabasca River mainstem flow) northward along Cree and Mamawi creeks and nearly doubled the inflow to Mamawi Lake, values that have been increasing ever since (De Boer et al. 1994, PADTS 1996, Timoney 2013).

Methods

Water balance of the numerous shallow, perched basins is controlled by variations in flux of input waters (river floodwater, precipitation) and evaporative losses. Previous studies have demonstrated groundwater does not substantially influence water balance of the delta's perched basins (PADPG 1973, Prowse et al. 1996). River floodwater, laden with inorganic sediment, provides an important source of inflow to these lakes, a record of which is preserved in their stratigraphic profiles (e.g., Wolfe et al. 2006). Flooding results in relatively high lake sediment inorganic matter content and low organic matter content due to influx of suspended mineral sediment carried by the rivers and suppression of aquatic plant production by increased water-column turbidity (Wiklund et al. 2010, McGowan et al. 2011, Wiklund et al. 2012). When lake

flooding is reduced, sediment organic matter content increases due to higher in-lake production of algae and aquatic plants and lower input of mineral sediment. We use measurement of organic and inorganic matter content profiles in sediment cores by loss-on-ignition methods to determine periods of increased or decreased flooding at nine shallow perched basins along an ~67 km transect (river distance) across the Athabasca Delta. Three lakes (PAD 76 [58° 31.386' N, 111° 32.294' W], 30 [local name: Mamawi Pond; 58° 30.605' N, 111° 31.025'W] and 31 [Johnny Cabin Pond; 58° 29.763',N 111° 31.101'W]) are located along Mamawi Creek north of the Embarras Breakthrough and six lakes (PAD 32 [58° 29.838' N, 111° 26.592'W], 26 [58° 25.192' N, 111° 16.171'W], M2 [Marta's Lake; 58° 25.099' N, 110° 54.823'W], M5 [Lake South of Tokyo Snye; 58° 30.149' N, 110° 47.585'W], M7 [Ross's Corner; 58° 26.172' N, 111° 02.801'W] and 71 [58° 33.441' N, 110° 52.531'W]) are located east and northeast of the Embarras Breakthrough and span the distance to the terminus of the Athabasca River (Figure 5.1).

Sediment cores were collected from the lakes in 2010 (PAD 31), 2015 (PAD M5, M7, 26, 32), 2016 (PAD 30, M2), 2017 (PAD 71) and 2018 (PAD 76) using a gravity corer (Glew 1989) operated from a small boat or pontoon of a helicopter. Sediment cores were described and sectioned within 24 h of collection into 1-cm intervals at a field base in Fort Chipewyan. Once sectioned, the samples were kept refrigerated (4 °C) and in the dark until analyzed at University of Waterloo.

Sediment cores were dated using gamma-ray spectrometric measurement of ^{210}Pb and ^{226}Ra (via daughters ^{214}Pb and ^{214}Bi) activity at alternating 1-cm intervals throughout the upper ~20–40 cm of each core. For each sample, 2–4 g of freeze-dried sediment was packed into pre-weighed tubes to 35-mm height. A silicone septum and 1ml of 2-ton clear epoxy were placed on top of the sediment, and ^{222}Rn and its decay products (^{214}Pb and ^{214}Bi) were allowed to reach equilibrium

with parent isotope ^{226}Ra for at least three weeks before measuring activity. Samples were run for 23–95 h at the University of Waterloo's WATER Lab Ortec co-axial HPGe Digital Gamma Ray Spectrometers interfaced with Maestro 32 software. For individual cores, total ^{210}Pb activity ranged 0.03–0.17 Bq g^{-1} and background ^{210}Pb activity was 0.03–0.05 Bq g^{-1}. Background depth was determined where total ^{210}Pb activity equals supported ^{210}Pb (=^{226}Ra) activity when accounting for their pooled measurement uncertainty (Binford 1990). The Constant Rate of Supply (CRS) model was used to calculate ^{210}Pb-based ages and sedimentation rates (Appleby 2001, Sanchez-Cabeza and Ruiz-Fernandez 2012). The reference accumulation rate approach was utilized (see Appleby 2001, Eq. 34) ensuring complete integration of the unsupported ^{210}Pb inventory. Dates below the unsupported ^{210}Pb horizon were extrapolated based on the mean dry mass accumulation rate during the ^{210}Pb-dateable portion of the records.

Subsamples of ~0.5–1 g wet mass from each 1-cm sediment interval were analyzed for moisture, organic matter, and carbonate content by weight loss on heating at temperatures of 90 °C (24 h), 550 °C (2 h), and 950 °C (2 h), respectively (Heiri et al. 2001). Mineral matter content was determined as the sediment mass remaining after final heating to 950 °C, and inorganic matter content as the sum of mineral plus carbonate contents. Organic and inorganic matter contents are expressed as a percentage of total dry sediment mass. Results are reported for the post-1900 intervals of the sediment cores.

Results and Interpretation

^{210}Pb activity profiles in sediment cores from the six perched basins located east and northeast of the Embarras Breakthrough (PAD 32, 26, M7, M2, M5, 71) and PAD 76, located north of the Embarras Breakthrough and partially sheltered by trees and shrubs, show a relatively consistent pattern of low values near the base and marked rise towards the top of the cores,

punctuated by occasional variability likely caused by episodic input of flood-supplied sediment with low ^{210}Pb activity (Figure 5.2). Background ^{210}Pb activity was reached between 7 and 39 cm depth, indicating variability in sedimentation rates among these lakes. In contrast, sediment cores from the other two perched basins located north of the Embarras Breakthrough show markedly different ^{210}Pb activity profiles, with low activity near the base of the cores, a rise to peak activity at mid-depths, and sharp decline in upper sediments (above 6 cm in PAD 30, 16 cm in PAD 31). The decline of ^{210}Pb activity in upper sediments coincides with a substantial rise in inorganic matter content of sediment and date to the early to mid-1980s (Figure 5.3).

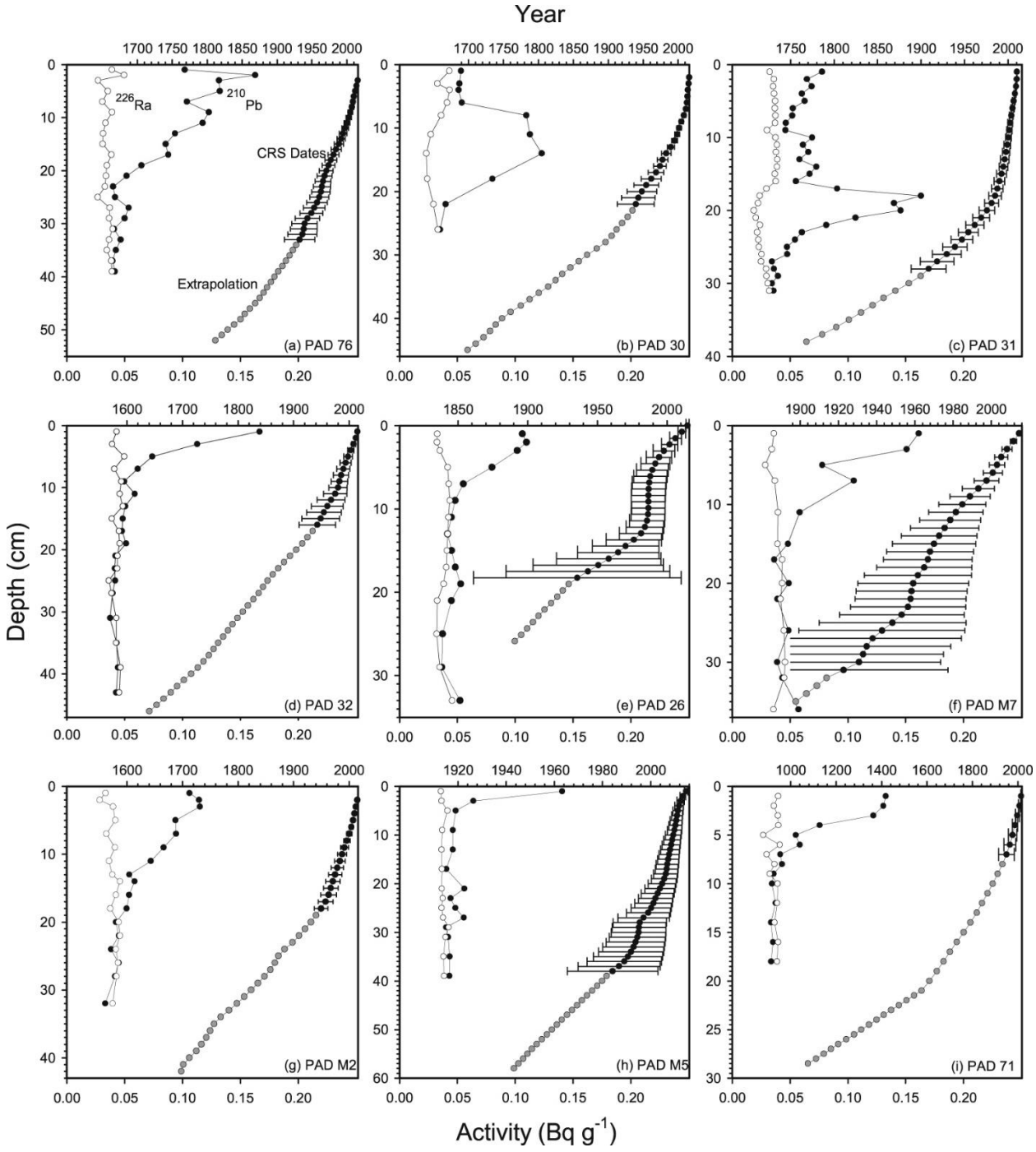

Figure 5.2 Graphs showing ^{210}Pb and ^{226}Ra activity profiles (left) and age-depth relations, including both estimated (black) and extrapolated (grey) values (right), for sediment cores collected from study lakes north of the Embarras Breakthrough: (a) PAD 76, (b) PAD 30 and (c) PAD 31, and along a proximal to distal transect to the east and northeast of the Embarras Breakthrough (d) PAD 32, (e) PAD 26, (f) PAD M7, (g) PAD M2, (h) PAD M5 and (i) PAD 71. Error bars = ±2 SD.

Despite challenges of dating cores by ^{210}Pb methods in dynamic sedimentary environments such as these floodplain lakes, accuracy of our established chronologies can be demonstrated through repeated, consistent dating of the clearly visible contact between overlying light-grey inorganic-rich sediment on top of deeper black organic-rich sediment at ~1982 in cores collected from PAD 31 in 2001 and 2010 (Figure 5.3).

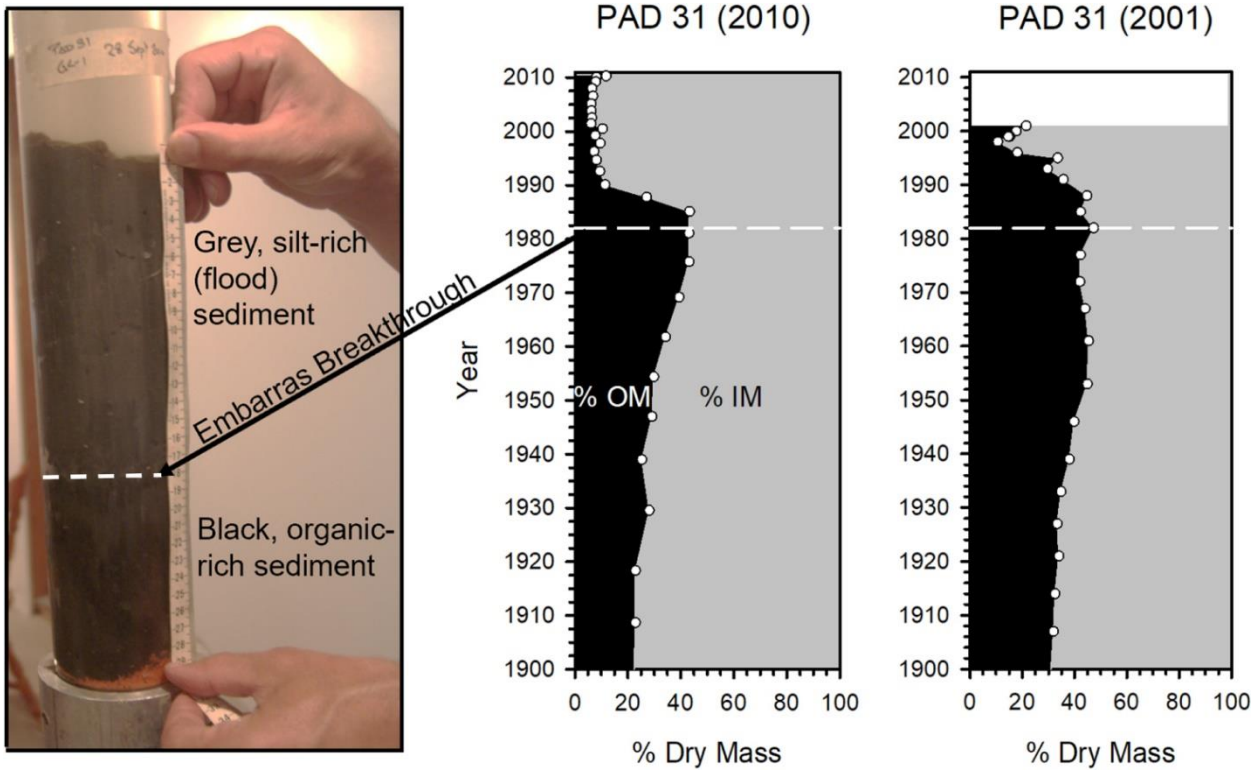

Figure 5.3 Photograph of a sediment core from lake PAD 31 collected in 2010 showing the contact between upper grey sediments rich in inorganic matter overlying deeper black organic-rich sediments as a consequence of the 1982 Embarras Breakthrough, a natural river avulsion which directed increasing river flow to PAD 31 and increased flood frequency to this lake. The graphs compare independently dated sediment core profiles of organic (black) and inorganic (grey) matter content in cores collected in 2010 and 2001, demonstrating the consistency of dating the contact produced by the 1982 Embarras Breakthrough (Wolfe et al. 2008b, Hall et al. 2012).

The stratigraphic profiles of organic and inorganic matter content demonstrate two patterns of temporal change in flood influence in the study lakes with respect to flow re-routed by the

Embarras Breakthrough after 1982 (Figure 5.4; Appendix E Tables E1–E9). Prior to 1982, sediments at PAD 30, 31 and 76, located north of the Embarras Breakthrough, possess relatively high organic matter content (25%–55%) compared to the other six perched basins located east and northeast of the Embarras Breakthrough, suggesting PAD 30, 31 and 76 were less frequently flooded. After 1982, inorganic matter content increased markedly at PAD 30 and 31 to 80%–90%, identifying a change to more frequent input of mineral sediment by river floodwaters. These results are consistent with prior multi-proxy analyses of a sediment core from PAD 31 (Wolfe et al. 2008b). At PAD 76, the rise of inorganic matter content was more gradual and delayed. In contrast, sediment cores from five of the six perched basins east and northeast of the Embarras Breakthrough (PAD 32, 26, M7, M5, 71) show the opposite pattern. High inorganic matter content (>90%) occurs prior to 1982, indicating frequent, strong influence of river flooding, and organic matter content increases after 1982, signalling that flood influence declined. Rising organic matter content began several years after 1982 in some of these lakes (e.g., ~1990 at PAD 32, 26, M5), which is consistent with knowledge that continual bank and river erosion at the site of the Embarras Breakthrough has increased capture of Athabasca and Embarras river flow by Cree and Mamawi creeks over time since 1982 (Timoney 2013). The resulting gradually increasing northward flow over time, and the more sheltered location of PAD 76, also likely explains the delayed post-2000 response to increase in river floodwater influence at this lake. Sediment composition did not change noticeably at PAD M2 after 1982, whereas organic matter content increased after ~1930 at several of the study lakes (PAD 76, 30, 31, 32, M7and M2; Figure 5.4). However, sediment cores from all nine study lakes show no directional change towards less frequent flooding coincident with Peace River regulation since 1968. Indeed, the only change recorded at 1968 in any of the nine lake sediment records is a short-lived increase of inorganic matter content at PAD

M2 during ~1965–1974, which is interpreted to indicate increased flooding to this lake during this interval. We considered other possible mechanisms to explain the organic matter profiles, such as diagenesis which commonly leads to down-core decline of organic matter content, but this cannot explain the profiles at PAD 30, 31 and 76, because organic matter content shows the opposite pattern. For the other lakes, given their variable sedimentation rates, diagenesis is highly improbable as a mechanism that could produce the temporally consistent increase in organic matter content after 1982.

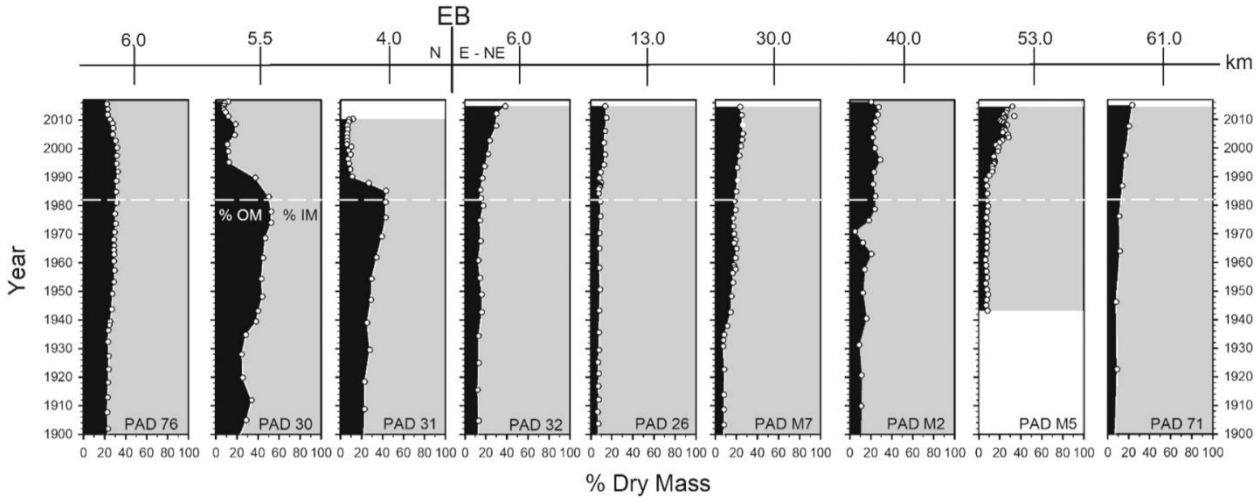

Figure 5.4 Stratigraphic patterns of change in organic (black; as % dry mass) and inorganic matter content (grey) in the study lakes arranged from west to east spanning a 67 river-kilometer transect across the Athabasca Delta. The white dashed line represents 1982, the year of the Embarras Breakthrough. PAD 31 record is from Hall et al (2012).

5.5 Discussion

In large, complex freshwater landscapes, recognition of the relative roles of anthropogenic and natural influences on hydrological conditions requires sufficient spatial and temporal perspectives. However, these data are rarely available because comprehensive long-term monitoring programs are often absent, or sampling locations are too sparse and records do not extend long enough to characterize reference conditions. In such situations, paleolimnological

studies have long been used to reconstruct pre-disturbance conditions and identify the timing and cause(s) of environmental change (e.g., Smol 1992, Smol 2008, Wolfe et al. 2008b, Lintern et al. 2016, Gell 2017).

Among the potential drivers of hydrological change in the Athabasca Delta, the Embarras Breakthrough is rarely mentioned or omitted in recent assessments (Beltaos 2014, MCFN 2014, 2016, WHC/IUCN 2017, IEC 2018), despite prior evidence of its hydrological effects (Wolfe et al 2008b, Timoney 2013). Results from the present study substantially expand upon the spatial coverage in Wolfe et al (2008b) and demonstrate clear evidence for the Embarras Breakthrough as the major driver of hydrological changes for perched basins across the Athabasca Delta. The Embarras Breakthrough directed Athabasca River flow, via the Embarras River, into Cree and Mamawi creeks and the low-lying central region of the PAD, which has led to more frequent flooding in a small, central region of the PAD (PAD 30, 31 and eventually PAD 76). Conversely, flood influence has declined since 1982 at the perched basins located to the east (PAD 32, 26, M7) and in the northeastern Athabasca River terminus region (M5, PAD 71). An exception is M2, which has remained strongly flood prone due to its proximal location to a sharp bend in the Athabasca River. Based on the organic and inorganic matter stratigraphic profiles from the perched basins along a ~67 river-km transect, the naturally occurring shift in distributary flow caused by the Embarras Breakthrough is the most influential hydrological change to occur during the past 115 years, consistent with findings of Wolfe et al. (2008b).

Declining Athabasca River discharge has been well documented (e.g., Schindler and Donahue 2006, Wolfe et al. 2011, Wolfe et al. 2012, Sauchyn et al. 2015) and is evident in lakes of the Athabasca Delta as rising organic matter content after ~1930 in sediment cores from five of the nine lakes in this study (PAD 76, 30, 31, 32, M7). But, the rapid (PAD 30, 31) and gradual

(PAD 76) decreases in sediment organic matter content after 1982 resulting from increased flooding caused by the Embarras Breakthrough has more than offset the effects of declining Athabasca River flow along Cree/Mamawi creeks. For lakes in the downstream terminus region of the Athabasca Delta, pronounced drying of perched basins is interpreted to be the consequence of substantial diversion of river flow away from this region by the Embarras Breakthrough superimposed upon the reduction of Athabasca River flow as a result of climate change. Clearly, perched basins in the Athabasca Delta have entered a new hydrological regime, one characterized by bi-directional change to drying in areas east and northeast of the Embarras Breakthrough and wetting to the north along the Cree and Mamawi creek corridor.

Conclusions and Implications

Our study demonstrates the critical role of the 1982 Embarras Breakthrough on distribution of floodwaters conveyed by the Athabasca and Embarras rivers and bi-directional hydrological changes to perched basins across a substantial portion of the Athabasca Delta. This natural river avulsion led to increased flooding of perched basins to the north along Cree and Mamawi creeks and reduced flooding to the east toward the Athabasca River terminus. Hydroelectric regulation of Peace River flow since 1968 could not have produced these patterns of hydrological change. Correct identification of the major factors causing the drying of the delta's perched basins, which lie at the center of concerns for deterioration of wildlife habitat and cultural land use, is important to inform impending decisions regarding designation of Wood Buffalo National Park as 'World Heritage in Danger' (WHC/IUCN 2017), and initiatives to protect the integrity of the PAD and its Outstanding Universal Values (WBNP 2019). For example, recommendations to mitigate presumed impacts of the WAC Bennett Dam on perched-basin hydrology in the Athabasca Delta by modifying the dam's operating regime may be largely unsuccessful if the dam has not led to

lake drying. The approaches used in this study are readily transferable to other complex, water- and lake-rich landscapes where causes of hydrological change are difficult to decipher.

Chapter 6: A Bayesian mixing model framework for quantifying temporal variation in source of sediment to lakes across broad hydrological gradients of floodplains

Citation: Kay, M.L., H.K. Swanson, J. Burbank, T.J. Owca, C.A.M. Savage, C.R. Remmer, L.K. Neary, J.A. Wiklund, B.B. Wolfe, R.I. Hall. 2021. A Bayesian mixing model framework for quantifying temporal variation in source of sediment to lakes across broad hydrological gradients of floodplains. Limnology and Oceanography Methods 19: 540-551. https://doi.org/10.1002/lom3.10443

Introduction

River floodplains and deltas are dynamic, ecologically diverse landscapes where episodic input of floodwaters maintain lake water balance, hydrologic connectivity, vegetation structure, and ecosystem services. Frequency and magnitude of flooding are influenced by inherent variation of natural processes and by anthropogenic activities, all of which typically operate over a range of temporal and spatial scales (Hughes et al. 2009; Lintern et al. 2016; Remmer et al. 2020a). Such complexity presents challenges to water resource managers, especially because monitoring records are often too short and sparse to adequately characterize natural variability, detect the timing and causes of hydrological and ecological change, and define limits of acceptable change (Gell 2017; Xenopoulos 2019; Heino et al. 2020; Wilkinson et al. 2020).

Paleolimnological studies conducted at large, hydrologically complex floodplain and deltaic landscapes often employ single site and multisite reconstructions to inform temporal and spatiotemporal perspectives about hydroecological change and variability (Michelutti et al. 2001; Brock et al. 2010; Velez et al. 2012; Wolfe et al. 2012; Lintern et al. 2016). Floodplain lakes situated in close proximity to rivers receive relatively frequent, high-energy floodwaters and their load of suspended sediment, which leads to lake sediments with high inorganic content. Thus, sediment cores from highly flood-prone lakes are well suited for analysis of stratigraphic variation in physical components, such as density, magnetic susceptibility, grain size, and mineralogy (Wolfe et al. 2006; Velez et al. 2012). In contrast, lakes at more distal and elevated locations

receive less frequent and weaker influence of floodwaters, and their sediments are typically organic-rich. Consequently, analysis of biological (e.g., diatoms, plant macrofossils) and organic geochemistry (e.g., carbon and nitrogen elemental and isotope composition) components are more effective to reconstruct past hydroecological change and variability (Wolfe et al. 2005, 2008b; Brock et al. 2010; Kuerten et al. 2013). Integration of paleolimnological records from multiple lakes that span the broad gradients of frequency and intensity of flooding may provide important additional insight into factors regulating hydroecological conditions across floodplain landscapes that are unavailable from analysis of one or a few lakes at either end of these energy gradients. However, reconciling records based on physical methods at some sites and biological and geochemical methods at other sites presents challenges, which frequently constrain reconstructions to qualitative or semiquantitative descriptions of past hydrological conditions (Wolfe et al. 2008a; Velez et al. 2012; Kuerten et al. 2013). Furthermore, analyses of most physical, biological, and geochemical variables in sediment cores do not inform about the source of floodwaters, which may be important to discriminate when more than one river has potential to be the source of flooding. Thus, development of a method that allows consistent measurement of the same variable in cores from lakes across the gradient of mineral-rich to organic-rich sediment and is capable of fingerprinting the source of sediment would represent a useful advance for elucidating drivers of hydroecological change in floodplains.

Fluvial sediment transported to floodplains possesses materials derived from potentially different regions within watersheds due to variation of the surficial geology, and these mixtures are deposited into lakes during flood events where they accumulate vertically and form a stratigraphic profile (Kitch et al. 2019). Sediments deposited into floodplain lakes, thus, provide an integrated temporal record of the parental sediment sources, each with their own geochemical

fingerprint (Collins et al. 2010, 2017; Blake et al. 2018). Sediment fingerprinting by trace element concentrations or isotope ratios has been used to discriminate among parental source materials (Walling and Woodward 1995; Hughes et al. 2009; Lamba et al. 2015a,b; Stewart et al. 2015). Unlike other measurements that vary in their efficacy across gradients of mineral and organic content, trace element concentrations can be quantified reproducibly across the spectrum from mineral-rich to organic-rich lake sediment, as occurs along gradients of river connectivity within floodplains and deltas (Lintern et al. 2016; Kay et al. 2020 [*included here as Chapter 2*]; Klemt et al. 2020). Thus, elemental concentrations may be ideal input tracers to track changes in the sources of sediment supplied to lakes across hydrologically complex floodplains, deltas, and other lake-rich landscapes where it is important to discriminate past variation of multiple sources of sediment, including floodwaters provided by one or more possible rivers. Indeed, mixing models have been used to quantify the role of anthropogenic disturbances within upland portions of watersheds on sediment deposition to downstream lakes (Cooper et al. 2015; Lizaga et al. 2019; Wynants et al. 2020). For instance, Wynants et al. (2020) recently used a Bayesian mixing model (BMM) framework and measurements of trace elements in lake and river sediment samples at strategically selected locations within Lake Manyara (Tanzania) and its many tributaries to quantify geochemical differences of river sediment supplied to the lake, and to reconstruct temporal variation in sediment sources from stratigraphic profiles. The approach revealed that a recent increase in siltation was linked to expansion of agricultural activities within the watershed of one of the lake's many tributaries—knowledge that assisted land management planning and protection of aquatic habitat and water quality of this large East-African Rift Lake. Defining (using concentrations of elements) and quantifying (using a BMM) the relative importance of sediment sources, and the temporal variability of these sediment sources, to lakes in floodplains, deltas and

lake-rich landscapes has the potential to enhance quantitative paleohydrological reconstructions, and better inform water resource management.

The approach elegantly demonstrated by Wynants et al. (2020) presents new opportunity to further probe the hydrological evolution of the Peace-Athabasca Delta (PAD) in northeastern Alberta (Canada), a site of intensive paleolimnological investigation for the past 20 years (Wolfe et al. 2012, 2020; Kay et al. 2019 *[included here as Chapter 5]*, 2020). The PAD is a 6000 km^2 boreal freshwater floodplain where episodic input of floodwaters caused by ice-jams on the Peace and Athabasca rivers recharges its abundant shallow, perched lakes. Several upstream and resistance forces may contribute to the occurrence of an ice-jam flood event (Prowse and Conly 1998, Beltaos and Bonsal 2021; Lamontagne et al. 2021), yet their magnitude and frequency have declined in recent decades raising concerns over deteriorating hydroecological conditions (Mikisew Cree First Nation [MCFN] 2014; WHC/IUCN 2017; Wood Buffalo National Park [WBNP] 2019). Paleolimnological studies have demonstrated the decline in magnitude and frequency of ice-jam flood events and lake level drawdown began in the early 20th century and have provided key insight into the paleohydrological record of individual lakes. However, spatial integration is not yet fully developed because different paleolimnological measurements have been used among lakes depending on the strongly varying mineral-rich to organic-rich sediment composition across the strong hydrological gradients of the delta.

Recent analysis of elemental concentrations in sediments of lakes across the PAD has demonstrated significantly higher concentrations of some elements in sediment conveyed by the Peace River compared to sediment sourced from the Athabasca River, which is attributed to the different underlying geological terrane of their catchments (Owca et al. 2020). This finding affords opportunity to develop a novel approach capable of quantitative reconstruction of sediment

supplied by the Peace River vs. Athabasca River to lakes, which is important in the vast low-relief PAD where multiple factors have potential to differentially alter flood regimes of these rivers, and large central areas of the delta may variously receive inflow from both rivers. In this study, we capitalize on differences in elemental concentrations in sediment supplied by the Peace River and Athabasca River, and from the local catchment in the absence of river floodwater, to evaluate the utility of a BMM (MixSIAR; Stock and Semmens 2016; Stock et al. 2018) in quantifying relative source contributions from these three end-members. We apply a MixSIAR model to stratigraphic profiles of elemental concentrations from sediment cores of two lakes in the PAD, where knowledge of past marked hydrological change and sediment composition has been previously obtained using more conventional methods (Wolfe et al. 2008b; Kay et al. 2019), to assess performance of the model. As we demonstrate, the methodology fosters opportunity for improved characterization and quantification of hydrological change over time and space in complex floodplain environments, such as the PAD, and is readily transferable to other comparable water-rich landscapes. This knowledge is important for stewardship decisions and mitigative actions to maintain abundance of water and ecological integrity.

Methods

Three steps were employed to develop, apply, and evaluate the methodological approach. First, samples of surficial lake sediment, river bottom sediment, and riverbank sediment were obtained from an array of sites that span the hydrological gradients of the PAD, and each sample was classified into one of three distinct a priori groups of allochthonous sediment input (hereafter referred to as end-members): (1) Athabasca River sediment, (2) Peace River sediment, and (3) local catchment. These three end-members represent the three major pathways of sediment delivery to lakes in the PAD under flood (Athabasca River, Peace River) and non-flood (local

catchment) conditions and are likely to be preserved in stratigraphic records. Samples were designated to an end-member based mainly on their geographic location, lake water isotope composition, and lake water chemistry data. Second, linear discriminant analysis (LDA) was conducted on sediment samples to select a subset of elements that best discriminated among the three end-members (via removal of collinear elements) and to determine if the elemental composition of each end-member differed significantly. Cross-validation was then performed to evaluate ability of the LDA to discriminate end-member sediment sources in the PAD based on differences in elemental composition of lake sediment. Third, means and standard deviations (SDs) of the elements, which differed significantly among Peace River, Athabasca River, and local catchment sediments (as identified by the LDA), were entered into a MixSIAR model to represent each of the three end-members. The MixSIAR model was then applied to stratigraphic profiles of element concentrations obtained from two lakes (PAD 30 and PAD 31) known to have experienced three distinct hydrological phases during the past 300 years and span a broad range of sediment composition (40–90% mineral matter; Wolfe et al. 2008b; Kay et al. 2019). This last step provided opportunity to evaluate performance of the model with independent data. Further details for each step are provided below.

Collection, analysis, and designation of sediment samples to the three end-members

During 2017–2019, samples of lake surface sediment, surficial river-bottom sediment, and riverbank sediment were collected in the PAD (Figure 6.1). Surface sediment samples were obtained using a mini-Glew gravity corer (Glew 1991) from a network of 44 lakes across the PAD in September 2017 (8 flooded by the Athabasca River, 3 flooded by the Peace River, 33 local catchment), and from a subset of 13 of those lakes in summer 2018 after they received floodwaters from an ice-jam flood event during that spring (6 flooded by the Athabasca River, 7 flooded by

the Peace River; Owca et al. 2020). Nine river-bottom samples were obtained in 2019 from the Peace River using a Petite Ponar grab sampler. No river-bottom samples were obtained from the Athabasca River. Riverbank sediment samples were collected from exposures along the Peace River (n = 10) and Athabasca River (n = 36) during summer 2019. The samples of lake surface sediment, river-bottom sediment, and riverbank sediment were homogenized, and subsamples were analyzed for a suite of elements at ALS Canada (Waterloo) following EPA method 202.2/6020A, which uses an aqua regia digestion.

To develop a geochemical fingerprint for each major source pathway, the sediment samples were assigned to one of the three end-members (Athabasca River sediment, Peace River sediment, or local catchment). Riverbank and river-bottom sediment samples were assigned to end-members of the river from which they were collected. Flooding in the PAD is variable between years, and lakes can be flooded by at least one of the Peace River or Athabasca River depending on the lake's geographic location and elevation (Remmer et al. 2020a). Lake surficial sediment samples collected in 2017 were assigned to the Peace River and Athabasca River end-members based on the sampling location, and determination of whether the sample likely incorporated inputs from river floodwaters was based on evidence from repeated seasonal measurements of lake water isotope composition and water chemistry during 2015–2019, following Remmer et al. (2020a). Surficial sediment samples from the non-flooded lakes were placed in the "local catchment" end-member. This end-member captures lake sediment signatures in the absence of recent flooding and includes fluvio-deltaic sediment eroded from the catchment. The 1-cm thick surficial sediment samples obtained from the lakes in 2017 likely captured sediment deposited within the prior 2–

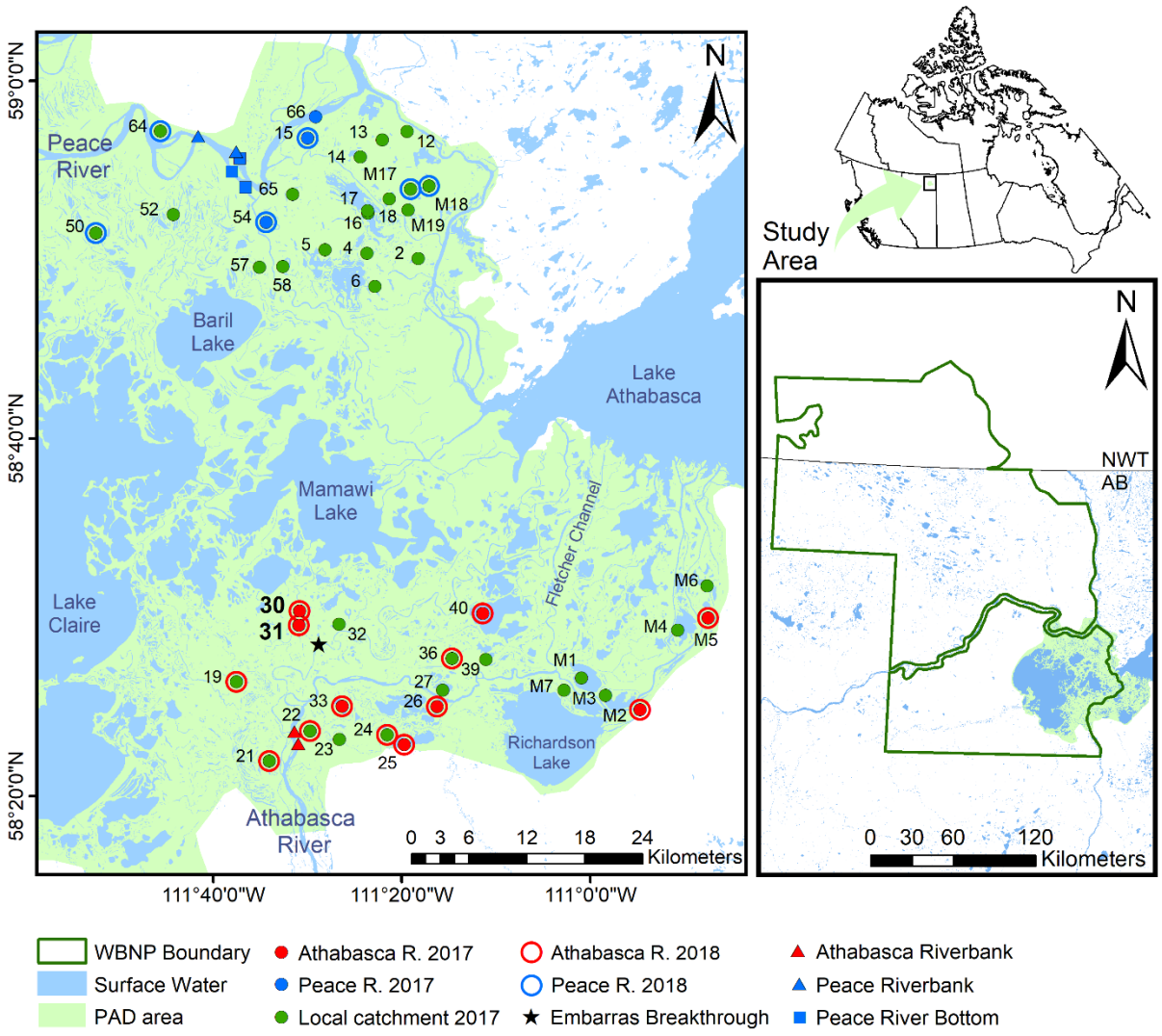

Figure 6.1 Map showing locations of sampling sites for river-bottom sediment (squares) and riverbank sediment (triangles) obtained in 2018 and 2019, and lake surface sediment (circles) collected in 2017 and 2018. The inner dot represents the flood status of lake sites in 2017, which have been color-coded to represent if they were flooded by the Athabasca River (red) or the Peace River (blue), or not-flooded (green). The outer ring represents the flood status of lakes in 2018 and color-coded to represent if they were flooded by either the Athabasca River (red) or Peace River (blue). Sites without a ring around the dot were not sampled in 2018 because they did not receive floodwaters. Inset maps show location of study region within Canada.

5 years based on our experience dating cores from > 30 lakes in the PAD (Wolfe et al. 2012; Kay et al. 2019). Lakes located in the central region of the delta were excluded from the study because sediment could be derived from multiple sources, which potentially confounds attempts to characterize the geochemical fingerprint of each of the three individual sources. Lake surficial sediment samples collected in 2018 were exclusively from lakes flooded in spring of that year and were assigned to the Peace River and Athabasca River end-members based on geographic location, following Remmer et al. (2020b) and Owca et al. (2020). Only the uppermost distinctive gray flood layer was collected to ensure that samples obtained exclusively represented sediment deposited during the spring ice-jam flood event. Lakes that were sampled in both 2017 and 2018 were allocated to an end-member in each year based on the above criteria and treated as independent samples in subsequent analyses.

In summary, we allocated sediment samples to the three end-members as follows. (1) The Athabasca River end-member is represented by the surface sediment samples from lakes in the southern Athabasca sector of the PAD considered to have recently received floodwater from the Athabasca River, plus the Athabasca River riverbank samples (total for end-member = 50). (2) The Peace River end-member is represented by the surface sediment samples from lakes in the northern Peace sector of the PAD considered to have recently received floodwater from the Peace River, plus the Peace River surficial river-bottom and riverbank sediment samples (total for end-member = 29). (3) The local catchment end-member is represented by surficial sediment samples from lakes in both the Peace and Athabasca sectors that were deemed to have not recently received river floodwaters (total for endmember = 33).

Linear discriminant analysis

Key requirements for successful application of mixing models include discrimination among end-members, and that input tracers are spatially and temporally conservative in their environmental behavior (Motha et al. 2002; Blake et al. 2018). This implies no changes in the composition of the tracers within sediment profiles before or after deposition (Koiter et al. 2013; Belmont et al. 2014; Laceby et al. 2017). Thus, prior to performing LDA, we removed elements from the initial suite known to exhibit nonconservative behavior (i.e., elements sensitive to redox reactions, mobile in sediments, or readily altered by diagenetic processes) from the analysis, as recommended by Smith et al. (2018). These elements included As, Fe, Mg, Mn, and Mo. Additionally, Sn and W were removed because their concentrations were consistently below detection limits. The remaining elements (Sb, Ba, Be, Bi, B, Cd, Ca, Cr, Co, Cu, Pb, Li, Ni, P, K, Se, Ag, Na, Sr, S, Tl, Ti, U, V, Zn, Zr) were geochemically normalized to Al, a lithogenic element, to account for influence of variation in grain size caused by a range of flow conditions (Loring 1991; Kersten and Smedes 2002). This was done to avoid characterization of differences in elemental concentrations that are due to shifting flow energy conditions, independent of source. For example, a single river may supply both coarse- and fine-grained sediment of differing elemental concentrations to lakes, and this can confound discrimination of sediment sources. Geochemical normalization is commonly applied to evaluate metals concentrations in lake and river sediment, and Al has been used as the normalizer in this region (Cooke et al. 2017; Kay et al. 2020; Klemt et al. 2020; Owca et al. 2020). We used information in Hugenholtz et al. (2009) to retrieve riverbank sediment samples deposited well before industrial development along the Peace River and Athabasca River. The river-bottom sediment samples and lake surface sediment samples show no indication of enrichment above preindustrial (pre-1920) concentrations (Wiklund et al.

2014; Owca et al. 2020), which allows an approach based, in large part, on contemporary samples to be applied for reconstruction of conditions prior to, and since, upstream industrial development within the river watersheds. LDA was performed using default settings in IBM SPSS Statistics version 27 and forward selection ($\alpha = 0.05$) based on Mahalanobis distance between the groups to determine a subset of elements that distinguish the three end-members. Leave-one-out cross-validation was then used to assess the ability of the LDA to categorize sediment samples to the end-members based on elemental concentrations.

Construction, application and assessment of the BMM

We selected MixSIAR (Stock and Semmens 2016; R Core Team 2020) as the BMM to quantify the source of sediment based on elemental composition, because it provides the flexibility to tailor the model to our specific data set (Blake et al. 2018; Stock et al. 2018). We used an uninformative prior (1, 1, 1) and the elemental concentrations were entered as the geochemical normalized means and SDs for each of the three end-members (as determined using LDA). Following recommendations by Wynants et al. (2020), we set the Markov Chain Monte Carlo parameters to: chain length = 3,000,000, burn = 2,700,000, thin = 500, and chains = 3. The model was run without fixed or continuous effects. Using the Gelman-Rubin diagnostic and criteria based on Gelman et al. (2013) and Stock et al. (2018), chain length did not require adjustment because < 5% of total variables exceeded 1.05. "Residual" and "process" errors were considered in our model to account for uncertainties introduced by the variable and nonconstant (i.e., pulsed) nature of sediment delivery to lakes across the PAD.

The MixSIAR model was applied to all contiguous freeze-dried 1-cm thick samples in a sediment core from PAD 30 (length: 45 cm; collected in 2016), and separately again for a core from PAD 31 (length: 38 cm; collected in 2010; Glew 1989), which were analyzed for elemental

concentrations at ALS Canada (Waterloo) using the same analytical methods as for end-member samples. The sediment cores were dated using gamma-ray spectrometric measurement of ^{210}Pb and ^{226}Ra activities and the Constant Rate of Supply model, as described in Kay et al. (2019). Results were used to assess the model's ability to reconstruct past changes in sediment sources associated with three previously determined, distinct hydrological phases during the past 300 years. PAD 30 (local name: Mamawi Pond; 58.509044°, -111.517280°) and PAD 31 (local name: Johnny Cabin Pond; 58.495582°, -111.518152°) are located ~1 km apart and on opposites sides of Mamawi Creek in the southern Athabasca sector of the PAD (Figure 6.1), and thus approximate replicate sites. However, PAD 31 lies at slightly lower elevation than PAD 30 and is slightly more flood-prone (Kay et al. 2019). During the three hydrological phases, mineral matter content in sediment cores varied from ~40% to ~90% (Wolfe et al. 2008b; Hall et al. 2012; Kay et al. 2019), which encompasses much of the range in lake sediment composition across the delta. During the first phase, from prior to ~1700 until ~1940, the lakes were inundated under a high-stand of Lake Athabasca supported by elevated flow of the Athabasca River. After ~1940, Lake Athabasca levels declined and both lakes entered a second isolated, closed-drainage hydrological phase of infrequent or absent flooding despite their location adjacent to Mamawi Creek, which became a relict (nonflowing) channel during this period. After 1982, both lakes entered a third hydrological phase when they became increasingly prone to river flooding following an avulsion of the Embarras River into Cree and Mamawi creeks (an event known as the Embarras Breakthrough). This has directed increasing Athabasca River flow via the Embarras River to Cree and Mamawi creeks and to adjacent low-lying areas where these lakes are located. Thus, elemental analysis on sediment cores from PAD 30 and PAD 31 and application of MixSIAR allows us to assess for accuracy and reproducibility of the methodology to reconstruct periods with flooding (under both

continuous diffuse flow with occasional pulse flood events pre-1940, and frequent episodic flood events after 1982) and without flooding (~1940–1982), and test if the methodology determines that the proximal Athabasca River is the major source of flood-supplied sediment.

Results

LDA identified 10 significant elements (Ag, Be, Ca, Li, Pb, S, Sb, Sr, Tl, V) that resulted in clear separation of sediment samples representing the three a priori end-members (Figure 6.2). The first axis captured 64.2% of the variation and separated elemental concentrations of sediment supplied by the Peace River, positioned to the right, from sediment supplied by the Athabasca River, positioned to the left. The first axis is most strongly associated with variation in concentrations of Sb, Li, V, and Be. Sb, Li, and V are relatively high in sediment supplied by the Peace River, whereas Be is relatively high in sediment supplied by the Athabasca River. The second axis captured 35.8% of the variation and separated sediment of flooded lakes, positioned low on axis 2, from non-flooded lakes (i.e., local catchment), positioned high on axis 2. Sediment of flooded lakes is relatively high in Pb and Ca, whereas Sr is relatively high in non-flooded lakes that received their sediment from the local catchment. Sample scores of riverbank and river-bottom sediments mostly plotted near the group centroids, as expected given that the Peace River and Athabasca River are the sole source of sediment in these samples. Sample scores of the lakes flooded by the Athabasca River are positioned adjacent to the river sediment samples collected from the Athabasca River, and sample scores of the lakes flooded by the Peace River are positioned adjacent to the river sediment samples collected from the Peace River. Notably, there is no overlap between sediment supplied by the Athabasca River vs. Peace River, and overlap is minimal between surficial sediment of flooded and non-flooded lakes. Overall, use of LDA identifies (1) the source of flood-supplied sediment (Peace River vs. Athabasca River) is the principal gradient

of variation in elemental concentrations, (2) variation due to presence or absence of flooding is a secondary gradient, and (3) centroids of the three end-members are distinct.

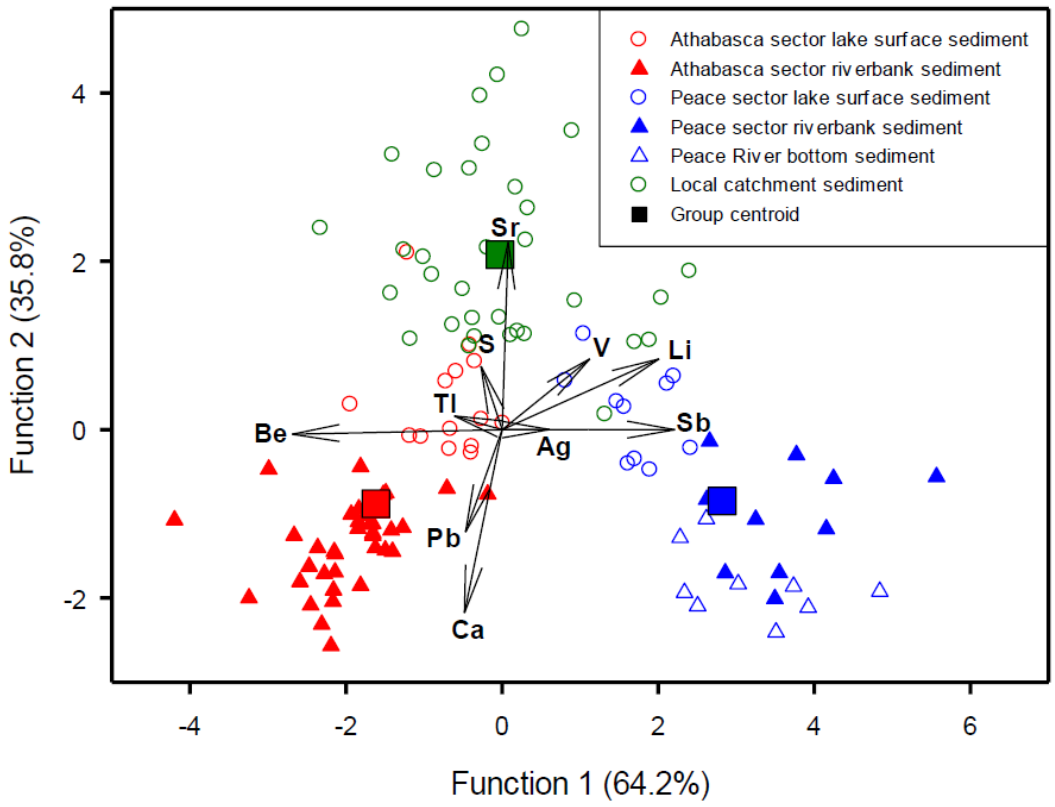

Figure 6.2 Ordination bi-plot based on LDA of concentrations of the 10 statistically significant elements in samples of surficial lake sediment (open circles), river-bottom sediment (open triangles), and riverbank sediment (solid triangles). The vectors for elemental concentrations depict their association with each of the three end-members. Samples are color-coded by their a priori designation to an end-member: Athabasca River (red), Peace River (blue), and local catchment (green).

Cross-validation of the LDA resulted in 90.2% of all sediment samples correctly categorized to their a priori endmember (Table 6.1). Classification accuracy was slightly higher for the Athabasca River and Peace River end-members (90.0% for Athabasca River, 93.1% for Peace River) than the local catchment end-member (87.9%), consistent with the small amount

overlap between sample scores in the LDA from the local catchment end-member with the two river end-members (Figure 6.2). Lower classification accuracy of the catchment end-member is not surprising given the lakes are situated in both sectors of the delta. However, the means and sample SDs of the sedimentary elemental concentrations for each end-member are used as input into MixSIAR, which are well separated on the LDA as captured by the centroids (Figure 6.2). Based on these outcomes, application of the mixing model is likely to provide a robust approach for reconstructing past variation in sediment delivered from the three main sources to lakes in the PAD.

Table 6.1 Results of leave-one-out cross-validation analysis by linear discriminant analysis. End membership of sediment samples are compared between *a priori* designations and designations predicted on the basis of elemental composition. Results are provided in raw counts and percentages.

			Predicted End-member			
			Athabasca R.	Peace R.	Catchment	Total
a priori designation	Count	Athabasca R.	46	0	4	50
		Peace R.	0	27	2	29
		Catchment	0	1	32	33
	Percentage	Athabasca R.	92.0	0.0	8.0	100.0
		Peace R.	0.0	93.1	6.9	100.0
		Catchment	0.0	3.0	97.0	100.0
Cross-validated	Count	Athabasca R.	45	1[1]	4[2]	50
		Peace R.	0	27	2[3]	29
		Catchment	1[4]	3[5]	29	33
	Percentage	Athabasca R.	90.0	2.0	8.0	100.0
		Peace R.	0	93.1	6.9	100.0
		Catchment	3.0	9.1	87.9	100.0

Footnote: superscripts denote misclassified samples:
[1] PAD 40 (2018)
[2] PAD 33 (2017), PAD 36 (2017), PAD 40 (2017), PAD 33 (2018)
[3] PAD 8 (2017), M18 (2018)
[4] M3 (2017)
[5] PAD 14 (2017), PAD 18 (2017), PAD 58 (2017)

The MixSIAR model was applied to elemental concentrations in stratigraphic records from PAD 30 and PAD 31 spanning the past ~300 yr to infer temporal patterns of variation in sediment source contribution (Figure 6.3). For independent validation, these temporal patterns were compared to variation in organic matter (OM) content, which varies inversely with magnitude of river floodwater influence (Kay et al. 2019). Results from the model produced remarkably similar temporal patterns of variation in sediment proportions at both lakes. During ~1680–1940, the MixSIAR model indicates that inputs from the Athabasca River dominated sediment composition at PAD 30 and PAD 31 (~80%), consistent with relatively low OM content during a period of known prolonged inundation of both lakes under a high-stand of Lake Athabasca. Interestingly, sediment attributed to the Peace River increased to ~20% during two episodes of this early phase at PAD 30 (~1720–1760 and ~1825–1845). At ~1940, results from MixSIAR suggest contribution of sediment from the Athabasca River decreased abruptly and supply from the local catchment rose to ~70–80% at both lakes. These changes coincided with marked rise in sediment OM content and identify onset of the second hydrological phase of PAD 30 and PAD 31 when water levels on Lake Athabasca declined, which caused both lakes to become hydrologically closed due to greatly reduced input of Athabasca River floodwater (Kay et al. 2019). A marked shift in sediment sources is inferred for both lakes in the 1970s, when contribution from the local catchment declined to near-zero and input from the Peace River and Athabasca River increased to ~57–69% and ~21–32%, respectively, at PAD 30 and PAD 31. This change was rapid and coincides with the largest ice-jam flood in the instrumental record in 1974, when widespread river flooding inundated the entire delta (Peters et al. 2006). Notably, this flood event is not captured in the OM stratigraphic records. Peace River and Athabasca River sediment continued to be the dominant sources to PAD 30 and PAD 31 until the early 1980s, possibly due to subsequent runoff that transported flood-

derived sediment from their local catchments to the coring location. After 1982, sediment from the Athabasca River is inferred to rise suddenly to >80% in both lakes, coincident with the Embarras Breakthrough which increased frequency of flooding at PAD 30 and PAD 31 by the Athabasca River (Wolfe et al. 2008b; Kay et al. 2019). This shift to the third hydrological phase is also captured by marked decline of sediment OM content due to greater influx of suspended mineral rich sediment in Athabasca River floodwaters (Kay et al. 2019).

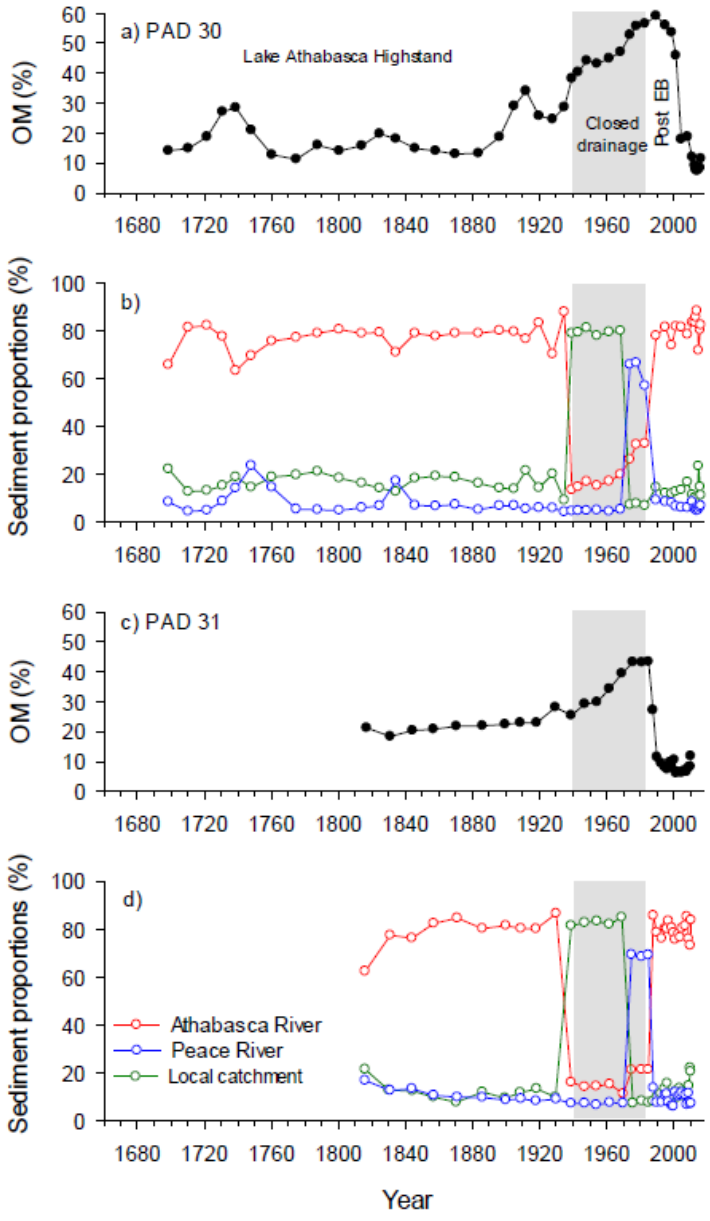

Figure 6.3 Graphs showing OM content and temporal variation of inferred proportion of sediment from the three end-member sources (Peace River [blue], Athabasca River [red], local catchment [green]) in sediment cores obtained from PAD 30 (a, b) and PAD 31 (c, d). The gray-shaded box identifies a closed-drainage hydrological phase of the lakes (ca. 1940–1982) when flooding was rare. A prior hydrological phase is defined by inundation by a highstand of Lake Athabasca and a later hydrological phase occurred as a result of the Embarras Breakthrough when the lakes became prone to frequent flooding from the Athabasca River. OM content and sediment core chronologies for PAD 30 and PAD 31 are reported in Wolfe et al. (2008a) and Kay et al. (2019).

Discussion

Paleolimnological analyses of multiple variables in sediment cores from aquatic basins have provided temporal perspectives about frequency and magnitude of flood events and other hydrological processes across floodplain landscapes (Wolfe et al. 2008b; Lintern et al. 2016). Yet, it remains challenging to integrate results at a landscape-scale because spatiotemporal variations in sediment composition in these dynamic aquatic environments necessitate use of different paleolimnological analyses with varying quantitative reconstruction potential. Thus, development and application of a single analysis that can be universally applied to quantify spatiotemporal patterns of variation in hydrological conditions across floodplains would provide an important advance. Here, we have demonstrated an effective methodology to quantify relative contributions of sediment from two rivers and from local catchments of lakes. We used measurements of elemental concentrations to trace inputs from three different sediment sources and employed a BMM, MixSIAR, to reconstruct variation in hydrological conditions from two lakes with previously described hydrologic history. A distinct advantage of the methodology is that elemental concentrations can be measured across the full spectrum of mineral-rich to organic-rich sediment typical of broad gradients of basin hydrology and river connectivity in floodplains.

A fundamental criterion for application of mixing models is characterization of distinct end-members (Smith and Blake 2014; Smith et al. 2015). We relied on geographic location, lake water isotope composition and lake water chemistry data, and knowledge accrued during 20 yr of fieldwork in the PAD, to define the three end-member allochthonous sources of sediment to lakes (Athabasca River, Peace River, local catchment). Clear separation of Al-normalized elemental concentrations among end-members in the LDA resulted in very high classification accuracy (90.2%) by cross-validation due to distinct geochemical fingerprints of Peace River sediment vs.

Athabasca River sediment. Such degree of separation of end-member centroids is uncommon among sediment-based mixing models (Upadhayay et al. 2018; Wynants et al. 2020). We achieved this outcome through a substantial effort over many years of fieldwork and knowledge of this complex landscape, yet we recognized this opportunity only after analysis and interpretation of lake surface sediment collected in 2017 for other purposes (Owca et al. 2020). More strategic and efficient sampling is possible elsewhere, which can improve transferability of the approach for use by others with lower investment.

Results of the MixSIAR model applied at PAD 30 and PAD 31 align remarkably well with the three known hydrological phases experienced at these lakes during the past ~300 years (Wolfe et al. 2008b; Kay et al. 2019), which capture most of the range of sediment composition for lakes across the PAD. Outputs from MixSIAR inferred that Athabasca River floodwaters were the dominant source of sediment to both PAD 30 and PAD 31 during the past 300 years, except for a brief period of reduced river influence between ~1940 and 1982. A novel inference, however, is that the largest magnitude flood on record in 1974 (Peters et al. 2006) resulted in delivery of a substantial proportion of sediment from Peace River floodwaters to both lakes. PAD 30 and PAD 31 are proximal (2.7–3.7 km) to the Athabasca River and distal (~45 km) to the Peace River, and these results suggest substantial southward penetration of Peace River floodwaters during the 1974 flood which is entirely plausible, based on aerial images of the flood event (Peters et al. 2006). Our methodological framework and application of MixSIAR clearly identifies the most proximal river (i.e., the Athabasca River and its distributary, the Embarras River, following the Embarras Breakthrough in 1982) as the main source of flood-derived sediment, except for the extreme flood of 1974 and possibly also unusually high-magnitude flooding that occurred in the mid-1700s and mid-1800s. Thus, the methodological approach appears to have detected previously unrecognized

importance of delivery of floodwater and sediment from the Peace River to the central and southern regions of the PAD during some extreme flood events. Unexpectedly, all three of these intervals of inferred increase of Peace River supplied sediment coincide with rise of sediment OM content, which could occur if the flux of Peace River sediment was insufficient to dilute subsequent within-lake production of organic sediment, and high energy flooding from the proximal Athabasca River did not occur. Overall, for the period of time captured in cores from both PAD 30 and PAD 31 (post ca. mid-1800s), application of the MixSIAR model to elemental concentrations resulted in very similar stratigraphic patterns of inferred sediment proportions from the three end-members at both lakes. Given the comparable hydrological setting of both lakes, we contend the methodology leads to reproducible results that match known temporal shifts in their basin hydrology, yet also identified extended reach of Peace River floodwaters during exceptionally large delta-wide flood events.

Conclusions

For application of the methodology to other floodplains, we recommend that sampling includes river sediment (riverbank, bottom, and suspended sediment) and lake surficial sediment. The river sediment samples are important to anchor the elemental composition of the source material in the mixing model, while the lake surficial sediment samples provide analogs for application to the lake sediment cores. We suggest caution should be exercised when interpreting results from the mixing model to stratigraphic profiles from floodplain lakes because sediment supplied by flood events are deposited on the landscape, which may be remobilized by snowmelt and rainfall events, and lead to inference of river contribution during non-flood intervals. This mechanism could account for inferred substantial Peace River sediment influence in a few samples deposited after the 1974 flood at PAD 30 and PAD 31.

Our methodology advances the important contributions of Wynants et al. (2020) in a new direction. They performed measurements of elemental concentrations in river and lake sediment and applied a BMM to quantify sediment delivery from several tributary watersheds to a single large lake. In contrast, our methodology is capable of quantifying the proportion of sediment contributed to multiple lakes across a floodplain landscape from two rivers during pulse flood events and during long-duration inundation, as well as from the local catchment during non-flood intervals. The approach is readily expandable to floodplains with more than two rivers if elemental concentrations of the fluvial sediment differ sufficiently or can be reduced to those with a single river source. Thus, we anticipate the methodology is transferable to many other floodplains, including the Mississippi River, Tigris and Euphrates rivers, and Yellow River, where flood regimes respond to variation in natural and anthropogenic processes (Richardson et al. 2005; Richardson and Hussain 2006; Nittrouer and Viparelli 2014; Zheng et al. 2017), and where the range of sediment composition may limit application of other paleolimnological measurements.

Chapter 7: Synthesis and Future Directions

Synthesis

The research presented in my PhD thesis has been motivated by concerns expressed by multiple stakeholders responsible for stewardship and use of the PAD, which centre on the widely held belief that the delta's aquatic ecosystems have been degraded by major energy projects located upstream on both the Peace and Athabasca rivers. The stakeholders include local Indigenous governments and organizations (Athabasca Chipewyan First Nation, Mikisew Cree First Nation, Fort Chipewyan Local 125 of the Métis Nation of Alberta), government agencies (e.g., Parks Canada, Alberta Environment & Parks, Environment and Climate Change Canada) and representatives of energy producers (e.g., members of the Canadian Oil Sands Innovation Alliance, BC Hydro). In conversations with these stakeholders during multiple visits to Ft. Chipewyan and at several workshops and conferences, many have expressed firm belief that water levels in the lakes and rivers in the PAD have declined since 1968 when the W.A.C. Bennett Dam began to regulate flow of the Peace River. They have also communicated concern that substances released by oil sands mining and processing activities to the air and the Athabasca River are polluting the water and biota downstream in the delta and at Fort Chipewyan.

During the 12 field sampling campaigns I participated in at the PAD between 2016 and 2019, and from the vantage point of many helicopter flights, I became keenly aware that the PAD is a vast (6,000 km^2), hydrologically complex, and dynamic floodplain landscape. For example, one can see areas that have recently flooded (e.g., trees and shrubs standing in water) as well as areas that have recently desiccated – at the same time but in different places! Concentric rings of dead and living willow shrubs within and adjacent to the delta's perched basins provide evidence of water-level changes that play out at multi-annual to multi-decadal timescales in response to

variations in climatic conditions and flood regimes. Along the shore of Lake Athabasca and on bedrock inliers that populate interior portions of the delta, there are former high-water marks that document an era from more than a century ago when Lake Athabasca was 2.3 m higher than at present and inundated substantial portions of the delta (Johnston et al. 2010). During airplane flights from Ft. McMurray to Ft. Chipewyan, which follow along the Athabasca River, I saw the massive scale of the bitumen mines that straddle the river but also extensive sections of the riverbank where the bitumen-rich McMurray Formation is exposed to the natural erosive forces that deliver substances of concern to the river and downstream. Thus, while industrial activities have potential to alter hydrological regimes and increase delivery of pollutants, it became evident to me that natural processes have long played influential roles. Unfortunately, existing hydrometric and sediment quality monitoring data are too short and too sparse to adequately distinguish the roles of natural versus anthropogenic influences on water quantity and water quality at the PAD. Based on research led by my supervisors since 2001, I recognized that paleolimnological analyses can generate critical information over sufficiently broad spatial and temporal scales to improve knowledge of their roles. Thus, over the course of my PhD research, I applied conventional and novel paleolimnological methods to sediment cores spanning two or more centuries from lakes in the PAD to discern effects of natural processes and anthropogenic stressors on basin hydrology and contaminant deposition via both fluvial and atmospheric pathways.

Stratigraphic analyses of trace elements (beryllium, chromium, lead, mercury, nickel (Ni), vanadium (V), and zinc) in sediment cores from floodplain and upland lakes were used to determine pre-disturbance concentrations and to quantify the extent to which they have become enriched since onset of oil sands development via fluvial and atmospheric pathways, respectively (Chapters 2-4). Results reveal no enrichment via fluvial pathways since the onset of oil sands

activities. Also, no enrichment was detected for pollution-indicator metals V and Ni, or for THg at upland lakes aligning with oil sands development. Rather, enrichment of THg was recorded at upland lakes from a more distant source beginning at ~1930, which is congruent with other lake sediment cores from western North America as a consequence of hemispheric patterns of pollution (Drevnick et al. 2016). Analysis of sediment records from lakes within regions of intense mining and processing of bitumen (Alberta Oil Sands Region) and gold (central Northwest Territories) detected enrichment via atmospheric pathways of pollution indicator metal(loid)s, which provide confidence in the sensitivity of the approach (Chapter 4).

Paleohydrological reconstructions of floodplain lakes in the Athabasca Delta have provided valuable insight into the drivers of hydrological change. Expanding upon the research conducted by Wolfe et al. (2008b), results from stratigraphic analyses of organic and inorganic matter content from nine floodplain lakes along the Athabasca River provide clear evidence that the 1982 Embarras Breakthrough has been a major cause of recent hydrological change in the Athabasca Delta (Chapter 5). After 1982, lakes located along Cree and Mamawi creeks have received more frequent flooding while flood frequency has declined at locations to the east and northeast of the Embarras Breakthrough. The Embarras Breakthrough is a natural geomorphic event that altered distributary flow in the Athabasca Delta and is the most influential hydrological change in the past ~120 years (Wolfe et al. 2008b; Chapter 5), yet it is rarely mentioned or is only acknowledged as a minor contributor of hydrological change in recent assessments of the ecological status of the PAD (WHC/IUCN 2017; IEC 2018).

During research that probed lake sediment records for evidence of trace metal pollution (see Chapter 2), a critical observation identified that sediment supplied by the Peace and Athabasca rivers differ in relative concentrations of a suite of trace elements, likely due to differing geological

terrane in their respective watersheds (Owca et al. 2020). This discovery occurred while I was enrolled in a graduate-level statistics course co-taught by Professors Heidi Swanson and Rebecca Rooney. Exposure to the merits of using mixing models for environmental assessment stimulated my interest to develop, apply, and test the approach using trace element concentrations in aquatic sediment, as presented in Chapter 6. This is a key advancement as sediment elemental concentrations can be measured across the full gradient of mineral-rich to organic-rich sediment, which is typical in floodplain landscapes, and it provides a universal approach for reconstructing sediment sources and, by inference, hydrological pathways of sediment delivery. Output of the mixing model, when applied to two floodplain lakes in the Athabasca Delta, align well with three previously described hydrological phases since ~1900 and produced a novel finding that Peace River sediment and floodwater penetrated into the Athabasca Delta during the historically significant 1974 ice-jam flood event.

The research presented in the five data chapters of this thesis is timely because it developed and evolved during a period when the World Heritage status of Wood Buffalo National Park was being evaluated by UNESCO, in response to a petition from the Mikisew Cree First Nation (MCFN 2014). A key recommendation that arose was for the Government of Canada to formulate an Action Plan to guide effective policies, decisions and actions to protect the 'Outstanding Universal Value' of Wood Buffalo National Park (WHC/IUCN 2017). One recommended action is to expand the scope of monitoring in the PAD to understand the effects of threats (WBNP 2019), but this requires knowledge at sufficient temporal and spatial scales. Thus, a key contribution of this thesis is the knowledge of pre-industrial baselines from several floodplain lakes should be crucial to underpin a comprehensive aquatic ecosystem monitoring program capable of detecting the effects of contaminant releases by oil sands mining and processing activities, as recommended by Remmer

et al. (2020a). Indeed, the pre-industrial metal(loid) baselines developed for the Peace and Athabasca rivers present a robust characterization of reference conditions for detecting enrichment of river-bottom sediment or surficial lake sediment as has been demonstrated at the PAD (Wiklund et al. 2014; Owca et al. 2020). Despite no current evidence of enrichment of river-bottom sediment and lake sediment at the PAD due to oil sand mining and processing activities (Wiklund et al. 2014; Owca et al. 2020; see Chapters 2-4), application of this approach is timely given that the Government of Alberta is considering approvals for release of treated oil sands process water directly into the Lower Athabasca River in coming years (Hicks and Scrimgeour 2019).

Final reflection on key scientific decisions

Results of the research that form this PhD Thesis provide considerable insight on drivers of hydrological changes in the Athabasca Delta and contaminant deposition across a broad swath of northwestern Canada. The Thesis was divided into two themes, contaminants and hydrology, but the sequence of the chapters does not reflect the chronological order that they were published in, or submitted to, peer-reviewed journals. As a result, the reader should be cautioned that evolution of the science and understanding is not captured by the sequence of the Thesis chapters. Below, I take the opportunity to reflect on several of the key scientific decisions that were made using 20 years of collective experience of the Hall/Wolfe Research Group working in complex floodplain environments and professional judgement I developed during the course of my PhD program.

Evaluation of the potential for deposition of trace elements in lakes due to industrial activities relied heavily on use of enrichment factor (EF) calculations, which may not reveal important information provided by the raw concentration values if attention is not also paid to them. For example, when calculating EFs at low concentrations of trace elements, moderate rises

in concentrations may result in a substantial increase of EFs even if the value is below risk of biological or ecological harm. Also, concentrations of aluminum approached the minimum detection limit of the analytical method in pre-disturbance sediment from some upland lakes, which can lead to EFs that are challenging to interpret with confidence. In situations where EFs demonstrated a rising trend above background and the data presented opportunity for further characterization, I typically completed additional analyses (e.g., computation of anthropogenic fluxes and excess inventories) to quantify anthropogenic influences. Notably, EFs may be confounded if reference (baseline) conditions are not adequately defined. Two different statistical methods were used to define baseline values throughout this Thesis including a mean pre-industrial value or a linear regression between the metal of interest and a geochemical normalizer. Geochemical normalization was used, when possible, throughout the Thesis but was not applied to elements that did not meet the criteria set by Loring (1991). Ideally, geochemical normalization would be applied consistently to every metal(loid), but a mean pre-industrial value was used for elements that possessed weak statistical relations with a geochemical normalizer or that are prone to post-depositional mobility in lake sediments. These decisions were rooted in scientific criteria set by Loring (1991), but also relied upon professional judgement, to avoid situations where inappropriate application of a geochemical normalizer may confound or mask a signal of enrichment.

An example of applying professional judgement occurred when interpreting elemental concentrations in the sediment core from PAD 30 for evidence of enrichment. There, concentrations of primary pollutants and vanadium were geochemically normalized to aluminum concentration to account for shifting grain size and energy conditions (Chapter 2), but concentrations of THg were not normalized (Chapter 3). Despite this difference in methodological

approaches to compute EFs, there was no evidence that any of these metal(loid)s became enriched since onset of oil sands mining and processing activities. Enrichment of Zn and THg was observed in the sediment records from PAD 30, but this occurred in the same few samples that included sediment deposited before oil sands development and was attributed to potentially local catchment processes (Chapter 2) or atmospheric deposition (Chapter 3). Given the nature of the analysis, it is very difficult to fully delineate the processes that led to enrichment of Zn and THg above background concentrations (but not other elements) and is likely to be a combination of both reduced flooding and local catchment processes.

Like other scientific analyses, radiometric dating of floodplain lake sediment cores, determination of metal(loid) concentrations and output of the Bayesian mixing model, for example, have uncertainties. Nonetheless, the uncertainties did not hamper delineation of consistent and repeatable trends in 'pristine' and industrialized landscapes. For instance, there is exceptional correspondence between the anthropogenic THg fluxes that were estimated based on analyses of sediment cores from upland lakes PAD 18 and AC5 even though the sediment cores were collected a decade apart, sectioned at different intervals (0.5- vs. 1-cm intervals, respectively) and THg concentrations were analyzed at two different laboratories that used different analytical methods. Strong correspondence of anthropogenic flux estimates between cores from these two lakes is unlikely if they are confounded by uncertainties associated radiometric dating and measurements of metal(loid) concentrations. In Chapter 5, I developed a novel mixing model framework that produced outputs entirely consistent with the interpretation of conventional stratigraphic data, yet the model output also provided a novel outcome of the extensive southward penetration of the Peace River waters during the 1974 flood event. As illustrated, mixing models are powerful tools that can provide robust results, but caution should be exercised as model

parameters are often tailored to specific studies and may not be applicable in other locations (Collins et al. 2020). Thus, a high degree of confidence can be garnered in the findings presented throughout the Thesis as the consistency, repeatability and large sample sizes greatly outweigh the concerns associated with uncertainty.

Application of the Bayesian mixing model to generate novel paleohydroscapes for the Peace-Athabasca Delta: a new research direction

Beyond the lake-specific application of the Bayesian mixing model (BMM; MixSIAR) demonstrated in Chapter 6, opportunity exists to employ the model at lakes throughout the PAD where sediment cores have been collected to generate novel 'paleohydroscapes' as maps of the delta showing spatial variation in inferred sources of sediment input (Figure 7.1-7.2). Application of the model presents an advancement over previous paleolimnological studies in the PAD aimed at improving our understanding of past hydrological change, which have often relied on stratigraphic profiles of several different variables across lakes leading to qualitative to semi-quantitative interpretations (e.g., Wolfe et al. 2008a, 2012). Below, I provide an early view of a new research direction that uses sediment elemental concentrations as tracers in the BMM from a network of lakes to delineate the spatio-temporal variation in sediment sources and, by inference, influence of Athabasca River and Peace River floodwaters to the delta.

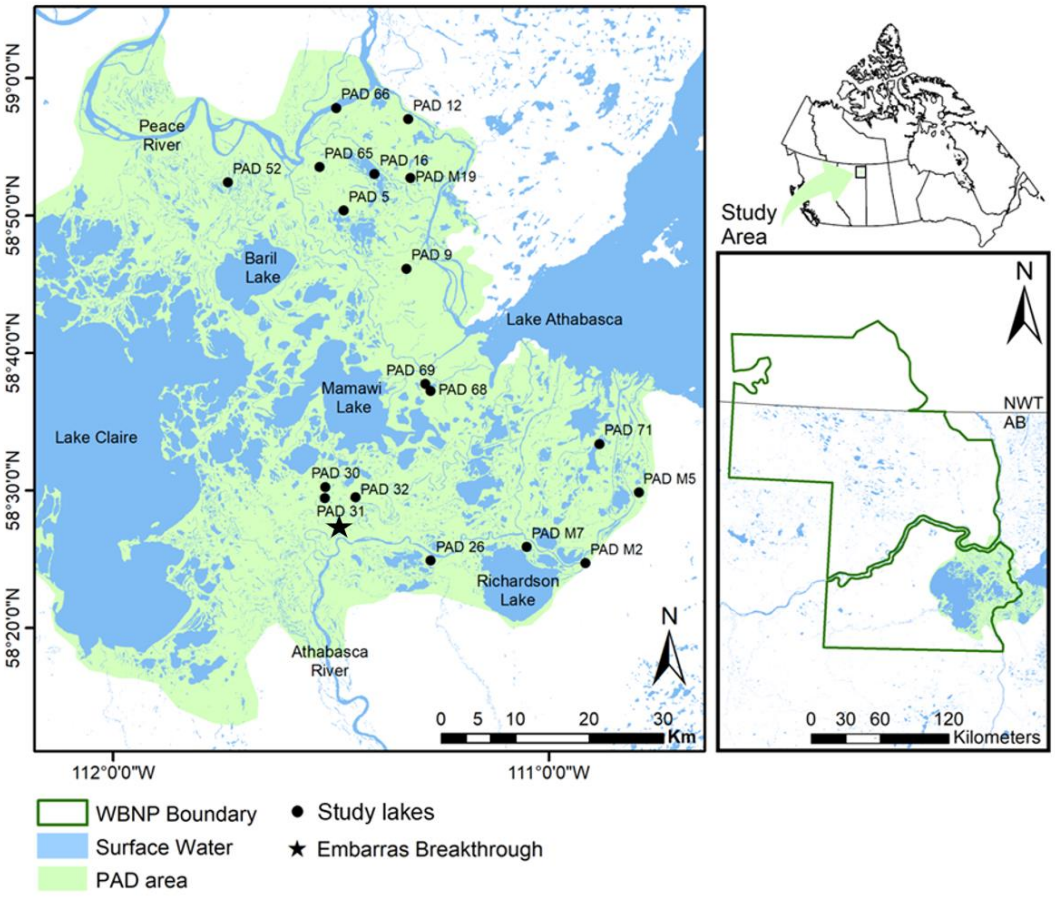

Figure 7.1 Maps showing lake sediment coring sites (black circles) in the Peace-Athabasca Delta (PAD) utilized in the MixSIAR model. In the left panel, the Wood Buffalo National Park boundary is denoted by the dark green line and the location of the Embarras Breakthrough is marked as a star. The Wood Buffalo National Park boundary is denoted by the dark green line in the bottom right panel. Source: Government of Canada (national park boundaries: https://open.canada.ca/data/en/dataset/9e1507cd-f25c-4c64-995b-6563bf9d65bd; water bodies: https://open.canada.ca/data/en/dataset/448ec403-6635-456b-8ced-d3ac24143add; PAD area: shapefile generated by Cory Savage.

The paleohydroscapes, as illustrated in Figure 7.2, were generated by applying the MixSIAR model to elemental concentrations in individual sediment samples selected at approximately decadal intervals from radiometrically-dated stratigraphic records of 18 lakes distributed across the PAD, with the exception of 2017, which was generated using surface

sediments from a larger number of lakes. Spatial interpolation was achieved by kriging, an approach similar to one used to develop 'isoscapes' in Remmer et al. (2020b). Results capture four distinct intervals of the influence of Athabasca River and Peace River floodwaters during the past ~150 years. The earliest interval (~1880 to ~1935) is denoted by strong influence of floodwaters from both the Peace and Athabasca rivers, which aligns with other paleoenvironmental records that have identified high river discharge and high-water levels at Lake Athabasca (Wolfe et al. 2006, 2008a, 2008b, 2011, 2012; Johnston et al. 2010; Sinnatamby et al. 2010; Chapter 5). The second interval (~1945 to ~1955) is marked by reductions in flood influence from both rivers. The third interval (~1965 to ~1975) displays a resurgence in the extent of floodwaters from both rivers, and straddles from just before to just after operation of the W.A.C. Bennett Dam. The paleohydroscape for ~1975 appears to capture the 1974 flood event and infers the maximum extent of floodwaters from the Peace River since ~1880, which penetrated well into the western portion of the Athabasca Delta. The fourth interval includes the paleohydroscapes since ~1985, which depict a shift to low spatial extent of floodwaters from both the Peace and Athabasca rivers, including at the Athabasca River terminus region. An exception is the inferred strong influence of Athabasca River floodwaters along the Mawami and Cree creek corridor displayed in these paleohydroscapes. The inferred pattern of reduced flood extent at the Athabasca River terminus and increased flood influence along the Mamawi and Cree creek corridor captures the hydrological effect of the 1982 Embarras Breakthrough (Wolfe et al. 2008b; Chapter 5). Since ~1985, only the paleohydroscape from ~2000 infers widespread flooding across the PAD, and it likely reflects influence of ice-jam flood events in 1996 and 1997, and possibly 2003.

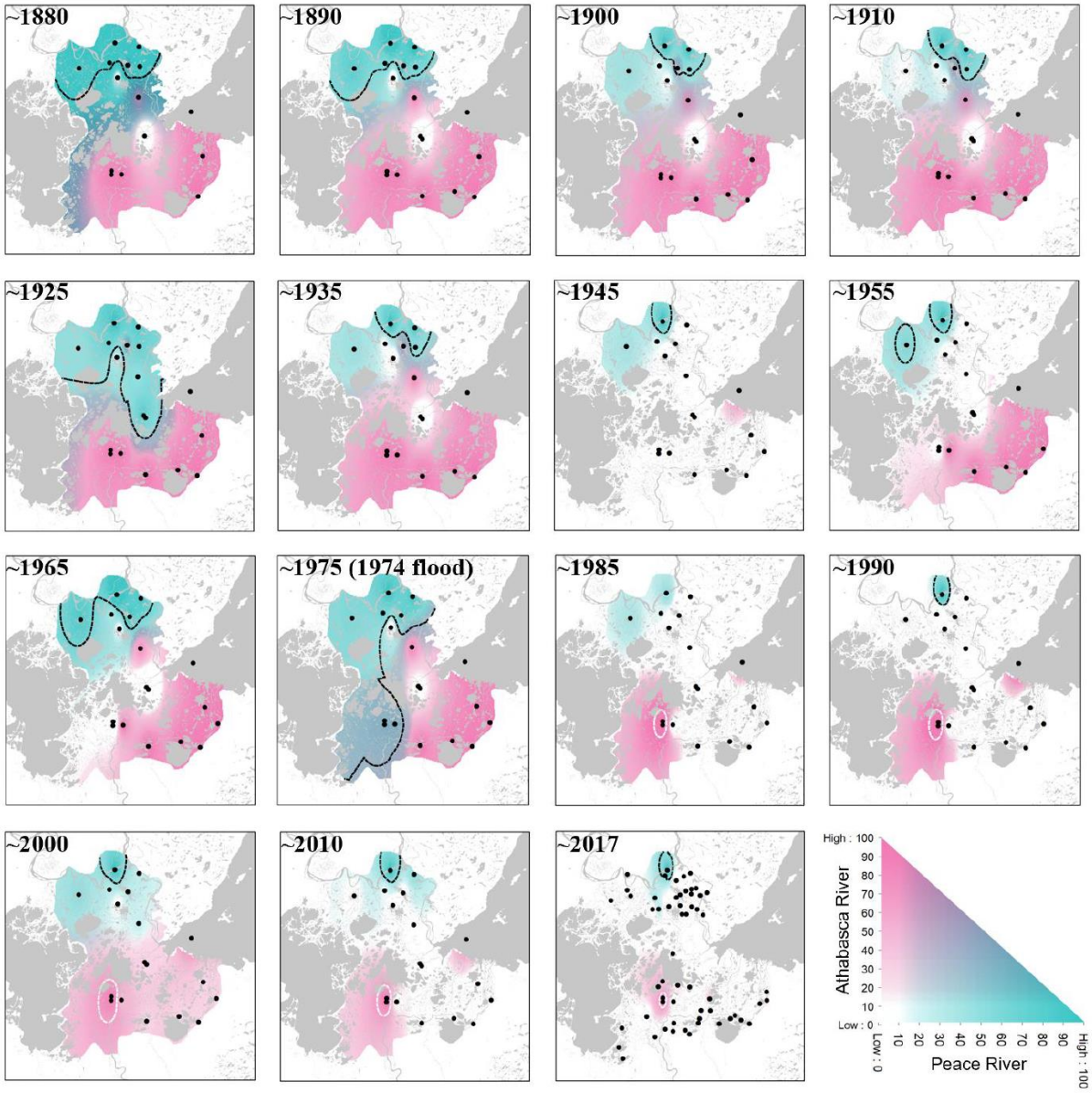

Figure 7.2 Time-series of paleohydroscapes at ~10-year intervals showing spatial interpolation of sediment proportion from the Peace River, Athabasca River, and local catchment across the Peace-Athabasca Delta during ~1880 to ~2017. The black dashed lines indicate regions of over 50% Peace River influence while the white dashed lines indicate regions of over 75% Athabasca River influence. The darker colours indicate greater influence of either the Peace River (green) or Athabasca River (pink) while white indicates the contribution of sediment from the local catchment in the absence of substantial flood influence (scale is presented in the bottom right panel). Individual lake locations (from Figure 7.1) that contribute to each time interval are identified as black circles.

Clearly, the visuals provided by the paleohydroscapes demonstrate marked spatio-temporal variability of hydrological conditions across the PAD, and at scales complementary to ongoing isotope-based monitoring and production of isoscapes (Remmer et al. 2020a,b). Combined, these methods provide a powerful approach to tracking hydrological change in the delta at a range of spatial and temporal scales relevant to inform environmental stewardship.

References

Abrahim, G.M.S., Parker, R.J., 2008. Assessment of heavy metal enrichment factors and the degree of contamination in marine sediments from Tamaki Estuary, Auckland, New Zealand. Environ. Monit. Assess. 136, 227–238.

Akaike, H., 1973. Information theory as an extension of the maximum likelihood principle. Ed: Petrov BN & Csaki F, Second international symposium on information theory. Budapest, Akaemiai Kiado, pp. 267–281.

Alexander, A.C., and Chambers, P.A. 2017. Assessment of seven Canadians rivers in relation to stages in oil sands industrial development. Environmental Reviews, 24: 484e494. https://doi.org/10.1139/er-2016-0033

Appleby, P.G. 2001. Chronostratigraphic techniques in recent sediments. In J.P. Smol (ed) Tracking Environmental Change Using Lake Sediments: Basin Analysis, Coring, and Chronological Techniques, Developments in Paleoenvironmental Research Vol 1 171–203.

Arciszewski, T.J., Hazewinkel, R.O., Dubé, M.G. 2021. A critical review of the ecological status of lakes and rivers from Canada's oil sands region. Integrated Environmental Assessment and Management, 18: 361-387. https://doi.org/10.1002/ieam.4524

Baker, L.F., Ciborowski, J.J., MacKinnon, M.D., 2012. Petroleum coke and soft tailing sediment in constructed wetlands may contribute to the uptake of trace metals by algae and aquatic invertebrates. Sci. Total Environ. 414, 177–186.

Barnett J, Lambert S and Fry I 2008 The hazards of indicators: insights from the environmental vulnerability index Annals of the Association of American Geographers 98 102–19

Batley, G.E., and Maher, W.A. 2001. Development and application of ANZECC and ARMCANZ sediment quality guidelines. Australasian Journal of Ecotoxicology, 7: 81-92.

Belmont, P., J. K. Willenbring, S. P. Schottler, J. Marquard, K. Kumarasamy, and J. M. Hemmis. 2014. Toward generalizable sediment fingerprinting with tracers that are conservative and nonconservative over sediment routing timescales. J. Soils Sediments 14: 1479–1492. doi: 10.1007/s11368-014-0913-5

Beltaos, S. 2014. Comparing the impacts of regulation and climate on ice-jam flooding of the Peace-Athabasca Delta. Cold Regions Science and Technology, 108: 49-58. https://doi.org/10.1016/j.coldregions.2014.08.006

Beltaos, S. 2018. Frequency of ice-jam flooding of Peace-Athabasca Delta. Canadian Journal of Civil Engineering, 45. https://doi.org/10.1139/cjce-2017-0434

Beltaos, S., and B. Bonsal. 2021. Climate change impacts on Peace River ice thickness and implications to ice-jam flooding of Peace-Athabasca Delta, Canada. Cold Reg. Sci. Technol. 186: 103279. doi: 10.1016/j.coldregions.2021.103279

Biester, H., Bindler, R., Martinez-Cortizas, A., and Engstrom, D.R. 2007. Modeling the past atmospheric deposition of mercury using natural archives. Environmental Science & Technology, 41: 4851–4860. http://dx.doi.org/10.1021/es0704232

Binford B W 1990 Calculation and uncertainty analysis of 210Pb dates for PIRLA project lake sediment cores J. Paleolimnol. 3 53–67

Birch, G.F. 2017. Determination of sediment metal background concentrations and enrichment in marine environments – A critical review. Science of the Total Environment, 580: 813-831. https://doi.org/10.1016/j.scitotenv.2016.12.028

Blais, J.M., Rosen, M.R., and Smol, J.P. 2015. Using natural archives to track sources and long-term trends of pollution: an introduction. In: Blais, J.M., Rosen, M.R., Smol, J.P. (Eds.), DPER Environmental Contaminants: Volume 18: Using Natural Archives To Track Sources And Long-Term Trends Of Pollution. Springer, New York, pp. 1–4.

Blake, W. H., and others. 2018. A deconvolutional Bayesian mixing model approach for river basin sediment source apportionment. Sci. Rep. 8: 13073. doi: 10.1038/s41598-018-30905-9

Blum, J.D., Johnson, M.W. Gleason, J.D., Demers, J.D., Landis, M.S., and Krupa, S. 2012. Mercury concentration and isotopic composition of epiphytic tree lichens in the Athabasca Oil Sands Region. In K.E. Percy (ed.) Developments in Environmental Science Vol 11, 373-390.

Boës, X., Rydberg, J., Martinez-Cortizas, A., Bindler, R., and Renberg, I. 2011. Evaluation of conservative lithogenic elements (Ti, Zr, Al, and Rb) to study anthropogenic element enrichments in lake sediments. Journal of Paleolimnology, 46: 75-87. https://doi.org/10.1007/s10933-011-9515-z

Bourbonniere, R.A., and Telford, S.L. 1996. Depositional history of sediment in Lake Athabasca: geochronology, bulk parameters, contaminants, and biogeochemical markers. Northern River Basins Study Project Report 72.

Bowman, M.F., and Somers, K.M. 2005. Considerations when using the reference condition approach for bioassessment of freshwater ecosystems. Water Quality Research Journal of Canada, 40: 347e360. https://doi.org/10.2166/wqrj.2005.039

Boyle, D., Brix, K.V., Amlund, H., Lundebye, A.K., Hogstrand, C., and Bury, N.R. 2008. Natural arsenic contaminated diets perturb reproduction in fish. Environmental Science and Technology, 42: 5354-5360. https://doi.org/10.1021/es800230w

Brady, J.P., Ayoko, G.A., Martens, W.N., and Goonetilleke, A. 2015. Development of a hybrid pollution index for heavy metals in marine and estuarine sediments. Environmental Monitoring & Assessment, 187: 306-319. https://doi.org/10.1007/s10661-015-4563-x

Brock, B. E., and others. 2010. Flood frequency variability during the past 80 years in the Slave River Delta, NWT, as determined from multi-proxy paleolimnological analysis. Can. Water Resour. 35: 281–300. doi: 10.4296/cwrj3503281

Brock, B.E., Martin, M.E., Mongeon, C.L., Sokal, M.A., Wesche, S.D., Armitage, D., Wolfe, B.B., Hall, R.I., and Edwards, T.W.D. 2010. Flood frequency variability during the past 80 years in the Slave River Delta, NWT, as determined from multi-proxy paleolimnological analysis. Canadian Water Resources Journal, 35: 281-300. https://doi.org/10.4296/cwrj3503281

Bromstad, M.J., Wrye, L.A., and Jamieson, H.E. 2017. The characterization, mobility, and persistence of roaster-derived arsenic in soils at Giant Mine, NWT. Applied Geochemistry, 82: 254-261. https://doi.org/10.1016/j.apgeochem.2017.04.004

Brown, K.C. 2022. Evaluating the role of local climate change on reduced freshwater availability at the Peace-Athabasca Delta using paleolimnology. UWSpace, http://hdl.handle.net/10012/18346

Burn D H, Abdul Aziz O I and Pietroniro A 2004 A comparison of trends in hydrological variables for two watersheds in the Mackenzie River Basin Canadian Water Resources Journal 29 283–98

Callender, E., and van Metre, P.C. 1997. Reservoir sediment cores show U.S. lead declines. Environmental Science & Technology, 31: 424A–428A. https://doi.org/10.1021/es972473k

Campbell, D., and Spitzer, A. 2007. High and Dry. Up Here: Explore Canada's Far North. September 2007.

Canadian Association of Petroleum Producers (CAPP). 2020. Retrieved from https://www.capp.ca/resources/publications/ on August 22nd, 2021.

Canadian Council of Ministers of the Environment. 1999. Canadian sediment quality guidelines for the protection of aquatic life: Mercury. In Canadian environmental quality guidelines, Canadian Council of Ministers of the Environment, Winnipeg.

Cheney, C.L., Eccles, K.M., Kimpe, L.E., Thienpont, J.R., Korosi, J.B., and Blais, J.M. 2017. Determining the effects of past gold mining using a sediment paleotoxicity model. Science of the Total Environment, 718: 136308. https://doi.org/10.1016/j/scitotenv.2020.137308

Chetelat, J., Cott, P.A., Rosabal, M., Houben, A., McClelland, C., Belle Rose, E., and Amyot, M. 2019. Arsenic bioaccumulation in subarctic fishes of a mine-impacted bay on Great Slave

Lake, Northwest Territories, Canada. PLoS One, 14: e0221361. https://doi.org/10.1371/journal.pone.0221361

Collins, A. L., D. Walling, L. Webb, and P. King. 2010. Apportioning catchment scale sediment sources using a modified composite fingerprinting technique incorporating property weightings and prior information. Geoderma 155: 249–261. doi: 10.1016/j.geoderma.2009.12.008

Collins, A. L., S. Pulley, I. D. L. Foster, A. Gellis, P. Porto, and A. J. Horowitz. 2017. Sediment source fingerprinting as an aid to catchment management: A review of the current state of knowledge and a methodological decision-tree for end-users. J. Environ. Manage. 194: 86–108. doi: 10.1016/j.jenvman.2016.09.075

Collins, A.L. et al. 2020. Sediment source fingerprinting: benchmarking recent outputs, remaining challenges and emerging themes. Journal of Soils and Sediments, 20: 4160-4193. https://doi.org/10.1007/s11368-020-02755-4

Conly, F.M., Crosley, R.W., Headley, J.V., Quagraine, E.K., 2007. Assessment of metals in bed and suspended sediments in tributaries of the Lower Athabasca River. J. Environ. Sci. Health 42 (8), 1021–1028.

Cooke, C.A., Kirk, J.L., Muir, D.C., Wiklund, J.A., Wang, X., Gleason, A., and Evans, M. S. 2017. Spatial and temporal patterns in trace element deposition to lakes in the Athabasca Oil Sands Region (Alberta, Canada). Environmental Research Letters, 12: 124001. https://doi.org/10.1088/1748-9326/aa9505

Cooper, R. J., N. Pedentchouk, K. M. Hiscock, P. Disdle, T. Krueger, and B. G. Rawlins. 2015. Apportioning sources of organic matter in streambank sediment: An integrated molecular

and compound specific stable isotope approach. Sci. Total Environ. 520: 187–197. doi: 10.1016/j.scitotenv.2015.03.058

Cott, P.A., Zajdlik, B.A., Palmer, M.J., and McPherson, M.D. 2016. Arsenic and mercury in lake whitefish and burbot near the abandoned Giant Mine on Great Slave Lake. Journal of Great Lakes Research, 42: 223-232. https://doi.org/10.1016/j.jglr.2015.11.004

Couture, R.M., Gobeil, C., and Tessier, A. 2008. Chronology of atmospheric deposition of arsenic inferred from reconstructed sedimentary records. Environmental Science and Technology, 42: 6508–6513. https://doi.org/10.1021/es800818j

Covelli, S., and Fontolan, G. 1997. Application of a normalization procedure in determining regional geochemical baselines. Environmental Geology, 30: 34-45. https://doi.org/10.1007/s002540050130

Cronmiller, J.G., Noble, B.F., 2018. The discontinuity of environmental effects monitoring in the Lower Athabasca region of Alberta, Canada: institutional challenges to long-term monitoring and cumulative effects management. Environ. Rev. 26 (2), 169–180.

De Boer A, Winhold T and Garner L 1994 Embarras River Breakthrough to Mamawi Creek Peace-Athabasca Delta Technical Studies Task 1–35 D.2

Déry S J and Wood E F 2005 Decreasing river discharge in northern Canada Geophys. Res. Lett. 32 L1040

Dillon, P., Dixon, G., Driscoll, C., Giesy, J., Hurlbert, S., Nriagu, J., 2011. Evaluation of four reports on contamination of the Athabasca River system by oil sands operations Prepared for the Government of Alberta.

Dolgova, S., Popp, B.N., Courtoreille, K., Espie, R.H.M., Maclean, B., McMaster, M. Straka, J.R., Tetreault, G.R., Wilkie, S. Hebert, C.E. 2018. Spatial trends in a biomagnifying contaminant: Application of amino acid compound–specific stable nitrogen isotope analysis to the interpretation of bird mercury levels. Environmental Toxicology and Chemistry, 37: 1466–1475.

Donner, M.W., Cuss, C.W., Poesch, M., Sinnatamby, R.N., Shotyk, W., and Siddique, T. 2018. Selenium in surface waters of the lower Athabasca River watershed: chemical speciation and implications for aquatic life. Environmental Pollution. 243: 1343e1351. https: doi.org/10.1016/j.envpol.2018.09.067

Donner, M.W., Javed, M.B., Shotyk, W., Francesconi, K.A., and Siddique, T. 2017. Arsenic speciation in the lower Athabasca River watershed: a geochemical investigation of the dissolved and particulate phases. Environmental Pollution, 224: 265e274. https://doi.org/10.1016/j.envpol.2017.02.004

Douglas, M.S.V., and Smol, J.P. 2000. Eutrophication and recovery in the high arctic: Meretta Lake (Cornwallis Island, Nunavut, Canada) revisited. Hydrobiologia, 431: 1932-204. https://doi.org/10.1023/A:1004000530997

Douglas, M.S.V., Hamilton, P.B., Pienitz, R., and Smol, J.P. 2004. In: Pienitz, R., Douglas, M.S.V, Smol, J.P (Eds.), Algal indicators of environmental change in arctic and Antarctic lakes and ponds, Long-term Environmental Change in Arctic and Antarctic Lakes. Springer. Netherlands, pp. 117-157.

Dowdeswell, L., Dillon, P., Ghoshal, S., Miall, A., Rasmussen, J., and Smol, J.P. 2010. A foundation for the future: Building an environmental monitoring system for the oil sands. A report submitted to the Minister of Environment. 1-49.

Drevnick, P.E., Cooke, C.A., Barraza, D., Blais, J.M., Coale, K.H., Curtis, C.J., Donahue, W.F., Eagle-Smith, C.A., Engstrom, D.R., Fitzgerald, W.F., Furl, C.V., Gray, J.E., Hall, R.I., Jackson, T.A., Laird, K.A., Lockhart, W.L., Macdonald, R.W., Mast, M.A., Mathieu, C., Muir, D.C.G., Outridge, P.M., Reinemann, S.A., Rothenberg, S.E., Ruiz-Fernández, A.C., St. Louis, V.L., Sanders, R.D., Sanei, H., Skierszkan, E.K., Van Metre, P.C., Veverica, T.J., Wiklund, J.A., and Wolfe, B.B. 2016. Spatiotemporal patterns of mercury accumulation in lake sediments of western North America. Science of the Total Environment, 568: 1157–1170. http://dx.doi.org/10.1016/j.scitotenv.2016.03.167

Driscoll, C.T., Mason, R.P., Chan, H.M., Jacob, D.J., and Pirrone, N. 2013. Mercury as global pollutant: sources, pathways, and effects. Environmental Science & Technology, 47: 4967-4983. https://doi.org/10.1021/es305071v

Dubé M G and Wilson J E 2012 Accumulated state assessment of the Peace-Athabasca-Slave River system Integrated Environmental Assessment and Management 9 405–25

Engstrom, D.R., Fitzgerald, W.F., Colin, A., Cooke, C.A., Lamborg, C.H., Drevnick, P.E., Swain, E.B., Balogh, S.J., Prentiss, H., and Balcom, P.H. 2014. Atmospheric Hg emissions from preindustrial gold and silver extraction in the Americas: a reevaluation from lake-sediment archives. Environmental Science & Technology, 48: 6533–6543. http://dx.doi.org/10.1021/es405558e

Evans, M., and Talbot, A. 2012. Investigations of mercury concentrations in walleye and other fish in the Athabasca River ecosystem with increasing oil sands development. Journal of Environmental Monitoring, 14: 1989-2003.

Evans, M.S., Billeck, B., Lockhart, L., Bechtold, J.P., Yunker, M.B., et al., 2002. PAH sediment studies in Lake Athabasca and the Athabasca River ecosystem related to the Fort McMurray oil sands operations: sources and trends. In: Brebbia, C.A. (Ed.), Oil and Hydrocarbon Spills III, Modelling, Analysis and Control. WIT Press, Southampton MA, pp. 365–374.

Evans, M.S., Davies, M., Janzen, K., Muir, D., Hazewinkel, R., Kirk, J., de Boer, D., 2016. PAH distributions in sediments in the oil sands monitoring area and western Lake Athabasca: concentration, composition and diagnostic ratios. Environ. Pollut. 213, 671–687.

Faber, J.A. 2020. Reconstructing hydrologic conditions and metals supplied by the Peace River to the Peace-Athabasca Delta. Theses and Dissertations (Comprehensive). 2317. Retrieved from https://scholars.wlu.ca/etd/2317 on August 22nd, 2021.

Fawcett, S.E., Jamieson, H.E., Nordstrom, D.K., and Blaine McCleskey, R. 2015. Arsenic and antimony geochemistry of mine wastes, associated waters and sediments at the Giant Mine, Yellowknife, Northwest Territories, Canada. Applied Geochemistry, 62: 3-17. https://doi.org/10.1016/j.apgeochem.2014.12.012

Finlayson, C.M., Clarke, S.J., Davidson, N.C., Gell, P., 2016. Role of palaeoecology in describing the ecological character of wetlands. Mar. Freshw. Res. 67, 687–694.

Forstner, U., Müller, G., 1981. Concentrations of heavy metals and polycyclic aromatic hydrocarbons in river sediments: geochemical background, man's influence and environmental impact. GeoJournal 5, 417–432.

Galloway, J.M., Palmer, M., Jamieson, H.E., Patterson, R.T., Nasser, N, Falck, H., Macumber, A.L., Goldsmith, S.A., Sanei, H., Normandeau, P., Hadlari, T., Roe, H.M., Neville, L.A., and Lemay, D. 2015. Geochemistry of lakes across ecozones in the Northwest Territories and implications for the distribution of arsenic in the Yellowknife region. Part 1: Sediments, Geological Survey of Canada, Open File 7908: 1 p.

Galloway, J.M., Sanei, H, Patterson, R.T., Mosstajiri, T., Hadlari, T., and Falck, H. 2012. Total arsenic concentrations of lake sediments near the city of Yellowknife, Northwest Territories. Geological Survey of Canada, Open File 7037: 47 p.

Galloway, J.M., Swindles, G.T., Jamieson, H.E., Palmer, M., Parsons, M.B., Sanei, H., Macumber, A.I., Patterson, R.T., and Falck, H. 2018. Organic matter control on the distribution of arsenic in lake sediments impacted by ~65 years of gold ore processing in subarctic Canada. Science of the Total Environment, 622-623: 1668-1679. https://doi.org/10.1016/j.scitotenv.2017.10.048

Gell, P. 2017. Using paleoecology to understand natural ecological character in Ramsar wetlands. Past Global Changes Magazine, 25: 86–7. https://doi.org/10.22498/pages.25.2.86

Gelman, A., J. B. Carlin, H. S. Stern, D. B. Dunson, A. Vehtari, and D. B. Rubin. 2013. Bayesian data analysis, 3rd Edition. Chapman and Hall/CRC

Gilmour, C.C., Henry, E.A., and Mitchell, R. 1992. Sulfate stimulation of mercury methylation in fresh-water sediments. Environmental Science & Technology, 26: 2281-2287. https://doi.org/10.1021/es00035a029

Gleick, P. 2003. Global freshwater resources: soft-path solutions for the 21st century. Science, 302: 1524–1528. https://doi.org/10.1126/science.1089967

Glew, J. R. 1988. A portable extruding device for close interval sectioning of unconsolidated core samples. Journal of Paleolimnology, 1: 235-239. https://doi.org/10.1007/BF00177769

Glew, J. R. 1989. A new trigger mechanism for sediment sampling. J. Paleolimnol. 2: 241–243. doi: 10.1007/BF00195474

Glew, J. R. 1991. Miniature gravity corer for recovering short sediment cores. J. Paleolimnol.5: 285–287. doi: 10.1007/BF00200351

Gobeil, C., Tessier, A., and Couture R.M.C. 2013. Upper Mississippi Pb as a mid-1800s chronostratigraphic marker in sediments from seasonally anoxic lakes in eastern Canada. Geochimica et Cosmochimica Acta, 113: 125-135. https://doi.org/10.1016/j.gca.2013.02.023

Gosselin, P., Hrudey, S., Naeth, A., Plourde, A., Therrien, R., van der Kraar, G., Xue, Z., 2010. Environmental and Health Impacts of Canada's Oil Sands Industry. The Royal Society of Canada, Ottawa, pp. 414.

Graney, J.R., Halliday, A.N., Keeler, G.J., Nriagu, J.O., Robbins, J.A., and Norton, S.A. 1995. Isotopic record of lead pollution in sediments from the Northeastern United States.

Geochimica et Cosmochimica Acta, 59: 1715-1728. https://doi.org/10.1016/0016-7037(95)00077-D

Hall R I, Wolfe B B Wiklund J A Edwards T W D Farwell A J and Dixon D G 2012 Has Alberta oil sands development altered delivery of polycyclic aromatic compounds to the Peace-Athabasca Delta? PLoS One 7 e46089

Hall, B.D., Manolopoulos, H., Hurley, J.P., Schauer, J.J., St. Louis, V.L., Kenski, D., Graydon, J., Babiarz, C.L. Cleckner, L.B., and Keeler, G.J. 2005. Methyl and total mercury in precipitation in the Great Lakes region. Atmospheric Environment, 39: 7557-7569. https://doi.org/10.1016/j.atmosenv.2005.04.042

Hall, R.I., Wolfe, B.B., Wiklund, J.A., Edwards, T.W.D., Farwell, A.J., and Dixon, D.G. 2012. Has Alberta Oil Sands Development Altered Delivery of Polycyclic Aromatic Compounds to the Peace-Athabasca Delta?. PLOS ONE, 7: e46089, https://doi.org/10.1371/journal.pone.0046089

Harris, R.C., Rudd, J.W.M., Amyot, M., Babiarz, C.L., Beaty, K.G., Blanchfield, P.J., Bodaly, R.A., Branfireun, B.A., et al. 2007. Whole-ecosystem study shows rapid fish-mercury response to changes in mercury deposition. Proceedings of the National Academy of Sciences of the United States of America, 104: 16586-16591. https://doi.org/10.1073/pnas.0704186104

Hassan, R., Scholes, R., and Ash, N. 2005. Millenium Ecosystem Assessment. Ecosystems and human well-being: Current state and trends, vol. 1. Washington, DC: Island Press.

Headley, J.V., Marsh, P., Akre, C.J., Peru, K.M., and Lesack, L. 2002. Origin of polycyclic aromatic hydrocarbons in lake sediments of the Mackenzie Delta. Journal of

Environmental Science and Health, Part A, 7: 1159-1180. https://doi.org/10.1081/ESE-120005979

Hebert, C. E., Campbell, D., Kindopp, R., MacMillan, S., Martin, P., Neugebauer, E., Patterson, L., and Shatford, J. 2013. Mercury trends in colonial waterbird eggs downstream of the oil sands region of Alberta, Canada. Environmental Science & Technology, 47: 11785–11792. https://doi.org/10.1021/es402542w

Hebert, C.E. 2019. The river runs through it: The Athabasca River delivers mercury to aquatic birds breeding far down stream. PLoS ONE, 14: e0206192. https://doi.org/10.1371/journal.pone.0206192

Heino, J., Culp, J.M., Erkinaro, J., Goedkoop, W., Lento, J., Rühland, K.M., and Smol, J.P. 2020. Abruptly and irreversibly changing Arctic freshwaters urgently require standardized monitoring. Journal of Applied Ecology, 57: 1192-1198. https://doi.org/10.1111/1365-2664.13645

Heiri O, Lotter A F and Lemcke G 2001 Loss on ignition as a method for estimating organic and carbonate content in sediments; reproducibility and comparability of results J. Paleolimnol. 25 101–10

Hicks, K., and Scrimgeour, G. 2019. A study design for enhanced environmental monitoring of the Lower Athabasca River, Government of Alberta, Ministry of Environment and Parks, open.alberta.ca/publications/9781460145364.

Hocking, D., Kuchar, P., Plambeck, J.A., and Smith, R.A. 1978. The impact of gold smelter emissions on vegetation and soils of a sub-arctic forest-tundra transition ecosystem. Journal

of the Air Pollution Control Association, 28: 133-137. https://doi.org/10.1080/00022470.1978.10470580

Houben, A.J., D'Onofrio, R., Kokelj, S.V., and Blais, J.M. 2016. Factors affecting elevated arsenic and methyl mercury concentrations in small shield lakes surrounding gold mines near the Yellowknife, NT, (Canada) region. PloS One, 11: e0150960. https://doi.org/10.1371/journal.pone.0150960

Hugenholtz, C. H., D. G. Smith, and J. M. Livingston. 2009. Application of floodplain stratigraphy to determine the recurrence of ice-jam flooding along the lower Peace and Athabasca Rivers, Alberta. Can. Water Resour. J. 34: 1–16. doi: 10.4296/cwrj3401079

Hughes, A. O., J. M. Olley, J. C. Croke, and L. A. McKergow. 2009. Sediment source changes over the last 250 years in a dry-tropical catchment, central Queensland, Australia. Geomorphology 104: 262–275. doi: 10.1016/j.geomorph.2008.09.003

Hutchinson, T.C., Aufreiter, S., and Hancock, R.G. 1982. Arsenic pollution in the Yellowknife Area from gold smelter activities. Journal of Radioanalytical Chemistry, 71: 59-73. https://doi.org/10.1007/BF02516141.

Independent Environment Consultants (IEC). 2018. Strategic environmental assessment of Wood Buffalo National Park World Heritage Site. Volume 1, Milestone 3 – Final SEA Report. Independent Environment Consultants (IEC), Markham, Ontario.

Indian and Northern Affairs Canada. 2007. Giant Mine Remediation Plan. Giant Mine Remediation Project Team, Prepared by SRK Consulting Inc. and SENES Consultants Limited, Department of Indian Affairs and Northern Development, Yellowknife, Northwest Territories.

IPCC. 2007. Climate Change 2007: The physical science basis. Contribution from Working Group 1 to the fourth assessment report of the Inter-Governmental Panel on Climate Change, in IPCC Fourth Assessment Report edited by Solomon, S., Quin, D., Manning, M., Marquis, M., Averyt, M., Tignor, M., Miller, H.L. Cambridge University Press, Cambridge, U.K.

Irwin, R.J., Vanmouwerik, M., Stevens, L., Seese, M.D., and Basham, W. 1997. Environmental Contaminants Encyclopedia Vanadium Entry, pp. 45. (www.nature.nps.gov/hazardssafety/toxic/vanadium.pdf)

Jacobs, F.S., Filby, R.H. (Ed). 1982. Trace element composition of Athabasca tar sands and extracted bitumen. Atomic and Nuclear Methods in Fossil Energy Research.

Jamieson, H.E. 2014. The legacy of arsenic contamination from mining and processing refractory gold ore at Giant Mine, Yellowknife, Northwest Territories, Canada. Reviews in Mineralogy & Geochemistry, 79: 533-551. https://doi.org/10.2138/rmg.2014.79.12

Jamieson, H.E., Maitland, K.M., Oliver, J.T., and Palmer, M.J. 2017. Regional distribution of arsenic in near-surface soils in the Yellowknife area. Northwest Territories Geological Survey, NWT Open File 2017-03, 28 p.

Jasiak, I., Wiklund, J.A., Leclerc, E., Telford, J.V., Couture, R.M.C., Venkiteswaran, J.J., Hall, R.I., and Wolfe, B.B. 2021. Evaluating spatiotemporal patterns of arsenic, antimony, and lead deposition from legacy gold mine emissions using lake sediment records. Applied Geochemistry, 134: 105053, https://doi.org/10.1016/j.apgeochem.2021.105053

Jautzy, J.J., Ahad, J.M.E., Hall, R.I., Wiklund, J.A., Wolfe, B.B., Gobeil, C., and Savard, M.M. 2015. Source apportionment of background PAHs in the Peace-Athabasca Delta (Alberta,

Canada) using molecular level radiocarbon analysis. Environmental Science & Technology, 49: 9056-9063. https://doi.org/10.1021/acs.est.5b01490

Johnson, J.W., Köster, D., Wolfe, B.B., Hall, R.I., Edwards, T.W.D., Endres, A., Martin, M.E., Wiklund, J.A., and Light, C. 2010. Quantifying Lake Athabasca (Canada) water level during the 'Little Ice Age' highstand from paleolimnological and geophysical analyses of a transgressive barrier-beach complex. The Holocene, 20: 801-811. https://doi.org/10.1177%2F0959683610362816

Juichang, R., Freedman, B., Coles, C., Zwicker, B., Holzbecker, J., Chatt, A., 1995. Vanadium contamination of lichens and tree foliage in the vicinity of three oilfired power plants in Eastern Canada. J. Air Waste Manag. Assoc. 45, 461–465.

Kabir, M.I., Lee, H., Kim, G., and Jun, T. 2011. Correlation assessment and monitoring of the potential pollutants in the surface sediments of Pyeongchang River, Korea. International Journal of Sedimentary Research, 26: 152-162. https:/doi.org/10.1016/S1001-6279 (11)60083-8

Karbassi, A.R., Monavari, S.M., Nabi Bidhedi, G.R., Nouri, J., and Nematour, K. 2008. Metal pollution assessment of sediment and water in the Shur River. Environmental Monitoring and Assessment, 147: 107-116. https://doi.org/10.1007/s10661-007-0102-8

Kay, M.L., Jasiak, I., Klemt, W.H., Wiklund, J.A., Faber, J.A., MacDonald, L.A., Telford, J.V.K., Savage, C.A.M., Cooke, C.A., Wolfe, B.B., and Hall, R.I. in review. Spatio-temporal patterns of metal(loid) enrichment in lake sediment records from large-scale mining operations in northwestern Canada: A synthesis. Submitted to Environmental Reviews, Manuscript ID: er-2021-0108.

Kay, M.L., Wiklund, J.A., Remmer, C.R., Neary, L.K., Brown, K., Ghosh, A., MacDonald. E., Thomson, K., Vucic, J.M., Wesenberg, K., Hall, R.I., and Wolfe, B.B. 2019. Bi-directional hydrological changes in perched basins of the Athabasca Delta (Canada) in recent decades caused by natural processes. Environmental Research Communications, 1: 081001. https://doi.org/10.1088/2515-7620/ab37e7

Kay, M.L., Wiklund, J.A., Remmer, C.R., Owca, T.J., Klemt, W.H., Neary, L.K. Brown, K., MacDonald, E., Thomson, K., Vucic, J.M., Wesenberg, K., Hall, R.I., and Wolfe, B.B. 2020. Evaluating temporal patterns of metals concentrations in floodplain lakes of the Athabasca Delta (Canada) relative to pre-industrial baselines. Science of the Total Environment, 20: 135309. https://doi.org/10.1016/j.scitotenv.2019.135309

Kay, M.L., Wiklund, J.A., Sun, X., Savage, C.A.M., Adams, J.K., MacDonald, L.A., Klemt, W.H., Brown, K.C., Hall, R.I., and Wolfe, B.B. 2022. Assessment of mercury enrichment in lake sediment records from Alberta Oil Sands development via fluvial and atmospheric pathways. Frontiers in Environmental Science, 10: 949339. https://doi.org/10.3389/fenvs.2022.949339.

Kelly, E.N., Schindler, D.W., Hodson, P.V., Short, J.W., Radmanovich, R., Nielsen, C.C., 2010. Oil sands development contributes elements toxic at low concentrations to the Athabasca River and its tributaries. Proc. Natl. Acad. Sci. 107 (37), 16178–16183.

Kelly, E.N., Short, J.W., Schindler, D.W., Hodson, P.V., Ma, M., Kwan, A.K., and Fortin, B.L. 2009. Oil sands development contributes polycyclic aromatic compounds to the Athabasca River and its tributaries. Proceedings of the National Academy of Sciences 106: 22346–22351. https://doi.org/10.1073/pnas.0912050106

Kersten, M., and Smedes, F. 2002. Normalization procedures for sediment contaminants in spatial and temporal trend monitoring. Journal of Environmental Monitoring, 4: 109-115. https://doi.org/10.1039/B108102K

Khalaf, F., Litherathy, P., Anderlini, V., 1982. Vanadium as a tracer of oil pollution in the sediments of Kuwait. Hydrobiologia 91, 147–154.

Kirk, J.L., Muir, D.C., Gleason, A., Wang, X., Lawson, G., Frank, R.A., Lehnherr, I., and Wrona, F. 2014. Atmospheric deposition of mercury and methylmercury to landscapes and waterbodies of the Athabasca Oil Sands Region. Environmental Science and Technology, 48: 7374-7383. https://doi.org/10.1021/es500986r

Kitch, J. L., J. Phillips, S. Peukert, A. Taylor, and W. H. Blake. 2019. Understanding the geomorphic consequences of enhanced overland flow in mixed agricultural systems: Sediment fingerprinting demonstrates the need for integrated upstream and downstream thinking. J. Soils Sediments 19:3319–3331. doi: 10.1007/s11368-019-02378-4

Klemt, W.H., Brua, R.B., Culp, J.M., Hicks, K., Wolfe, B.B., and Hall, R.I. 2021. Evaluating Lower Athabasca River sediment metals concentrations from Alberta Oil Sands monitoring programs using predevelopment baselines. Environmental Science and Technology, 55: 8817-8828. https://doi.org/10.1021/acs.est.1c01761

Klemt, W.H., Kay, M.L., Wiklund, J.A., Wolfe, B.B., and Hall, R.I. 2020. Assessment of vanadium and nickel enrichment in Lower Athabasca River floodplain lake sediment within the Athabasca Oil Sands

Koiter, A., P. N. Owens, E. Petticrew, and D. Lobb. 2013. The behavioural characteristics of sediment properties and their implications for sediment fingerprinting as an approach for

identifying sediment sources in river basins. Earth Sci. Rev. 125: 24–42. doi: 10.1016/j.earscirev.2013.05.009

Korosi, J.B., Thienpont, J.R., Smol, J.P., and Blais, J.M. 2017. Paleo-ecotoxicology: What can lake sediments tell us about ecosystem responses to environmental pollutants? Environmental Science and Technology, 51: 9446-9457. https://doi.org/10.1021/acs.est.7b02375

Kuerten, S., M. Parolin, M. L. Assine, and M. M. McGlue. 2013. Sponge spicules indicate Holocene environmental changes on the Nabileque River floodplain, southern Pantanal, Brazil. J. Paleolimnol. 49: 171–183. doi: 10.1007/s10933-012-96520z

Kurek, J., Kirk, J.L., Muir, D.C., Wang, X., Evans, M.S. and Smol, J.P. 2013. Legacy of a half century of Athabasca oil sands development recorded by lake ecosystems. Proceedings of the National Academy of Sciences, 110: 1761-1766. https://doi.org/10.1073/pnas.1217675110

Laceby, J. P., O. Evrard, H. G. Smith, W. H. Blake, J. M. Olley, J. P. Minella, and P. N. Owens. 2017. The challenges and opportunities of addressing particle size effects in sediment source fingerprinting: A review. Earth Sci. Rev. 169: 85–103. doi: 10.1016/j.earscirev.2017.04.009

Lamba, J., K. G. Karthikeyan, and A. M. Thompson. 2015a. Apportionment of suspended sediment sources in an agricultural watershed using sediment fingerprinting. Geoderma 239–240: 25–33. doi: 10.1016/j.geoderma.2014.09.024

Lamba, J., K. G. Karthikeyan, and A. M. Thompson. 2015b. Using radiometric fingerprinting and phosphorus to elucidate sediment transport dynamics in an agricultural watershed. Hydrol. Process. 29: 2681–2693. doi: 10.1002/hyp.10396

Lamontagne, J. R., M. Jasek, and J. D. Smith. 2021. Coupling physical understanding and statistical modeling to estimate ice jam flood frequency in the northern Peace-Athabasca Delta under climate change. Cold Reg. Sci. Technol, 192: 103383. https://doi.org/10.1016/j.coldregions.2021.103383

Laresen, J.N. et al. 2014. Polar regions. In Barros, V.R., Field, C.B., Dokken, D.J., Mastrandrea, M.D., Mach, K.J., Bilir, T.E., and White, L.L., Climate change 2014: impacts, adaptation, and vulnerability. Part B: Regional aspects. Contributions of Working Group II to the Fifth Assessment Report of the Intergovernmental Panel on Climate Change (pp. 1567-1612). Cambridge, UK and New York, NY: Cambridge University Press.

Leclerc, E., Venkiteswaran, J.J., Jasiak, I., Telford, J.V., Wolfe, B.B., Hall, R.I., Schultz, M.D.J., and Couture, R.M.C. 2021. Quantifying arsenic post-depositional mobility in lake sediments impacted by gold ore roasting in sub-arctic Canada using inverse diagenetic modelling. Environmental Pollution, 288: 117723. https://doi.org/10.1016/j.envpol.2021.117723

Lindenmayer, D.B., and Likens, G.E. 2009. Adaptive monitoring: a new paradigm for long-term research and monitoring. Trends in Ecology & Evolution, 24: 482-486. https://doi.org/10.1016/j.tree.2009.03.005

Lindenmayer, D.B., Likens, G.E., 2008. Adaptive monitoring: a new paradigm for long-term research and monitoring. Trends Ecol. Evol. 24 (9), 482–486.

Lintern, A., P. J. Leahy, H. Heijnis, A. Zawadzki, P. Gadd, G. Jacobsen, A. Deletic, and D. T. McCarthy. 2016. Identifying heavy metal levels in historical flood water deposits using sediment cores. Water Res. 105: 34–46. doi: 10.1016/j.watres.2016.08.041

Lizaga, I., L. Gaspar, W. H. Blake, B. Latorre, and A. Navas. 2019. Fingerprinting changes of source apportionments from mixed land uses in stream sediments before and after an exceptional rainstorm event. Geomorphology 341: 216–226. doi: 10.1016/j.geomorph.2019.05.015

Loring, D.H. 1991. Normalization of heavy-metal data from estuarine and coastal sediments. ICES Journal of Marine Science, 48: 101-115. https://doi.org/10.1093/icesjms/48.1.101

Lotter, A.F., Pienitz, R., and Schmidt R. 1999. Diatoms as indicators of environmental change near arctic and alpine treeline. In The Diatoms: Applications for the Environmental and Earth Sciences, Stoermer EF and Smol JP (eds). Cambridge University Press: Cambridge; 227-244.

MacDonald, L.A., Wiklund, J.A., Elmes, M.C., Wolfe, B.B., and Hall, R.I. 2016. Paleolimnological assessment of riverine and atmospheric pathways and sources of metal deposition at a floodplain lake (Slave River Delta, Northwest Territories, Canada). Science of the Total Environment, 544: 811-823. https://doi.org/10.1016/j.scitotenv.2015.11.173

Mazerolle, M.J., 2017. AICcmodavg: Model Selection and Multimodel Inference Based on (Q)AIC(c). R Package Version 2.1-1. R Package Version 2.1-1. Available at https://cranr-project.org/web/packages/AICcmodavg/AICcmodavg.pdf.

MCFN (Mikisew Cree First Nation). 2014. Petition to the World Heritage Committee requesting Inclusion of Wood Buffalo National Park on the List of World Heritage in Danger, 1-18.

MCFN 2016 Water is everything Prepared by the Mikisew Cree First Nations for the UNESCO World Heritage Site 1–24

McGowan S, Leavitt P R Hall R I Wolfe B B,Edwards T W D Karst-Riddoch T and Vardy S R 2011 Interdecadal declines in flood frequency increase primary production in lakes of a northern river delta Global Change Biol. 17 1212–24

McMartin, I., Henderson, P.J., and Nielsen, E. 1999. Impact of base metal smelter on the geochemistry of soils of the Flin Flon region Manitoba and Saskatchewan. Canadian Journal of Earth Science, 36: 141-160. https://doi.org/10.1139/e98-001

Michelutti, N., Hermanson, M.H., Smol, J.P., Dillon, P.J., and Douglas, M.S.V. 2007. Delayed response of diatom assemblages to sewage inputs in an arctic lake. Aquatic Sciences, 69: 523-533. https://doi.org/10.1007/s00027-007-0928-8

Michelutti, N., M. B. Hay, P. Marsh, L. Lesack, and J. P. Smol. 2001. Diatom changes in lake sediments from the Mackenzie Delta, N.W.T., Canada: Palaeohydrological applications. Arct. Antarct. Alp. Res. 33: 1–12. doi: 10.1080/15230430.2001.12003398

Moir, K.E., Windle, M.J.S., Cumming, B.F., and Ridal, J.J. 2021. Nearshore sedimentary mercury concentrations reflect legacy point sources and variable sedimentation patterns under a natural recovery strategy. Environmental Toxicology and Chemistry, 40: 1788-1789. https://doi.org/10.1002/etc.5009

Mongeon, C. 2008. Paleohydrologic reconstruction of three shallow basins, Slave River Delta, NWT, Using Stable Isotope Methods. Theses and Dissertations (Comprehensive). 870. https://scholars.wlu.ca/etd/870.

Motha, J., P. Wallbrink, P. Hairsine, and R. Grayson. 2002. Tracer properties of eroded sediment and source material. Hydrol. Process. 16: 1983–2000. doi: 10.1002/hyp.397

Mudroch, A., and Clair, T. 1986. Transport of arsenic and mercury from gold mining activities through an aquatic system. Science of the Total Environment, 57: 205-216. https://doi.org/10.1016/0048-9697(86)90024-0

Muir, D.C.G., Wang, X., Yang, F., Nguyen, N., Jackson, T.A., Evans, M.S., Douglas, M., Köck, G., Lamoureux, S., Pienitz, R., Smol, J.P., Vincent, W.F., and Dastoor, A. 2009. Spatial trends and historical deposition of mercury in eastern and northern Canada inferred from lake sediment cores. Environmental Science & Technology, 43: 4802–4809. http://dx.doi.org/10.1021/es8035412

National Pollutant Release Inventory. Retrieved from https://www.ec.gc.ca/inrp-npri/ on August 22nd, 2021.

Neary, L.K., Remmer, C.R., Kirst, J., Wolfe, B.B., and Hall, R.I. 2021. A new lake classification scheme for the Peace-Athabasca Delta (Caanda) characterizes hydrological processes that cause lake-level variation. Journal of Hydrology: Regional Studies, 38: 100948. https://doi.org/10.1016/j.ejrh.2021.100948

Nesbitt, J.A., and Lindsay, B.J. 2017. Vanadium geochemistry of oil sands fluid petroleum coke. Environmental Science and Technology, 51: 3102-3109. https: doi.org/10.1021/acs.est.6b05682

Nittrouer, J. A., and E. Viparelli. 2014. Sand as a stable and sustainable resource for nourishing the Mississippi River delta. Nat. Geosci. 7: 350–354. doi: 10.1038/ngeo2142

Owca, T.J., Kay, M.L., Faber, J., Remmer, C.R., Zabel, N., Wiklund, A.J., Wolfe, B.B., Hall, R.I., 2020. Use of pre-industrial baselines to monitor anthropogenic enrichment of metals concentrations in recently deposited sediment of floodplain lakes in the Peace-Athabasca Delta (Alberta, Canada). Environmental Monitoring and Assessment. 192, 106. https://doi.org/10.1007/s10661-020-8067-y

Palmer, M.J., Chetelat, J., Richardson, M., Jamieson, H.E., and Galloway, J.M. 2019. Seasonal variation of arsenic and antimony in surface waters of small subarctic lakes impacted by legacy mining pollution near Yellowknife, NT, Canada. Science of the Total Environment, 684: 326-339. https://doi.org/10.1016/j.scitotenv.2019.05.258

Palmer, M.J., Galloway, J.M., Jamieson, H.E., Patterson, R.T., Falck, H., and Kokelj, S.V. 2015. The concentration of arsenic in lake waters of the Yellowknife area, Northwest Territories Geological Survey, NWT Open File 2015-06. 25 p.

Peace-Athabasca Delta Project Group (PADPG). 1973. Peace-Athabasca Delta Project, Technical Report; volume 2. p. 9

Peace-Athabasca Delta Technical Studies (PADTS). 1996. Final Report. PADTS Steering Committee, Fort Chipewyan, Alberta; p. 106.

Pelletier, N., Chetelat, J., Cousens, B., Zhang, S., Stephner, D., Muir, D.C.G., and Vermaire, J.C. 2020. Lead contamination from gold mining in Yellowknife Bay (Northwest Territories), reconstructed using stable lead isotopes. Environmental Pollution, 259: 113888. https://doi.org/10.1016/j.envpol.2019.113888

Peters, D. L., T. D. Prowse, A. Pietroniro, and R. Leconte. 2006. Flood hydrology of the Peace-Athabasca Delta, northern Canada. Hydrol. Process. 20: 4073–4096. doi: 10.1002/hyp.6420

Pirrone, N., Allegrini, I., Keeler, G.J., Nriagu, J.O., Rossman, R., Robbins, J.A. 1998. Historical atmospheric mercury emissions and depositions in North America compared to mercury accumulations in sedimentary records. Atmospheric Environment. 32: 929–940. http://dx.doi.org/10.1016/S1352-2310(97)00353-1.

Prowse T D, Peters D L and Marsh P 1996 Modelling the water balance of Peace–Athabasca Delta perched basins Peace–Athabasca Delta Technical Studies National Hydrology Research Institute

Prowse, T. D., and F. M. Conly. 1998. Impacts of climatic variability and flow regulation on ice-jam flooding of a northern delta. Hydrol. Process. 12: 1589–1610. doi: 10.1002/(SICI)1099-1085(199808/09)12:10/11%3C1589::AID-HYP683%3E3.0.CO;2-G

Prowse, T.D., and Conly, F.M. 2002. A review of hydroecological results of the Northern River Basins Study, Canada. Part 2. Peace-Athabasca Delta. River Research and Applications, 18: 450-454. https://doi.org/10.1002/rra.682

Prowse, T.D., Wrona, F.J., Reist, J.D., Gibson, J.J., Hobbie, J.E., Lévesque, L.M., and Vincent, W.F. 2006. Climate change effects on hydroecology of Arctic freshwater ecosystems. Ambio, 35: 347-358. https://doi.org/10.1579/0044-7447(2006)35[347:cceoho]2.0.co;2

R Core Team, 2018. R: A Language and Environment for Statistical Computing. Vienna: R Foundation for Statistical Computing. Available online at: https://www.R-project.org/.

Remmer, C. R., L. K. Neary, M. L. Kay, B. B. Wolfe, and R. I. Hall. 2020a. Multi-year isoscapes of lake water balances across a dynamic northern freshwater delta. Environ. Res. Lett. 15: 104066. doi: 10.1088/1748-9326/abb267

Remmer, C. R., T. Owca, L. Neary, J. A. Wiklund, M. Kay, B. B. Wolfe, and R. I. Hall. 2020b. Delineating extent and magnitude of river flooding to lakes across a norther delta using water isotope tracers. Hydrol. Process. 34: 303–320. doi: 10.1002/hyp.13585

Remmer, C.R., Neary, L.K., Wolfe, B.B., and Hall, R.I. 2020c. Technical report for monitoring lakes in the Peace-Athabasca Delta, Alberta. Prepared for Wood Buffalo National Park.

Reuther, R., 2009. Lake and river sediment Monitoring. Environmental monitoring Encyclopedia of Life Support Systems (EOLSS) 2, 120–147.

Richardson, C. J., and N. A. Hussain. 2006. Restoring the Garden of Eden: An ecological assessment of the marshes of Iraq. Bioscience 56: 477–488. doi: 10.1641/0006-3568(2006)56[477:RTGOEA]2.0.CO;2

Richardson, C. J., P. Reiss, N. A. Hussain, A. J. Alwash, and D. J. Pool. 2005. The restoration of potential of the Mesopotamian marshes of Iraq. Science 307: 1307–1311. doi: 10.1126/science.1105750

Roberts, D., Hazewinkel, R.O., Arciszewski, T.J., Beausoleil, D., Davidson, C., Horb, E.C., Sayanda, D., Wentworth, G.R., Wyatt, F., and Dubé, M.G. 2021. An integrated knowledge synthesis of regional ambient monitoring in Canada's oil sands. Integrated Environmental Assessment and Management, 18: 428-441. https://doi.org/10.1002/ieam.4505

Rood S B, Samuelson G M, Braatne J H, Gourley CR, Hughes F M and Mahoney JM 2005 Managing river flows to restore floodplain forests The Ecological Society of America 3 193–201

Rooney, R.C., Bayley, S.E., and Schindler, D.W. 2012. Oil sands mining and reclamation cause massive loss of peatland and stored carbon. Proceedings of the National Academy of Sciences, 109: 4933-4937. https://doi.org/10.1073/pnas.1117693108

Rosen, M.R. 2015. The influence of hydrology on lacustrine sediment contaminant records. In: Blais, J.M., Rosen, M.R., Smol, J.P. (Eds.), DPER Environmental Contaminants: Volume 18: Using Natural Archives To Track Sources And Long-Term Trends Of Pollution. Springer, New York, pp. 5–34.

Rühland, K.M., Paterson, A.M., Keller, W., Michelutti, N., and Smol, J.P. 2013. Global warming triggers the loss of a key Arctic refugium. Proceedings of the Royal Society Biological Sciences, 280: 20131887. https://doi.org/10.1098/rspb.2013.1887

Salat, A.P.J., Eickmeyer, D.C., Kempe, L.E., Hall, R.I., Wolfe, B.B., Mundy, L.J., Trudeau, V.L., and Blais, J.M. 2021. Integrated analysis of petroleum biomarkers and polycyclic aromatic compounds in lake sediment cores from an oil sands region. Environmental Pollution, 270: 116060. https://doi.org/10.1016/j.envpol.2020.116060

Sanchez-Cabeza, J.A., and Ruiz-Fernandez, A.C. 2012. 210Pb sediment radiochronology: An integrated formulation and classification of dating models. Geochimica et Cosmochimica Acta, 82: 183-200. https://doi.org/10.1016/j.gca.2010.12.024

Sandlos, J., and Keeling, A. 2012. Claiming the New North: Development and Colonialism at the Pine Point Mine, Northwest Territories, Canada. Environment and History, 18: 5-34. https://doi.org/10.3197/096734012X13225062753543

Sauchyn, D.J., St-Jacques, J.M., and Luckman, B.H. 2015. Long-term relaibility of the Athabasca River (Alberta, Canada) as the water source for oil sands mining. Proceedings of the National Academy of Sciences USA, 112: 12621-6. https://doi.org/10.1073/pnas.1509726112

Scalzitti J, Strong C and Kochanski A 2016 Climate change impact on the roles of temperature and precipitation in the western US snowpack variability Geophys. Res. Lett. 43 5361–9

Schindler D W and Donahue W F 2006 An impending water crisis in Canada's western prairie provinces Proceedings of the National Academy of Sciences, United States of America 103 7210–6

Schindler, D.W. 2010. Tar sands need solid science. Nature, 468: 499. https://doi.org/10.1038/468499a

Schindler, D.W., and Smol, J.P. 2006. Cumulative effects of climate warming and other human activities on freshwaters of Arctic and subarctic North America. Ambio, 35: 160-168. https://doi.org/10.1579/0044-7447(2006)35[160:ceocwa]2.0.co;2

Schindler, D.W., Donahue, W.F., 2006. An impending water crisis in Canada's western prairie provinces. Proc. Natl. Acad. Sci. USA 103 (19), 7210–7216.

Schuh, C.E., Jamieson, H.E., Palmer, M.J., and Martin, A.J. 2018. Solid-phase speciation and post-depositional mobility of arsenic in lake sediments impacted by ore roasting at legacy gold

mines in the Yellowknife area, Northwest Territories, Canada. Applied Geochemistry, 91: 208-220. https://doi.org/10.1016/j.apgeochem.2017.10.025

Shotyk, W., Bicalho, B., Cuss, C., Donner, M., Grant-Weaver, I., Javed, M.B., and Noernberg, T. 2021. Trace elements in the Athabasca Bituminous Sands: A geochemical explanation for the paucity of environmental contamination by chalcophile elements. Chemical Geology, 581: 120392. https://doi.org/10.1016/j.chemgeo.2021.120392

Simpson, G.L. 2018. Modelling palaeoecological time series using generalised additive models. Frontiers in Ecology and Evolution, 6: 1-21. https://doi.org/10.3389/fevo.2018.00149

Simpson, S.L., Batley, G.E., Chariton, A.A., Stauber, J.L., King, C.K., Chapman, J.C., Hyne, R.V., Gale, S.A., Roach, A.C., and Maher, W.A. 2005. Handbook for Sediment Quality Assessment, CSIRO, Bangor NSW.

Sinnatamby, R.N., Yi, Y., Sokal, M.A., Clogg-Wright, K.P., Asada, T., Vardy, S.R., Karst-Riddoch, T.L., Last, W.M., Johnston, J.W., Hall, R.I., Wolfe, B.B., Edwards, T.W.D. 2010. Historical and paleolimnological evidence for expansion of Lake Athabasca (Canada) during the Little Ice Age. Journal of Paleolimnology, 43: 705-717. https://doi.org/10.1007/s10933-009-9361-4

Smith, H. G., and W. H. Blake. 2014. Sediment fingerprinting in agricultural catchments: A critical reexamination of source discrimination and data corrections. Geomorphology 204: 177–191. doi: 10.1016/j.geomorph.2013.08.003

Smith, H. G., D. S. Karam, and A. T. Lennard. 2018. Evaluating tracer selection for catchment sediment fingerprinting. J. Soils Sediments 18: 3005–3019. doi: 10.1007/s11368-018-1990-7

Smith, H. G., O. Evrard, W. H. Blake, and P. N. Owens. 2015. Preface—addressing challenges to advance sediment fingerprinting research. J. Soils Sediments 15: 2033–2037. doi: 10.1007/s11368-015-1231-2

Smol J P 1992 Paleolimnology: an important tool for effective ecosystem management Journal of Aquatic Ecosystem Health 1 49–58

Smol J P 2008 Pollution of Lakes and Rivers: A Paleoenvironmental Perspective 2nd edn (Oxford: Blackwell Publishing)

Sokal, M.A., Hall, R.I., and Wolfe, B.B. 2008. Relationships between hydrological and limnological conditions in lakes of the Slave River Delta (NWT, Canada) and quantification of their roles on sedimentary diatom assemblages. Journal of Paleolimnology, 39: 533-550. https://doi.org/10.1007/s10933-007-9128-8

Stewart, H. A., A. Massoudieh, and A. Gellis. 2015. Sediment source apportionment in Laurel Hill Creek, PA, using Bayesian chemical mass balance and isotope fingerprinting. Hydrol. Process. 29: 2545–2560. doi: 10.1002/hyp.10364

Stock, B. C., A. L. Jackson, E. J. Ward, A. C. Parnell, D. L. Phillips, and B. X. Semmens. 2018. Analyzing mixing systems using a new generation of Bayesian tracer mixing models. PeerJ 6: e5096. doi: 10.7717/peerj.5096

Stock, B. C., and B. X. Semmens. 2016. MixSIAR GUI user manual. Version 3.1. Available from https://github.com/brianstock/MixSIAR/. (Accessed 21 July 2020)

Stubley, M.P., and Irwin, D. 2019. Bedrock geology of the Slave Craton, Northwest Territories and Nunavut. Northwest Territories Geological Survey, NWT Open File 2019-01. ESRI and Adobe digital files.

Telford, J.V., Kay, M.L., Vander Heide, H., Wiklund, J.A., Owca, T.J., Faber, J.A., Wolfe, B.B., and Hall, R.I. 2021. Building upon open-barrel corer and sectioning systems to foster the continuing legacy of John Glew. Journal of Paleolimnology, 65: 271-277. https://doi.org/10.1007/s10933-020-00162-w

Thienpont, J.R., Korosi, J.B., Hargan, K.E., Williams, T., Eickmeyer, D.C., Kimpe, L.E., Palmer, M.J., Smol, J.P., and Blais, J.M. (2016). Multi-trophic level response to extreme metal contamination from gold mining in a subarctic lake. Proceedings of the Royal Society B: Biological Sciences, 283: 20161125. https://doi.org/10.1098/rspb.2016.1125

Timoney K 2013 The Peace-Athabasca Delta: Portrait of a Dynamic Ecosystem (Edmonton: University of Alberta Press)

Timoney, K.P. 2002. A dying delta? A case study of a wetland paradigm. Wetlands, 22: 285-291. https://doi.org/10.1672/0277-5212(2002)022[0282:ADDACS]2.0.CO;2

Timoney, K.P., and Lee, P. 2009. Does the Alberta tar sands industry pollute? The scientific evidence. The Open Conservation Biology Journal, 3: 65-81. http://dx.doi.org/10.2174/1874839200903010065

Timoney, K.P., and Lee, P. 2011. Polycyclic aromatic hydrocarbons increase in Athabasca River Delta sediment: temporal trends and environmental correlates. Environment Science and Technology. 4: 4278e4284. https://doi.org/10.1021/es104375d

Ullrich, S.M., Tanton, T.W., and Abdrashitova, S.A. 2001. Mercury in the aquatic environment: a review of factors affecting methylation. Environmental Science & Technology, 31: 241-293.

Upadhayay, H. R., H. G. Smith, M. Griepentrog, S. Bode, R. M. Bajracharya, W. H. Blake, W. Cornelis, and P. Boeckx. 2018. Community managed forests dominate the catchment sediment cascade in the mid-hills of Nepal: A compound-specific stable isotope analysis. Sci. Total Environ. 637: 306–317. doi: 10.1016/j.scitotenv.2018.04.394

Van Den Berghe, M.D., Jamieson, H.E., and Palmer, M.J. 2018. Arsenic mobility and characterization in lakes impacted by gold ore roasting, Yellowknife, NWT, Canada. Environmental Pollution, 234: 630-641. https://doi.org/10.1016/j.envpol.2017.11.062

Velez, M. I., J. I. Martínez, and F. Suter. 2012. Late Holocene history of the floodplain lakes of the Cauca River, Columbia. J. Paleolimnol. 49: 591–604. doi: 10.1007/se0933-012-9663-9

Vincent, W.F., Callaghan, T.V., Dahl-Jensen, D., Johansson, M.W.F., Kovacs, K.M., Michel, C., Prowse, T., Reist, J.D., and Sharp, M. 2011. Ecological implications of changes in the Arctic cryosphere. Ambio, 40: 87–99. https://dx.doi.org/10.1007%2Fs13280-011-0218-5

Wagemann, R., Snow, N.B., Rosenberg, D.M., and Lutz, A. 1978. Arsenic in sediments, water and aquatic biota from lakes in the vicinity of Yellowknife, Northwest Territories, Canada. Archives of Environmental Contamination and Toxicology, 7: 169-191. https://doi.org/10.1007/BF02332047

Walker, S.R., Jamieson, H.E., Lanzirotti, A., Andrade, C.F., and Hall, G.E. 2005. The speciation of arsenic in iron oxides in mine wastes from the Giant gold mine, N.W.T.: application of

synchrotron micro-xrd and micro-xanes at the grain scale. The Canadian Mineralogist, 43: 1205-1224. https://doi.org/10.2113/gscanmin.43.4.1205

Walker, S.R., Jamieson, H.E., Lanzirotti, A., Hall, G.E., and Peterson, R.C. 2015. The effect of ore roasting on arsenic oxidation state and solid phase speciation in gold mine tailings. Geochemistry: Exploration, Environment, Analysis, 15: 273-291. https://doi.org/10.1144/geochem2013-238

Walling, D. E., and J. C. Woodward. 1995. Tracing suspended sediment sources in river basins: A case study of the River Culm, Devon, UK. Mar. Freshw. Res. 46: 327–336. doi: 10.1071/MF9950327

Wasiuta, V., Kirk, J.L., Chambers, P.A., Alexander, A.C., Wyatt, F.R., Rooney, R.C., and Cooke, C.A. 2019. Accumulating mercury and methylmercury burdens in watersheds impacted by Oil Sands pollution. Environmental Science & Technology, 2019, 53: 12856−12864.

WHC/IUCN. 2017. Reactive monitoring mission to Wood Buffalo National Park Canada, p. 1–79. Technical Report. Available from https://whc.unesco.org/en/documents/156893

WHC/IUCN. 2021. United Nations Educational, Scientific and Cultural Organization Convention concerning the protection of the world cultural and natural heritage. China, online meeting, pp 188. Retrieved from https://whc.unesco.org/en/sessions/44com/ on February 11th, 2022.

Wiklund J A, Bozinovski N Hall R I and Wolfe B B 2010 Epiphytic diatoms as flood indicators J. Paleolimnol. 44 25–42

Wiklund, J.A., Hall, R.I., Wolfe, B.B., Edwards, T.W.D, Farwell, A.J. and Dixon, D.G. 2014. Use of pre-industrial floodplain lake sediments to establish baseline river metal concentrations downstream of Alberta oil sands: a new approach for detecting pollution of rivers. Environmental Research Letters, 9: 124019. https://doi.org/10.1088/1748-9326/9/12/124019

Wiklund, J.A., Hall, R.I., Wolfe, B.B., Edwards, T.W.D, Farwell, A.J., and Dixon, D.G. 2012. Has Alberta oil sands development increased far-field delivery of airborne contaminants to the Peace–Athabasca Delta?. Science of the Total Environment, 433: 379-382. https://doi.org/10.1016/j.scitotenv.2012.06074

Wiklund, J.A., Kirk, J.L., Muir, D.C.G., Evans, M., Yang, F., Keating, J., and Parsons, M.T. 2017. Anthropogenic mercury deposition in Flin Flon Manitoba and the Experimental Lakes Area Ontario (Canada): A multi-lake sediment core reconstruction. Science of the Total Environment, 586: 685-695. https://doi.org/10.1016/j.scitotenv.2017.02.046

Wilkinson, G. M., J. Walter, R. Fleck, and M. L. Pace. 2020. Beyond the trends: The need to understand multiannual dynamics in aquatic ecosystems. Limnol. Oceanogr.: Lett. 5: 281–286. doi: 10.1002/lol2.10153

Wolfe, B. B., Hall, R. I., Wiklund, J. A., and Kay, M. L. 2020. Past variations in Lower Peace River ice-jam flood frequency. Environ. Rev. 28: 209–217. doi: 10.1139/er-2019-0047

Wolfe, B. B., T. L. Karst-Riddoch, S. R. Vardy, M. D. Falcone, R. I. Hall, and T. W. D. Edwards. 2005. Impacts of climate and river flooding on the hydro-ecology of a floodplain basin, Peace-Athabasca Delta, Canada since A.D. 1700. Quatern. Res. 64: 147–162. doi: 10.1016/j.yqres.2005.05.001

Wolfe, B.B., Edwards, T.W.D., Hall, R.I., and Johnston, J.W. 2011. A 5200-year record of freshwater availability for regions in western North America fed by high-elevation runoff. Geophysical Research Letters, 38: L11404. https://doi.org/10.1029/2011GL047599

Wolfe, B.B., Hall, R.I., Edwards, T.W.D., and Johnston, J.W. 2012. Developing temporal hydroecological perspectives to inform stewardship of a northern floodplain landscape subject to multiple stressors: Paleolimnological investigations of the Peace-Athabasca Delta. Environmental Reviews, 20: 192-206. https://doi.org/10.1139/a2012-008

Wolfe, B.B., Hall, R.I., Edwards, T.W.D., Jarvis, S.R., Sinnatamby, R.N., Yi, Y., and Johnston, J.W. 2008a. Climate-driven shifts in quantity and seasonality of the river discharge over the past 1000 years from the hydrographic apex of North America. Geophysical Research Letters, 35: L24402. https://doi.org/10.1029/2008GL036125

Wolfe, B.B., Hall, R.I., Edwards, T.W.D., Vardy, S.R., Falcone, M.D., Sjunneskog, C., Sylvestre, F., McGowan, S., Leavitt, P.R., and van Driel, P. 2008. Hydroecological responses of the Athabasca Delta, Canada, to changes in river flow and climate during the 20th century. Ecohydrology, 1: 142–148. https://doi.org/10.1002/eco.13

Wolfe, B.B., Hall, R.I., Last W.M., Edwards, T.W.D., English, M.C., Karst-Riddoch, T., Paterson, A., and Palmini, R. 2006. Reconstruction of multi-century flood histories from oxbow lake sediments, Peace-Athabasca Delta, Canada. Hydrological Processes, 20: 4131–4153. https://doi.org/10.1002/hyp.6423

Wood Buffalo National Park (WBNP). 2019. World heritage site action plan, p. 1–96. Available from https://www.pc.gc.ca/en/pn-np/nt/woodbuffalo/info/action. (Accessed 17 March 2019)

Wood, S.N., 2017. Generalized Additive Models: An Introduction with R. CRC Press, Boca Raton, FL.

Woodward, G., Perkins, D., and Brown, L. 2010. Climate change and freshwater ecosystems: Impacts across multiple levels of organization. Philosophical Transactions of the Royal Society: Biological Science, 365: 2093-2106. https://doi.org/10.1098/rstb.2010.0055

Wynants, M., and others. 2020. Determining tributary sources of increased sedimentation in East-African Rift Lakes. Sci. Total Environ. 717: 137266. doi: 10.1016/j.scitotenv.2020.137266

Xenopoulos, M. A. 2019. Editorial: Long-term studies in limnology and oceanography. Limnol. Oceanogr. 64: S1. doi: 10.1002/lno.11112

Yi, Y. Brock, B.E., Falcone, M.D., Wolfe, B.B., and Edwards, T.W.D. 2008. A couple isotope tracer method to characterize input water to lakes. Journal of Hydrology, 350: 1-13. https://doi.org/10.1016/j.jhydrol.2007.11.008

Zheng, S., B. Wu, K. Wang, G. Tan, S. Han, and C. Thorne. 2017. Evolution of the Yellow River delta, China: Impacts of channel avulsion and progradation. Int. J. Sediment Res.32: 34–44. doi: 10.1016/j.ijsrc.2016.10.001

Zubot, W., MacKinnon, M.D., Chelme-Ayala, P., Smith, D.W., and Gamal El-Din, M. 2012. Petroleum coke adsorption as a water management option for oil sands process-affected water. Science of the Total Environment, 427-428: 364-372. https://doi.org/10.1016/j.scitotenv.2012.04.024

Appendix A

Appendix A provides crossplots for primary pollutants not shown in main text of Chapter 2, AICc results and base data for metals concentrations.

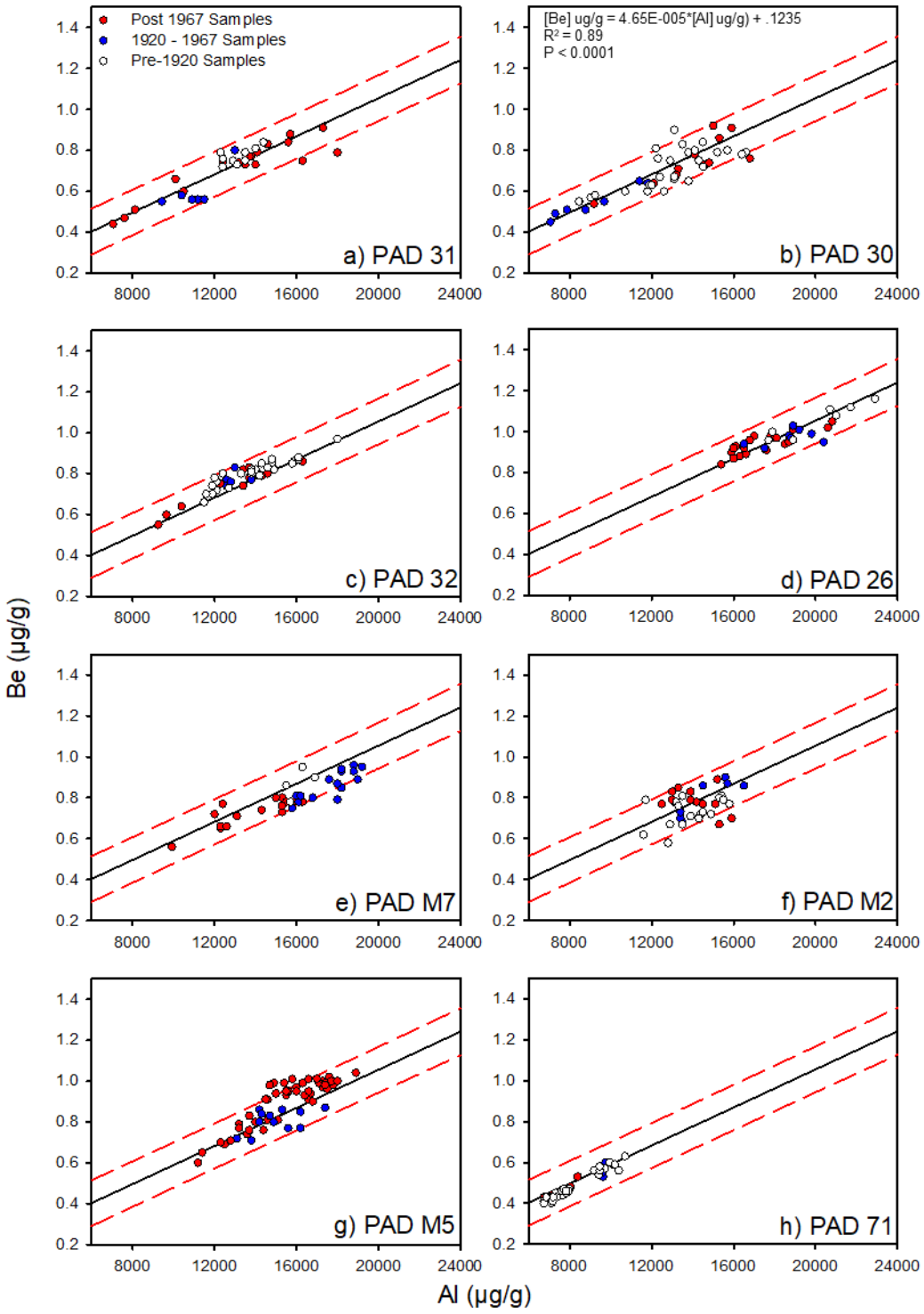

Figure A1. The linear relations between sediment concentrations of beryllium and aluminum in pre-1920 floodplain lake sediment (black line) and 95% prediction intervals (red dashed line denoting range of natural variability). Sediment samples are distinguished by time intervals (pre-1920 [open circles], 1920-1967 [blue circles], and post-1967 [red circles]).

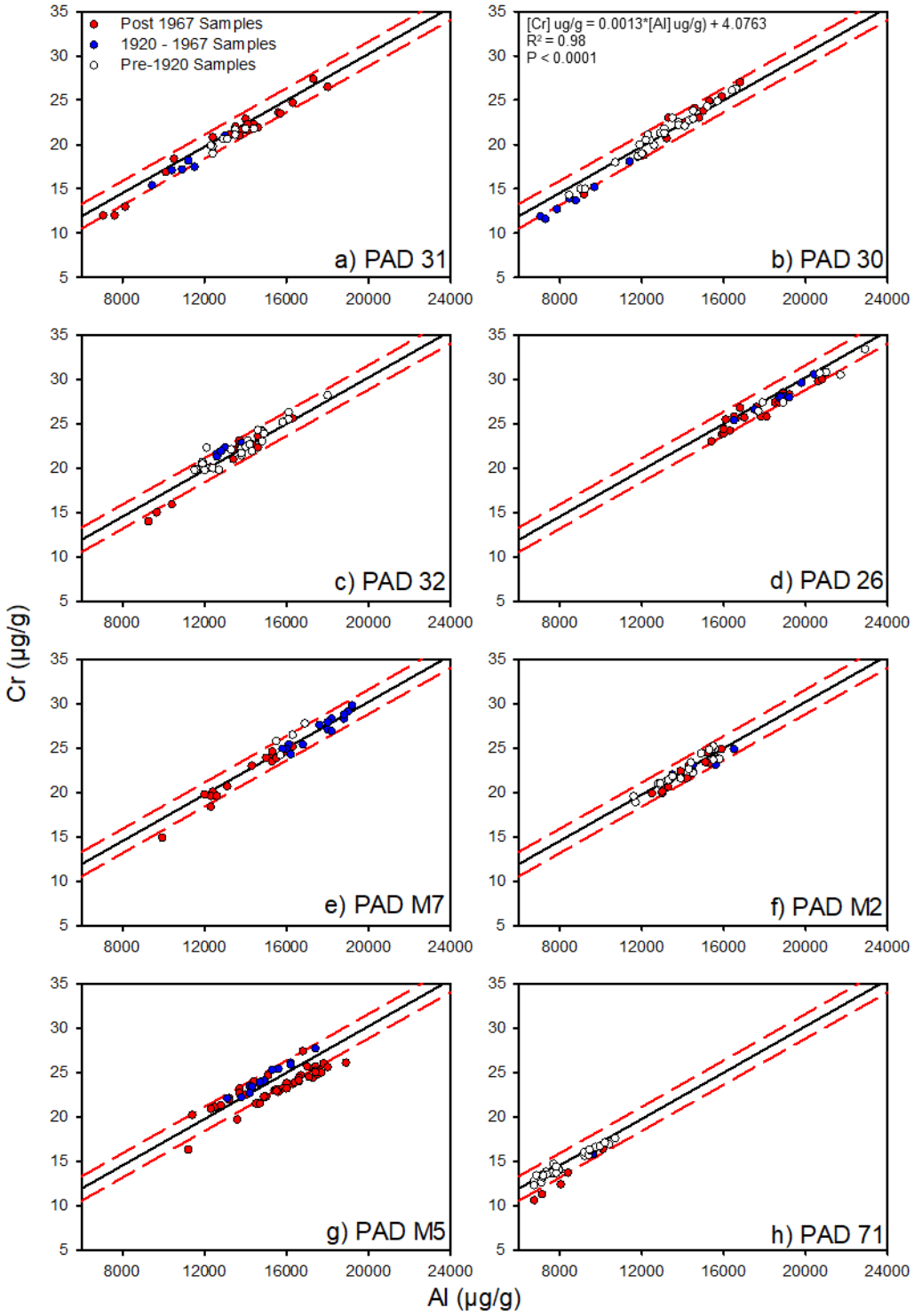

Figure A2. The linear relations between sediment concentrations of chromium and aluminum in pre-1920 floodplain lake sediment (black line) and 95% prediction intervals (red dashed line denoting range of natural variability). Sediment samples are distinguished by time intervals (pre-1920 [open circles], 1920-1967 [blue circles], and post-1967 [red circles]).

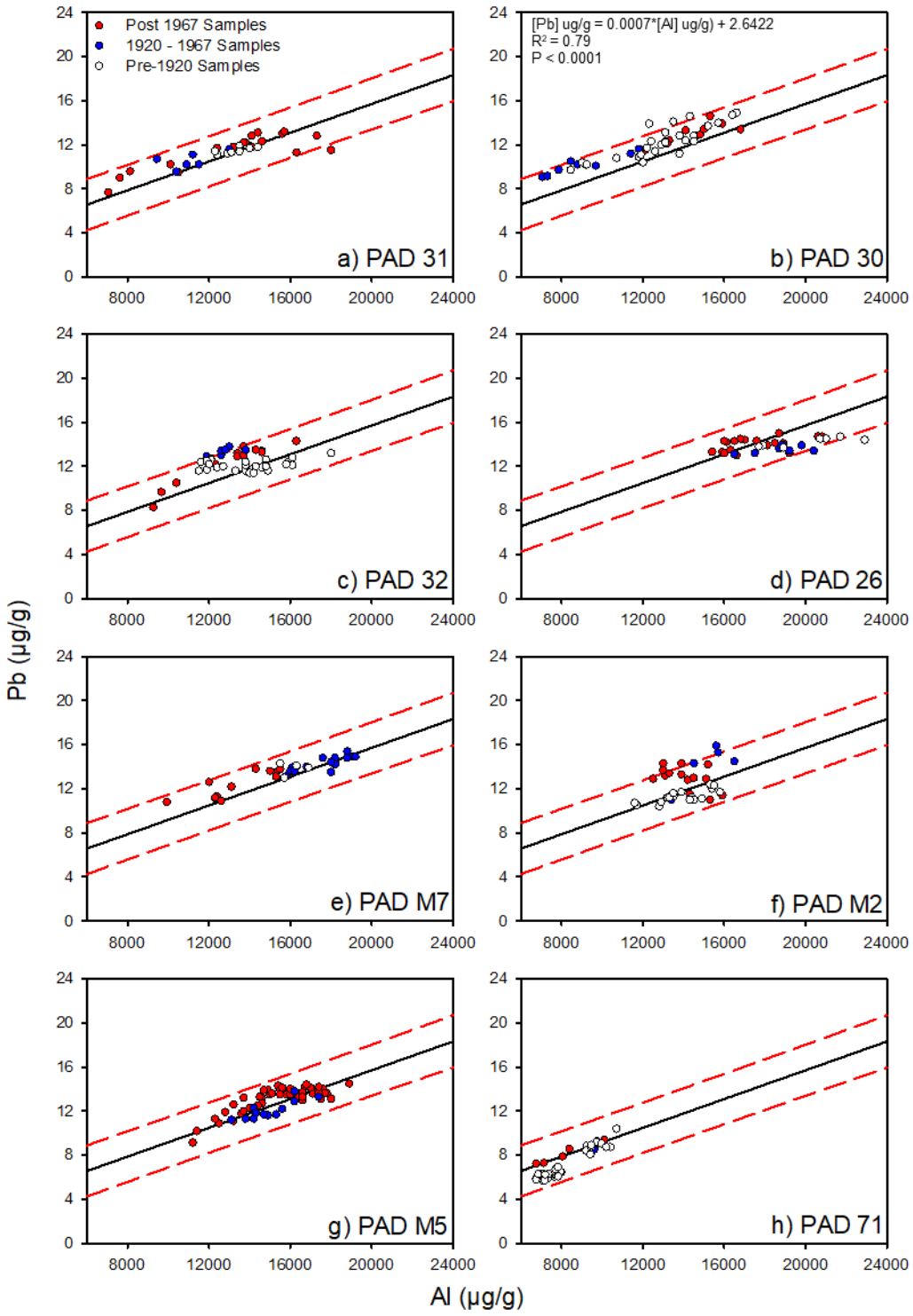

Figure A3. The linear relations between sediment concentrations of lead and aluminum in pre-1920 floodplain lake sediment (black line) and 95% prediction intervals (red dashed line denoting range of natural variability). Sediment samples are distinguished by time intervals (pre-1920 [open circles], 1920-1967 [blue circles], and post-1967 [red circles]).

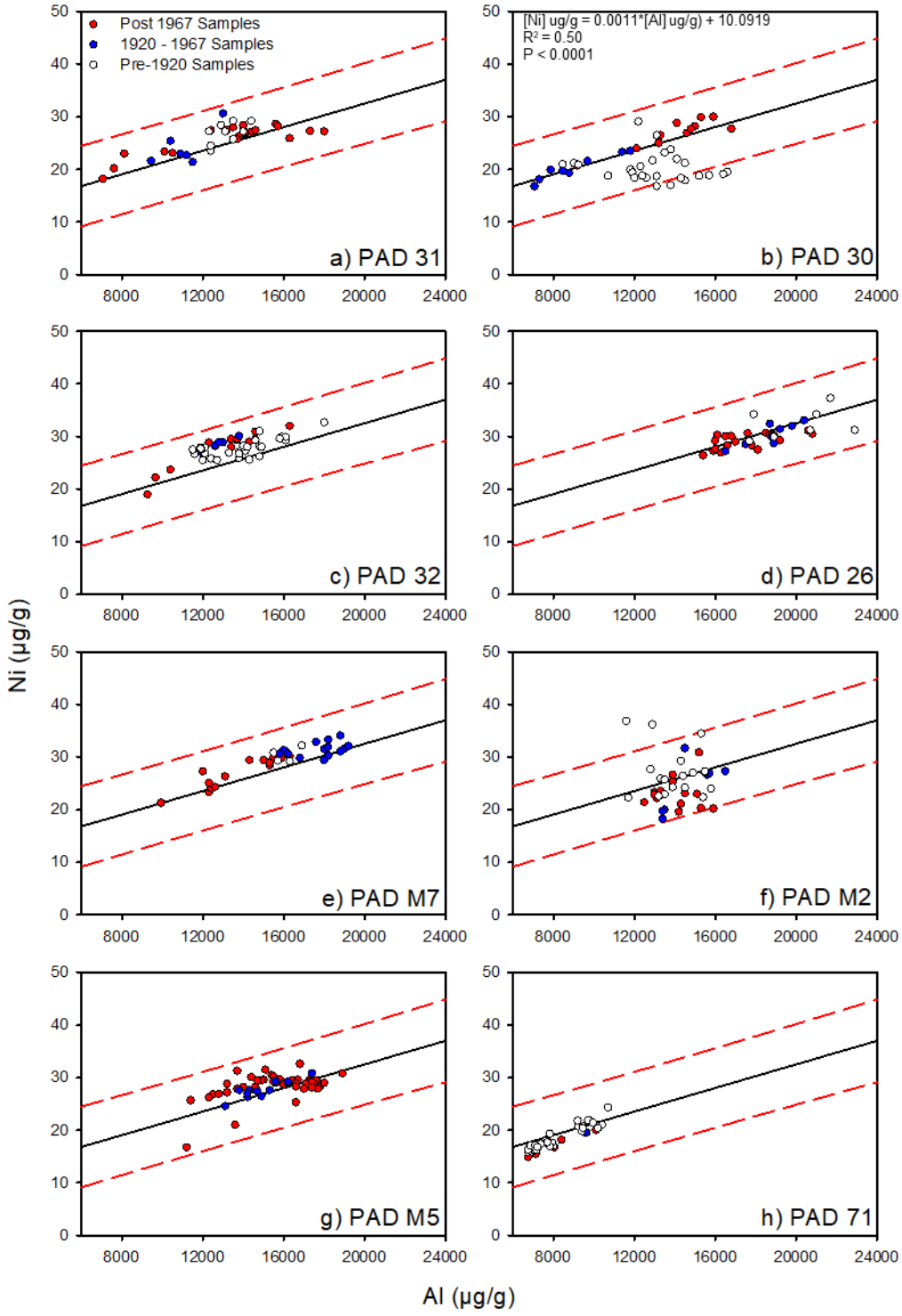

Figure A4. The linear relations between sediment concentrations of nickel and aluminum in pre-1920 floodplain lake sediment (black line) and 95% prediction intervals (red dashed line denoting range of natural variability). Sediment samples are distinguished by time intervals (pre-1920 [open circles], 1920-1967 [blue circles], and post-1967 [red circles]).

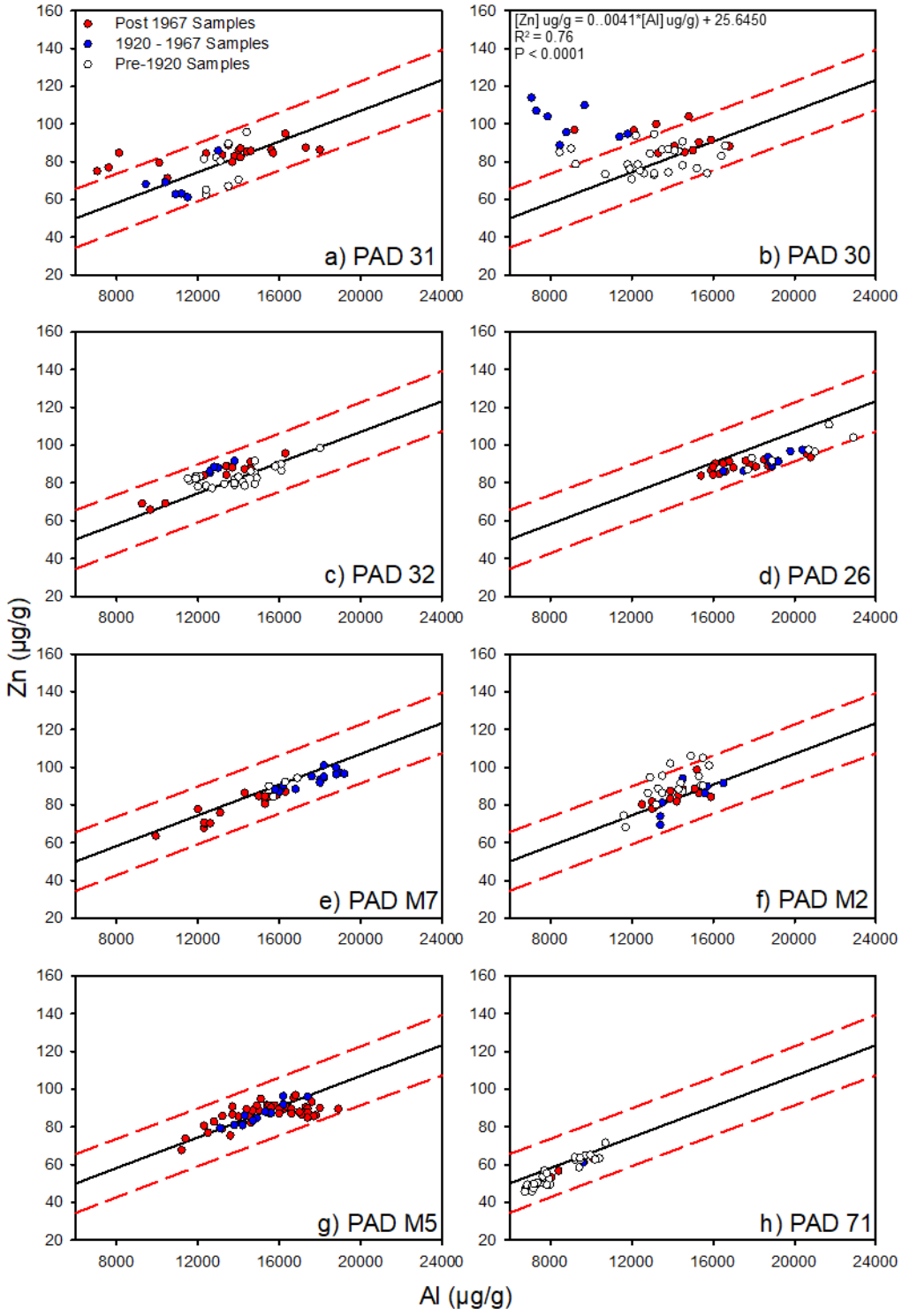

Figure A5. The linear relations between sediment concentrations of zinc and aluminum in pre-1920 floodplain lake sediment (black line) and 95% prediction intervals (red dashed line denoting range of natural variability). Sediment samples are distinguished by time intervals (pre-1920 [open circles], 1920-1967 [blue circles], and post-1967 [red circles]).

Table A1. AICc values, changes in AICc values and model weights for a set of models used to test which normalizing agent best predicts metals concentrations in floodplain lakes located in the Athabasca Delta. AICc model computations (K = 3 for all models) were performed using the package *AICcmodavg* in R version 3.5.2 (Mazerolle, 2017; R Core Team, 2019).

Model	AICc	ΔAICc	AICc weights
Be ~ Al	-349.64	0	1
Be ~ Li	-243.39	106.25	0
Cr ~ Al	253.01	0	1
Cr ~ Li	560.15	307.14	0
Pb ~ Al	377.35	0	1
Pb – Li	484.50	107.15	0
Ni ~ Al	664.27	15.35	0
Ni ~ Li	648.27	0	1
V ~ Al	467.78	0	1
V ~ Li	713.86	246.08	0
Zn ~ Al	834.86	0	1
Zn ~ Li	929.59	94.72	0

Reference:

Mazerolle, M. J. (2017). AICcmodavg: Model Selection and Multimodel Inference Based on (Q)AIC(c). R Package Version 2.1-1. Available at https://cran.r-project.org/web/packages/AICcmodavg/AICcmodavg.pdf

Table A2. Estimated year and metals concentrations for the sediment core from PAD 31 in the Peace-Athabasca Delta.

Depth (cm)	Year	Al (ug/g)	Be (ug/g)	Cr (ug/g)	Pb (ug/g)	Ni (ug/g)	V (ug/g)	Zn (ug/g)
0	2010.3	16300.00	0.75	24.70	11.30	25.90	43.50	94.90
1	2010.1	18000.00	0.79	26.50	11.50	27.20	46.20	86.40
2	2009.3	17300.00	0.91	27.40	12.80	27.30	47.60	87.50
3	2008.0	13500.00	0.73	22.00	11.80	28.00	36.20	88.70
4	2006.6	12400.00	0.74	20.80	11.70	27.40	33.20	84.50
5	2005.2	13200.00	0.74	21.10	11.80	27.50	33.30	83.50
6	2003.8	14000.00	0.73	22.90	11.90	28.40	36.60	86.10
7	2002.5	13800.00	0.77	21.60	12.20	26.30	35.70	83.00
8	2001.5	10500.00	0.60	18.40	9.51	23.10	30.70	71.30
9	2000.5	13700.00	0.77	21.00	12.20	25.70	36.00	79.90
10	1999.2	14400.00	0.84	22.30	13.10	27.10	36.60	85.30
11	1997.8	14100.00	0.79	21.60	12.80	26.80	36.60	82.40
12	1996.3	15600.00	0.84	23.60	13.00	28.60	38.70	86.50
13	1994.7	15700.00	0.88	23.50	13.20	28.20	38.70	84.60
14	1992.6	14600.00	0.83	21.90	12.30	27.40	37.10	85.80
15	1990.1	14100.00	0.79	22.30	11.80	27.10	37.70	87.20
16	1987.8	10100.00	0.66	16.90	10.20	23.40	29.60	79.50
17	1985.1	7050.00	0.44	12.00	7.68	18.20	23.00	75.10
18	1981.1	7610.00	0.47	12.00	9.01	20.20	25.00	77.00
19	1975.8	8120.00	0.51	13.00	9.60	23.00	27.20	84.80
20	1969.2	9440.00	0.55	15.40	10.70	21.60	30.40	68.20
21	1961.8	11200.00	0.56	18.20	11.10	22.70	34.20	63.20
22	1954.4	11500.00	0.56	17.50	10.20	21.40	31.90	61.20
23	1947.0	10900.00	0.56	17.20	10.20	23.00	31.30	62.90
24	1939.0	10400.00	0.58	17.10	9.56	25.40	30.90	69.20
25	1929.6	13000.00	0.80	21.00	11.60	30.60	38.10	85.90
26	1918.4	12400.00	0.72	19.00	11.20	23.50	33.70	62.60
27	1908.7	13500.00	0.79	21.70	11.90	25.70	38.80	67.10
28	1899.6	12400.00	0.76	19.80	11.10	24.50	36.70	65.20
29	1886.0	14000.00	0.81	21.80	11.70	27.20	39.50	70.60
30	1870.5	12300.00	0.79	19.90	11.40	27.20	34.60	81.50
31	1856.8	12900.00	0.75	20.60	11.20	28.40	36.20	82.30
32	1844.3	13100.00	0.73	20.60	11.30	27.20	36.60	80.50
33	1831.0	13500.00	0.75	21.10	11.40	29.20	37.00	89.80
34	1816.9	14400.00	0.84	21.80	11.80	29.20	36.90	95.80

Table A3. Estimated year and metals concentrations for the sediment core from PAD 30 in the Peace-Athabasca Delta.

Depth (cm)	Year	Al (ug/g)	Be (ug/g)	Cr (ug/g)	Pb (ug/g)	Ni (ug/g)	V (ug/g)	Zn (ug/g)
0	2016.37	13300.00	0.71	23.00	12.40	26.50	39.10	84.70
1	2015.92	14600.00	0.73	24.10	12.80	26.90	40.30	85.10
2	2014.94	16800.00	0.76	27.00	13.40	27.70	45.30	88.10
3	2014.01	15000.00	0.92	23.80	13.40	28.20	38.30	86.10
4	2013.39	15300.00	0.86	24.90	14.60	29.90	39.70	90.40
5	2012.66	15900.00	0.91	25.40	13.90	30.00	40.90	91.60
6	2011.19	14100.00	0.78	22.50	13.30	28.80	39.50	88.30
7	2008.44	14800.00	0.74	23.00	12.90	27.70	41.30	104.00
8	2004.70	13200.00	0.68	20.70	12.10	25.00	37.00	100.00
9	2001.45	12100.00	0.64	18.80	11.50	24.00	33.60	96.70
10	1998.93	9180.00	0.54	14.40	10.20	20.70	27.40	96.90
11	1995.11	11400.00	0.65	18.10	11.20	23.30	31.90	93.20
12	1989.71	11800.00	0.64	18.60	11.60	23.50	33.30	94.80
13	1983.06	9680.00	0.55	15.20	10.10	21.60	29.50	110.00
14	1977.85	7060.00	0.45	11.90	9.07	16.80	24.30	114.00
15	1973.99	7300.00	0.49	11.60	9.16	18.10	24.20	107.00
16	1968.53	7860.00	0.51	12.70	9.71	19.90	25.90	104.00
17	1961.64	8780.00	0.51	13.70	10.20	19.30	26.70	95.60
18	1954.42	8460.00	0.55	13.90	10.50	19.70	26.90	88.70
19	1948.17	9020.00	0.57	15.00	10.40	21.20	29.00	86.90
20	1943.13	8450.00	0.55	14.30	9.72	21.00	27.40	85.10
21	1939.43	9240.00	0.58	15.00	10.20	20.90	28.10	78.80
22	1934.86	11800.00	0.60	18.70	10.90	20.00	30.60	78.60
23	1927.96	12600.00	0.60	19.90	11.40	18.40	32.90	74.00
24	1919.72	11900.00	0.63	20.00	11.10	19.40	32.50	76.30
25	1911.91	12000.00	0.63	19.00	10.40	18.40	31.80	70.80
26	1904.91	10700.00	0.60	18.00	10.80	18.80	30.90	73.50
27	1896.22	12400.00	0.67	20.50	12.30	18.80	35.10	75.30
28	1883.61	13100.00	0.66	21.20	12.30	16.80	33.80	73.00
29	1869.79	13800.00	0.65	22.50	12.80	17.00	36.60	74.40
30	1858.09	14500.00	0.72	23.80	12.80	17.90	39.20	78.10
31	1845.80	15200.00	0.79	24.30	13.70	18.80	41.50	76.60
32	1834.32	12300.00	0.76	21.10	13.90	20.60	37.20	78.60
33	1824.65	12900.00	0.75	21.30	12.00	21.70	37.60	84.40
34	1814.00	13100.00	0.67	21.80	12.20	18.70	35.60	73.90
35	1800.52	15700.00	0.80	24.90	14.00	18.90	40.70	73.90
36	1787.63	16600.00	0.79	26.30	14.90	19.50	43.00	88.60
37	1774.89	16400.00	0.78	26.10	14.70	19.10	42.80	83.10
38	1760.35	14300.00	0.75	22.70	14.60	18.30	35.80	85.70
39	1748.05	13500.00	0.83	23.00	14.10	23.20	41.60	86.60
40	1738.76	13100.00	0.90	21.30	13.10	26.50	40.60	94.60
41	1730.90	12200.00	0.81	20.50	11.70	29.10	37.30	94.00
42	1721.64	13800.00	0.79	22.20	11.20	23.80	36.80	86.80
43	1710.38	14100.00	0.80	22.10	12.40	22.00	38.00	86.00
44	1698.62	14500.00	0.84	22.90	12.30	21.20	38.80	90.70

Table A4. Estimated year and metals concentrations for the sediment core from PAD 32 in the Peace-Athabasca Delta.

Depth (cm)	Year	Al (ug/g)	Be (ug/g)	Cr (ug/g)	Pb (ug/g)	Ni (ug/g)	V (ug/g)	Zn (ug/g)
0	2014.7	9260.00	0.55	14.00	8.29	19.00	26.30	69.00
1	2012.2	9660.00	0.60	15.00	9.66	22.20	28.10	65.80
2	2007.9	10400.00	0.64	15.90	10.50	23.70	30.40	69.20
3	2002.8	12300.00	0.75	20.10	12.20	28.80	36.90	83.90
4	1998.0	14600.00	0.83	22.30	13.40	29.40	40.00	87.60
5	1993.7	16300.00	0.86	25.60	14.30	32.00	45.10	95.70
6	1989.5	14600.00	0.80	23.60	13.30	30.90	42.30	91.30
7	1985.5	13400.00	0.82	22.10	13.20	29.50	38.30	89.00
8	1982.5	13400.00	0.74	21.00	12.90	28.00	37.50	84.30
9	1979.9	13700.00	0.78	22.60	13.00	29.30	39.50	88.60
10	1974.8	14300.00	0.79	22.70	13.50	29.00	40.10	87.40
11	1967.6	13700.00	0.83	23.10	13.80	29.50	40.40	88.10
12	1960.7	13800.00	0.77	22.80	13.50	30.10	39.20	91.70
13	1954.7	13000.00	0.83	22.30	13.80	28.90	38.00	88.10
14	1948.9	11900.00	0.74	20.00	12.90	27.10	35.00	82.30
15	1942.8	12600.00	0.77	21.60	13.00	28.20	36.30	85.40
16	1934.4	12600.00	0.74	21.30	13.40	28.30	35.80	86.50
17	1924.9	12800.00	0.76	21.90	13.50	28.90	37.70	88.60
18	1915.5	12100.00	0.76	20.00	12.70	26.80	33.80	83.10
19	1904.7	12100.00	0.72	22.30	12.60	27.90	35.70	83.50
20	1893.8	11900.00	0.70	20.70	12.40	27.50	34.90	83.50
21	1882.8	11600.00	0.70	19.90	12.40	26.70	33.40	81.30
22	1872.3	11900.00	0.74	20.20	12.50	27.90	34.60	83.30
23	1862.6	11500.00	0.66	19.80	11.60	27.50	34.60	82.30
24	1853.3	15900.00	0.86	25.30	12.40	29.90	44.50	89.60
25	1845.2	14800.00	0.86	24.20	12.60	31.00	42.60	91.80
26	1837.2	13800.00	0.80	22.20	11.60	27.10	38.70	81.80
27	1827.8	14800.00	0.85	24.10	12.10	28.10	42.10	85.20
28	1817.9	16100.00	0.87	25.50	12.80	29.30	44.80	86.70
29	1808.5	14100.00	0.80	23.10	11.70	27.30	40.30	81.50
30	1798.9	14000.00	0.82	22.40	11.40	28.20	40.20	83.20
31	1790.1	14200.00	0.79	22.70	11.40	28.00	40.00	80.50
32	1782.0	13300.00	0.80	22.10	11.60	26.90	38.90	79.40
33	1773.3	16100.00	0.88	26.30	12.10	29.90	45.60	90.00
34	1764.5	14900.00	0.82	23.90	11.60	28.00	41.70	82.60
35	1756.2	18000.00	0.97	28.20	13.20	32.70	49.50	98.50
36	1747.4	15800.00	0.85	25.20	12.20	29.60	44.40	88.80
37	1737.9	14600.00	0.83	24.30	11.90	29.30	41.90	86.20
38	1727.6	11900.00	0.74	20.50	11.70	27.70	35.20	82.30
39	1715.7	14800.00	0.87	23.00	12.00	26.20	41.00	79.40
40	1702.6	12400.00	0.80	20.00	11.90	25.80	34.70	78.60
41	1690.5	12000.00	0.78	19.80	12.20	25.50	34.30	78.10
42	1678.9	14300.00	0.85	21.90	12.00	25.60	38.90	78.60
43	1666.4	13800.00	0.82	21.40	12.10	25.90	37.20	78.90
44	1653.7	13800.00	0.81	21.70	12.40	26.70	37.50	79.90
45	1640.4	12700.00	0.73	19.80	12.00	25.50	34.90	77.20

Table A5. Estimated year and metals concentrations for the sediment core from PAD 26 in the Peace-Athabasca Delta.

Depth (cm)	Year	Al (ug/g)	Be (ug/g)	Cr (ug/g)	Pb (ug/g)	Ni (ug/g)	V (ug/g)	Zn (ug/g)
0	2014.8	17800.00	0.98	25.80	14.00	28.30	44.90	90.10
1	2010.7	18100.00	0.97	25.80	13.90	27.50	45.00	88.60
2	2006.1	16300.00	0.88	24.20	13.50	26.90	42.10	84.70
3	2001.9	15400.00	0.84	23.00	13.30	26.40	40.50	83.90
4	1997.8	15900.00	0.90	23.80	13.30	27.30	42.40	86.60
5	1994.3	16000.00	0.87	23.90	13.20	27.60	42.50	84.40
6	1991.7	16600.00	0.89	25.60	13.00	28.30	44.00	86.00
7	1989.5	16500.00	0.92	25.80	14.30	30.00	44.90	90.30
8	1988.0	16100.00	0.93	25.50	14.20	30.30	44.50	90.40
9	1987.3	16000.00	0.92	24.40	14.30	29.20	42.90	88.60
10	1986.9	17000.00	0.98	25.70	14.40	29.00	44.90	88.10
11	1986.8	16800.00	0.96	26.80	14.50	30.10	46.30	91.40
12	1986.7	17600.00	0.91	26.90	14.30	30.60	46.40	91.70
13	1986.7	18500.00	0.94	27.40	14.10	30.70	46.90	92.30
14	1986.4	20600.00	1.02	29.80	14.70	31.10	52.70	95.40
15	1985.7	20800.00	1.05	30.00	14.70	30.50	52.60	93.60
16	1984.2	18900.00	1.02	28.50	13.90	29.70	49.10	88.80
17	1981.4	18900.00	1.01	28.40	14.10	30.20	49.10	90.10
18	1976.3	18700.00	0.95	27.40	15.00	30.30	49.30	89.10
19	1970.4	19200.00	1.01	28.30	13.20	29.30	49.10	91.60
20	1965.0	20400.00	0.95	30.60	13.40	33.10	53.70	97.50
21	1958.2	18700.00	0.98	27.90	13.60	32.40	48.90	93.80
22	1950.7	16500.00	0.94	25.40	13.10	27.20	43.40	86.30
23	1943.3	18900.00	1.03	28.10	13.90	28.70	47.90	89.10
24	1935.6	18800.00	0.97	28.00	13.90	30.00	48.30	91.10
25	1929.5	19800.00	0.99	29.60	13.90	32.00	50.30	96.90
26	1925.3	17500.00	0.92	26.60	13.20	28.50	45.20	86.40
27	1921.3	19200.00	1.01	28.00	13.40	31.40	49.20	91.30
28	1916.8	17900.00	1.00	27.40	13.90	34.20	47.20	93.20
29	1912.2	18900.00	0.96	27.40	13.70	29.90	46.90	91.70
30	1907.8	21000.00	1.08	30.80	14.50	34.20	54.20	96.50
31	1903.8	20700.00	1.11	30.70	14.50	31.20	54.80	97.60
32	1899.6	22900.00	1.16	33.40	14.40	31.20	61.80	104.00
33	1895.4	21700.00	1.12	30.50	14.70	37.30	54.50	111.00
34	1890.8	17700.00	0.96	26.40	13.80	29.10	46.30	87.10

Table A6. Estimated year and metals concentrations for the sediment core from PAD M7 in the Peace-Athabasca Delta.

Depth (cm)	Year	Al (ug/g)	Be (ug/g)	Cr (ug/g)	Pb (ug/g)	Ni (ug/g)	V (ug/g)	Zn (ug/g)
0	2014.5	9930.00	0.56	14.90	10.80	21.30	27.60	63.60
1	2011.6	12300.00	0.65	18.40	11.10	23.30	33.70	67.70
2	2008.2	12400.00	0.77	20.10	11.30	24.10	37.00	70.00
3	2005.2	12300.00	0.66	19.60	11.20	25.10	35.70	70.60
4	2003.0	12600.00	0.66	19.60	10.90	24.30	36.30	70.40
5	2000.8	13100.00	0.71	20.70	12.20	26.30	38.40	75.90
6	1997.5	12000.00	0.72	19.80	12.60	27.30	36.50	77.80
7	1993.2	15300.00	0.73	24.10	13.50	29.00	44.60	82.60
8	1988.8	15300.00	0.80	23.50	13.10	28.40	43.10	80.50
9	1984.8	15500.00	0.78	23.90	13.80	29.90	44.20	84.30
10	1981.4	15000.00	0.80	23.90	13.60	29.40	42.70	84.70
11	1978.5	14300.00	0.74	23.00	13.80	29.40	41.10	86.30
12	1975.6	15700.00	0.78	24.20	13.00	29.30	43.40	84.40
13	1972.7	16300.00	0.78	25.20	14.00	30.10	44.80	87.00
14	1970.0	15300.00	0.76	24.60	13.10	28.90	43.80	84.70
15	1967.9	15900.00	0.78	24.60	13.20	29.80	44.50	85.30
16	1966.8	16100.00	0.78	25.40	13.90	31.00	46.20	88.70
17	1964.9	16000.00	0.81	24.90	13.60	31.30	46.70	87.00
18	1961.6	15800.00	0.75	24.90	13.10	30.60	46.00	88.10
19	1959.2	16200.00	0.81	24.30	13.60	30.60	43.50	90.40
20	1958.3	16800.00	0.80	25.40	14.00	29.80	47.00	88.40
21	1957.8	18200.00	0.85	28.30	14.40	33.30	50.70	101.00
22	1956.4	18000.00	0.79	27.10	13.50	31.50	49.40	93.30
23	1953.2	18200.00	0.93	26.90	14.20	31.90	48.40	94.30
24	1948.3	17600.00	0.89	27.60	14.80	32.90	49.20	95.10
25	1942.7	18800.00	0.96	28.30	15.40	34.10	50.50	99.90
26	1937.9	18200.00	0.94	28.30	14.80	30.30	48.70	95.00
27	1934.8	19000.00	0.89	29.10	14.90	31.60	49.90	97.00
28	1932.9	18800.00	0.93	28.80	14.80	31.10	49.90	96.20
29	1930.8	19200.00	0.95	29.80	14.90	32.10	52.00	96.50
30	1922.6	18000.00	0.87	27.90	14.40	29.40	47.90	91.80
31	1913.8	16900.00	0.90	27.80	13.90	32.20	48.10	94.30
32	1908.6	15500.00	0.86	25.80	14.30	30.80	43.30	90.00
33	1903.2	16300.00	0.95	26.50	14.10	29.20	45.10	92.20
34	1897.6	15700.00	0.78	24.20	13.00	29.30	43.40	84.40

Table A7. Estimated year and metals concentrations for the sediment core from PAD M2 in the Peace-Athabasca Delta.

Depth (cm)	Year	Al (ug/g)	Be (ug/g)	Cr (ug/g)	Pb (ug/g)	Ni (ug/g)	V (ug/g)	Zn (ug/g)
0	2016.2	15900.00	0.70	24.90	11.40	20.20	40.80	84.20
1	2014.4	15300.00	0.67	23.30	11.00	20.30	39.30	86.30
2	2011.8	14300.00	0.70	23.00	11.50	21.10	39.40	85.10
3	2009.5	14200.00	0.78	21.60	12.80	19.60	38.00	81.80
4	2007.0	15100.00	0.77	23.40	12.90	23.00	42.40	88.60
5	2003.8	14500.00	0.77	22.40	13.00	23.10	40.90	88.50
6	2000.1	12500.00	0.77	19.90	12.90	21.40	36.50	80.30
7	1996.0	13100.00	0.78	20.40	13.20	22.20	37.70	78.70
8	1991.7	13000.00	0.79	19.90	13.70	23.30	37.60	81.80
9	1987.4	13000.00	0.83	20.10	14.30	22.90	38.30	78.00
10	1983.3	13300.00	0.85	20.60	13.40	23.50	39.40	80.10
11	1978.8	13900.00	0.79	21.90	13.30	25.30	40.00	83.40
12	1974.8	13900.00	0.83	22.40	14.30	26.60	39.40	87.50
13	1970.9	15200.00	0.89	24.50	14.20	30.90	43.00	98.60
14	1966.9	14500.00	0.86	23.10	14.30	31.70	40.20	94.00
15	1963.0	16500.00	0.86	24.90	14.50	27.30	41.70	91.60
16	1957.7	15600.00	0.90	23.10	15.90	26.60	40.60	86.20
17	1949.5	15700.00	0.87	23.80	15.30	26.90	39.10	89.90
18	1940.6	13500.00	0.68	22.00	11.40	20.00	34.60	81.20
19	1931.3	13400.00	0.70	21.50	11.40	19.70	35.10	74.00
20	1920.6	13400.00	0.73	21.50	11.00	18.20	34.20	69.40
21	1909.8	15400.00	0.81	24.80	12.00	22.40	38.90	90.30
22	1898.2	13500.00	0.67	21.70	11.30	22.90	38.30	95.50
23	1884.0	15800.00	0.77	23.80	11.70	24.00	40.40	101.00
24	1872.6	13900.00	0.71	21.60	11.70	24.30	37.40	102.00
25	1866.3	14900.00	0.72	24.40	11.10	27.00	41.30	106.00
26	1858.4	15500.00	0.79	25.20	12.30	27.10	42.60	105.00
27	1847.5	14400.00	0.72	23.40	11.20	26.40	38.50	91.60
28	1835.7	14500.00	0.73	22.20	11.00	24.20	36.30	87.20
29	1823.5	13200.00	0.78	21.30	11.20	22.60	35.20	80.30
30	1811.2	14300.00	0.70	22.60	11.00	29.20	36.80	88.30
31	1798.0	15300.00	0.80	24.80	12.40	34.50	40.30	95.20
32	1783.7	15500.00	0.79	23.70	12.30	27.30	41.70	90.20
33	1769.0	11700.00	0.79	18.90	10.50	22.30	36.40	68.20
34	1757.0	11600.00	0.62	19.60	10.70	36.80	34.40	74.40
35	1749.9	12800.00	0.58	21.00	10.40	27.70	36.20	86.30
36	1743.0	12900.00	0.67	21.00	10.80	36.20	38.50	94.70
37-39	1734.0	13300.00	0.76	21.40	11.20	25.90	37.40	88.70
40	1725.2	13500.00	0.81	21.80	11.60	25.70	36.80	86.40

Table A8. Estimated year and metals concentrations for the sediment core from PAD M5 in the Peace-Athabasca Delta.

Depth (cm)	Year	Al (ug/g)	Be (ug/g)	Cr (ug/g)	Pb (ug/g)	Ni (ug/g)	V (ug/g)	Zn (ug/g)
0	2014.7	11200.00	0.60	16.30	9.15	16.70	30.30	67.70
1	2013.4	13600.00	0.74	19.70	11.80	21.00	37.30	75.40
2	2012.5	16600.00	0.91	24.00	13.00	25.30	44.10	88.30
3	2011.8	17300.00	0.97	24.40	14.00	29.70	45.00	90.50
4	2011.4	15400.00	0.99	23.00	14.30	30.50	41.70	91.60
5	2011	15000.00	0.94	22.30	13.50	29.60	41.70	88.90
6	2010.6	15500.00	0.93	23.10	13.90	30.20	42.60	91.40
7	2010.3	14900.00	0.99	22.30	13.90	29.50	40.80	91.30
8	2009.9	16700.00	0.94	24.70	14.20	29.60	45.00	95.50
9	2009.4	17600.00	1.02	25.30	14.00	29.50	46.90	93.30
10	2008.9	16300.00	0.99	23.70	13.70	29.20	43.50	89.70
11	2008.5	15800.00	1.01	23.20	13.50	29.70	44.40	91.30
12	2008.1	15600.00	0.95	22.80	14.10	29.00	43.40	90.30
13	2007.6	14600.00	0.91	21.50	13.20	27.80	39.90	85.40
14	2007.3	14500.00	0.91	21.50	13.30	27.80	40.10	85.70
15	2006.9	16400.00	0.93	23.90	13.30	29.50	43.90	90.40
16	2006.7	16600.00	1.01	24.40	13.70	28.90	45.90	89.60
17	2006.3	16000.00	0.97	23.80	13.50	28.90	44.40	89.60
18	2005.6	16600.00	0.95	24.10	13.30	28.30	44.80	87.10
19	2004.8	15500.00	0.95	22.90	13.50	29.30	44.30	87.30
20	2003.9	14700.00	0.98	21.50	13.90	29.40	43.00	88.70
21	2002.9	16000.00	0.95	23.20	14.00	28.70	42.70	87.20
22	2002.1	17500.00	0.96	24.80	13.10	28.90	45.10	86.30
23	2001.2	17300.00	1.00	25.40	13.80	29.20	47.30	88.00
24	2000.2	17100.00	0.99	24.50	13.60	28.80	44.90	86.60
25	1999	17800.00	0.98	26.00	13.60	28.30	47.40	86.20
26	1997.1	17700.00	1.00	25.00	13.60	27.90	44.50	85.60
27	1995.5	17400.00	0.98	25.70	13.40	29.20	45.00	89.90
28	1995.1	18000.00	1.00	25.60	13.10	29.00	44.40	90.10
29	1995	17400.00	0.99	25.20	13.60	29.10	44.00	87.60
30	1994.5	17000.00	1.01	25.70	14.10	27.90	44.90	88.00
31	1993.7	17400.00	0.98	25.00	14.20	28.10	44.30	84.90
32	1992.9	18900.00	1.04	26.10	14.50	30.80	46.30	89.60
33	1991.9	13700.00	0.83	23.20	13.20	31.30	37.60	90.80
34	1990.6	16800.00	0.90	27.40	14.40	32.60	45.40	96.80
35	1989	14600.00	0.81	23.80	12.70	28.20	38.90	82.30
36	1986.9	14400.00	0.76	24.00	12.50	30.10	38.80	89.40
37	1984.2	13200.00	0.79	22.10	12.60	28.80	35.60	85.80
38	1981.7	14000.00	0.80	22.50	12.30	28.20	36.20	85.60
39	1979.8	15100.00	0.81	24.70	13.60	31.50	39.50	94.90
40	1977.8	13200.00	0.77	21.90	11.10	27.20	36.60	79.00
41	1975.7	11400.00	0.65	20.20	10.20	25.70	32.70	73.80
42	1973.6	12500.00	0.69	21.10	10.90	26.80	35.40	77.00
43	1971.5	12300.00	0.70	20.90	11.30	26.20	34.10	80.50
44	1969.4	13700.00	0.76	22.70	12.00	27.90	36.80	86.60
45	1967.4	12800.00	0.71	21.30	11.90	26.90	34.20	82.80

46	1965.2	13800.00	0.71	22.20	11.30	27.60	36.70	81.10
47	1963.1	15600.00	0.77	25.40	12.20	29.30	42.60	87.40
48	1961	16200.00	0.77	26.10	12.90	29.00	43.20	91.90
49	1959	17400.00	0.87	27.70	13.30	30.80	45.90	96.00
50	1956.9	16200.00	0.85	25.90	13.80	29.20	42.30	96.30
51	1954.8	13100.00	0.72	22.10	11.20	24.60	36.00	79.40
52	1952.7	14900.00	0.80	24.10	11.60	26.50	38.60	84.70
53	1950.7	14700.00	0.83	23.90	11.70	27.40	38.80	83.40
54	1948.9	14200.00	0.86	23.50	12.30	26.30	37.60	81.60
55	1947	14300.00	0.84	23.40	11.80	27.60	37.80	86.10
56	1945.1	14200.00	0.80	22.70	11.30	27.00	37.50	80.90
57	1943.2	15300.00	0.86	25.30	11.70	27.60	30.30	88.00

Table A9. Estimated year and metals concentrations for the sediment core from PAD 71 in the Peace-Athabasca Delta.

Depth (cm)	Year	Al (ug/g)	Be (ug/g)	Cr (ug/g)	Pb (ug/g)	Ni (ug/g)	V (ug/g)	Zn (ug/g)
0	2015.0	6750.00	0.43	10.60	7.25	14.90	17.80	47.00
1	2007.6	7130.00	0.44	11.30	7.29	15.50	18.90	49.30
2	1997.4	8050.00	0.48	12.40	7.89	16.70	21.00	53.30
3	1986.8	8390.00	0.53	13.70	8.57	18.20	23.30	56.80
4	1976.1	10100.0	0.59	16.40	9.39	20.00	27.50	63.10
5	1963.9	9640.00	0.53	15.80	8.88	19.60	26.50	61.30
6	1946.2	9600.00	0.55	15.80	8.52	19.50	25.70	61.10
7	1922.6	9740.00	0.60	16.50	9.26	21.90	27.10	64.80
8	1898.0	9230.00	0.56	15.60	8.83	20.70	25.70	62.70
9	1874.0	10700.0	0.63	17.60	10.40	24.30	29.50	71.60
10	1848.8	9200.00	0.56	16.00	8.42	21.80	25.80	63.90
11	1822.4	9720.00	0.57	16.60	9.22	21.90	28.10	64.90
12	1796.5	9960.00	0.60	16.70	9.05	21.40	28.70	65.10
13	1766.0	9420.00	0.54	15.70	8.07	19.80	26.10	58.50
14	1732.9	9470.00	0.56	16.20	8.73	20.70	26.20	62.50
15	1699.9	9460.00	0.58	16.30	8.92	20.40	25.80	63.60
16	1666.9	10400.0	0.56	16.90	8.73	21.00	27.30	63.40
17	1635.5	10200.0	0.59	17.10	8.73	20.40	27.10	62.80
18	1602.9	6750.00	0.41	12.80	5.83	15.90	20.90	46.70
19	1566.7	7990.00	0.47	14.00	6.44	17.00	23.10	49.50
20	1529.3	7080.00	0.43	13.40	6.32	16.10	22.70	45.80
21	1492.5	6750.00	0.40	12.30	5.77	16.30	19.20	45.70
22	1455.8	7660.00	0.44	13.60	6.05	18.20	22.70	50.90
23	1419.0	6860.00	0.43	13.40	6.28	17.10	21.30	49.40
24	1381.4	7650.00	0.46	13.90	6.25	17.60	23.50	50.20
25	1345.4	7320.00	0.45	13.80	5.92	17.20	22.90	49.70
26	1310.7	7740.00	0.46	14.00	6.15	17.60	24.20	52.60
27	1273.4	7620.00	0.46	13.70	6.50	18.00	23.20	53.70
28	1236.3	7370.00	0.43	13.50	6.30	17.40	22.90	50.40
29	1201.5	7100.00	0.40	12.60	5.69	17.10	20.60	48.70
30	1163.7	7170.00	0.41	13.20	5.72	16.20	20.60	47.50
31	1124.9	7200.00	0.43	13.40	6.23	16.80	21.50	49.80
32	1089.0	7940.00	0.46	14.00	6.51	17.60	23.40	52.40
33	1055.3	7830.00	0.45	13.70	6.06	16.90	22.30	49.40
34	1017.2	7700.00	0.47	14.70	6.71	17.70	23.30	56.90
35	977.6	7820.00	0.46	14.40	6.91	19.30	23.20	55.40

Appendix B: Peace-Athabasca Delta pre-1920 baseline concentrations used develop linear regressions between the metal of interest and geochemical normalizer (Al) for Chapter 4.

Table B1. Athabasca Delta pre-1920 baseline concentrations

Location	Depth (cm)	Year	Al (ug/g)	Be (ug/g)	Cd (ug/g)	Cr (ug/g)	Cu (ug/g)	Pb (ug/g)	Ni (ug/g)	V (ug/g)	Zn (ug/g)
PAD 31	26	1918.40	12400	0.72	0.345	19.0	26.8	11.2	23.5	33.7	62.6
PAD 31	27	1908.70	13500	0.79	0.338	21.7	22.8	11.9	25.7	38.8	67.1
PAD 31	28	1899.60	12400	0.76	0.330	19.8	26.1	11.1	24.5	36.7	65.2
PAD 31	29	1886.00	14000	0.81	0.408	21.8	23.6	11.7	27.2	39.5	70.6
PAD 31	30	1870.50	12300	0.79	0.370	19.9	26.4	11.4	27.2	34.6	81.5
PAD 31	31	1856.80	12900	0.75	0.404	20.6	24.0	11.2	28.4	36.2	82.3
PAD 31	32	1844.30	13100	0.73	0.364	20.6	24.5	11.3	27.2	36.6	80.5
PAD 31	33	1831.00	13500	0.75	0.321	21.1	24.0	11.4	29.2	37.0	89.8
PAD 31	34	1816.90	14400	0.84	0.389	21.8	24.6	11.8	29.2	36.9	95.8
PAD 30	24	1919.72	11900	0.63	0.381	20.0	24.1	11.1	19.4	32.5	76.3
PAD 30	25	1911.91	12000	0.63	0.352	19.0	22.9	10.4	18.4	31.8	70.8
PAD 30	26	1904.91	10700	0.60	0.434	18.0	24.4	10.8	18.8	30.9	73.5
PAD 30	27	1896.22	12400	0.67	0.361	20.5	25.2	12.3	18.8	35.1	75.3
PAD 30	28	1883.61	13100	0.66	0.256	21.2	19.5	12.3	16.8	33.8	73.0
PAD 30	29	1869.79	13800	0.65	0.271	22.5	21.6	12.8	17.0	36.6	74.4
PAD 30	30	1858.09	14500	0.72	0.270	23.8	23.4	12.8	17.9	39.2	78.1
PAD 30	31	1845.80	15200	0.79	0.304	24.3	25.2	13.7	18.8	41.5	76.6
PAD 30	32	1834.32	12300	0.76	0.401	21.1	28.0	13.9	20.6	37.2	78.6
PAD 30	33	1824.65	12900	0.75	0.459	21.3	27.2	12.0	21.7	37.6	84.4
PAD 30	34	1814.00	13100	0.67	0.325	21.8	24.4	12.2	18.7	35.6	73.9
PAD 30	35	1800.52	15700	0.80	0.261	24.9	24.9	14.0	18.9	40.7	73.9
PAD 30	36	1787.63	16600	0.79	0.312	26.3	28.3	14.9	19.5	43.0	88.6
PAD 30	37	1774.89	16400	0.78	0.267	26.1	25.5	14.7	19.1	42.8	83.1
PAD 30	38	1760.35	14300	0.75	0.320	22.7	25.8	14.6	18.3	35.8	85.7
PAD 30	39	1748.05	13500	0.83	0.449	23.0	30.4	14.1	23.2	41.6	86.6
PAD 30	40	1738.76	13100	0.90	0.596	21.3	33.2	13.1	26.5	40.6	94.6

PAD 30	41	1730.90	12200	0.81	0.787	20.5	31.6	11.7	29.1	37.3	94.0
PAD 30	42	1721.64	13800	0.79	0.534	22.2	26.1	11.2	23.8	36.8	86.8
PAD 30	43	1710.38	14100	0.80	0.569	22.1	26.3	12.4	22.0	38.0	86.0
PAD 30	44	1698.62	14500	0.84	0.509	22.9	26.2	12.3	21.2	38.8	90.7
PAD 32	18	1915.50	12100	0.76	0.331	20.0	24.2	12.7	26.8	33.8	83.1
PAD 32	19	1904.70	12100	0.72	0.342	22.3	24.4	12.6	27.9	35.7	83.5
PAD 32	20	1893.80	11900	0.70	0.326	20.7	24.2	12.4	27.5	34.9	83.5
PAD 32	21	1882.80	11600	0.70	0.337	19.9	23.4	12.4	26.7	33.4	81.3
PAD 32	22	1872.30	11900	0.74	0.334	20.2	24.3	12.5	27.9	34.6	83.3
PAD 32	23	1862.60	11500	0.66	0.326	19.8	24.1	11.6	27.5	34.6	82.3
PAD 32	24	1853.30	15900	0.86	0.358	25.3	26.1	12.4	29.9	44.5	89.6
PAD 32	25	1845.20	14800	0.86	0.354	24.2	26.8	12.6	31.0	42.6	91.8
PAD 32	26	1837.20	13800	0.80	0.311	22.2	23.5	11.6	27.1	38.7	81.8
PAD 32	27	1827.80	14800	0.85	0.345	24.1	24.4	12.1	28.1	42.1	85.2
PAD 32	28	1817.90	16100	0.87	0.345	25.5	25.2	12.8	29.3	44.8	86.7
PAD 32	29	1808.50	14100	0.80	0.315	23.1	23.7	11.7	27.3	40.3	81.5
PAD 32	30	1798.90	14000	0.82	0.325	22.4	24.0	11.4	28.2	40.2	83.2
PAD 32	31	1790.10	14200	0.79	0.319	22.7	23.6	11.4	28.0	40.0	80.5
PAD 32	32	1782.00	13300	0.80	0.305	22.1	23.0	11.6	26.9	38.9	79.4
PAD 32	33	1773.30	16100	0.88	0.345	26.3	25.9	12.1	29.9	45.6	90.0
PAD 32	34	1764.50	14900	0.82	0.324	23.9	23.9	11.6	28.0	41.7	82.6
PAD 32	35	1756.20	18000	0.97	0.366	28.2	27.9	13.2	32.7	49.5	98.5
PAD 32	36	1747.40	15800	0.85	0.355	25.2	25.7	12.2	29.6	44.4	88.8
PAD 32	37	1737.90	14600	0.83	0.341	24.3	24.9	11.9	29.3	41.9	86.2
PAD 32	38	1727.60	11900	0.74	0.339	20.5	23.7	11.7	27.7	35.2	82.3
PAD 32	39	1715.70	14800	0.87	0.317	23.0	22.0	12.0	26.2	41.0	79.4
PAD 32	40	1702.60	12400	0.80	0.327	20.0	22.0	11.9	25.8	34.7	78.6
PAD 32	41	1690.50	12000	0.78	0.325	19.8	22.5	12.2	25.5	34.3	78.1
PAD 32	42	1678.90	14300	0.85	0.328	21.9	22.1	12.0	25.6	38.9	78.6
PAD 32	43	1666.40	13800	0.82	0.321	21.4	22.2	12.1	25.9	37.2	78.9

PAD 32	44	1653.70	13800	0.81	0.326	21.7	23.0	12.4	26.7	37.5	79.9
PAD 32	45	1640.40	12700	0.73	0.315	19.8	22.2	12.0	25.5	34.9	77.2
PAD 26	28	1916.80	17900	1.00	0.414	27.4	26.1	13.9	34.2	47.2	93.2
PAD 26	29	1912.20	18900	0.96	0.400	27.4	26.1	13.7	29.9	46.9	91.7
PAD 26	30	1907.80	21000	1.08	0.377	30.8	26.6	14.5	34.2	54.2	96.5
PAD 26	31	1903.80	20700	1.11	0.467	30.7	25.9	14.5	31.2	54.8	97.6
PAD 26	32	1899.60	22900	1.16	0.453	33.4	28.8	14.4	31.2	61.8	104.0
PAD 26	33	1895.40	21700	1.12	0.491	30.5	26.9	14.7	37.3	54.5	111.0
PAD 26	34	1890.80	17700	0.96	0.440	26.4	25.8	13.8	29.1	46.3	87.1
M7	31	1913.80	16900	0.90	0.304	27.8	25.9	13.9	32.2	48.1	94.3
M7	32	1908.60	15500	0.86	0.287	25.8	24.1	14.3	30.8	43.3	90.0
M7	33	1903.20	16300	0.95	0.338	26.5	25.1	14.1	29.2	45.1	92.2
M7	34	1897.60	15700	0.78	0.337	24.2	24.6	13.0	29.3	43.4	84.4
M2	21	1909.80	15400	0.81	0.342	24.8	24.9	12.0	22.4	38.9	90.3
M2	22	1898.20	13500	0.67	0.406	21.7	24.9	11.3	22.9	38.3	95.5
M2	23	1884.00	15800	0.77	0.412	23.8	25.7	11.7	24.0	40.4	101.0
M2	24	1872.60	13900	0.71	0.424	21.6	25.0	11.7	24.3	37.4	102.0
M2	25	1866.30	14900	0.72	0.391	24.4	24.7	11.1	27.0	41.3	106.0
M2	26	1858.40	15500	0.79	0.414	25.2	26.1	12.3	27.1	42.6	105.0
M2	27	1847.50	14400	0.72	0.384	23.4	23.6	11.2	26.4	38.5	91.6
M2	28	1835.70	14500	0.73	0.406	22.2	23.3	11.0	24.2	36.3	87.2
M2	29	1823.50	13200	0.78	0.349	21.3	21.0	11.2	22.6	35.2	80.3
M2	30	1811.20	14300	0.70	0.383	22.6	22.5	11.0	29.2	36.8	88.3
M2	31	1798.00	15300	0.80	0.4	24.8	24.9	12.4	34.5	40.3	95.2
M2	32	1783.70	15500	0.79	0.43	23.7	26.1	12.3	27.3	41.7	90.2
M2	33	1769.00	11700	0.79	0.451	18.9	27.1	10.5	22.3	36.4	68.2
M2	34	1757.00	11600	0.62	0.393	19.6	24.2	10.7	36.8	34.4	74.4
M2	35	1749.90	12800	0.58	0.371	21.0	23.8	10.4	27.7	36.2	86.3
M2	36	1743.00	12900	0.67	0.477	21.0	27.9	10.8	36.2	38.5	94.7
M2	37-39	1734.00	13300	0.76	0.451	21.4	25.0	11.2	25.9	37.4	88.7
M2	40	1725.20	13500	0.81	0.4	21.8	24.0	11.6	25.7	36.8	86.4
PAD 71	8	1898.00	9230	0.56	0.318	15.6	17.1	8.8	20.7	25.7	62.7
PAD 71	9	1874.00	10700	0.63	0.367	17.6	20.5	10.4	24.3	29.5	71.6
PAD 71	10	1848.80	9200	0.56	0.285	16.0	15.6	8.4	21.8	25.8	63.9
PAD 71	11	1822.40	9720	0.57	0.299	16.6	16.6	9.2	21.9	28.1	64.9
PAD 71	12	1796.50	9960	0.60	0.308	16.7	16.3	9.1	21.4	28.7	65.1
PAD 71	13	1766.00	9420	0.54	0.235	15.7	13.5	8.1	19.8	26.1	58.5
PAD 71	14	1732.90	9470	0.56	0.244	16.2	13.8	8.7	20.7	26.2	62.5
PAD 71	15	1699.90	9460	0.58	0.252	16.3	14.6	8.9	20.4	25.8	63.6
PAD 71	16	1666.90	10400	0.56	0.244	16.9	14.1	8.7	21.0	27.3	63.4

PAD 71	17	1635.50	10200	0.59	0.239	17.1	13.6	8.7	20.4	27.1	62.8
PAD 71	18	1602.90	6750	0.41	0.162	12.8	7.7	5.8	15.9	20.9	46.7
PAD 71	19	1566.70	7990	0.47	0.178	14.0	9.2	6.4	17.0	23.1	49.5
PAD 71	20	1529.30	7080	0.43	0.218	13.4	8.7	6.3	16.1	22.7	45.8
PAD 71	21	1492.50	6750	0.40	0.164	12.3	8.1	5.8	16.3	19.2	45.7
PAD 71	22	1455.80	7660	0.44	0.207	13.6	9.9	6.1	18.2	22.7	50.9
PAD 71	23	1419.00	6860	0.43	0.197	13.4	9.8	6.3	17.1	21.3	49.4
PAD 71	24	1381.40	7650	0.46	0.221	13.9	10.4	6.3	17.6	23.5	50.2
PAD 71	25	1345.40	7320	0.45	0.222	13.8	9.8	5.9	17.2	22.9	49.7
PAD 71	26	1310.70	7740	0.46	0.261	14.0	10.4	6.2	17.6	24.2	52.6
PAD 71	27	1273.40	7620	0.46	0.286	13.7	10.7	6.5	18.0	23.2	53.7
PAD 71	28	1236.30	7370	0.43	0.231	13.5	10.5	6.3	17.4	22.9	50.4
PAD 71	29	1201.50	7100	0.40	0.203	12.6	9.0	5.7	17.1	20.6	48.7
PAD 71	30	1163.70	7170	0.41	0.170	13.2	9.0	5.7	16.2	20.6	47.5
PAD 71	31	1124.90	7200	0.43	0.218	13.4	9.8	6.2	16.8	21.5	49.8
PAD 71	32	1089.00	7940	0.46	0.220	14.0	10.3	6.5	17.6	23.4	52.4
PAD 71	33	1055.30	7830	0.45	0.185	13.7	9.5	6.1	16.9	22.3	49.4
PAD 71	34	1017.20	7700	0.47	0.257	14.7	11.1	6.7	17.7	23.3	56.9
PAD 71	35	977.60	7820	0.46	0.262	14.4	11.9	6.9	19.3	23.2	55.4
ALV1 -1.025	**Athabasca Levee 1**		3820	0.23	0.089	7.9	3.7	4.1	9.1	13.9	24.0
ALV1 -1.05	Lat	Long	5070	0.32	0.125	9.6	5.6	4.9	11.7	17.8	31.8
ALV1 -1.26	58.396	-111.525	2770	0.22	0.087	5.8	2.7	4.1	8.7	11.2	21.7
ALV1 -1.36			3660	0.27	0.124	7.3	4.0	4.5	10.0	13.6	26.6
ALV1 -1.59			3410	0.26	0.112	7.9	4.2	4.2	9.9	13.0	27.0
ALV1 -1.87			6780	0.43	0.180	13.0	9.8	6.5	15.2	22.9	40.3
ALV1 -1.97			3030	0.19	0.067	6.6	2.5	3.5	7.7	11.7	19.9
ALV1 -2.09			9180	0.56	0.227	16.2	14.1	8.2	19.1	28.5	49.9
ALV1 -2.17			5920	0.39	0.171	11.5	8.7	6.1	14.2	20.5	36.8
ALV1 -2.275			4930	0.35	0.142	9.7	6.6	5.4	12.7	17.6	34.0

ALV1-2.20			3760	0.27	0.116	7.6	4.8	4.5	10.4	13.8	27.5
ALV1-2.53			4200	0.28	0.124	8.3	4.7	4.7	10.7	15.6	28.4
ALV1-2.60			4830	0.31	0.135	9.7	5.7	5.0	12.3	17.4	31.5
ALV2-1.26	**Athabasca Levee 2**		12100	0.88	0.119	21.1	20.9	13.4	25.6	39.8	52.2
ALV2-1.39	Lat	Long	13800	0.95	0.241	23.7	27.2	14.0	39.4	46.0	64.7
ALV2-1.50	58.385	-111.517	8010	0.53	0.099	14.4	12.2	8.3	19.9	25.5	42.4
ALV2-1.64			2270	0.17	0.027	4.7	2.3	2.8	5.3	8.8	15.6
ALV2-1.70			809	<0.10	<0.020	1.7	0.8	1.2	2.2	3.1	5.5
ALV2-1.85			1830	0.12	0.023	4.1	1.8	2.1	4.3	7.4	11.8
ALV2-1.94			1060	<0.10	0.022	2.6	1.1	1.4	3.3	4.6	6.5
ALV2-2.15			827	<0.10	<0.020	1.8	1.1	1.1	2.6	3.1	5.0
ALV2-2.20			17000	0.90	0.163	27.0	27.5	15.4	32.3	45.2	71.5
ALV2-2.25			17100	0.94	0.191	27.6	29.9	15.4	37.0	44.0	78.5
ALV2-2.30			18200	1.01	0.218	28.5	33.2	17.6	38.8	44.4	87.4
ALV2-2.38			20300	1.00	0.242	30.9	32.3	17.6	38.0	52.6	85.7
ALV2-2.46			11700	0.68	0.129	19.2	17.4	9.9	23.2	34.6	52.4
ALV2-2.52			737	<0.10	0.071	1.2	1.1	0.8	4.6	2.6	3.6
ALV2-2.63			463	<0.10	<0.020	1.3	0.5	0.7	1.3	2.4	2.7
ALV2-2.70			720	<0.10	0.021	1.3	0.8	0.8	2.5	2.9	3.5
ALV2-2.80BT			1570	0.32	0.173	7.3	6.9	6.0	15.9	36.1	19.0
ALV2-2.85			852	0.10	0.037	3.5	1.7	1.5	3.2	7.7	6.3
ALV2-2.90			662	<0.10	<0.020	1.2	<0.50	0.7	1.5	2.9	3.4
ALV2-3.10			622	<0.10	<0.020	2.0	<0.50	0.9	1.4	3.1	3.7
ALV2-3.25			620	<0.10	<0.020	1.6	<0.50	0.9	1.2	2.8	3.3
ALV2-3.35			695	<0.10	<0.020	1.5	0.5	0.9	1.4	2.6	3.9
ALV2-3.60			647	<0.10	<0.020	1.4	0.8	0.9	2.1	2.5	5.0

Table B2. Peace Delta pre-1920 baseline concentrations

Location	Depth (cm)	Year	Al (ug/g)	Be (ug/g)	Cd (ug/g)	Cr (ug/g)	Cu (ug/g)	Pb (ug/g)	Ni (ug/g)	V (ug/g)	Zn (ug/g)
PAD 65	27	1915.42	13000	0.78	0.624	23.1	30.1	14.0	35.9	40.8	108.0
PAD 65	28	1909.28	12100	0.77	0.596	22.0	29.3	13.8	34.1	39.4	105.0
PAD 65	29	1903.01	11500	0.67	0.584	20.1	27.3	12.8	32.5	35.3	99.9
PAD 65	30	1897.06	10900	0.66	0.533	18.7	26.4	11.7	30.7	33.8	95.2
PAD 65	31	1890.80	11200	0.65	0.528	18.7	25.9	11.7	30.0	34.6	92.7
PAD 65	32	1884.82	10000	0.64	0.548	18.0	24.8	11.0	28.5	33.2	90.3
PAD 65	33	1879.27	10800	0.68	0.676	18.2	25.3	11.2	29.3	33.8	92.8
PAD 65	34	1873.32	10400	0.6	0.536	19.2	25.3	11.0	29.6	35.6	91.8
PAD 65	35	1867.04	10700	0.62	0.571	19.4	25.9	11.5	31.0	36.0	93.6
PAD 65	36	1860.16	10500	0.58	0.566	18.9	25.1	13.3	29.9	35.8	91.3
PAD 65	37	1852.51	10400	0.57	0.498	18.4	24.6	11.0	29.8	34.4	89.0
PAD 65	38	1845.27	9360	0.58	0.526	17.8	24.9	11.1	29.6	33.5	90.3
PAD 65	39	1838.28	10100	0.62	0.524	18.3	25.6	11.4	30.6	34.3	91.2
PAD 65	40	1830.77	11400	0.62	0.511	19.4	25.3	11.5	30.2	36.6	90.7
PAD 65	41	1823.22	11400	0.65	0.527	19.6	25.4	11.5	30.7	37.4	92.6
PAD 65	42	1816.00	11100	0.62	0.517	19.7	25.1	11.2	30.6	37.5	91.8
PAD 65	43	1808.43	11500	0.68	0.568	20.8	26.4	11.3	31.8	38.6	95.5
PAD 65	44	1800.25	10800	0.64	0.553	19.1	26.2	11.4	31.1	33.6	95.0
PAD 65	45	1791.98	10400	0.66	0.473	17.9	23.4	12.2	27.2	32.6	84.8
PAD 65	46	1784.12	9890	0.58	0.458	17.7	22.6	10.1	26.3	32.8	81.7
PAD 65	47	1776.58	12100	0.66	0.581	22.2	28.2	12.2	32.7	40.8	102.0
PAD 65	48	1768.60	12300	0.61	0.563	22.1	27.6	11.7	32.2	40.3	98.7
PAD 65	49	1759.98	10400	0.65	0.526	19.1	24.5	11.5	28.7	34.9	88.3
PAD 65	50	1751.74	11500	0.75	0.525	20.1	25.5	13.1	29.7	36.1	92.1
PAD 65	51	1743.32	10200	0.95	0.475	18.4	23.5	18.0	27.3	34.3	83.2

PAD 65	52	1734.55	11600	0.64	0.544	21.4	27.0	11.9	31.5	39.3	96.0
PAD 65	53	1726.16	12800	0.74	0.561	22.5	28.8	11.9	33.2	41.6	103.0
PAD 67	20	1916.60	15400	0.87	0.593	26.6	32.0	13.7	39.5	49.2	126.0
PAD 67	21	1908.11	20300	1.16	0.809	34.6	40.9	17.6	50.8	65.6	163.0
PAD 67	22	1899.89	16300	1.03	0.782	28.7	36.0	16.6	46.1	54.2	147.0
PAD 67	23	1892.12	16500	0.99	0.817	29.4	36.4	16.3	47.1	56.3	150.0
PAD 67	24	1884.61	16300	0.98	0.807	28.7	32.7	15.3	42.4	57.8	137.0
PAD 67	25	1878.07	15200	0.96	0.772	27.8	33.6	14.8	49.9	56.8	141.0
PAD 67	26	1872.60	11200	0.75	0.55	19.7	24.7	11.2	35.2	40.1	102.0
PAD 67	27	1867.36	10800	0.71	0.497	19.5	23.5	10.8	34.8	39.5	96.5
PAD 67	28	1862.94	10100	0.66	0.485	18.5	22.9	10.4	31.8	37.6	92.4
PAD 67	29	1856.68	10300	0.7	0.51	18.3	23.3	10.4	31.3	35.5	93.5
PAD 67	30	1848.42	13500	0.8	0.607	24.0	28.1	12.8	39.2	46.9	113.0
PAD 67	31	1840.62	11800	0.74	0.529	20.1	26.5	11.3	34.0	40.9	95.9
PAD 67	32	1832.18	16500	0.95	0.699	29.2	33.9	14.7	43.8	55.8	128.0
PAD 67	33	1821.18	16400	0.93	0.721	28.9	33.0	14.7	42.9	55.5	124.0
PAD 67	34	1809.86	15300	0.9	0.72	27.5	32.6	15.3	43.2	52.8	126.0
PAD 67	35	1800.38	16400	0.92	0.671	29.2	34.4	14.6	44.9	54.6	130.0
PAD 67	36	1791.08	18700	1.07	0.713	32.5	38.3	16.4	47.7	61.3	145.0
PAD 67	37	1780.96	16000	0.96	0.628	27.9	33.9	15.7	39.4	50.5	126.0
PAD 67	38	1769.77	16100	0.91	0.719	28.0	33.9	14.9	42.7	53.3	136.0
PAD 67	39	1758.28	12300	0.74	0.607	22.1	26.6	12.3	32.2	41.4	104.0
PAD 67	40	1744.92	13600	0.77	0.648	24.2	28.9	13.3	34.5	46.5	110.0
PAD 67	41	1728.88	14900	0.85	0.733	27.0	32.0	15.0	38.9	50.9	120.0
PAD 67	42	1713.89	15600	0.93	0.755	27.9	34.6	15.6	42.3	52.9	134.0
PAD 67	43	1700.50	15500	0.9	0.724	27.8	33.8	15.5	39.4	51.4	127.0
PAD 67	44	1686.34	18400	1	0.799	30.6	35.6	16.4	41.2	56.4	138.0

PAD 67	45	1671.27	17400	0.95	0.714	28.8	33.2	15.6	39.5	53.5	127.0
PAD 67	46	1655.18	18900	1.04	0.82	33.3	37.3	17.8	45.0	60.1	145.0
PAD 67	47	1638.98	15900	0.94	0.683	27.8	32.1	15.7	38.5	50.9	124.0
PAD 67	48	1623.60	19900	1.08	0.796	33.2	38.8	17.2	46.3	61.1	149.0
PAD 67	49	1608.83	20400	1.13	0.835	35.3	40.6	18.8	50.1	65.6	156.0
PAD 67	50	1594.70	19600	1.15	0.81	34.3	39.6	18.1	47.0	63.2	152.0
PAD 67	51	1577.39	16300	0.9	0.759	27.8	34.6	16.1	40.6	49.6	131.0
PAD 67	52	1561.34	16500	0.91	0.705	29.2	33.8	15.9	39.1	53.2	125.0
PAD 67	53	1548.52	15100	0.9	0.706	27.4	33.2	15.1	40.9	52.8	122.0
PAD 67	54	1535.64	13900	0.77	0.619	24.9	29.6	13.2	35.7	46.8	109.0
PAD 67	55	1522.82	11700	0.71	0.549	21.6	26.0	12.3	31.7	40.4	97.3
PAD 52	21	1914.94	12900	0.69	0.529	23.4	27.2	13.6	32.2	45.0	99.6
PAD 52	22	1906.27	15900	0.78	0.644	29.0	33.9	16.2	39.3	54.6	122.0
PAD 52	23	1899.36	14800	0.81	0.667	28.0	35.1	17.4	40.6	50.8	129.0
PAD 52	24	1886.78	14100	0.76	0.624	26.1	30.9	15.5	35.6	46.7	113.0
PAD 52	25	1876.36	14300	0.76	0.610	26.1	31.2	15.3	36.8	48.5	112.0
PAD 52	26	1866.22	15400	0.78	0.611	27.9	30.9	15.0	37.3	52.8	115.0
PAD 52	27	1855.04	17000	0.88	0.649	29.8	33.7	16.4	39.4	56.0	127.0
PAD 52	28	1844.90	12900	0.67	0.530	23.4	27.1	13.2	32.5	42.6	104.0
PAD 52	29	1831.92	15000	0.74	0.577	27.0	29.6	14.0	34.7	49.3	113.0
PAD 52	30	1820.61	16300	0.83	0.630	28.7	30.4	15.1	36.8	53.4	122.0
PAD 52	31	1811.29	15200	0.78	0.611	27.4	30.5	14.9	36.8	50.4	119.0
PAD 52	32	1802.88	17200	0.90	0.642	30.6	34.6	16.7	40.3	57.0	130.0
PAD 52	33	1793.66	16400	0.85	0.691	29.0	32.6	16.0	38.6	52.8	131.0
PAD 52	34	1783.41	13800	0.73	0.583	24.6	28.0	13.8	33.4	44.8	110.0
PAD 52	35	1772.55	14100	0.75	0.595	25.1	28.3	14.4	33.2	45.5	115.0
PAD 52	36	1766.40	16300	0.84	0.550	28.7	31.0	15.9	35.2	52.0	123.0

PLV1-1.20	**Peace Levee 1**		5920	0.28	0.182	15.7	7.8	5.7	18.5	30.4	45.4
PLV1-1.96	Lat	Long	8160	0.30	0.136	17.0	4.9	6.5	11.0	34.2	65.4
PLV1-2.10	58.923	-111.619	6170	0.29	0.113	18.4	7.1	6.0	19.8	35.4	40.2
PLV1-2.30			5210	0.25	0.226	15.6	8.6	5.5	25.5	29.8	42.5
PLV1-2.65			5130	0.23	0.209	14.3	8.6	5.5	21.0	26.5	46.0
PLV1-2.72			8410	0.41	0.150	18.4	12.0	7.7	18.3	30.0	42.3
PLV2-1.70	**Peace Levee 2**		7960	0.43	0.514	17.6	19.1	9.1	25.4	30.1	70.1
PLV2-2M	Lat	Long	5480	0.28	0.279	14.1	9.4	5.8	17.8	25.0	45.5
PLV2-2.40	58.936	-111.638	11000	0.55	0.695	23.2	27.5	12.3	33.3	37.2	92.1
PLV2-2.44			10400	0.55	0.621	21.7	24.8	11.0	30.7	35.5	93.6
PLV2-2.60			9880	0.48	0.611	20.4	24.3	10.9	29.4	32.5	90.0
PLV2-2.74			5490	0.28	0.266	15.4	10.1	5.5	17.1	24.7	47.6
PLV3-3.15	**Peace Levee 3**		4740	0.20	0.351	12.2	6.1	5.2	17.9	23.2	40.8
PLV3-2.85	Lat	Long	4680	0.20	0.294	12.9	7.4	4.9	17.1	22.9	41.5
PLV3-2.40	58.950	-111.707	9100	0.44	0.440	19.6	20.5	9.5	26.0	30.7	76.7
PLV3-1.96			9150	0.40	0.512	18.5	19.0	8.4	26.7	28.6	71.8

Appendix C:

This Appendix provides tables with lake and sediment core information and base data for THg concentrations presented in Chapter 3. Figures provide activity profiles of radioisotopes used in ^{210}Pb and ^{137}Cs dating of cores from all lakes and PAD 30 THg and Zn enrichment factor temporal trends.

Table C1. Lake and sediment core information for floodplain lakes in the AOSR and PAD and upland lakes in the PAD (and vicinity) in northeastern Alberta.

Lake ID	Hydrological Setting	Coordinates (decimal degrees)	Distance from AR6 (km)	Lake Depth* (m)	Core Length (cm)
Down 1	Floodplain	57.025, - 111.485	1	0.6	54
Down 26	Floodplain	57.218, -111.604	26	0.5	42
Down 58	Floodplain	57.524, -111.523	58	1.3	45
PAD 23	Floodplain	58.389, -111.440	~170	1.3	43
PAD 30	Floodplain	58.509, -111.517	~170	0.8	45
PAD 31	Floodplain	58.494, -111.518	~170	0.9	36
PAD 32	Floodplain	58.496, -111.447	~170	1.0	46
M2	Floodplain	58.417, -110.914	~170	1.3	42
M5	Floodplain	58.437, -111.050	~170	0.9	58
PAD 18	Upland	58.896, -111.360	~210	8.6	49
AC5	Upland	58.441, -110.676	~165	4.2	83.5

*Corresponds to lake depth when the sediment core was extracted from the lake.

Table C2. Depth (top of interval), estimated year, organic matter content (%OM) and THg concentration for the sediment core from Down 1 in the Alberta Oil Sands Region. %OM and THg concentrations are expressed per dry weight.

Depth (cm)	Year	%OM	THg (mg/kg)
0	2010.05	52.89	0.04005
1	2007.76	53.35	0.0411
2	2003.84	52.51	0.0424
3	2001.06	50.96	0.0435
4	1995.16	49.70	0.0443
5	1990.89	47.67	0.0459
6	1987.55	48.09	0.0491
7	1984.04	46.94	0.0470
8	1980.31	47.26	0.0488
9	1976.50	47.42	0.0438
10	1972.62	44.87	0.0461
11	1968.89	44.76	0.0499
12	1965.15	43.74	0.0479
13	1961.18	42.83	0.0449
14	1956.84	42.58	0.0438
15	1952.65	41.98	0.0423
16	1949.00	40.23	0.0423
17	1944.84	38.57	0.0436
18	1940.38	37.72	0.0431
19	1935.64	36.44	0.0399
20	1930.12	34.24	0.0362
21	1923.81	34.56	0.0385
22	1917.05	34.20	0.0354
23	1910.82	33.81	0.0359
24	1905.06	31.89	0.0373
25	1899.19	31.29	0.0357
26	1893.29	30.81	0.0346
27	1887.92	31.21	0.0339
28	1882.43	32.03	0.0338
29	1875.31	34.01	0.0328
30	1867.20	35.55	0.0322
31	1859.41	35.71	0.0400
32	1851.74	35.20	0.0374
33	1844.40	33.67	0.0353
34	1837.36	32.58	0.0366
35	1830.41	31.47	0.0365
36	1823.71	31.61	0.0356
37	1817.13	32.73	0.0322
38	1810.58	34.31	0.0362
39	1803.49	34.70	0.0370

40	1796.86	34.28	0.0349
41	1790.53	37.28	0.0281
42	1783.78	37.37	0.0286
43	1777.09	37.76	0.0353

Table C3. Depth (top of interval), estimated year, organic matter content (%OM) and THg concentration for the sediment core from Down 26 in the Alberta Oil Sands Region. %OM and THg concentrations are expressed per dry weight.

Depth (cm)	Year	%OM	THg (mg/kg)
0	2017.68	41.67	0.0367
1	2017.05	34.63	0.0287
2	2016.28	27.17	0.0394
4	2012.40	16.91	0.0596
6	2007.19	16.15	0.0545
8	2000.76	11.57	0.0588
10	1994.00	11.10	0.0600
12	1986.50	11.01	0.0665
14	1976.21	9.48	0.0677
16	1963.00	6.84	0.0677
18	1948.67	7.01	0.0605
20	1936.57	7.77	0.0570
22	1926.40	9.45	0.0587
24	1916.98	11.30	0.0531
26	1908.83	13.26	0.0518
28	1898.57	11.48	0.0511
30	1885.36	7.40	0.0575
32	1870.75	7.77	0.0600
34	1858.46	8.28	0.0611
36	1846.44	7.43	0.0564
38	1834.49	9.65	0.0606
40	1823.20	11.41	0.0622

Table C4. Depth (top of interval), organic matter content (%OM) and THg concentration for the sediment core from Down 58 in the Alberta Oil Sands Region. %OM and THg concentrations are expressed per dry weight.

Depth (cm)	%OM	THg (mg/kg)
0	9.08	0.0609
1	7.75	0.0617
2	8.05	0.0626
3	6.44	0.0643
4	5.98	0.0595
5	7.10	0.0645
6	7.69	0.0546
7	9.18	0.0555
8	8.50	0.0559
9	7.22	0.0616
10	7.34	0.0561
11	8.27	0.0685
12	7.96	0.0540
13	8.17	0.0577
14	7.39	0.0592
15	5.53	0.0720
16	5.11	0.0600
17	5.89	0.0573
18	5.56	0.0537
19	6.58	0.0818
20	7.10	0.0524
21	7.87	0.0593
22	6.62	0.0536
23	6.25	0.0581
24	5.66	0.0529
25	5.71	0.0582
26	6.51	0.0710
27	6.71	0.0611
28	7.70	0.0582
29	6.73	0.0633
30	5.41	0.0938
31	4.75	0.0536
32	6.07	0.0578
33	8.04	0.0447
34	6.17	0.0600
35	6.47	0.0646
36	5.75	0.0894
37	5.66	0.0633
38	6.89	0.0624

39	6.55	0.0621
40	6.90	0.0380
41	6.87	0.0532
42	5.35	0.0955
43	5.37	0.0535
44	5.35	0.0860

Table C5. Depth (top of interval), estimated year, organic matter content (%OM) and THg concentration for the sediment core from PAD 23 in the Peace-Athabasca Delta. %OM and THg concentrations are expressed per dry weight.

Depth (cm)	Year	%OM	THg (mg/kg)
0	2010.74	59.32	0.0490
2	2007.67	58.64	0.0522
4	2005.83	56.34	0.0438
5.5	2001.33	55.69	0.0507
7	1998.28	55.15	0.0518
8.5	1993.27	52.56	0.0567
10	1990.69	49.41	0.0525
11	1988.34	49.08	0.0596
12	1986.13	47.13	0.0567
13	1983.21	45.98	0.0581
14	1981.06	47.51	0.0575
15	1978.53	46.43	0.0523
16	1974.84	44.17	0.0495
17	1972.08	44.27	0.0505
18	1968.41	40.12	0.0512
19	1965.39	41.36	0.0483
20	1962.24	41.47	0.0461
21	1957.40	39.93	0.0442
22	1953.07	38.27	0.0530
23	1948.33	37.95	0.0499
24	1944.34	33.98	0.0509
25	1939.22	36.43	0.0482
26	1933.13	39.60	0.0510
27	1927.97	33.41	0.0497
28	1923.56	29.65	0.0482
29	1917.49	28.95	0.0493
30	1911.24	31.68	0.0488
31	1906.80	31.49	0.0496
32	1903.25	28.25	0.0509

Table C6. Depth (top of interval), estimated year, organic matter content (%OM) and THg concentration for the sediment core from PAD 30 in the Peace-Athabasca Delta. %OM and THg concentrations are expressed per dry weight.

Depth (cm)	Year	%OM	THg (mg/kg)
0	2016.37	11.47	0.0745
1	2015.92	8.36	0.0738
2	2014.94	7.63	0.0755
3	2014.01	7.36	0.0741
5	2012.66	9.16	0.0632
7	2008.44	18.72	0.0792
9	2001.45	45.92	0.0969
10	1998.93	53.63	0.1007
12	1989.71	59.17	0.0708
13	1983.06	56.50	0.0987
15	1973.99	52.74	0.1041
17	1961.64	44.95	0.1023
19	1948.17	44.15	0.0802
21	1939.43	38.23	0.0743
23	1927.96	24.63	0.0567
25	1911.91	34.06	0.0672
27	1896.22	18.66	0.0598
29	1869.79	12.97	0.0636
31	1845.80	14.85	0.0650
33	1824.65	19.75	0.0601
35	1800.52	14.06	0.0640
37	1774.89	11.25	0.0647
39	1748.05	20.94	0.0607
41	1730.90	27.09	0.0559
43	1710.38	14.87	0.0588
44	1698.62	14.09	0.0600

Table C7. Depth (top of interval), estimated year, organic matter content (%OM) and THg concentration for the sediment core from PAD 31 in the Peace-Athabasca Delta. %OM and THg concentrations are expressed per dry weight.

Depth (cm)	Year	%OM	THg (mg/kg)
0	2010.29	11.84	0.0525
1	2009.85	8.27	0.0577
2	2008.67	7.95	0.0593
3	2007.29	6.54	0.0606
4	2005.87	6.87	0.0630
5	2004.44	6.25	0.0620
6	2003.17	6.26	0.0623
7	2001.89	6.43	0.0624
8	2001.03	6.14	0.0528
9	1999.98	10.53	0.0537
10	1998.50	7.80	0.0573
11	1997.07	9.64	0.0570
12	1995.49	7.34	0.0609
13	1993.90	8.22	0.0597
14	1991.30	9.46	0.0620
15	1988.88	11.44	0.0619
16	1986.70	27.15	0.0534
17	1983.54	43.36	0.0772
18	1978.67	43.10	0.0594
19	1972.88	43.17	0.0479
20	1965.50	39.39	0.0431
21	1958.08	34.25	0.0456
22	1950.74	29.82	0.0469
23	1943.30	29.21	0.0449
24	1934.70	25.36	0.0450
25	1924.40	28.10	0.0431
26	1912.36	22.91	0.0501
27	1905.04	22.93	0.0401
28	1894.12	22.39	0.0414
29	1877.85	21.91	0.0421
30	1863.15	21.78	0.0423
31	1850.50	20.77	0.0429
32	1838.01	20.35	0.0430
33	1823.92	18.38	0.0420
34	1809.85	21.19	0.0493

Table C8. Depth (top of interval), estimated year, organic matter content (%OM) and THg concentration for the sediment core from PAD 32 in the Peace-Athabasca Delta. %OM and THg concentrations are expressed per dry weight.

Depth	Year	%OM	THg
0	2014.73	38.46	0.0651
1	2012.20	30.18	0.0694
2	2007.92	29.86	0.0709
3	2002.82	23.87	0.0717
4	1998.03	22.22	0.0725
5	1993.74	18.90	0.0726
6	1989.53	16.87	0.0708
7	1985.46	14.97	0.0693
8	1982.50	15.54	0.0713
9	1979.91	17.36	0.0720
10	1974.78	14.41	0.0728
11	1967.58	15.02	0.0707
12	1960.74	12.99	0.0696
13	1954.66	14.41	0.0719
14	1948.88	16.11	0.0717
15	1942.76	16.26	0.0713
16	1934.40	13.05	0.0681
17	1924.91	13.28	0.0687
18	1915.48	12.27	0.0677
19	1904.70	13.11	0.0684
20	1893.76	11.38	0.0681
21	1882.81	11.15	0.0686
22	1872.32	15.39	0.0684
23	1862.59	14.21	0.0689
24	1853.25	17.29	0.0689
25	1845.21	18.87	0.0688
26	1837.22	20.47	0.0688
27	1827.77	15.77	0.0702
28	1817.90	16.90	0.0675
29	1808.46	16.28	0.0674
30	1798.94	17.06	0.0666
31	1790.12	18.15	0.0672
32	1781.96	23.50	0.0653
33	1773.34	20.99	0.0646
34	1764.50	15.19	0.0671
35	1756.23	24.04	0.0663
36	1747.39	16.56	0.0642
37	1737.87	14.54	0.0670
38	1727.62	13.35	0.0661
39	1715.68	11.96	0.0666
40	1702.60	12.88	0.0681

41	1690.45	13.18	0.0659
42	1678.93	12.02	0.0700
43	1666.41	11.91	0.0675
44	1653.70	15.54	0.0700
45	1640.36	12.67	0.0682

Table C9. Depth (top of interval), estimated year, organic matter content (%OM) and THg concentration for the sediment core from M2 in the Peace-Athabasca Delta. %OM and THg concentrations are expressed per dry weight.

Depth	Year	%OM	THg
0	2016.22	20.51	0.0693
1	2014.44	27.68	0.0792
2	2011.81	26.80	0.0794
4	2006.95	23.42	0.0787
6	2000.05	24.20	0.0782
8	1991.66	23.21	0.0754
10	1983.26	24.54	0.0716
12	1974.76	18.46	0.0652
13	1970.88	5.11	0.0639
15	1963.04	12.85	0.0651
17	1949.44	12.75	0.0609
19	1931.27	9.02	0.0636
21	1909.81	11.20	0.0606
23	1872.55	12.34	0.0642
25	1858.38	18.93	0.0613
27	1835.70	12.21	0.0601
29	1823.50	11.74	0.0598
31	1797.98	12.83	0.0596
33	1768.96	10.65	0.0803
35	1749.88	28.79	0.0605
37	1733.99	14.36	0.0634
39	1712.42	31.69	0.0636

Table C10. Depth (top of interval), estimated year, organic matter content (%OM) and THg concentration for the sediment core from M5 in the Peace-Athabasca Delta. %OM and THg concentrations are expressed per dry weight.

Depth	Year	%OM	THg
0	2014.7	32.06	0.0660
1	2013.3	26.77	0.0811
2	2012.4	25.88	0.0726
3	2011.8	23.97	0.0719
4	2011.3	33.98	0.0750
5	2010.9	25.25	0.0764
6	2010.6	24.13	0.0726
7	2010.2	22.10	0.0759
8	2009.8	20.58	0.0701
9	2009.3	21.87	0.0728
10	2008.9	24.08	0.0742
11	2008.4	26.05	0.0753
12	2008.0	26.74	0.0744
13	2007.6	23.89	0.0788
14	2007.2	23.54	0.0762
15	2006.9	22.99	0.0726
16	2006.6	23.91	0.0752
17	2006.3	25.23	0.0747
18	2005.6	23.00	0.0729
19	2004.7	27.92	0.0769
20	2003.8	28.67	0.0795
21	2002.8	22.61	0.0718
22	2002.0	19.87	0.0698
23	2001.1	16.60	0.0767
24	2000.1	18.91	0.0739
25	1999.0	18.37	0.0681
26	1997.0	14.40	0.0682
27	1995.5	15.41	0.0682
28	1995.1	15.08	0.0674
29	1994.9	14.91	0.0705
30	1994.4	14.58	0.0661
31	1993.7	12.73	0.0675
32	1992.8	13.05	0.0679
33	1991.8	12.82	0.0658
34	1990.5	10.18	0.0681
35	1989.0	7.10	0.0657
36	1986.8	7.72	0.0672
37	1984.1	8.04	0.0662
38	1981.7	8.02	0.0652
39	1979.8	8.74	0.0648
40	1977.8	8.17	0.0633
41	1975.6	7.04	0.0601
42	1973.5	8.50	0.0606
43	1971.4	8.26	0.0623
44	1969.4	8.05	0.0666

45	1967.3	7.78	0.0636
46	1965.2	7.62	0.0647
47	1963.1	7.64	0.0648
48	1961.0	6.39	0.0651
49	1958.9	7.11	0.0640
50	1956.9	7.46	0.0654
51	1954.8	7.98	0.0633
52	1952.6	6.96	0.0612
53	1950.6	7.79	0.0605
54	1948.8	8.82	0.0618
55	1947.0	7.76	0.0670
56	1945.0	7.07	0.0607
57	1943.2	8.41	0.0612

Table C11. Depth (top of interval), estimated year, organic matter content (%OM) and THg concentration for the sediment core from PAD 18 in the Peace-Athabasca Delta. %OM and THg concentrations are expressed per dry weight.

Depth	Year	%OM	THg
0	2010.0	52.89	0.0401
1	2007.7	53.35	0.0411
2	2003.8	52.51	0.0424
3	2001.0	50.96	0.0435
4	1995.1	49.70	0.0443
5	1990.8	47.67	0.0459
6	1987.5	48.09	0.0491
7	1984.0	46.94	0.0470
8	1980.3	47.26	0.0488
9	1976.5	47.42	0.0438
10	1972.6	44.87	0.0461
11	1968.8	44.76	0.0499
12	1965.1	43.74	0.0479
13	1961.1	42.83	0.0449
14	1956.8	42.58	0.0438
15	1952.6	41.98	0.0423
16	1949.0	40.23	0.0423
17	1944.8	38.57	0.0436
18	1940.3	37.72	0.0431
19	1935.6	36.44	0.0399
20	1930.1	34.24	0.0362
21	1923.8	34.56	0.0385
22	1917.0	34.20	0.0354
23	1910.8	33.81	0.0359
24	1905.0	31.89	0.0373
25	1899.1	31.29	0.0357
26	1893.2	30.81	0.0346
27	1887.9	31.21	0.0339
28	1882.4	32.03	0.0338
29	1875.3	34.01	0.0328
30	1867.2	35.55	0.0322
31	1859.4	35.71	0.0400
32	1851.7	35.20	0.0374
33	1844.4	33.67	0.0353
34	1837.3	32.58	0.0366
35	1830.4	31.47	0.0365
36	1823.7	31.61	0.0356
37	1817.1	32.73	0.0322
38	1810.5	34.31	0.0362
39	1803.4	34.70	0.0370
40	1796.8	34.28	0.0349
41	1790.5	37.28	0.0281
42	1783.7	37.37	0.0286
43	1777.0	37.76	0.0353

Table C12. Depth (top of interval), estimated year, organic matter content (%OM) and THg concentration for the sediment core from AC5, located southeast of the Peace-Athabasca Delta. %OM and THg concentrations are expressed per dry weight.

Depth	Year	%OM	THg
0	2018.8	67.82	0.0544
1	2017.4	70.50	0.0524
2	2015.9	67.74	0.0592
3	2014.1	64.32	0.0680
4	2012.2	65.44	0.0755
5	2009.9	65.58	0.0727
6	2007.5	61.97	0.0721
7	2004.7	63.25	0.0712
8	2001.6	62.14	0.0721
9	1998.2	61.95	0.0714
10	1994.4	59.94	0.0744
11	1990.4	55.91	0.0855
12	1986.1	56.44	0.0834
13	1981.8	54.19	0.0851
14	1977.2	52.03	0.0795
15	1972.1	51.98	0.0842
16	1966.8	52.99	0.0871
17	1962.0	54.37	0.0851
18	1957.3	53.84	0.0725
19	1951.8	53.80	0.0662
20	1946.2	52.15	0.0646
21	1940.1	53.42	0.0636
22	1933.9	54.52	0.0582
23	1928.1	53.75	0.0509
24	1922.4	50.19	0.0541
25	1916.0	50.76	0.0492
26	1909.1	49.60	0.0462
27	1902.6	49.38	0.0486
29	1897.2	50.60	0.0525
32	1892.2	52.43	0.0432
34	1867.2	50.32	0.0439
36	1858.3	49.84	0.0322
38	1853.0	52.44	0.0360
40	1842.0	50.24	0.0346
42	1831.8	51.66	0.0340
44	1821.9	50.00	0.0267
46	1813.7	49.80	0.0227
48	1803.5	48.80	0.0216

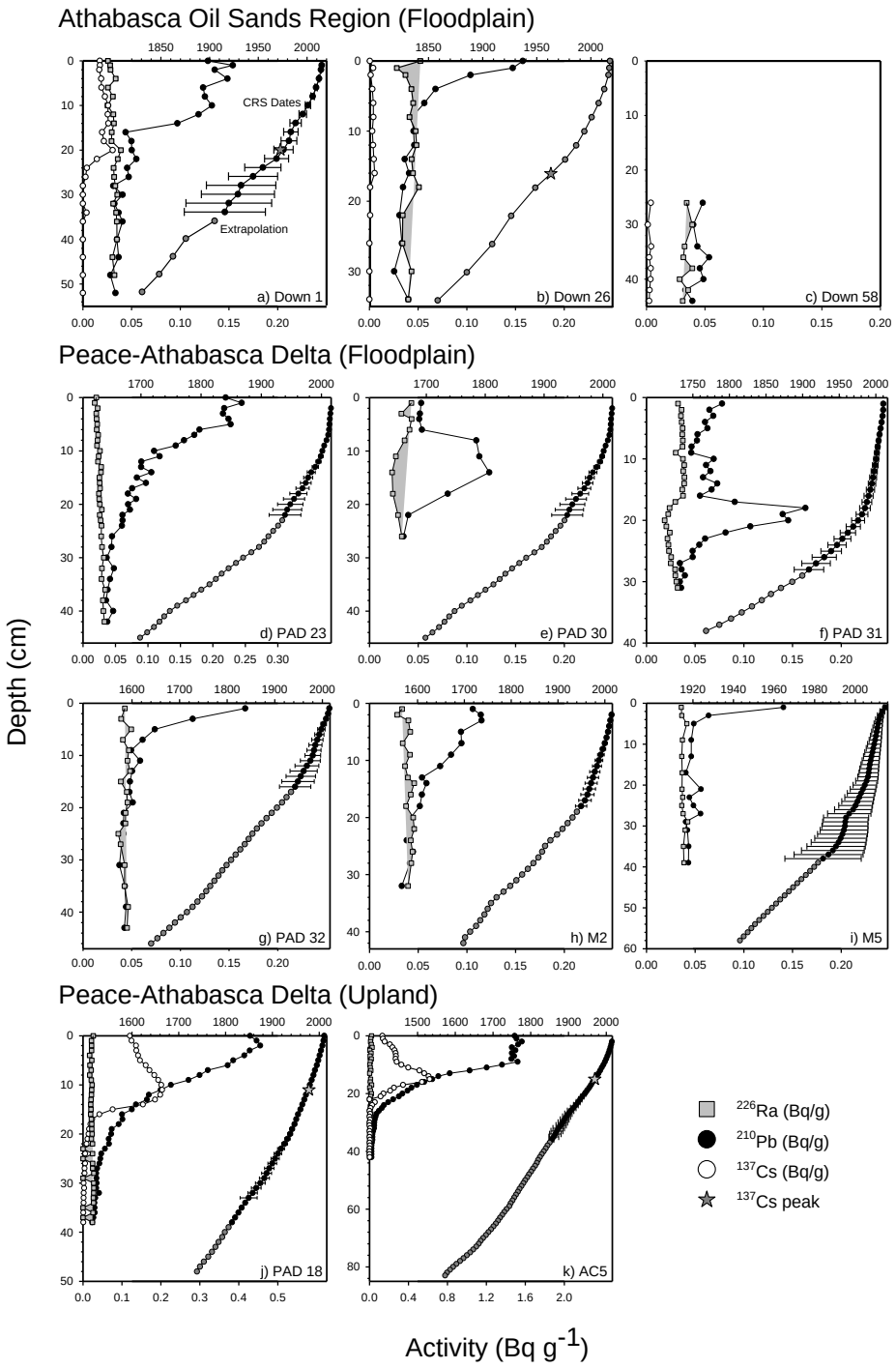

Figure C1. Graphs showing ^{210}Pb, ^{226}Ra and ^{137}Cs activity profiles (left) and age-depth relations (right), which includes both estimated (black) and extrapolated (grey) values for study lakes. The ^{137}Cs peak is denoted by a grey star and the error bars = ±2 SD. Previously published profiles include Down 1, Down 26 and Down 58 (Klemt et al. 2020), PAD 23 (Hall et al. 2012), PAD 30, PAD 31, PAD 32, M2 and M5 (Kay et al. 2019), and PAD 18 (Wiklund et al. 2012). AC5 (Brown 2022).

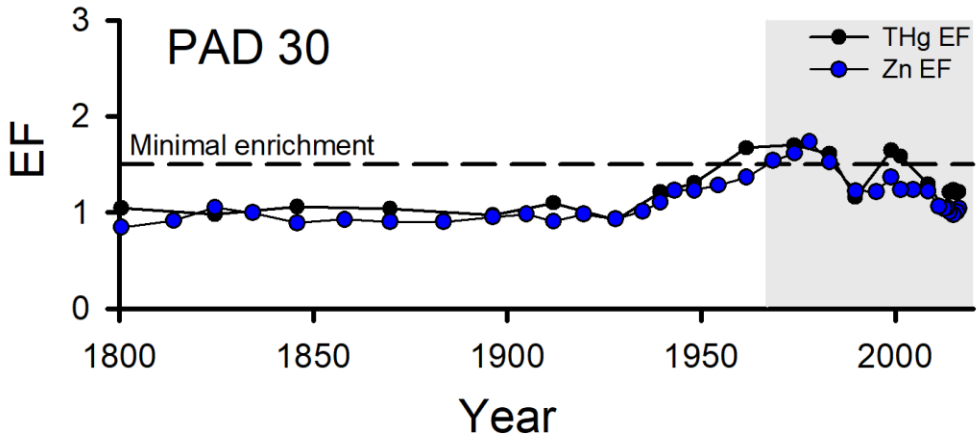

Figure C2. Time-series of enrichment factors relative to pre-industrial baselines for THg and Zn at PAD 30. The grey shaded region denotes the interval of oil sands mining and processing activities on the Lower Athabasca River beginning in 1967. The Zn data were published in Kay et al. (2020).

Appendix D:

This Appendix contains equations and text to perform the calculations used in Chapter 4 associated with the semi-empirical predictive model for estimating total excess (i.e., anthropogenic) As and Sb inventories at various distances from Giant and Con mines.

Derivation of landscape excess inventories for As and Sb

We expected the total excess inventory of "excess" metalloid deposition from lake sediment cores in the central NWT to decrease with distance from the Giant/Con Mine smelter complex moderated by prevailing winds. Sixty-six years (1953 - 2019) of hourly wind data were compiled from the Environment Canada climate monitoring station Yellowknife A (Climate ID #: 2204100), located at 205.7 m.a.s.l., 62.46° N, 114.44° W. Wind direction data were classified into an eight-pointed wind rose (N, NE, E, SE, etc.) and each lake was assigned a downwind rose direction with respect to the smelter (Table D1). Sediment core inventories of focus factor corrected excess metalloid ('Me'; As or Sb; see equation 5 of Wiklund et al. 2017) were then weighted by the proportion of time the wind blew from the direction of the smelter stack towards the lake as follows:

$$\text{Weighted } I_{\text{ex Me}} = I_{\text{ex Me}} / \left(\frac{\%downwind}{(\%totalwind/8)} \right) \quad \text{Eq. D1)}$$

where: $I_{\text{ex Me}}$ is the focus factor corrected excess As or Sb inventories computed following equation 5 of Wiklund et al. (2017) and reported in Jasiak et al. (2021).

%downwind = % of time that the wind blows from the direction of the smelter stack towards a given lake.

%totalwind = % of time that the wind blows (= 100 % - % calm conditions). The factor 8 corresponds to the 8 directions of the compass rose.

The focus factor corrected excess As or Sb inventories vs distance were then modeled following Kelly et al. (2010) and Wiklund et al. (2017) using linear regression after natural-log transformation of the excess metalloid inventories (see Figure D1):

$$\text{Ln } I_{\text{ex Me}} = y - kx \quad \text{Eq. D2)}$$

where: x = the distance (km) from the smelter stack

k = the slope describing the decline in fallout inventory with distance

y = a constant, the antilog of which ($e^y = a$) is equal to the inferred inventory of excess metalloid (g km^{-2}) at x = 0

e = base of the natural logarithm (2.71828)

Equation D2) can be re-expressed as: $I_{\text{ex Me}} = ae^{-kx}$ Eq. D3)

The total mass (M_{ex}) in g of excess As or Sb inventory deposited on the landscape within a given distance x (e.g., 50 km) from the smelter was then estimated as described by Kelly et al. (2010) and Wiklund et al. (2017) using the expression:

$$M_{\text{ex Me}} = 2\pi a \left(\frac{1-(kx+1)e^{-kx}}{k^2}\right) \quad \text{Eq. D4)}$$

Equation D3) can be rearranged to predict the total excess inventory of As or Sb for a given distance and cardinal direction due to atmospheric deposition by inserting the wind-weighting term for the direction of interest. For example, for a location 10 km due west of Giant Mine (a location not cored in this study) we would predict the total excess As inventory due to atmospheric deposition sourced from smelter operations to be:

$$I_{\text{ex As 10km West}} = \left(\frac{22.7}{(100/8)}\right) 9.012e^{(-0.0659)(10)}$$

So applied, Equation D3) becomes a semi-empirical model that predicts the total atmospheric anthropogenic deposition of As or Sb for any cardinal direction and distance (≤100 km) from Giant Mine (see Figure 4.4).

Table D1. Wind rose direction and average wind speed (1953-2019) for Yellowknife A Meteorological Station (Climate ID: 2204100; 62.46° N, 114.44° W). Note that this gives the direction the wind blows *towards* a direction and is simply the 180° inverse of station wind data which reports where direction the wind blows *from*. Note that wind rarely blows towards the NE from Yellowknife. Sediment cores were collected from lakes along the NW and NE downwind directions (bolded).

Downwind direction	Frequency (%)	Average wind speed (km hr^{-1})
S	18.0%	11.1
SW	13.2%	11.5
W	22.7%	13.5
NW	10.1%	15.0
N	9.8%	15.4
NE	2.6%	8.2
E	8.3%	11.5
SE	15.2%	14.3

Table D2. Central NWT Lake properties, distance, and direction to Giant Mine (GM), and excess As and Sb inventories after Focus Factor (FF) correcting and wind source weighting.

	Watershed Area CA m^2	Lake Area LA m^2	Direction and distance to GM	km	FF corrected Excess inventories Sb mg m^{-2}	As mg m^{-2}	Wind Weighting Factor	FF corrected & Wind Weighted Excess inventories Sb mg m^{-2}	As mg m^{-2}
NW80	$1.04x10^{-6}$	$9.44x10^{-4}$	NW	79	2	120	0.8064	2.5	149
NW70	$3.43x10^{-5}$	$9.22x10^{-4}$	NW	72.5	4	17	0.8064	5.0	21
NW60	$3.78x10^{-6}$	$3.17x10^{-5}$	NW	55.7	7	234	0.8064	8.7	290
NW50	$3.50x10^{-6}$	$5.61x10^{-5}$	NW	49.6	18	995	0.8064	22.3	1234
NW40	$1.01x10^{-7}$	$5.21x10^{-5}$	NW	40.7	7	117	0.8064	8.7	145
NW30	$1.90x10^{-5}$	$1.65x10^{-4}$	NW	29.8	30	434	0.8064	37.2	538
NW20	$1.17x10^{-6}$	$2.06x10^{-5}$	NW	17.8	19	6929	0.8064	23.6	8593
NW10	$3.58x10^{-5}$	$4.18x10^{-4}$	NW	10.5	82	4826	0.8064	101.7	5985
NE20	$1.10x10^{-6}$	$2.08x10^{-5}$	NE	20.9	7	318	0.2088	33.5	1523
NE40	$5.82x10^{-5}$	$4.23x10^{-4}$	NE	41.2	3	46	0.2088	14.4	220

* See Wiklund et al. (2017) and Jasiak et al. (2021) for explanation of excess inventories calculations and focus factor corrections.

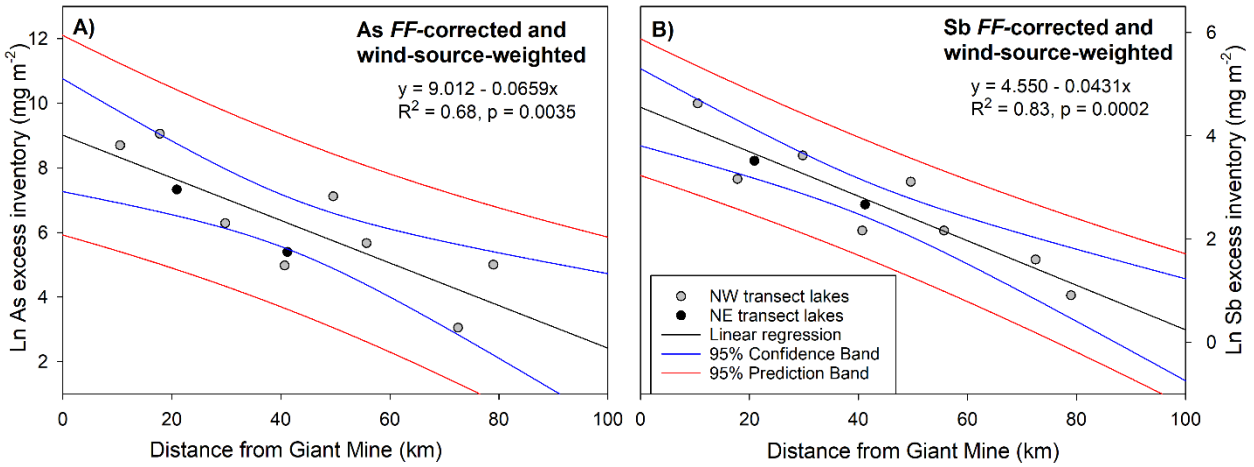

Figure D1. Total lake sediment excess or anthropogenic A) As and B) Sb inventories focus factor (FF)-corrected and wind-source-weighted vs distance from Giant Mine. See Table D2 for references for focus factors.

References

Jasiak, I., Wiklund, J.A., Leclerc, E., Telford, J.V., Couture, R.M.C., Venkiteswaran, J.J., Hall, R.I., and Wolfe, B.B. 2021. Evaluating spatiotemporal patterns of arsenic, antimony, and lead deposition from legacy gold mine emissions using lake sediment records. Applied Geochemistry, **134**: 105053, https://doi.org/10.1016/j.apgeochem.2021.105053

Kelly, E.N., Schindler, D.W., Hodson, P.V., Short, J.W., Radmanovich, R., and Nielsen, C.C. 2010. Oil sand development contributes elements toxic at low concentrations to the Athabasca River and its tributaries. Proceedings of the National Academy of Sciences, **107**: 16178-16183. https://doi.org/10.1073/pnas.1008754107

Wiklund, J. A. Kirk, J.L., Muir, D.C.G., Evans, M., Yang, F., Keating, J., Parsons, M.T. 2017. Anthropogenic mercury deposition in Flin Flon Manitoba and the experimental lakes area Ontario (Canada): a multi-lake sediment core reconstruction. Sci. Total Environ., **586**: 685-695. https://doi.org/10.1016/j.scitotenv.2017.02.046

Appendix E:

This Appendix provides the base data for organic and inorganic matter content (expressed as % of dry mass) and sediment age from Figure 5.4 in Chapter 5.

Table E1. Estimated year and organic and inorganic matter content (expressed as % of dry mass) for the sediment core from lake PAD 76 in the Peace-Athabasca Delta

PAD 76

Year	% OM	% MM	Year	% OM	% MM
2018.35	25.79	74.21	1891.14	22.55	77.45
2017.14	22.22	77.78	1885.65	21.20	78.80
2015.48	22.18	77.82	1880.72	19.98	80.02
2013.73	23.17	76.83	1875.22	15.33	84.67
2011.84	22.96	77.04	1868.89	17.16	82.84
2010.12	25.46	74.54	1861.13	13.26	86.74
2008.71	27.70	72.30	1853.85	13.74	86.26
2007.10	28.38	71.62	1847.84	12.45	87.55
2004.91	28.14	71.86	1838.65	11.32	88.68
2002.60	30.59	69.41	1829.26	10.72	89.28
2000.17	32.07	67.93	1820.74	10.75	89.25
1997.41	31.77	68.23	1811.77	11.34	88.66
1994.62	31.54	68.46			
1991.86	32.80	67.20			
1988.55	31.28	68.72			
1984.75	31.15	68.85			
1980.91	31.46	68.54			
1977.05	29.94	70.06			
1973.64	30.64	69.36			
1970.67	29.71	70.29			
1968.06	28.93	71.07			
1965.91	29.20	70.80			
1964.32	29.11	70.89			
1962.83	29.24	70.76			
1960.55	28.99	71.01			
1957.29	29.69	70.31			
1953.28	29.20	70.80			
1949.13	27.46	72.54			
1943.68	26.97	73.03			
1939.37	25.33	74.67			
1938.23	24.76	75.24			
1936.39	23.71	76.29			
1932.38	23.35	76.65			
1927.32	24.15	75.85			
1922.73	24.09	75.91			
1918.07	23.47	76.53			
1912.90	23.07	76.93			
1907.64	22.66	77.34			
1901.89	23.43	76.57			
1896.34	22.73	77.27			

Table E2. Estimated year and organic and inorganic matter content (expressed as % of dry mass) for the sediment core from lake PAD 30 in the Peace-Athabasca Delta

	PAD 30	
Year	% IM	% OM
2016.37	88.53	11.47
2015.92	91.64	8.36
2014.94	92.37	7.63
2014.01	92.64	7.36
2013.39	92.28	7.72
2012.66	90.84	9.16
2011.19	88.04	11.96
2008.44	81.28	18.72
2004.70	82.08	17.92
2001.45	89.01	10.99
1998.93	88.28	11.72
1995.11	87.46	12.54
1989.71	62.32	37.68
1983.06	49.67	50.33
1977.85	47.32	52.68
1973.99	47.26	52.74
1968.53	52.94	47.06
1961.64	55.05	44.95
1954.42	56.82	43.18
1948.17	55.85	44.15
1943.13	59.64	40.36
1939.43	61.77	38.23
1934.86	71.37	28.63
1927.96	75.37	24.63
1919.72	74.28	25.72
1911.91	65.94	34.06
1904.91	71.00	29.00
1896.22	81.34	18.66
1883.61	86.75	13.25
1869.79	87.03	12.97
1858.09	85.93	14.07
1845.80	85.15	14.85
1834.32	81.92	18.08
1824.65	80.25	19.75
1814.00	84.23	15.77
1800.52	85.94	14.06
1787.63	84.08	15.92
1774.89	88.75	11.25
1760.35	87.27	12.73
1748.05	79.06	20.94
1738.76	71.51	28.49
1730.90	72.91	27.09
1721.64	81.30	18.70
1710.38	85.13	14.87
1698.62	85.91	14.09

Table E3. Estimated year and organic and inorganic matter content (expressed as % of dry mass) for the sediment core from lake PAD 31 in the Peace-Athabasca Delta

	PAD 31	
Year	% IM	% OM
2010.29	88.16	11.84
2010.07	91.73	8.27
2009.26	92.05	7.95
2007.98	93.46	6.54
2006.58	93.13	6.87
2005.16	93.75	6.25
2003.81	93.74	6.26
2002.53	93.57	6.43
2001.46	93.86	6.14
2000.50	89.47	10.53
1999.24	92.20	7.80
1997.78	90.36	9.64
1996.28	92.66	7.34
1994.69	91.78	8.22
1992.60	90.54	9.46
1990.09	88.56	11.44
1987.79	72.85	27.15
1985.12	56.64	43.36
1981.11	56.90	43.10
1975.78	56.83	43.17
1969.19	60.61	39.39
1961.79	65.75	34.25
1954.41	70.18	29.82
1947.02	70.79	29.21
1939.00	74.64	25.36
1929.55	71.90	28.10
1918.38	77.09	22.91
1908.70	77.07	22.93
1899.58	77.61	22.39
1885.99	78.09	21.91
1870.50	78.22	21.78
1856.82	79.23	20.77
1844.25	79.65	20.35
1830.96	81.62	18.38
1816.89	78.81	21.19
1802.42	82.84	17.16
1786.35	85.51	14.49
1768.15	84.28	15.72

Table E4. Estimated year and organic and inorganic matter content (expressed as % of dry mass) for the sediment core from lake PAD 32 in the Peace-Athabasca Delta

	PAD 32	
Year	% IM	% OM
2014.73	61.54	38.46
2012.20	69.82	30.18
2007.92	70.14	29.86
2002.82	76.13	23.87
1998.03	77.78	22.22
1993.74	81.10	18.90
1989.53	83.13	16.87
1985.46	85.03	14.97
1982.50	84.46	15.54
1979.91	82.64	17.36
1974.78	85.59	14.41
1967.58	84.98	15.02
1960.74	87.01	12.99
1954.66	85.59	14.41
1948.88	83.89	16.11
1942.76	83.74	16.26
1934.40	86.95	13.05
1924.91	86.72	13.28
1915.48	87.73	12.27
1904.70	86.89	13.11
1893.76	88.62	11.38
1882.81	88.85	11.16
1872.32	84.61	15.39
1862.59	85.79	14.21
1853.25	82.71	17.29
1845.21	81.13	18.87
1837.22	79.53	20.47
1827.77	84.23	15.77
1817.90	83.10	16.90
1808.46	83.72	16.28
1798.94	82.94	17.06
1790.12	81.85	18.15
1781.96	76.50	23.50
1773.34	79.01	20.99
1764.50	84.81	15.19
1756.23	75.96	24.04
1747.39	83.44	16.56
1737.87	85.46	14.54
1727.62	86.65	13.35
1715.68	88.04	11.96
1702.60	87.12	12.88
1690.45	86.82	13.18
1678.93	87.98	12.02
1666.41	88.09	11.91
1653.70	84.46	15.54
1640.37	87.33	12.67

Table E5. Estimated year and organic and inorganic matter content (expressed as % of dry mass) for the sediment core from lake PAD 26 in the Peace-Athabasca Delta

	PAD 26	
Year	% IM	% OM
2014.77	86.23	13.77
2010.71	85.28	14.72
2006.09	86.39	13.61
2001.91	87.59	12.41
1997.82	86.41	13.59
1994.32	87.64	12.36
1991.71	90.65	9.35
1989.54	91.90	8.10
1988.04	90.24	9.76
1987.27	91.46	8.54
1986.91	90.99	9.01
1986.75	91.02	8.98
1986.71	91.49	8.51
1986.66	91.93	8.07
1986.42	91.63	8.37
1985.71	92.53	7.47
1984.22	92.64	7.36
1981.40	90.81	9.19
1976.26	90.83	9.17
1970.36	91.75	8.25
1965.00	91.92	8.08
1958.22	91.74	8.26
1950.70	91.20	8.80
1943.30	92.00	8.00
1935.64	92.10	7.90
1929.48	92.28	7.72
1925.25	93.19	6.81
1921.26	92.59	7.41
1916.82	92.99	7.01
1912.15	92.51	7.49
1907.78	93.62	6.38
1903.76	92.87	7.13
1899.60	93.25	6.75
1895.38	92.66	7.34
1890.82	94.06	5.94

Table E6. Estimated year and organic and inorganic matter content (expressed as % of dry mass) for the sediment core from lake PAD M7 in the Peace-Athabasca Delta

	M7	
Year	% IM	% OM
2014.49	76.52	23.48
2011.60	74.74	25.26
2008.21	73.92	26.08
2005.17	73.65	26.35
2003.00	74.46	25.54
2000.82	75.54	24.46
1997.47	77.04	22.96
1993.23	79.20	20.80
1988.82	78.67	21.33
1984.83	80.15	19.85
1981.44	81.60	18.40
1978.46	80.70	19.30
1975.55	82.99	17.01
1972.69	82.92	17.08
1970.01	82.04	17.96
1967.91	80.83	19.17
1966.80	82.19	17.81
1964.90	79.71	20.29
1961.59	80.74	19.26
1959.15	82.24	17.76
1958.29	81.67	18.33
1957.75	80.79	19.21
1956.41	83.42	16.58
1953.15	83.12	16.88
1948.30	84.61	15.39
1942.73	85.39	14.61
1937.90	88.60	11.40
1934.79	91.51	8.49
1932.90	92.26	7.74
1930.79	92.38	7.62
1922.64	91.59	8.41
1913.80	91.85	8.15
1908.63	91.75	8.25
1903.24	91.85	8.15
1897.64	92.12	7.88

Table E7. Estimated year and organic and inorganic matter content (expressed as % of dry mass) for the sediment core from lake PAD M2 in the Peace-Athabasca Delta

	M2	
Year	% IM	% OM
2016.22	79.49	20.51
2014.44	72.32	27.68
2011.81	73.20	26.80
2009.47	75.38	24.62
2006.95	76.58	23.42
2003.84	77.99	22.01
2000.05	75.80	24.20
1995.98	70.98	29.02
1991.66	76.79	23.21
1987.41	77.69	22.31
1983.26	75.46	24.54
1978.75	76.05	23.95
1974.76	81.54	18.46
1970.88	94.89	5.12
1966.91	87.24	12.76
1963.04	79.41	20.59
1957.69	85.55	14.45
1949.45	87.25	12.75
1940.55	84.09	15.91
1931.27	90.98	9.02
1920.62	88.58	11.42
1909.81	88.80	11.20
1898.22	89.20	10.80
1884.00	87.66	12.34
1872.55	84.15	15.85
1866.29	81.07	18.93
1858.38	87.49	12.51
1847.47	87.79	12.21
1835.70	86.86	13.14
1823.50	88.26	11.74
1811.17	86.30	13.70
1797.98	87.17	12.83
1783.73	91.55	8.45
1768.96	89.35	10.65
1757.02	85.04	14.96
1749.88	79.84	20.16
1743.02	71.21	28.79
1733.99	85.64	14.36
1725.15	68.31	31.69
1712.42	81.82	18.18
1701.54	57.45	42.55

Table E8. Estimated year and organic and inorganic matter content (expressed as % of dry mass) for the sediment core from lake PAD M5 in the Peace-Athabasca Delta

	M5				
Year	% IM	% OM	Year	% IM	% OM
2014.71	67.94	32.06	1963.11	92.36	7.64
2013.37	73.23	26.77	1961.02	93.61	6.39
2012.45	74.12	25.88	1958.99	92.89	7.11
2011.82	76.03	23.97	1956.91	92.54	7.46
2011.35	66.02	33.98	1954.82	92.02	7.98
2010.98	74.75	25.25	1952.68	93.04	6.96
2010.63	75.87	24.13	1950.66	92.21	7.79
2010.27	77.90	22.10	1948.86	91.18	8.82
2009.86	79.42	20.58	1947.02	92.24	7.76
2009.38	78.13	21.87	1945.08	92.93	7.07
2008.93	75.92	24.08	1943.21	91.59	8.41
2008.49	73.95	26.05			
2008.06	73.26	26.74			
2007.63	76.11	23.89			
2007.25	76.46	23.54			
2006.92	77.01	22.99			
2006.65	76.09	23.91			
2006.30	74.77	25.23			
2005.62	77.00	23.00			
2004.77	72.08	27.92			
2003.85	71.33	28.67			
2002.89	77.39	22.61			
2002.06	80.13	19.87			
2001.17	83.40	16.60			
2000.19	81.09	18.91			
1999.00	81.63	18.37			
1997.06	85.60	14.40			
1995.51	84.59	15.41			
1995.14	84.92	15.08			
1994.96	85.09	14.91			
1994.49	85.42	14.58			
1993.73	87.27	12.73			
1992.88	86.95	13.05			
1991.85	87.18	12.82			
1990.58	89.82	10.18			
1989.01	92.90	7.10			
1986.88	92.28	7.72			
1984.17	91.96	8.04			
1981.72	91.98	8.02			
1979.80	91.26	8.74			
1977.80	91.83	8.17			
1975.69	92.96	7.04			
1973.55	91.50	8.50			
1971.49	91.74	8.26			
1969.44	91.95	8.05			
1967.35	92.22	7.78			
1965.24	92.38	7.62			

Table E9. Estimated year and organic and inorganic matter content (expressed as % of dry mass) for the sediment core from lake PAD 71 in the Peace-Athabasca Delta

	PAD 71	
Year	% IM	% OM
2015.00	76.65	23.35
2007.64	79.45	20.55
1997.39	83.18	16.82
1986.77	85.81	14.19
1976.13	88.88	11.12
1963.92	88.37	11.63
1946.17	91.98	8.02
1922.56	91.04	8.96
1897.98	93.02	6.98
1874.02	91.37	8.63
1848.84	93.98	6.02
1822.42	92.58	7.42
1796.53	93.58	6.42
1765.95	95.43	4.57
1732.90	95.54	4.46
1699.88	95.02	4.98
1666.92	94.98	5.02
1635.47	94.76	5.24
1602.88	96.06	3.94
1566.69	96.98	3.02
1529.28	96.87	3.14
1492.51	96.41	3.59
1455.78	95.74	4.26
1419.00	96.79	3.21
1381.40	96.90	3.10
1345.40	96.43	3.57
1310.69	96.72	3.28
1273.44	95.76	4.24
1236.28	96.59	3.41
1201.54	96.41	3.59
1163.73	96.45	3.55
1124.92	97.16	2.84
1089.01	96.76	3.24
1055.31	97.44	2.56
1017.19	96.96	3.04
977.56	96.23	3.77